UTS UNIVERSITY OF TECHNOLOGY SYDNEY

Airflow-Oximetry Combined Signal Based Automatic Detection of Sleep Apnea in Adults

by Md Bashir Uddin

Thesis submitted in fulfilment of the requirements for the degree of

Doctor of Philosophy in Biomedical Engineering

under the supervision of

Associate Professor Steven Su (Principal Supervisor)
Dr Steve Ling (Co-Supervisor)
Associate Professor Chin Moi Chow (External Supervisor)
Faculty of Medicine and Health, The University of Sydney

University of Technology Sydney
Faculty of Engineering and Information Technology

December 2020

Certificate of Original Authorship

I, Md Bashir Uddin declare that this thesis is submitted in fulfilment of the requirements for the award of Doctor of Philosophy (PhD), in the School of Biomedical Engineering, Faculty of Engineering and Information Technology (FEIT) at the University of Technology Sydney (UTS).

This thesis is wholly my work unless otherwise referenced or acknowledged. In addition, I certify that all information sources and literature used are indicated in the thesis.

This document has not been submitted for qualifications at any other academic institution.

This research is supported by the Australian Government Research Training Program.

Production Note:
Signature removed prior to publication.

.....

(Md Bashir Uddin)

December 2020

To my beloved parents

*(Mrs **Alya Begum** & Late **Ali Asgar Moral**)*

for all your immeasurable love, unlimited support, and endless encouragement

Acknowledgement

I would like to acknowledge the support and contributions of everyone who has made my research journey a stimulating and a rewarding experience. I am indebted to my incredible primary supervisor, Associate Professor Steven Su, who has always been full of inspiration, support, and cheer. His unconditional support and encouragement throughout the research and invaluable feedback and comments have been extremely helpful. His style of supervision was stimulating and very effective. I have greatly enjoyed working with him. Besides being a supervisor, Prof Su cared for my well-being and always promoted a healthy work-life balance.

I am grateful to my co-supervisor, Dr Steve Ling for his valuable support to my thesis. His direction and support to my research have been helpful.

I acknowledge the immense support and contribution of my external supervisor Associate Professor Chin Moi Chow from The University of Sydney. I valued her concise explanation and critical analysis of critical aspects of my work that ultimately enhanced the quality of my research. Her guidance, direction, and support in my research especially in algorithm development, interpretation with practical scenarios, technical paper writing and correction, and thesis-writing and formatting have been extraordinary. Moreover, I must acknowledge her contribution as an editor of this thesis. I am thankful to Prof Chow for proofreading my thesis. It would not be possible to complete this thesis without her tremendous contribution. Besides being a great mentor, Prof Chow always cared for my well-being.

I am thankful to Professor Joanne Tripper, Professor Gyorgy Hutvagner, Associate Professor Adel Al-Jumaily, Associate Professor Ananda Sanagavarapu, Dr Rifai Chai, and Dr Daniel Carter for their feedback and support as members of the assessment panel at different times of my candidature. Their suggestions and valuable comments have made my thesis meaningful and significant. I am also thankful to the examiners who have reviewed this thesis and provided important feedback and suggestions.

I am grateful to the University of Technology Sydney for providing financial support through two scholarships namely UTS International Research Scholarship (IRS) and UTS President's Scholarship (UTSP). Without these scholarships and the associated supports from the University of Technology Sydney, my research journey would not have been possible.

Special thanks to the authors of the Sleep Heart Health Study (SHHS) who collected and processed nocturnal PSG data and made these datasets freely available. Without their sleep data, it would have been difficult to manage my research goals.

Thanks to all my colleagues and friends from the Faculty who have contributed to making my journey enjoyable – a special thanks to Kairui Guo, Wenhui Chen, Dr Shakil Ahamed Khan, Md Noman Habib Khan, K M Anamul Hossain, Md Rabiul Islam, Dr Md Zakir Hossain, and Dr Md Arafat Hossain. I would also like to thank all my friends in Australia. They care about me and are always there to help when I need it. My life in Australia is much more colourful in their presence.

I am fortunate to have a wonderful wife, Aysha Siddiqa Joti, who has been a very supportive partner during my PhD. She took care of me and did all the household activities. She took the time to do those little things that always filled my heart with joy and love.

I sincerely thank my mother Alya Begum, who has done everything for my study since my childhood. I am also grateful to my late father Ali Asgar Moral. I would like to acknowledge the support and contributions of my brothers Md Shirazul Islam, Md Mahtab Moral, Md Mohasin Moral, Md Joshim Moral, and Md Nasir Moral for their limitless love, invaluable support, encouragement, and understanding in seeing me through the most challenging endeavour in my life. I also thank my uncles, aunties, cousins, father-in-law, mother-in-law, and the friends in Bangladesh or anywhere in the world, for their encouragement. I would like to dedicate this thesis to the wonderful memories of my beloved parents for their unexplainable love and support.

Format of Thesis

This thesis by compilation is structured as a single manuscript that comprises a combination of chapters and published/publishable works (i.e., papers). This thesis presents each chapter/paper logically and coherently by the addition of linking text to establish the relationship between one chapter/paper and the next. This thesis by compilation includes:

- An introduction to the basic physiology and terms linked to the research study.
- A chapter or paper that describes a review of the literature.
- A chapter or paper that describes the electroencephalogram spectral power with varying apnea duration.
- A chapter or paper that describes the automatic diagnosis of sleep apnea.
- A chapter or paper that describes the modified algorithm for the diagnosis of sleep apnea.
- A final discussion of the research study and proposed future works.

List of Papers/Publications

This thesis includes the following papers/publications. The status of each paper and its corresponding chapter in the thesis are also included at the last of each paper.

1. **Uddin, M. B.**, Chow, C. M., and Su, S. W. (2018). Classification methods to detect sleep apnea in adults based on respiratory and oximetry signals: a systematic review. *Physiological Measurement*, *39*(3), 03TR01. DOI: 10.1088/1361-6579/aaafb8. (**Published**) – ***Chapter 2***
2. **Uddin, M. B.**, Su, S. W., Chen, W., and Chow, C. M. (2019). Dynamic changes in electroencephalogram spectral power with varying apnea duration in older adults. *Journal of Sleep Research*, *28*(6), e12850. DOI: 10.1111/jsr.12850. (**Published**) – ***Chapter 3***
3. **Uddin, M. B.**, Chow, C. M., Ling, S. H., and Su, S. W. (2020). *A robust airflow envelope tracking and digitization approach for automatic detection of apnea and hypopnea event*. Paper presented at the 7th IEEE Asia-Pacific Conference on Computer Science and Data Engineering. (**Accepted and Presented**) – ***Chapter 4***
4. **Uddin, M. B.**, Chow, C. M., Ling, S. H., and Su, S. W. (2020). A novel algorithm for automatic diagnosis of sleep apnea from airflow and oximetry signals. *Physiological Measurement, 42*(1). DOI: 10.1088/1361-6579/abd238 (**Published**) – ***Chapter 4***
5. **Uddin, M. B.**, Chow, C. M., Ling, S. H., and Su, S. W. (2020). *A per-sample digitized algorithm for automatically detecting apnea and hypopnea events from airflow and oximetry*. Paper presented at the 42nd Annual International Conference of the IEEE Engineering in Medicine and Biology Society.
   DOI: 10.1109/EMBC44109.2020.9176212 (**Published**) – ***Chapter 5***
6. **Uddin, M. B.**, Chow, C. M., Ling, S. H., and Su, S. W. (2020). An algorithm for automatic diagnosis of sleep apnea hypopnea syndrome from per-sample encoding of airflow and oximetry. *IEEE Journal of Biomedical and Health Informatics*. (**Under review**) – ***Chapter 5***

Contribution of Authors

Md Bashir Uddin is the primary contributor and has contributed to the whole thesis and all papers presented in this thesis. The specific contributions of all authors listed in the previous papers/publications are mentioned below:

Md Bashir Uddin (**Uddin, M. B.**): This author is the primary contributor to all papers/publications listed in this thesis. The main contributions are:

- Performing systematic review of literature.
- Electroencephalogram (EEG) spectral analysis with varying apnea durations.
- Designing an automatic algorithm with subsequent modifications for sleep apnea diagnosis based on airflow (AF) and oximetry (SpO_2) signals.
- Writing, correction, and submission related tasks of all technical papers.

Steven Su (**Su, S. W.**): This author is the secondary contributor to all papers/publications listed in this thesis. The main contributions are:

- Guiding the tasks related to the systematic review of literature.
- EEG spectral power calculation in different frequency bands.
- Reviewing the design processes of the automatic algorithms.
- Modification and corrections to all technical papers listed in this thesis.

Chin Moi Chow (**Chow, C. M.**): This author is the secondary contributor to all papers/publications listed in this thesis. The main contributions are:

- Guiding and modifying the tasks related to the systematic review of literature.
- Guiding the statistical analysis linked to apnea events and EEG spectral powers.
- Correcting the design of the automatic algorithm from the physiological aspects.
- Modification and corrections to all technical papers listed in this thesis.

Steve Ling (**Ling, S. H.**): The main contributions of this author are:

- Guiding the tasks related to the design of the automatic diagnostic algorithm.
- Modification and corrections to some technical papers.

Wenhui Chen (**Chen, W.**): The main contributions of this author are:

- Significant contribution to the statistical analysis for EEG spectral powers.

Contents

Abbreviations

Abbreviations	Full-Form
AASM	American Academy of Sleep Medicine
AAT	After apnea termination
AE	Abdominal effort
AF	Airflow
AHI	Apnea hypopnea index
ANN	Artificial neural network
ANOVA	Analysis of variance
AUC	Area under ROC curve
BAT	Before apnea termination
BHC	Binary hierarchical
BMI	Body mass index
BS	Backward shifting
BS SpO_2	Backward shifted oximetry
CA	Clustering algorithms
CART	Classification and regression trees
CO_2	Carbon dioxide
CPAP	Continuous positive airway pressure
CGE	Center of gravity engine
CSA	Central sleep apnea
dB	Decibel
ECG	Electrocardiography
EEG	Electroencephalography
EMG	Electromyography
EOG	Electrooculography
FCM	Fuzzy *c*-means
FIR	Finite impulse response
FIS	Fuzzy inference system
FN	False negative
FP	False positive
GLM	Generalized linear models
HR	Heart rate
KM	K-means

KNN	*k*-nearest neighbors
LDA	Linear discriminant analysis
LoA	Limits of agreement
LRA	Logistic regression analysis
LRM	Linear regression model
LS-SVM	Least squares support vector machine
ML	Machine learning
MLP	Multi-layer perceptron
MLR	Multiple linear regression
MRT	Modified recording time
MSA	Mixed sleep apnea
NAF	Nasal airflow
NN	Neural network
NPV	Negative predictive value
NREM	Non-rapid eye movement
O_2	Oxygen
O_2 desat	Oxygen desaturation
OLS	Orthogonal least squares
OSA	Obstructive sleep apnea
PAP	Positive airway pressure
PLA	Piecewise linear approximation
PNN	Probabilistic neural network
PPV	Positive predictive value
PSG	Polysomnography
PVDF	Polyvinylidene fluoride
QDA	Quadratic discriminant analysis
RBF	Radial basis function
RDI	Respiratory disturbance index
REM	Rapid eye movement
RERA	Respiratory effort-related arousal
RFC	Random forest classifier
RIP	Respiratory inductance plethysmography
ROC	Receiver operating characteristic
RSS	Random subspace
SpO_2	Oximetry/Oxygen saturation
SD	Standard deviation

SHHS	Sleep Heart Health Study
SVM	Support vector machine
SWS	Slow-wave sleep
TDNN	Time-delay neural network
TE	Thoracic effort
TN	True negative
TP	True positive
TST	Total sleep time
TRT	Total recording time

List of Figures

List of Tables

Abstract

Sleep apnea, a common sleep disorder, can significantly decrease the quality of life and is closely associated with major health risks such as cardiovascular disease, sudden death, depression, and hypertension. It also elicits brain and physiological changes that vary across the night. Conventional diagnosis of sleep apnea using polysomnography (PSG) is costly and time-consuming, requiring manual scoring of sleep stages and respiratory events. Current automatic diagnostic algorithms used to detect sleep apnea vary in approaches with the use of different physiological signals. An effective, reliable, and accurate automatic method for the diagnosis of sleep apnea will be time-efficient and economical.

This thesis is a narration of the work that led to the development of a novel algorithm suitable for the automatic diagnosis of sleep apnea. A systematic literature review of the existing methods (approaches and algorithms) was performed before designing the algorithm. This review presented an overview of methods to diagnose sleep apnea using respiratory and oximetry signals. The review identified the research gaps with indicating the major concerns, challenges, benefits, and limitations of using respiratory and oximetry signals for the diagnosis of sleep apnea.

This thesis examined the electroencephalogram (EEG) spectral powers resulting from apnea duration of varying length and reported the changes in the relative powers in EEG frequency bands before and at apnea termination. The study was carried out for the purpose of justifying the usability of EEG for the automatic diagnosis of sleep apnea. It investigated the spectral power changes in delta, theta, alpha, sigma, and beta frequency bands of EEG as a function of apnea duration from 375 events. The study revealed a significant reduction in EEG relative powers (the low frequency theta, alpha, and sigma powers) both before and at apnea termination. The findings from the EEG spectral analysis suggests that the application of EEG signal in sleep apnea diagnosis is not reliable due to the random variations in spectral powers as well as the major challenges associated with EEG acquisition and its processing. Due to the limitations associated with the EEG for an unattended home diagnosis of sleep apnea, the EEG signal was excluded from the automatic detection approach.

An automatic method that employed an airflow (AF) envelope tracking and subsequent digitization approach for the diagnosis of sleep apnea was developed. The automatic detection process includes the detection of apnea, hypopnea, sleep time, and apnea hypopnea index (AHI). In designing the algorithms, 988 PSG records were randomly selected from a recognized database of the Sleep Heart Health Study (SHHS). The dataset was further divided into a development (n = 45) and a validation (n = 943) set. Total sleep time (TST) was estimated from the analysis of AF and oximetry (SpO_2) signals. The algorithm detected apnea events by a digitization process,

following the determination of the peak excursion from AF envelopes. Hypopnea events were determined from the AF envelope and oxygen desaturation with a correction to a time lag in SpO_2. The AHI was estimated from the number of detected events divided by the estimated TST. For performance evaluation, the estimated AHI was compared to the SHHS manually scored data. The automatic algorithm showed strong correlations between the estimated and actual AHI. In addition, the Bland-Altman plot showed very good agreements between estimated and actual AHI, with small mean bias and narrow limits of agreement. Binary (two) class diagnosis was reported where positive (sleep apnea) and negative (normal) classes were identified using different AHI cut-offs (≥5, ≥15, and ≥30 events/h). In addition, 4 classes (normal, mild, moderate, and severe) of diagnosis were estimated for performance evaluation. The overall 2 class diagnostic accuracies were found to be 90.7%, 91%, and 96.7% for AHI cut-offs ≥5, ≥15, and ≥30 events/h respectively. Moreover, good accuracy (78.9%) and kappa (0.70) were observed for 4 class diagnosis. Though the envelope-based automatic approach performed well, some possible limitations were addressed.

A modified method was developed for the automatic diagnosis of sleep apnea where all possible limitations in the previous envelope-based designed method have been addressed and minimised. The modified approach used a sample-to-sample encoding of the AF signal for the precise detection of apnea events. The per-sample encoding approach accurately detected peak excursion by the exact detection of peak and trough amplitudes. Thus, the limitation (incorrect detection of peak excursion due to fluctuations in the upper boundary) found in the envelope tracking method was minimized. In addition, per-sample encoding of SpO_2 signals correctly identified the start and end of each oxygen desaturation phase, whereas a fixed window method may overestimate the duration of desaturations. Moreover, the adjustment of all possible time lags (0, 10, 20, and 30 s) made the modified algorithm more accurate than the envelope tracking method. The overall 2 class diagnostic accuracies were found 93.5%, 92.4%, and 96.6% for AHI cut-offs ≥5, ≥15, and ≥30 events/h respectively. Moreover, excellent overall accuracy (83.4%) and kappa (0.77) were observed for 4 class diagnosis. Comparing to envelope-based approach, the overall increments in 2 and 4 class diagnostic accuracies were 1.4% and 4.5% respectively, whereas 4 class kappa significantly improved from 0.70 to 0.77. Thus, the modified algorithm performed significantly better than the envelope-based approach.

The new algorithm overperformed than any other existing methods for the automatic diagnosis of sleep apnea. It is applicable to any portable sleep screeners especially for the home diagnosis of sleep apnea.

Chapter 1

Introduction

1.1 Sleep Apnea

1.1.1 Sleep apnea event

Sleep breathing disorders, defined by disturbances of the normal breathing process during sleep, can cause the development of central nervous, organic, physical, and metabolic disorders (Varady, Micsik, Benedek, & Benyo, 2002). There are various types of sleep breathing disorders, namely obstructive sleep apnea (OSA), central sleep apnea (CSA), and mixed sleep apnea (MSA).

Figure 1.1 depicts the different types of apnea events. An episode of OSA occurs when there is complete obstruction of the air passage and cessation of airflow but continued respiratory efforts (abdominal and thoracic) against a closed airway. A CSA episode occurs when there is a complete cessation of breathing with no respiratory efforts. Both these events must last 10 seconds or more during sleep for them to be scored as such in adults (Berry et al., 2017; Berry et al., 2012). MSA is defined by a central respiratory pause followed, in a relatively short duration of time, by obstruction of the airway (Koves, 1999;Berry et al., 2017; Berry et al., 2012). OSA is the most prevalent sleep disorder (Berger et al., 1997) with CSA and MSA being relatively less predominant. There are major differences in sleep and respiratory physiology between children and adults. Sleep apnea in children is defined as the cessation of airflow for at least two respiratory cycles, and it is different from the definition of apneas in adults (Alsubie & BaHammam, 2017).

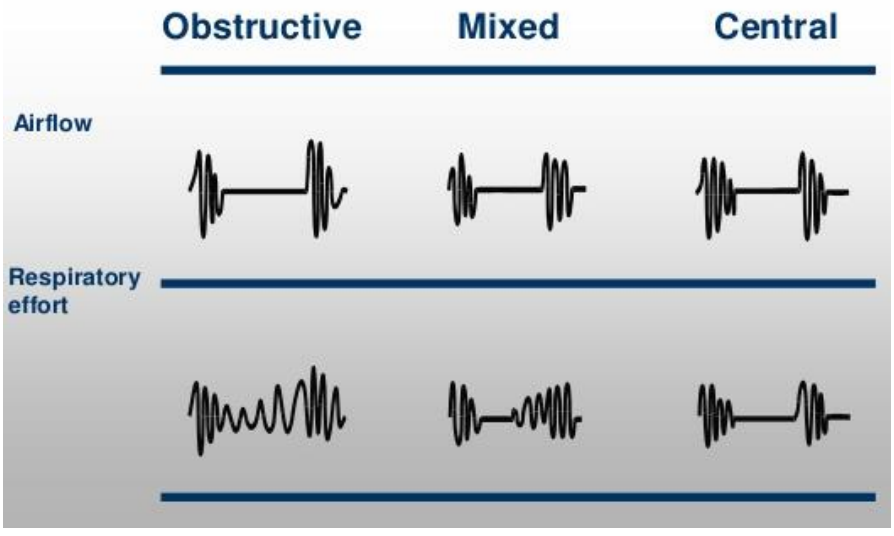

Figure 1.1. Sleep apnea event types with physiological signals.

OSA is the most serious form of sleep disorder and it is the focus of this thesis.

OSA affects about 2-5% of the total human population and over 30% of the elderly male population (Koves, 1999). The prevalence of sleep apnea is approximately 3% in children (Chang & Chae, 2010), 9% in women, and 17% in men with age ranging from 50 to 70 years (Peppard et al., 2013).

OSA is a serious sleep disorder, where patients stop breathing repeatedly during sleep, sometimes more than hundreds of times due to airways obstruction. Figure 1.2 depicts the anatomical location of an obstructive apnea at the level of the pharynx. An apnea that is prolonged results in a progressive lack of oxygen to the brain and the rest of the body.

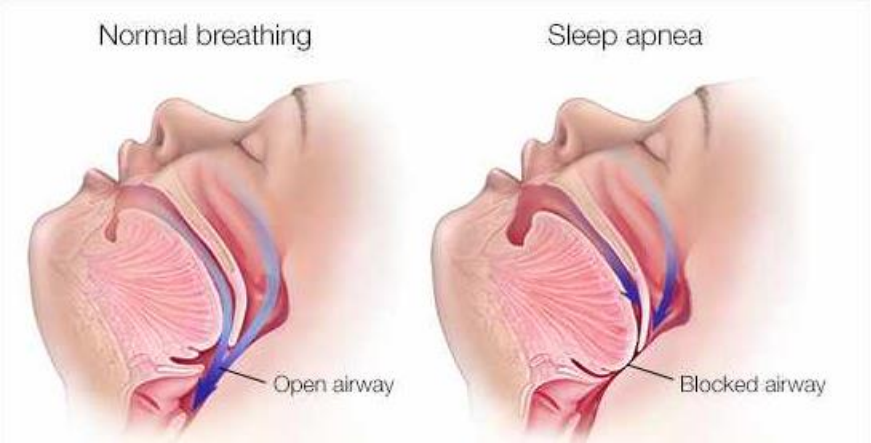

Figure 1.2. Airway pattern during normal breathing and an obstructive sleep apnea event.

An obstructive apnea event can be detected by employing physiological signals that detect airflow (e.g., use of nasal pressure or thermal sensor) and respiratory effort (e.g., use of inductance plethysmography) (Figure 1.3).

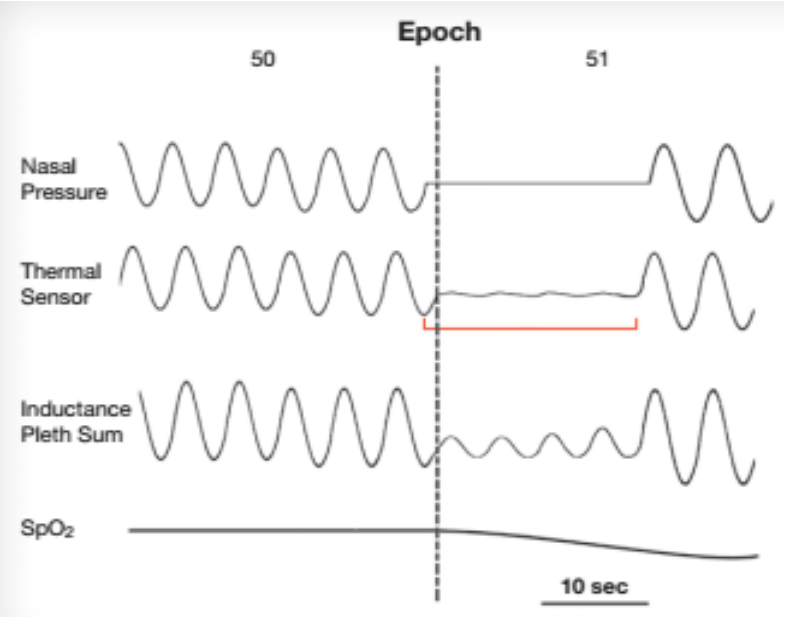

Figure 1.3. Sleep apnea event with physiological signals (Pleth = Plethysmography).

The respiratory disturbances due to sleep apnea may cause arousal from sleep (Gleeson, Zwillich, & White, 1990). Sleep disruption and excessive daytime sleepiness are the most common presenting complaint (Slater & Steier, 2012). Other major symptoms include snoring, fatigue, falling asleep, headaches, weight gain, and memory loss. Because of such complications, the quality of life can be significantly decreased as well as an increased major risk of associated health problems (Ben-Israel, Tarasiuk, & Zigel, 2010). In addition, sleep apnea may go undiagnosed for years because of a person's unawareness (Kryger, Roos, Delaive, Walld, & Horrocks, 1996). Notably, there are around a hundred million people in the world who are suspected to have sleep apnea but undiagnosed (Cruz, 2007). In this regard, several challenges regarding sleep apnea diagnosis, assessment, and treatment are of major concerns in public health.

1.1.2 Sleep hypopnea event

Shallow breathing, also known as hypopnea, is often associated with partial obstruction (or high airway resistance) of the upper airway. Hypopnea is typically defined by a decreased amount of air movement into the lungs and can cause oxygen level in the blood to drop as illustrated in Figure 1.4. Hypopnea during sleep is considered a sleep breathing event, although less severe than apnea. During severe hypopnea, sleep is disturbed such that despite a full night's sleep, patients did not feel rested because they were aroused frequently during sleep. This breathing disruption causes a drop in blood oxygen level, which may in turn disrupt the stages of sleep.

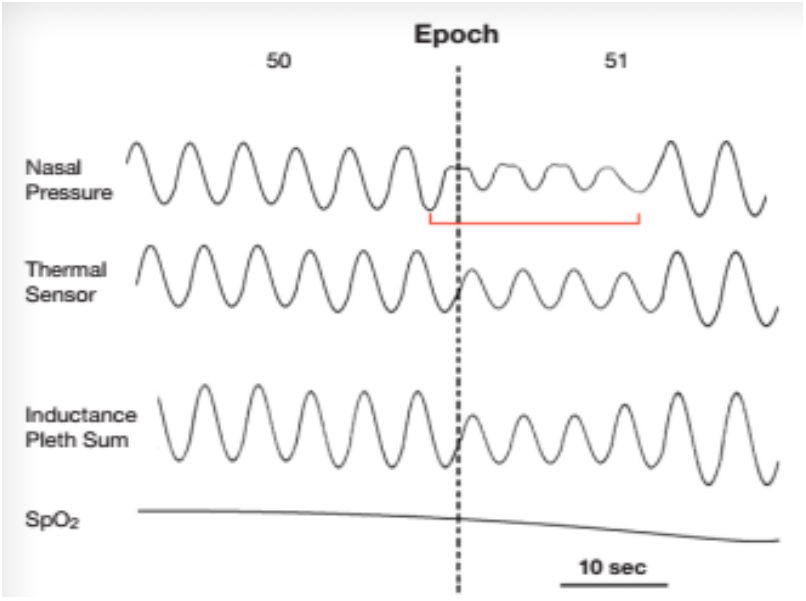

Figure 1.4. Sleep hypopnea event with physiological signals.

People with sleep breathing disorder (apnea/hypopnea) often have loud and heavy snoring. The most common symptom of sleep breathing disorder is excessive sleepiness, which results from constant sleep interruption. Not all people with hypopnea experience all these symptoms

and not everyone who has these symptoms has hypopnea. Other symptoms may include loss of energy, depression, nervousness, forgetfulness, morning headaches, mood or behavior changes, and trouble concentrating. These symptoms may cause traffic accidents and may lead to diminished productivity in the workplace and emotional problems, thus compromising the quality of life. Cardiovascular consequences of apnea/hypopnea events may include hypertension, myocardial infarction and coronary heart disease as well as other problems such as stroke, psychiatric problems, impotence, cognitive dysfunction, and memory loss.

1.2 Conventional Diagnosis of Sleep Apnea

1.2.1 Polysomnography

Polysomnography (PSG), considered the gold standard and reliable method for sleep apnea diagnosis, is a multichannel signal recording process throughout the night. The major parameters of a standard diagnostic nocturnal PSG (Chesson et al., 1997; Kushida et al., 2005) include recording of electrocardiogram (ECG), electroencephalogram (EEG), electrooculogram (EOG), electromyogram (EMG), nasal airflow (NAF), abdominal and/or thoracic efforts (AE and/or TE), body position, snoring sounds, and pulse oximetry (SpO_2). In portable devices, a limited-channel Level 3 or 4 home study is also frequently used for apnea diagnosis. A limited-channel study includes one or more of the following signal channels: NAF, abdominal, and/or thoracic movements, SpO_2, and heart rate (HR) derived from ECG (Ferber et al., 1994).

A sleep apnea test with PSG involves an overnight diagnostic study in a sleep laboratory, where electrodes are attached to the skin surface and scalp to record physiological signals as illustrated in Figure 1.5. Patients may not be able to sleep well due to wires hanging from one's head and body. Sleep technologists monitor and manually review the overnight study for designating sleep stages and apnea type and length according to the American Academy of Sleep Medicine (AASM) guidelines.

1.2.2 Scoring an apnea event

According to the last update of the American Academy of Sleep Medicine (AASM) guidelines (Berry et al., 2017; Berry et al., 2012), scoring a respiratory event as apnea is done when both of the following criteria are met:

- There is a drop in the peak signal excursion by ≥90% of the pre-event baseline using an oronasal thermal sensor (diagnostic study), positive airway pressure (PAP) device flow (titration study), or an alternative apnea sensor (diagnostic study).

- The duration of the ≥90% drop in sensor signal is ≥10 seconds.

Figure 1.5. Complete setup for polysomnography.

(https://www.alamy.com/stock-photo/polysomnography.html)

The pre-event baseline is defined as the mean amplitude of stable breathing and oxygenation in the 2 minutes preceding onset of the event (in individuals who have a stable breathing pattern during sleep) or the mean amplitude of the 3 largest breaths in the 2 minutes preceding onset of the event (in individuals without a stable breathing pattern). When baseline breathing amplitude cannot be easily determined (and when underlying breathing variability is large), events can also be terminated when either there is a clear and sustained increase in breathing amplitude, or in the case where a desaturation has occurred, there is event-associated resaturation of at least 2%. When the oronasal thermal airflow sensor is not functioning or the signal is not reliable during the diagnostic study, one of the alternative apnea sensors such as nasal pressure transducer, respiratory inductance plethysmography sum (RIPsum), respiratory inductance plethysmography flow (RIPflow), or polyvinylidene fluoride sum (PVDFsum) can be used. For scoring either apnea or a hypopnea, the event duration is measured from the nadir preceding the first breath that is clearly reduced to the beginning of the first breath that approximates the baseline breathing amplitude as illustrated in the red brackets of Figure 1.3 and Figure 1.4.

Scoring an apnea as obstructive if it meets apnea criteria and is associated with continued or increased inspiratory effort throughout the entire period of absent airflow. Scoring an apnea as central if it meets apnea criteria and is associated with absent inspiratory effort throughout the entire period of absent airflow. Scoring an apnea as mixed if it meets apnea criteria and is

associated with the absent inspiratory effort in the initial portion of the event, followed by the resumption of inspiratory effort in the second portion of the event. There is insufficient evidence to support a specific duration of the central and obstructive components of a mixed apnea; thus, specific durations of these components are not recommended (Berry et al., 2017).

The identification of apnea does not require a minimum desaturation criterion. If a portion of a respiratory event that would otherwise meet the criteria for a hypopnea meets the criteria for apnea, the entire event should be scored as an apnea (Berry et al., 2017). If the apnea or hypopnea event begins or ends during an epoch that is scored as sleep, then the corresponding respiratory event can be scored and included in the computation of the apnea hypopnea index (AHI). This situation usually occurs when an individual has a high AHI with events occurring so frequently that sleep is severely disrupted that resulted in epochs being scored as wake, even though <15 second of sleep is present during the epoch containing that portion of the respiratory event (Berry et al., 2017). However, if the apnea or hypopnea occurs entirely during an epoch scored as wake, it should not be scored or counted towards the apnea-hypopnea index because of the difficulty of defining a denominator in this situation. If these occurrences are a prominent feature of a polysomnogram and/or interfere with sleep onset, their presence should be mentioned in the narrative summary of the study.

1.2.3 Scoring a hypopnea event

According to updated AASM guidelines (Berry et al., 2017; Berry et al., 2012), scoring a respiratory event as a hypopnea is done if all of the following criteria are met:

- The peak signal excursions drop by ≥30% of the pre-event baseline using nasal pressure (diagnostic study), PAP device flow (titration study), or an alternative hypopnea sensor (diagnostic study).
- The duration of the ≥30% drop in the signal excursion is ≥10 seconds.
- There is a ≥3% oxygen desaturation from pre-event baseline or the event is associated with an arousal.

The criteria used to score a respiratory event as a hypopnea (≥3% oxygen desaturation with or without arousal) should be specified in the PSG report. It is the responsibility of the individual practitioner to confirm and follow the criteria that should be used for reporting to the patient's payer to be reimbursed and qualify the patient for therapy. When the nasal pressure transducer is not functioning or the signal is not reliable during a diagnostic study, one of the alternative hypopnea sensors such as an oronasal thermal sensor, RIPsum, RIPflow, dual thoracoabdominal RIP belts, or PVDFsum can be used. Supplemental oxygen may blunt desaturation. There are currently no scoring guidelines for when a patient is on supplemental oxygen and no desaturation

is noted. If the diagnostic study is performed while the individual is on supplemental oxygen, its presence should be mentioned in the narrative summary of the study.

1.2.4 Scoring a hypopnea event with EEG arousal

Electroencephalography (EEG) is an electrophysiological monitoring signal that records the electrical activity of the brain. It is typically non-invasive, with the electrodes placed on the scalp, although invasive electrodes are sometimes used, as in electrocorticography. EEG measures voltage fluctuations resulting from ionic current within the neurons of the brain (Niedermeyer & da Silva, 2005). Clinically, EEG refers to the recording of the brain's spontaneous electrical activity over a while, as recorded from multiple electrodes placed on the scalp (Niedermeyer & da Silva, 2005). Diagnostic applications generally focus either on event-related potentials or on the spectral content of EEG. The analyses of neural oscillations (popularly called 'brain waves') that can be observed in EEG signals in the frequency domain.

EEG is usually used to score arousal from sleep. An EEG arousal is an abrupt shift in EEG frequency, which may include alpha and/or theta waves and/or delta waves and/or frequencies greater than 16 Hz lasting at least 3 seconds and starting after at least 10 continuous seconds of sleep. An EEG arousal often occurs at the termination of an apnea event (Figure 1.6). An EEG arousal is required for scoring a hypopnea event when the peak excursion of airflow drops ≥30% from the pre-event baseline with a duration of ≥10 s but not associated with ≥3% oxygen desaturation (Berry et al., 2017; Berry et al., 2012).

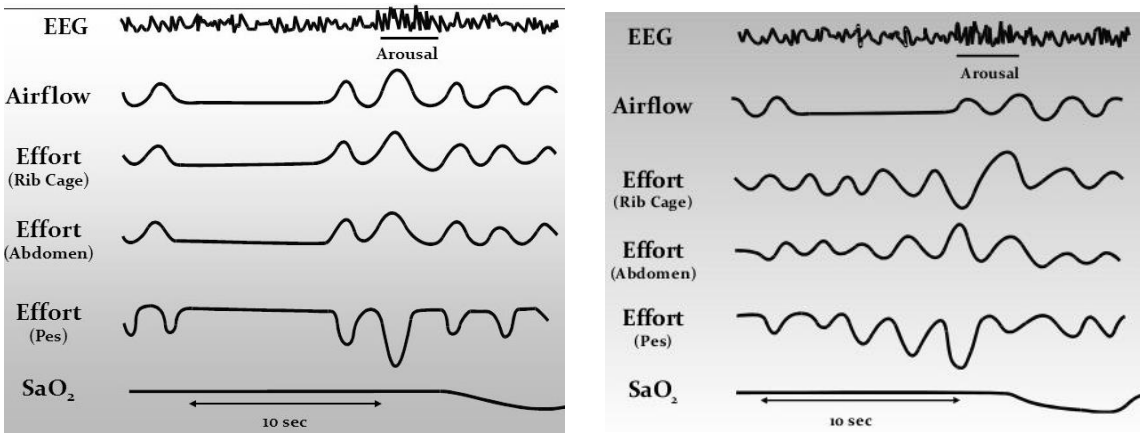

(a) (b)

Figure 1.6. EEG arousals corresponding to (a) CSA and (b) OSA events.

1.2.5 Scoring total sleep time and AHI

An overnight PSG record usually contains sleep and wake segments that are scored using EEG signal. Sleep and wake portions can be distinguished based on EEG rhythms/frequency

bands according to Rechtschaffen and Kales criteria ((Berry et al., 2017; Berry et al., 2012). Thus, the analysis of EEG can provide the total sleep time (TST) by subtracting the wake durations from the PSG recording duration. The AHI is calculated from the total number of apnea and hypopnea events divided by TST.

1.2.6 Severity of sleep apnea

The severity of sleep apnea is measured by the number of episodes per hour, using several indexes such as the apnea index (AI), hypopnea index (HI), and apnea-hypopnea index (AHI) or respiratory disturbance index (RDI). AHI is the most used severity index. In individuals with apnea or hypopnea throughout the night, there can be 5 to 15 episodes per hour in mild cases, 15 to 30 episodes per hour in moderate cases, and more than 30 episodes per hour in severe cases in adults (Grover & Pittman, 2008; Kryger, 2000). The severity of sleep apnea is also different in children with 1 to 5 episodes per hour classified as Mild, 5 to 10 episodes per hour as Moderate, and more than 10 episodes per hour as Severe (Alsubie & BaHammam, 2017; Kljajic et al., 2017).

1.3 Automatic Diagnosis of Sleep Apnea

Sleep apnea is a serious sleep disorder that affects the quality of sleep. Early diagnosis is the pre-requisite to the proper treatments for sleep apnea. Conventional/manual diagnosis (visual scoring) is time-consuming and costly and requires skilled personnel. Automatic diagnosis can remove the drawbacks of manual diagnosis. Thus, a robust and most accurate automatic diagnostic method needs to be developed that can produce a reliable diagnosis of sleep apnea.

An automatic method can analyze the respiratory-related physiological signals and detect the episodes of apnea and hypopnea events for proper diagnosis without any involvement of humans. Though automatic processes have been developed obviating the manual process, they are not sufficiently robust for reliable and accurate diagnosis of sleep apnea. Thus, a new automatic method (algorithm) is required for the accurate diagnosis of sleep apnea.

This thesis developed an automatic algorithm for the diagnosis of sleep apnea from AF and SpO_2 signals. A systematic literature review of the existing methods (approaches and algorithms) was required for designing a reliable automatic algorithm. In addition, the analysis of the electroencephalogram (EEG) spectral powers from apnea duration of varying length was required to justify the use of the EEG for the automatic approach for home application.

An automatic method that employed an airflow (AF) envelope tracking and subsequent digitization approach for the diagnosis of sleep apnea was developed. The automatic detection process includes the detection of apnea, hypopnea, sleep time, and apnea hypopnea index (AHI).

A modified method of the AF envelope tracking method developed for the automatic diagnosis of sleep apnea where all possible limitations in the previous designed method have been addressed and minimised.

1.4 Research Questions, Hypotheses, and Study Approach

Three main research questions were raised in this thesis with relevant hypotheses and study approach.

Question 1: Are the EEG spectral features effective for sleep apnea diagnosis?

Hypothesis 1: The features of spectral power may not be used for sleep apnea diagnosis.

Study approach:

- Analysis of the EEG spectral powers to investigate the changes related to apnea termination.
- Comparison of spectral powers in different apnea duration groups.
- Justification of the use of EEG for the automatic diagnosis of sleep apnea.

Question 2: Is the envelope tracking approach with subsequent digitization, based on AF and SpO_2 signals, effective for the automatic diagnosis of sleep apnea?

Hypothesis 2: An envelope tracking and subsequent digitization approach would be effective for reliable diagnosis of sleep apnea.

Study approach:

- Detection of apnea and hypopnea events using AF envelope tracking with subsequent digitization.
- The estimation of TST from the auto-analysis of AF and SpO_2 signals.
- Validation of the automatic algorithm with a large dataset.
- Comparison of the performance with the existing approaches.

Question 3: Can per-sample encoding of AF and SpO_2 produce better performance than envelope-based approach?

Hypothesis 3: Sample-to-sample encoding would be superior to detecting apnea and hypopnea events compared to the envelope-based approach.

Study approach for Hypothesis 3:

- Detection of apnea events by sample-to-sample encoding of AF signal with satisfying the updated AASM guidelines.
- Detection of the timing of oxygen desaturations from per-sample encoding of SpO_2 signal.
- Detection of hypopnea events by applying all possible amount of time lags in SpO_2 signal.
- Estimation of AHI from overall detected apneas and hypopneas and validate the algorithm with a large dataset.
- Comparison of the performance with envelope-based and other existing approaches.

1.5 Contribution to Knowledge

This thesis contributed significantly to knowledge as follows:

- A review of the literature that led to identifying the major concerns, challenges, and limitations of the existing automatic methods. In addition, the potential research gaps and possible directions were addressed for developing a new and reliable automatic approach.
- Description of EEG spectral power resulting from apnea of different durations. The EEG spectral power in sleep apnea episodes varied significantly with the change of apnea durations. The spectral analysis showed the link between spectral power changes and varying apnea duration and suggested the effectiveness of using EEG signal for the automatic diagnosis of sleep apnea.
- Development of algorithms for the automatic diagnosis of sleep apnea using an envelope tracking technique and a sample-to-sample encoding technique. Envelope tracking was proposed as a new technique for the diagnosis of sleep apnea though some limitations exist throughout the automatic diagnostic process. A modified algorithm minimized the problems associated with envelope-based approach and outperformed over other automatic approaches. This novel algorithm is proposed for the ease of computational implications in event scoring and applicable to used-friendly home diagnosis of sleep apnea.

1.6 Thesis Outline

This thesis is a narration of the work that led to the development of a novel algorithm suitable for the automatic diagnosis of sleep apnea:

Chapter 1 provided an overview of the basic physiology and terms linked to sleep apnea.

Chapter 2 is a systematic literature review of the existing methods (approaches and algorithms) used for sleep apnea diagnosis.

Chapter 3 examined the electroencephalogram (EEG) spectral powers resulting from apnea duration of varying length and reported the changes in the relative powers in EEG frequency bands before and at apnea termination.

Chapter 4 reported an automatic method that employed an airflow (AF) envelope tracking and subsequent digitization approach for the diagnosis of sleep apnea. The automatic detection process includes the detection of apnea, hypopnea, sleep time, and apnea hypopnea index (AHI).

Chapter 5 reported a modified method of the AF envelope tracking method developed for the automatic diagnosis of sleep apnea where all possible limitations in the previous designed method have been addressed and minimised.

Chapter 6 provided a summary, final discussion and addressed future works for developing new algorithms for the diagnosis of sleep apnea.

Chapter 2

Literature Review

2.1 Introduction

A systematic review of existing literature based on sleep apnea diagnosis is required where computerized techniques may overcome the limitations of manual processes. In addition, the systematic review addresses the research gaps for future investigations.

Physiological signals also referred to as biological or biomedical signals, are elemental in sleep apnea diagnosis. They are the measurements or recordings that are generated in the physiological process of human beings, e.g., heart rate, respiratory frequency, skin conductance, electric muscle current, and brain electrical activity. Respiratory signals (nasal airflow/pressure) along with efforts generated by respiratory muscles (thoracic and abdominal effort manifest as pressure waves), and pulse oximetry (SpO_2) are fundamental signals employed to detect sleep apnea. Obstructive, central, and mixed apnea types can be easily distinguished by airflow, thoracic and abdominal efforts. Besides, sleep apnea severity (mild, moderate, and severe) can be calculated using the number of events per hour. In addition, every apnea event of 10 seconds or more results in a reduction of oxygen level. Thus, the level of oxygen desaturation is applied to detect apnea/hypopnea cases. Other physiological signals such as EEG, ECG, and snore sound are also used to detect sleep apnea but the reliability of sleep apnea detection using these signals is very poor.

Many researchers have employed different classification methods to detect sleep apnea using physiological signals. The common signals used include oxygen saturation (Oeverland, Skatvedt, Kvaerner, & Akre, 2002; Zamarron, Romero, Gude, Amaro, & Rodriguez, 2001), airflow (Morsy & Al-Ashmouny, 2006; Nazeran, Almas, Behbehani, Burk, & Lucas, 2001), snore sounds (Ben-Israel, Tarasiuk, & Zigel, 2012), ECG (Song, Liu, Zhang, Chen, & Xian, 2016; Travieso, Alonso, del Pozo, Ticay, & Castellanos-Dominguez, 2014), EEG (Tagluk & Sezgin, 2011), or a combination of these signals (W. Huang, Guo, Shen, & Tang, 2017; Kaimakamis et al., 2016; Varady et al., 2002). The cost of the detection system is proportional to the number of sensors used to collect physiological signals. Many studies have used only one physiological signal to detect sleep apnea (Mendez et al., 2010; Selvaraj & Narasimhan, 2013), whereas others have used multiple physiological signals (Al-Mardini, Aloul, Sagahyroon, & Al-Husseini, 2014; Alvarez-Estevez & Moret-Bonillo, 2009; Kaimakamis, Bratsas, Sichletidis, Karvounis, & Maglaveras,

2009; Otero, Felix, Barro, & Zamarron, 2012). Reducing the processing cost is not the primary target of sleep apnea detection, but the accuracy of the system designed is the first priority.

Detecting sleep apnea using the main signals, respiratory and oximetry, would be more realistic and result in better detection accuracy. There are several reasons for selecting these signals. Firstly, the manual scoring of sleep apnea events is based on respiratory and oximetry signals, where data segments or epochs are annotated using these signals. Secondly, sleep apnea detection that uses additional signals of EEG, ECG, and snore sound is done using the same annotations based on these signals. Finally, the detection accuracy found in different classification methods is the measure that is based on these annotations.

In addition, adults and children are two distinct entities in sleep apnea detection. Sleep architecture, respiratory physiology, apnea definition, and apnea severity in adults differ from children/pediatric subjects (Alsubie & BaHammam, 2017; Kljajic et al., 2017). Besides, the algorithms for sleep apnea detection in pediatric subjects are quite different and usually need special consideration or criteria to obtain better detection results. According to these differences between adults and pediatric subjects, this review focuses only on the adult population.

Detection of sleep apnea using respiratory and oximetry signals often includes a four-stage methodology as illustrated in Figure 2.1: acquisition of respiratory and oximetry signals, features extraction, features selection, followed by apnea detection. One or more respiratory and oximetry signals are recorded from the adult population (healthy and apnea or both types). Features are extracted from respiratory and oximetry signals and in some cases with a large set of features; the features selection step is applied to select more distinctive features. Finally, features are applied to the classifiers to detect sleep apnea.

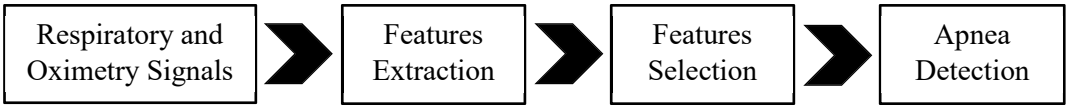

Figure 2.1. The conceptual workflow of decision-making.

Detection of sleep apnea using respiratory and oximetry signals often includes a four-stage methodology Respiratory and oximetry signals are the most effective physiological signals on which a reliable and accurate sleep apnea detection system is based. To design such a system, a review of the existing literature on respiratory and oximetry signals has shown greater acceptability in sleep apnea detection. However, the benefits, drawbacks, and challenges associated with the use of these signals as well as the existing classification methods in sleep apnea detection are unknown. Thus, this systematic review will address these issues to advance

the techniques of sleep apnea detection to enable the development of a reliable and accurate system. In addition, this paper will address the rationales for and the process of decision-making on the multiple sleep apnea scenarios, including their concept, model, performance, plus beneficial and challenging outcomes. The main research questions were (1) Which respiratory and/or oximetry signals provide the best discriminatory support for decision-making on sleep apnea? (2) Which classification methods result in high accuracy in sleep apnea detection with respiratory and oximetry signals? (3) What are the beneficial and challenging effects associated with the use of these physiological signals and classification methods?

2.2 Methods

2.2.1 Inclusion and exclusion criteria

Studies were included in this review if they met the following criteria: (1) presented a method or systematic approach to detecting sleep apnea, (2) written in English, (3) included adult participants only, (4) classification methods based on the use of one or more respiratory and oximetry signals, (5) decisions made on normal or apnea (or different classes of apnea or their severity), and (6) presented definitive overall detection results in the form of accuracy, sensitivity, specificity, and other parameters. These criteria were also applied to studies obtained from cross-reference tracking. Studies that satisfied the above criteria were extracted and included in this review. Articles from conference proceedings were reviewed critically and only extended versions that were published as journal articles were included. Studies were also excluded even though they met the above inclusion criteria: (1) case report of a single subject, and (2) studies where participants have co-morbidities of chronic heart and kidney diseases, diabetes, stroke, etc.

2.2.2 Search strategy

The phrase ‘Sleep apnea detection’ is inter-related to the research fields of Health, Engineering (Biomedical), and Information Technology. sleep apnea is a medical or health complication where knowledge of Engineering and Information Technology is applied to detect or solve this problem. In this regard, the selection of specific databases to extract related articles is a crucial factor. A systematic search was conducted on the following five major electronic databases that are basic sources of articles in the fields of Health, Engineering, and Information Technology: Medline (Ovid), Scopus (Elsevier), ACM Digital Library, IEEE Xplore Digital Library, and ProQuest Science & Technology. Studies published in English from January 2001 to July 2017 were included in this study according to the inclusion and exclusion criteria mentioned above.

Databases search was performed using the following words or phrases and all possible combinations: apnea or sleep apnea or obstructive sleep apnea or sleep apnea-hypopnea syndrome or sleep-disordered breathing, and the noun or verbal form of classification or detection or identification or prediction or recognition or screening. Following limiting conditions were applied as well during the search: English language, adult human subject, and the stated range of years of publication. All references found in five databases were imported to EndNote for rigorous manual screening after deleting duplicates. Thus, identified articles were screened for eligible studies. Detailed investigation of eligible studies and their bibliographies retrieved additional pertinent references. Finally, inclusion and exclusion criteria were applied to extract desired articles for qualitative synthesis.

The flow diagram of the systematic review process is presented in Figure 2.2. The combined electronic searches identified 4111 studies. Rigorous screening of titles and abstracts excluded 3963 studies due to irrelevancy. The remaining 148 full-text articles were eligible for detailed investigation.

A rigorous manual search of bibliographies of mentioned full-text articles was performed to extract eligible additional references and new full-text studies. In this way of cross-reference tracking, 7 new full-text articles were added. Of 155 full-text articles, 93 failed to satisfy the eligibility criteria. The remaining 62 full-text articles that met the inclusion criteria but not met the exclusion criteria were included for qualitative synthesis.

2.2.3 Extraction of study characteristics

The data extracted from the included studies through qualitative synthesis were studies with the year of publication, the number of subjects, type of respiratory and/or oximetry signals used, main decision, classification methods, and metrics for classification method evaluation (detection rate). The metrics (based on per-subject or per-recording and per-segment or per-epoch detection) appear in the last four columns (Table 2.2). The parameters and equations used to evaluate the metrics (accuracy, sensitivity, specificity, and other parameters) are set out in Table 2.1. True positive (TP) represents a positive input detected as positive, whereas true negative (TN) represents a negative input detected as negative. False positive (FP) represents a negative input detected as positive, whereas false negative (FN) represents a positive input detected as negative.

The main outcome measuring parameters (accuracy, sensitivity, and specificity) are evaluated based on TP, TN, FP, and FN. Other parameters are positive predictive value (PPV), negative predictive value (NPV), F-measure, g-means, and area under ROC (receiver operating characteristic) curve (AUC). The qualitative analysis of included articles based on respiratory and oximetry signals (single signal or multiple signals) is tabulated in Table 2.2.

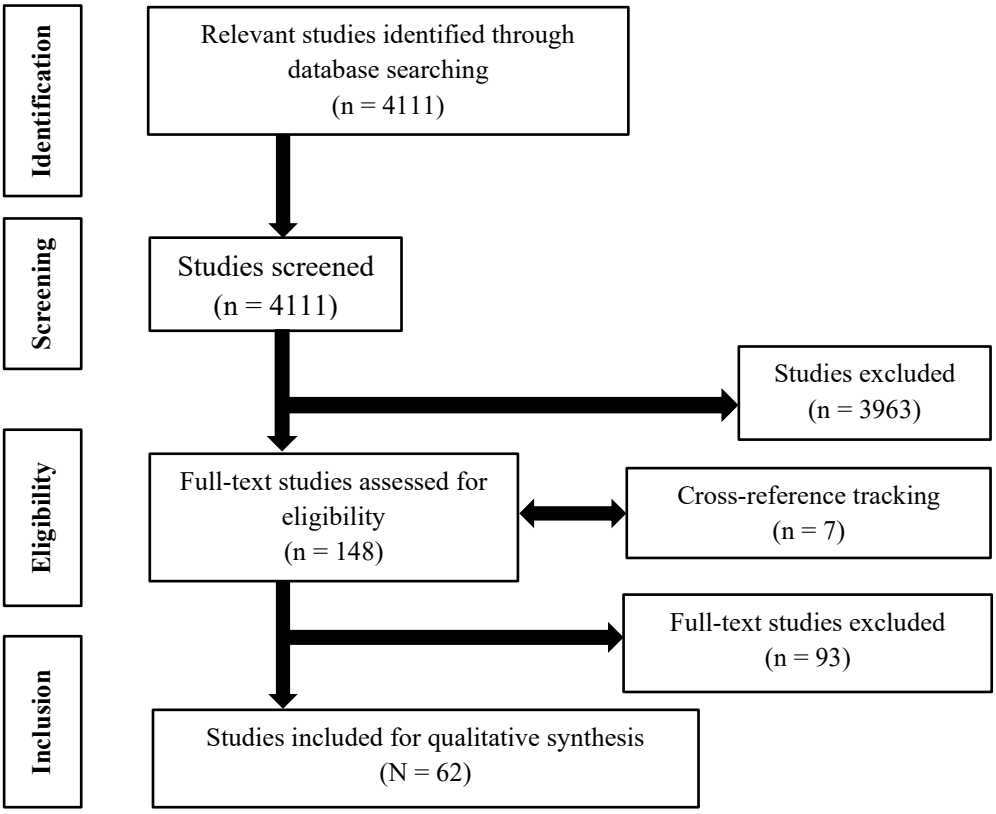

Figure 2.2. Flow diagram of the systematic review process.

Table 2.1. Parameters for evaluating metrics used in classification methods.

Parameters[a]	Definition[b]
Accuracy (Ac)	$\frac{TP+TN}{TP+TN+FP+FN} \times 100\%$
Sensitivity (Se)	$\frac{TP}{TP+FN} \times 100\%$
Specificity (Sp)	$\frac{TN}{TN+FP} \times 100\%$
Positive predictive value (PPV)	$\frac{TP}{TP+FP} \times 100\%$
Negative predictive value (NPV)	$\frac{TN}{TN+FN} \times 100\%$
F-measure	$2 \times \frac{PPV \times Sensitivity}{PPV + Sensitivity}$
g-means	$\sqrt{Sensitivity \times Specificity}$
Receiver operating characteristic (ROC) curve	A plot of sensitivity versus 1-specificity
Area under ROC curve (AUC)	A performance measurement for the classification problems at various threshold settings. AUC represents the degree of separability between classes.

[a]Parameters symbols: AUC = Area under ROC curve, NPV = Negative predictive value, PPV = Positive predictive value, ROC = Receiver operating characteristic

[b]Definition terms: FN = False negative, FP = False positive, TN = True negative, TP = True positive

Table 2.2. Included studies to detect sleep apnea based on respiratory and oximetry signals.

Study	No. of subjects	Signal[a]	Decision[b]	Classification method[c] (*) best when multiple mentioned	Metrics[d,e] (%)			
					Ac	*Se*	*Sp*	*Other*
Nazeran et al. (2001)	9	AF	A/H	FIS (Fuzzy rules)	83.0			
Zamarron et al. (2001)	197	SpO_2	O^+/O^-	Threshold-based	(77.0)	(58.0)	(92.0)	PPV (87.0)
Oeverland et al. (2002)	100	SpO_2	Mi/Mo-Se	Threshold-based		(88.6)	(76.9)	
Varady et al. (2002)	16	AF+TE+AE	A/H/N	ANN	90.0			
Varady, Bongar, and Benyo (2003)	6	TE+AE	C/O	PLA				PPV 90.6
Y. K. Lee, Bister, Blanchfield, and Salleh (2004)	7	SpO_2	O/N	Threshold-based	96.6	95.7	97.0	
Fontenla-Romero, Guijarro-Berdinas, Alonso-Betanzos, and Moret-Bonillo (2005)	6	AF+TE	C/M/O	ANN	83.8			
Morsy and Al-Ashmouny (2006)	10	AF	A/N	FIS (fuzzy rules) + CGE		100	97.0	
Tian and Liu (2006)	30	AF+SpO_2	A/H/N	TDNN		83.7	82.9	
Alvarez, Hornero, Abasolo, del Campo, and Zamarron (2006)	187	SpO_2	O^+/O^-	Threshold-based	(87.2)	(90.1)	(82.9)	AUC (96.7)
Alvarez, Hornero, Garcia, et al. (2006)	74	SpO_2	O^+/O^-	Threshold-based	(86.5)	(95.5)	(73.3)	AUC (87.0)

del Campo, Hornero, Zamarron, Abasolo, and Alvarez (2006)	187	SpO_2	O^+/O^-	Threshold-based		(88.3)	(82.9)	AUC (92.1)
Alvarez, Hornero, Garcia, del Campo, and Zamarron (2007)	187	SpO_2	O^+/O^-	Threshold-based	(87.2)	(90.1)	(82.9)	AUC (92.4)
Alvarez, Hornero, Marcos, del Campo, and Lopez (2007)	74	SpO_2	O^+/O^-	CA (KM*, FCM, Hierarchical)	(90.5)	(95.5)	(83.3)	
Hornero, Alvarez, Abasolo, del Campo, and Zamarron (2007)	187	SpO_2	O^+/O^-	Threshold-based		(82.1)	(87.0)	
Marcos, Hornero, Alvarez, del Campo, and Lopez (2007)	187	SpO_2	O^+/O^-	NN (MLP, RBF*)	(86.3)	(89.9)	(81.1)	AUC (96.0)
Salisbury and Sun (2007)	34	AF	O/N	Threshold-based		93.3	100	
Han, Shin, Jeong, and Park (2008)	24	AF	A/N	Threshold-based		92.4	88.3	
Marcos, Hornero, Alvarez, del Campo, Lopez, et al. (2008)	187	SpO_2	O^+/O^-	NN (KM*, FCM, OLS)	(86.1)	(89.4)	(81.4)	AUC (91.0)
Marcos, Hornero, et al. (2008b)	187	SpO_2	O^+/O^-	NN (MLP)	(85.5)	(89.8)	(79.4)	AUC (90.0)
Marcos, Hornero, et al. (2008a)	157	SpO_2	O^+/O^-	GLM	(88.0)	(79.6)	(100)	AUC (92.0)

Ng et al. (2008)	26	TE+AE	A/N	Threshold-based				AUC 90.9
Otero, Felix, Alvarez, and Zamarron (2008)	5	AF	A/H	Fuzzy rules	95.0			
Alvarez-Estevez and Moret-Bonillo (2009)	12	AF+TE+AE+SpO_2	A/H	Fuzzy rules		88.5	88.5	AUC 88.0
Kaimakamis et al. (2009)	86	AF+TE+SpO_2	O/N	Decision tree (C4.5)	(84.9)			
Marcos, Hornero, Alvarez, del Campo, and Zamarron (2009a)	187	SpO_2	O^+/O^-	LDA*, QDA, KNN, LRA	(87.6)	(91.1)	(82.6)	AUC (92.5)
Marcos, Hornero, Alvarez, del Campo, and Zamarron (2009b)	149	SpO_2	O^+/O^-	SVM	(88.0)	(84.4)	(93.3)	AUC (92.1)
Morillo, Rojas, Crespo, Leon, and Gross (2009)	117	SpO_2	Mi/Mo-Se	Threshold-based		(90.9)	(84.0)	AUC (95.0)
Sezgin and Tagluk (2009)	21	TE+AE	C/M/O	ANN	86.8			
Akin and Sezgin (2010)	21	AE	C/M/O	ANN	77.9			
Alvarez, Gutierrez, Marcos, del Campo, and Hornero (2010)	148	AF+SpO_2	O^+/O^-	Threshold-based	(84.5)	(84.0)	(85.4)	AUC (90.4)
Alvarez, Hornero, Marcos, and del Campo (2010)	148	SpO_2	O^+/O^-	LRA	(89.7)	(92.0)	(85.4)	AUC (96.7)
Burgos, Goni, Illarramendi, and Bermudez (2010)	8	SpO_2	A/N	Bagging with ADTree	93.0	92.4	93.5	AUC 98.5
Caseiro, Fonseca-Pinto, and Andrade (2010)	41	AF	O/N	Threshold-based		(81.0)	(95.0)	

Marcos, Hornero, Alvarez, del Campo, and Aboy (2010)	214	SpO_2	O^+/O^-	LDA	(93.0)	(97.0)	(79.3)	AUC (95.0)
Tagluk and Sezgin (2010)	21	AE	C/M/O	ANN	85.6			
Marcos, Hornero, Nabney, Alvarez, and del Campo (2011)	96	SpO_2	O^+/O^-	Threshold-based	(81.3)	(81.3)	(81.3)	AUC (87.0)
Guijarro-Berdinas, Hernandez-Pereira, and Peteiro-Barral (2012)	6	AF+TE	C/M/O	ANN	93.5	90.3	95.1	
Gutierrez-Tobal, Hornero, Alvarez, Marcos, and del Campo (2012)	148	AF	O^+/O^-	LRA	(82.4)	(88.0)	(70.8)	AUC (90.3)
Otero et al. (2012)	10	AF+SpO_2	A/N	Fuzzy rules	90.0			
Gutierrez-Tobal, Alvarez, Marcos, del Campo, and Hornero (2013)	148	AF	O^+/O^-	MLR, NN (MLP*, RBF)	(91.5)	(92.5)	(89.5)	PPV (94.9)
Koley and Dey (2013)	36	AF	A/N	SVM	94.9			
Maali and Al-Jumaily (2013)	5	AF+TE+AE	A/N	ANN				AUC 87.0
Morillo and Gross (2013)	115	SpO_2	O^+/O^-	PNN	(93.9)	(92.4)	(95.9)	AUC (96.1)
Selvaraj and Narasimhan (2013)	200	AF	A/N	Logical algorithm		(83.6)	(100)	PPV (72.3)
Thommandram, Eklund, and McGregor (2013)	8	TE	A/N	KNN		95.7	88.1	AUC 96.0
J. Zhang, Zhang, Wang, and Qiu (2013)	40	SpO_2	A/N	SVM	90.0			

Bianchi, Lipoma, Darling, Alameddine, and Westover (2014)	116	TE+AE	A/N	Event detection algorithm				AUC (92.0)
Carmes, Kempfner, Sorensen, and Jennum (2014)	109	TE+AE+SpO_2	A/N	Elastic net		(86.8)	(95.4)	AUC (97.9)
Koley and Dey (2014)	34	SpO_2	A/N	SVM	95.4			
Sanchez-Morillo, Lopez-Gordo, and Leon (2014)	115	SpO_2	Mi/Mo/Se/N	BHC	(82.6)			
Avci and Akbas (2015)	8	AF+TE+AE	A/N	RFC*, AdaBoost, RSS	98.7			F-measure 98
Ciolek, Niedzwiecki, Sieklicki, Drozdowski, and Siebert (2015)	30	AF	A/H	Envelope detection algorithm	95.0	90.0	96.0	
S. H. Huang et al. (2015)	387	SpO_2	O/N	Decision tree (C4.5)	(94.7)	(98.7)	(90.7)	g-means (94.6)
Jin and Sanchez-Sinencio (2015)	5	AF	A/N	Threshold-based		100	85.9	
Gutierrez-Tobal, Alvarez, del Campo, and Hornero (2016)	317	AF	A/N	AdaBoost (LDA, CART*)	(86.5)	(89.0)	(80.0)	
Kagawa, Tojima, and Matsui (2016)	35	TE+AE	Mi/Mo-Se	Threshold-based		96.4	100	AUC 100
Kaimakamis et al. (2016)	100	AF+TE+SpO_2	O/N	LRM*, Decision tree	(88.6)	(92.9)	(71.4)	
H. Lee, Park, Kim, and Lee (2016)	50	AF	A/H	Rule-based algorithm		(86.4)		PPV (84.5)
W. Huang et al. (2017)	30	AF+SpO_2	A/H	Respiratory events algorithm		97.6		PPV 95.7

Morales et al. (2017)	79	SpO_2	A/N	KNN*, LS-SVM	(93.7)	(96.9)	(78.6)	
Rolon, Larrateguy, di Persia, Spies, and Rufiner (2017)	954	SpO_2	Mi/Mo-Se	NN (MLP)	(85.8)	(85.6)	(85.9)	AUC (93.7)

[a]Signal symbols: AF = Airflow, AE = Abdominal effort, TE = Thoracic effort, and SpO_2 = Pulse oximetry.

[b]Decision symbols: A/N = Apnea or Normal, A/H = Apnea or Hypopnea, A/H/N = Apnea or Hypopnea or Normal, O/N = OSA or Normal, O^+/O^- = OSA positive or OSA negative, C/O = CSA or OSA, C/M/O = CSA or OSA or MSA, Mi/Mo-Se = Mild OSA or Moderate-to-Severe OSA, Mi/Mo/Se/N = Mild OSA or Moderate OSA or Severe OSA or Normal.

[c]Classification methods symbols: ANN = Artificial neural network, BHC = Binary hierarchical, CA = Clustering algorithm, CART = Classification and regression trees, CGE = Center of gravity engine, FCM = Fuzzy c-means, FIS = Fuzzy inference system, GLM = Generalized linear models, KM = k-means, KNN = k-nearest neighbors, LDA = Linear discriminant analysis, LRA = Logistic regression analysis, LRM = Linear regression model, LS-SVM = Least squares support vector machine, MLP = Multi-layer perceptron, MLR = Multiple linear regression, NN = Neural network, OLS = Orthogonal least squares, PLA = Piecewise linear approximation, PNN = Probabilistic neural network, QDA = Quadratic discriminant analysis, RBF = Radial basis function, RFC = Random forest classifier, RSS = Random subspace, SVM = Support vector machine, TDNN = Time-delay neural network.

[d]Metrics: Results based on per-recording detection are enclosed by brackets, whereas results without brackets indicate per-epoch detection.

[e]Decision symbols: Ac = Accuracy, AUC = Area under ROC curve, PPV = Positive predictive value, ROC = Receiver operating characteristic, Se = Sensitivity, Sp = Specificity.

2.3 Results

A year on year distribution of published articles for sleep apnea detection is shown in Figure 2.3. The number of published articles concerning each publication year is illustrated here. The bar chart shows an increasing tendency of use of respiratory and oximetry signals by year to detect sleep apnea in adults. The highest number of publications (11.3%) was found in the year 2010 and 2013 each. Table 2.3 displays the number and percent of articles found to detect sleep apnea using respiratory and oximetry signals and the number of articles used to make decisions on the types of sleep apnea. Of the 62 studies retrieved, 70.97% (44 articles) were categorized based off single respiratory or oximetry signal, whereas 29.03% (18 articles) based off multiple respiratory and oximetry signals (Table 2.3). Sleep apnea detection based on single signals was further clustered as: airflow (AF) signal based detection (22.58%, 14 articles), thoracic effort (TF) signal based detection (1.61%, 1 article), abdominal effort (AE) signal based detection (3.23%, 2 articles), and pulse oximetry (SpO_2) based detection (43.55%, 27 articles).

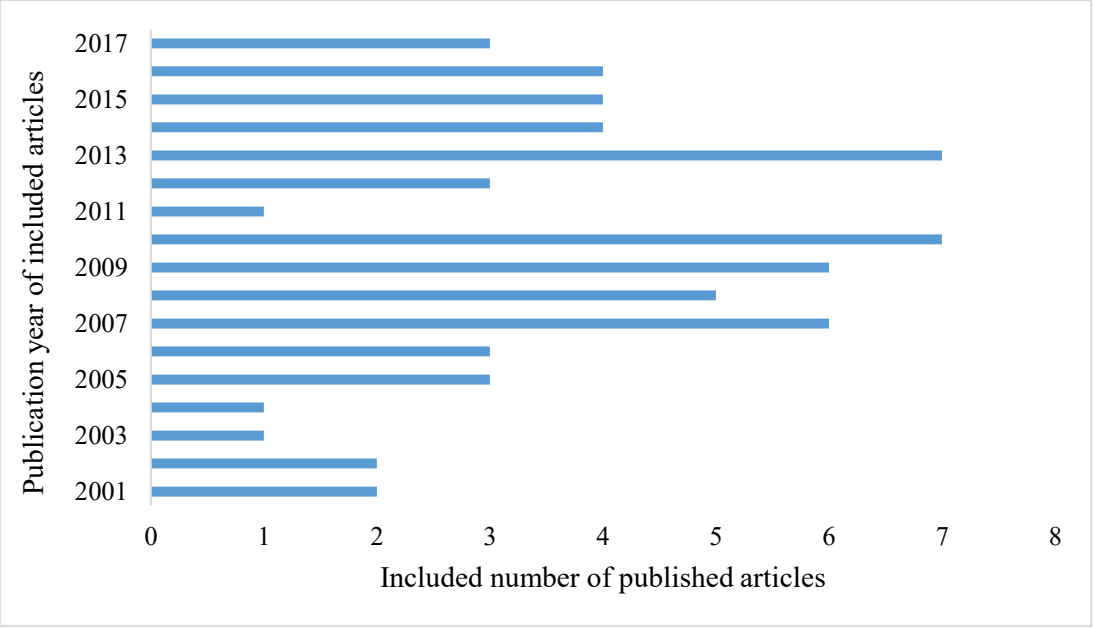

Figure 2.3. The proportion of articles employing respiratory and oximetry signals for sleep apnea detection.

In addition, as presented in Table 2.3, the decision-making process is substantiated by the following scenarios: applying a binary decision (in 54 articles, 87.09%) such as apnea or normal, apnea or hypopnea, OSA or normal, OSA positive or OSA negative, CSA or OSA, and mild OSA or moderate-to-severe OSA; a three-option decision (in 7 articles, 11.29%) such as apnea or hypopnea or normal and CSA or MSA or OSA; and a four-option decision (in 1 article, 1.62%) such as mild OSA or moderate OSA or severe OSA or normal.

Table 2.3. Decisions made based on single/multiple respiratory and oximetry signals.

Decision[a]	Single-signal[b]				Multi-signal	Number of articles (%)
	AF	*TE*	*AE*	*SpO_2*		
A/N	6	1		4	6	17 (27.42%)
A/H	4				2	6 (9.68%)
A/H/N					2	2 (3.23%)
O/N	2			2	2	6 (9.68%)
O^+/O^-	2			17	1	20 (32.26%)
C/O					1	1 (1.61%)
C/M/O			2		3	5 (8.06%)
Mi/Mo-Se				3	1	4 (6.45%)
Mi/Mo/Se/N				1		1 (1.61%)
Number of articles	14	1	2	27	18	62
%	22.58	1.61	3.23	43.55	29.03	(100%)

[a]Decision symbols: A/N = Apnea or Normal, A/H = Apnea or Hypopnea, A/H/N = Apnea or Hypopnea or Normal, O/N = OSA or Normal, O^+/O^- = OSA positive or OSA negative, C/O = CSA or OSA, C/M/O = CSA or OSA or MSA, Mi/Mo-Se = Mild OSA or Moderate-to-Severe OSA, Mi/Mo/Se/N = Mild OSA or Moderate OSA or Severe OSA or Normal.

[b]Signal symbols: AF = Airflow, AE = Abdominal effort, TE = Thoracic effort, and SpO_2 = Pulse oximetry.

2.3.1 Decision-making combined with classification methods

Decision-making on the sleep apnea types according to different classification methods is tabulated in Table 2.4. Sixty-two studies revealed single or a combination of classification methods that were clustered as follows: machine learning methods (64.52%), threshold-based methods (27.42%), and other methods (8.06%). A conceptual mind-map of different classification methods used in this review is depicted in Figure 2.4.

Machine learning (ML) has revolutionized the possibility to deal with large and complex data sets. Different ML approaches were applied to detect sleep apnea using respiratory and oximetry signals. Out of sixty-two, four studies applied multiple approaches of ML for detection purposes. In total, forty out of sixty-two studies applied different ML approaches that included 64.52% of total classification methods. ML approaches were further segmented as follows: neural networks (22.58%), linear methods (14.52%), regularization (1.61%), instance-based (11.29%), clustering (1.61%), dimensionality reduction (3.23%), ensemble learning (6.45%), and decision trees (3.23%).

The neural network (NN) is a powerful tool for data analytics. The aim of artificial neural networks (ANNs) is to perform tasks analogous to biological brains based on the connections

among many simple processing elements, known as neurons. These neurons are organized into layers, where outputs from one layer are used as inputs into the following layer. Other neural networks techniques reported in this review are time-delay neural network (TDNN), radial basis function (RBF) neural network (Haykin, 1994), multilayer perceptron (MLP) neural network, and the probabilistic neural network (PNN). A TDNN can recognize features independent of time-shift (Waibel, Hanazawa, Hinton, Shikano, & Lang, 1995). The RBF neural network is commonly used for modeling nonlinear problems through a fixed nonlinear transformation (Pombo, Garcia, Felizardo, & Bousson, 2014). An MLP is a class of feedforward ANN that utilizes a supervised learning technique and can distinguish data that are not linearly separable (Cybenko, 1989). Finally, the PNN introduced by Specht (1990) is also a feedforward NN that uses probability distributions.

Support vector machine (SVM) and least squares support vector machine (LS-SVM) (Suykens & Vandewalle, 1999) are the most popular linear methods for data analytics. Other linear methods found in this review are the logistic regression analysis (LRA) (Harrell Jr, Lee, Califf, Pryor, & Rosati, 1984), the multiple linear regression (MLR) (Draper & Smith, 2014), the linear regression model (LRM) (Efron, Hastie, Johnstone, & Tibshirani, 2004), the piecewise linear approximation (PLA) (Hamann & Chen, 1994), and the generalized linear model (GLM) (Nelder & Baker, 1972).

Another ML approach included in this study is the instance-based that includes the *k*-nearest neighbors (KNN) (Dudani, 1976) and the fuzzy rules (Zadeh, 1965). Less information is used in dimensionality reduction models to summarize or describe data. Two such techniques are the linear discriminant analysis (LDA) (Belhumeur, Hespanha, & Kriegman, 1997) and the quadratic discriminant analysis (QDA).

Ensemble learning obtains the overall detection by combining multiple independent models. Several methods observed are the AdaBoost (Bishop, 2006), the Bagging (Breiman, 1996), the binary hierarchical (BHC) (Casasent & Wang, 2005), the random forest classifier (RFC), and the random subspace (RSS). Decision tree (C4.5), clustering, and regularization (elastic net) techniques are also reported in this review.

The threshold-based classification methods are dependent on the selection of appropriate values (Coenen & Leng, 2007) or different limits (typically support and confidence thresholds). Seventeen articles out of sixty-two included in this study were based on threshold-based classification methods (Uddin et al., 2018). Five articles employed different algorithms for sleep apnea detection. The algorithms included in this study are the logical algorithms, event detection algorithms, envelope detection algorithms, rule-based algorithms, and respiratory events algorithms.

Table 2.4. Decision-making according to classification methods.

Decision[a]	Machine learning								Threshold-based	Other methods
	Neural networks	*Linear methods*	*Regularization*	*Instance-based*	*Clustering*	*Dimensionality reduction*	*Ensemble learning*	*Decision tree*		
A/N	1	4	1	4			3		3	2
A/H				3						3
A/H/N	2									
O/N		1						3	3	
O^+/O^-	5	6		1	1	2			8	
C/O		1								
C/M/O	5									
Mi/Mo-Se	1								3	
Mi/Mo/Se/N							1			
%	22.58	14.52	1.61	11.29	1.61	3.23	6.45	3.23	27.42	8.06

[a]Decision symbols: A/N = Apnea or Normal, A/H = Apnea or Hypopnea, A/H/N = Apnea or Hypopnea or Normal, O/N = OSA or Normal, O^+/O^- = OSA positive or OSA negative, C/O = CSA or OSA, C/M/O = CSA or OSA or MSA, Mi/Mo-Se = Mild OSA or Moderate-to-Severe OSA, Mi/Mo/Se/N = Mild OSA or Moderate OSA or Severe OSA or Normal.

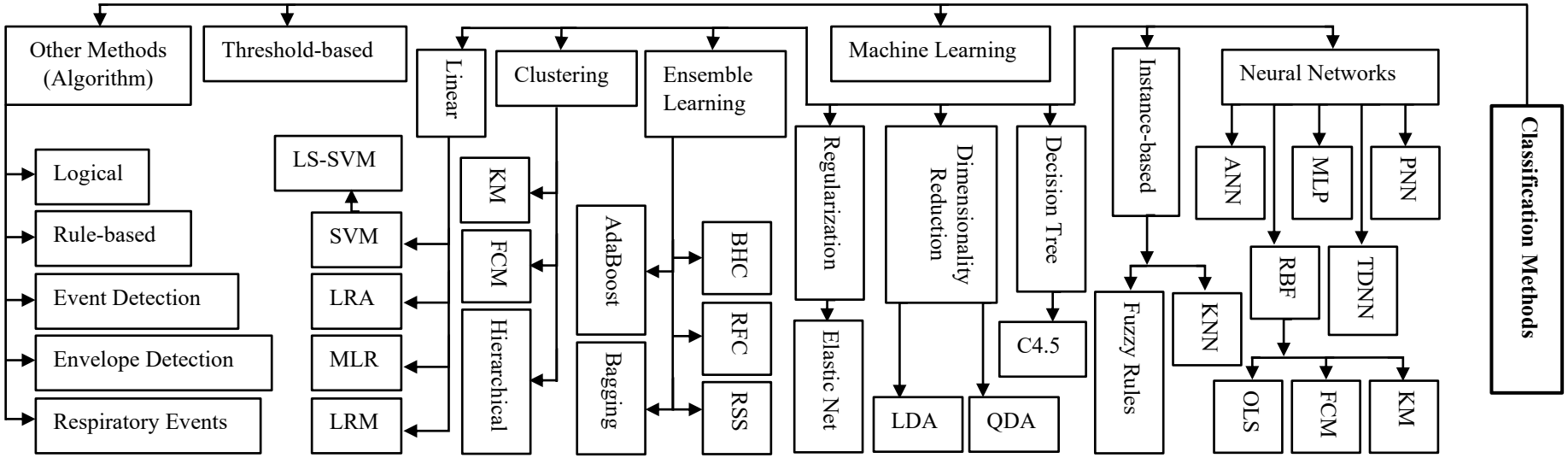

Figure 2.4. Mind map of the observed classification methods (machine learning, threshold-based, and other techniques).

2.3.2 Sleep apnea detection based on single signals

In this section, sleep apnea detection based on the single respiratory signals of AF, TE, and AE, and SpO_2 is discussed in the following four sub-sections considering the published articles.

The AF signal is the most important respiratory signal used to detect sleep apnea because the impact of airway obstruction is reflected in this signal. The authors of this review found 14 articles that used only an AF signal to detect sleep apnea as indicated in Table 2.2 and Table 2.3. Most of those articles distinguished between apnea and normal events using binary classification methods. Nazeran et al. (2001) reported poor performance of fuzzy inference systems (FIS) to detect apnea events using a respiratory AF signal from nine adults. Another approach to detecting sleep apnea applied an adaptive fuzzy logic to the AF signal of ten subjects (Morsy & Al-Ashmouny, 2006). Two classification engines (fuzzy logic-based and center of gravity) were used in series to distinguish normal and abnormal (apnea) events. This two-step, the adaptive approach allowed high accuracy and permitted testing with a large clinical dataset.

A daytime AF recording of short duration (5 min), as opposed to the occurrence of night-time apnea events, was proposed to separate obstructive and normal events (Salisbury & Sun, 2007). A nonlinear and nonstationary signal analysis technique (Hilbert–Huang transformation) was applied to extract features from the AF signal and a threshold-based technique resulted in significant advantages over the previous methods. Han et al. (2008) introduced a new algorithm to detect apneic events based on the mean magnitude of the second derivatives of the NAF signal. The suggested algorithm was found to be robust and useful due to a good overall agreement rate between the algorithm and manual scoring. An automated method was proposed by Otero et al. (2008) to distinguish apnea from hypopnea events by applying fuzzy set theory. Further evaluation of this proposed approach was needed due to the use of very small sample size (five subjects).

Caseiro et al. (2010) screened and separated OSA patients from normal using 5 min oronasal airway pressure signal during waking. Though the approach did not require a whole night of recording, the performance of the separation technique was poor. Two studies published by Gutierrez-Tobal et al. (2013) and Gutierrez-Tobal et al. (2012) used the same large dataset (148 patients) to distinguish between OSA positive and OSA negative. In the first study, an LRA model was used but performance improved using an MLP model in the second study. A real-time adaptive apnea event detection method was proposed by Koley and Dey (2013) using a two-stage classifier model. An SVM classifier was used to distinguish normal and abnormal (apnea) episodes that resulted in good accuracy. A per-second basis logical algorithm separated

apnea and normal patients but further improvement in the classification approach was needed to get acceptable performance (Selvaraj & Narasimhan, 2013).

Ciolek et al. (2015) reported an automated detection approach of apnea and hypopnea events using AF envelope tracking and achieved good accuracy that can be implemented in portable sleep apnea monitoring devices. A micro-electro-mechanical systems sensor-based home sleep apnea screening device was proposed by Jin and Sanchez-Sinencio (2015) that detected apnea and normal events using a threshold-based classification method. An AdaBoost algorithm reported by Gutierrez-Tobal et al. (2016) to distinguish normal and apnea patients with classification and regression trees (CARTs) resulted in good accuracy over LDA. H. Lee et al. (2016) proposed a rule-based algorithm for automatic real-time detection of apnea and hypopnea events using a NAF signal. The proposed approach achieved good performance for detecting apnea and hypopnea events regardless of AHI severity.

Sleep apnea detection using only a TE signal appears almost impossible and only one article was found that used a TE signal for the mentioned purpose (Table 2.2 and Table 2.3). Thommandram et al. (2013) used a chest movement waveform (also known as respiratory impedance signal) for sleep apnea detection. Four clinical features were extracted from each 1 min epoch of respiratory impedance waveform and a KNN classifier was used to separate apnea from normal epochs. The results of this study were promising but the size of the sample was small (only eight records) and demands further testing using a much larger dataset.

Two studies reported the application of an AE signal to distinguish central, mixed, and obstructive sleep apnea events (Table 2.2 and Table 2.3). In one study, AE signals were separated into spectral components using a multi-resolution wavelet transform (Akin & Sezgin, 2010). The coefficients of discrete wavelet transform were fed to the input of the ANN to separate the apnea types. Tagluk and Sezgin (2010) used sub-band spectral energy instead of wavelet coefficients to minimize the size of the input vector and reported improved performance. It should be mentioned here that the above two studies were not solely dependent on the AE signal but also used the AF signal in the initial stage. AF signals were used to select the corresponding sections of the AE signals related to sleep apnea events, and then the selected AE sections were used to extract features as well as to detect apnea events. It is almost impossible to distinguish sleep apnea types using an AE signal only.

Like the AF signal, SpO_2 is another important physiological signal used to detect sleep apnea. We found 27 articles that used only the SpO_2 signal to detect sleep apnea as listed in Tables 2.2 and Table 2.3. Zamarron et al. (2001) distinguished OSA positive and OSA negative patients with HR analysis from nocturnal pulse oximetry recording with poor accuracy, whereas Oeverland et al. (2002) reported comparatively improved performance separating mild and

moderate-to-severe patients using a threshold-based technique. Y. K. Lee et al. (2004) reported good detection accuracy using wavelet transform and global threshold with a very small sample size (seven subjects). Several articles used nonlinear analysis of nocturnal oximetry signal to distinguish OSA positive and OSA negative patients (Alvarez, Hornero, Abasolo, et al., 2006; Alvarez, Hornero, Garcia, et al., 2007; Alvarez, Hornero, Garcia, et al., 2006; Alvarez, Hornero, Marcos, et al., 2007; del Campo et al., 2006; Hornero et al., 2007; Marcos et al., 2011), whereas Marcos et al. (2007) and Alvarez, Hornero, et al. (2010) added spectral analysis with nonlinear analysis to improve performance. Marcos, Hornero, Alvarez, del Campo, Lopez, et al. (2008) and Marcos, Hornero, et al. (2008b) proposed NN, whereas Marcos, Hornero, et al. (2008a) applied a GLM-based classification method using features from linear and nonlinear analyses. The performance of different classifiers to detect OSA positive and OSA negative patients were reported by Marcos et al. (2009a), Marcos et al. (2009b), and Marcos et al. (2010), whereas Morillo et al. (2009) separated mild OSA from moderate-to-severe OSA patients using the threshold method.

An alternative proposal that promoted not only a transmission of oximetry data but also a real-time analysis of those data locally with a mobile device was presented by Burgos et al. (2010) and reported the best performance when using the Bagging classifier with an ADTree classifier. A novel multivariate system using PNN was proposed by Morillo and Gross (2013) that over-performed the existing univariate and multivariate approaches. J. Zhang et al. (2013) presented a real-time auto-adjustable smart pillow system for apnea detection and treatment but the approach needs further improvement in event detection. Koley and Dey (2014) used an SVM classifier to detect apnea from normal events, whereas Sanchez-Morillo et al. (2014) used a BHC classifier to detect four classes (mild, moderate, severe, and normal). A decision tree (C4.5) was applied to detect a large set of the obstructive and normal populations and reported good detection accuracy (S. H. Huang et al., 2015). A recent study (Rolon et al., 2017) reported a discriminative method to detect mild and moderate-to-severe patients using MLP NN. Another recent study by Morales et al. (2017) performed better with KNN than LS-SVM to detect apnea and normal subjects.

2.3.3 Sleep apnea detection based on multi-signals

A combination of different respiratory signals (AF, TE, and AE) and an oximetry or SpO_2 signal has been also used to detect sleep apnea. A combined application of AF, TE, and AE signals was used to detect apnea, hypopnea, and normal events (Varady et al., 2002), whereas only TE and AE signals were applied to distinguish central and obstructive events (Varady et al., 2003). Fontenla-Romero et al. (2005) detected different apnea types (central, mixed, and obstructive) using an ANN applying AF and TE signals, whereas Tian and Liu (2006) applied

AF and SpO_2 signals to detect apnea and hypopnea events using TDNN. Ng et al. (2008) used a threshold-based technique to separate apnea and normal events using AE and TE signals. Alvarez-Estevez and Moret-Bonillo (2009) applied three respiratory signals (AF, TE, and AE), and a SpO_2 signal to detect apnea and hypopnea events using fuzzy logic, whereas Kaimakamis et al. (2009) applied two respiratory signals (AF and TE) and a SpO_2 signal to separate obstructive and normal patients using a decision tree (C4.5) algorithm. Energy-based features were applied to an ANN to detect central, mixed, and obstructive events using TE and AE signals (Sezgin & Tagluk, 2009). Alvarez, Gutierrez, et al. (2010) applied a nonparametric threshold-based method to distinguish OSA positive and OSA negative subjects using AF and SpO_2 signals.

Guijarro-Berdinas et al. (2012) reported a good detection accuracy with an ANN. They used AF and TE signals with a small sample size to separate apnea types. Apnea and normal events were separated by a multivariable fuzzy temporal profile model (Otero et al., 2012) and an ANN (Maali & Al-Jumaily, 2013) using the different combinations of respiratory and oximetry signals. Combined signals were used to separate apnea and normal patients using an event detection algorithm (Bianchi et al., 2014) and elastic net classifier (Carmes et al., 2014). Avci and Akbas (2015) reported an outstanding detection accuracy where RFC was applied to detect apnea and normal events. Though the detection accuracy was very high, the sample size was small (eight subjects). Kagawa et al. (2016) using Doppler radar proposed a non-contact diagnosis of mild and moderate-to-severe OSA from TE and AE signals. LRM resulted in better than decision trees to detect obstructive and normal subjects (Kaimakamis et al., 2016). A very recent study by W. Huang et al. (2017) reported good precision in detecting apnea and hypopnea events using a respiratory events detection algorithm.

2.3.4 Per-epoch and per-recording based detection

Per-epoch- and per-recording-based detection is another distinguishing point of interest in this review. This review found 27 articles based on per-epoch detection (last four columns of Table 2.2, numbers not in brackets), whereas the remaining 35 articles were based on per-recording detection (indicated with brackets, Table 2.2). Per-recording detection was used to detect patients as OSA positive or OSA negative without addressing sleep apnea severity. On the other hand, per-epoch detection was used to detect each epoch as apnea or normal, and OSA positive or OSA negative. In the case of per-epoch detection, varying epoch length (5 s, 15 s, 30 s, 1 min, and so on) was applied. The selection of epoch length is critical. However, it is challenging to determine an epoch length that is suitable for good reliability and accuracy since it also depends on classification methods. It is currently not possible to guide how best to select epoch length or the entire recording that is equally applicable to all situations.

2.4 Discussion

In this study, the authors presented an overview of the respiratory and oximetry signals used to detect sleep apnea. The authors also presented the metrics (accuracy, sensitivity, specificity, and other parameters) of corresponding classification methods by conducting a systematic review study on articles published from 2001–2017. From a high-level overview, the observed detection of sleep apnea fell into two categories, single-signal (only one respiratory or oximetry signal) based and multi-signal (i.e. a combination of more than one respiratory and oximetry signal) based. Detection based on a single-signal was further sub-divided into the four signals of AF, TE, AE, and SpO_2. This review reveals that respiratory and oximetry signals have increasingly been used in sleep apnea detection. On the other hand, as presented in Table 2.3, decision-making was based on both respiratory and oximetry signals as well as classification methods (ML, threshold-based, and other techniques) (Table 2.4). The most common scenario observed was based on the use of the SpO_2 signal (43.55%) to detect sleep apnea and most of the decisions were made on binary classes.

2.4.1 Single and multi-signals for apnea detection

Single respiratory- or oximetry signal-based sleep apnea detection was done more in the case of binary classes (Ciolek et al., 2015; Gutierrez-Tobal et al., 2013; Y. K. Lee et al., 2004; Marcos et al., 2010), whereas multi-signal application was done to detect multi-classes (Guijarro-Berdinas et al., 2012; Sanchez-Morillo et al., 2014; Sezgin & Tagluk, 2009; Varady et al., 2002). AF and SpO_2 signals used separately to detect sleep apnea were effective, whereas TE and AE signals alone were almost unable to detect sleep apnea. A combined application of TE and/or AE with AF was effective for multiclass detection (Avci & Akbas, 2015; Varady et al., 2002), which was challenging when using a single respiratory or oximetry signal. A combination of the respiratory signals with the SpO_2 signal resulted in good detection accuracy (W. Huang et al., 2017; Otero et al., 2012).

Evidently, signals from both single-channel and dual-channel devices are used for binary decision-making (e.g., decision-making between apnea and normal) but not for multi decision-making (e.g., decision-making between CSA, OSA, MSA, and normal). Signals from multi-channel devices would be more effective because multi decision-making is also applied automatically to binary decision-making. Thus, the application of multi-signals from multi-parameter systems (e.g., acquisition of AF, TE, and AE with/without SpO_2) would be systematically better than a single-channel (e.g., acquisition of AF or SpO_2) or dual-channel (e.g., acquisition of AF and SpO_2) devices.

2.4.2 Major concerns and benefits

In addition to the use of respiratory and oximetry signals to detect sleep apnea, sample size and classification methods are the two major concerns for the evaluation of any sleep apnea detective systems. This review found the intensive use of ML methods for sleep apnea detection using respiratory and oximetry signals. Some ML methods (SVM, RFC, AdaBoost, and KNN) were comparatively better than other methods (FIS, ANN, LRA, and LDA). The choice of appropriate ML methods is critical with the use of respiratory and oximetry signals to get high detection accuracy. Despite high detection accuracy with certain classifiers, the sample size used was often small (Avci & Akbas, 2015; Guijarro-Berdinas et al., 2012; Jin & Sanchez-Sinencio, 2015). Studies that used highly specific datasets, which were confined to small samples, suffered from limitations of generalizability of results and thus, further investigation is needed to validate the generality of classification models to detect sleep apnea on large datasets or within different populations. Apart from yielding high performance, an automated system with acceptable accuracy remains a major concern.

The benefit of using oximetry signal to detect sleep apnea is its ease of use. The finger-tip pulse oximeter is comfortable for the patient, where respiratory sensors are not. Respiratory sensors are worn around the nose. These sensors can be uncomfortable and annoying for some patients. Though the respiratory sensors are uncomfortable, the respiratory signals are the fundamental signals for the reliable diagnosis of sleep apnea. Respiratory and oximetry signals without artefacts are reliable. The number of electrical cables required to acquire respiratory and oximetry signals is less than the other physiological signals such as EEG, ECG, and EMG. Moreover, the latter signals are easily affected by noise and complex processing is required to remove signal noise. On the other hand, the reliability of using respiratory and oximetry signals for sleep apnea detection is very high. Different devices have been developed which can record overnight respiratory and oximetry signals with good signal quality and less noise. Acquisition of good quality respiratory and oximetry signals would result in better detection of sleep apnea events and diagnosis.

2.4.3 Main challenges and limitations

PSG requires an exhaustive test in a hospital setting, skilled experts, high cost, and discomfort to the patient, so the implementation of a non-invasive, accurate, and home-based automated technique based on a simple set of respiratory and oximetry signals would be recommended. The main challenge of using respiratory and oximetry signals is to develop an accurate automated system to detect sleep apnea events. Acquisition of reliable, noise- and distortion-free respiratory and oximetry signals is paramount for an accurate sleep apnea

detection system. The acquisition of NAF using a nasal pressure transducer is superior to using thermal-based oronasal AF sensors. Thermal sensors detect a change in the temperature of exhaled air. However, they may fail to detect minor, although significant, changes in AF. Thus, they may underestimate hypopneas (Norman, Ahmed, Walsleben, & Rapoport, 1997). SpO_2 acquisition usually uses finger-based sensors rather than a forehead reflectance oximeter. Overnight recording of SpO_2 using forehead sensors is quite challenging and can cause patient discomfort and thus affect sleep quality. On the other hand, a finger-based oximeter is less obtrusive and easy to incorporate in a home-based sleep apnea detection system.

Despite a higher sleep apnea detection rate reported in several articles using different classification methods (Avci & Akbas, 2015; Guijarro-Berdinas et al., 2012; Jin & Sanchez-Sinencio, 2015), some major challenges exist with ML techniques. Firstly, a high detection rate was reported mostly in articles that used a small sample size or a fixed number of records from a fixed database. The overall detection accuracy changes with the sample size and database used. For this reason, the accuracy of those detection methods may deviate when the same methods are applied to other datasets or a greater proportion of records. Secondly, each ML technique is linked to a basic step of feature extraction. Features selection is an optional stage used when the number of features extracted is numerous and some of them are redundant. Extraction and selection of many weakly relevant and redundant features are the key reasons for poor detection accuracy. On the other hand, efficient feature extraction and sometimes robust feature selection should result in good detection of sleep apnea events. It is difficult to extract relevant and distinguishing features as well as to manage efficient and robust features from a wide range of features sets. Thirdly, selecting an appropriate classification method to provide reasonable, reliable, and consistent decisions is very critical. The selection of any classification method is need-based and depends on the nature of the extracted and selected features set. Finally, appropriate training of ML classifiers is a pre-requisite to getting better testing accuracy. Inappropriate training of ML classifiers results in poor performance. If the ML classifiers are poorly trained or overtrained, the testing accuracy will be affected. In addition, parameter selection and training time are two crucial points when training a classifier. Training time increases when new samples are added and thus affect the performance of the classifier. It is challenging to manage the above criteria that deal with ML classifiers to obtain acceptable detection accuracy.

Several automated methods of sleep apnea detection have already been developed (Bianchi et al., 2014; Ciolek et al., 2015; Marcos et al., 2010) but the reliability reported is not quite high enough to implement in practical cases. In addition, many researchers have employed a single oximetry signal to detect sleep apnea (Alvarez, Hornero, Abasolo, et al., 2006; Alvarez, Hornero, et al., 2010; Marcos et al., 2007; Marcos, Hornero, Alvarez, del Campo, Lopez, et al., 2008;

Marcos et al., 2009a) and reported accuracy close to 90%. It is challenging to achieve a higher accuracy (e.g. over 90%). However, further improvement in accuracy would be possible, for example, by (1) employing multiple signals such as AF and SpO_2. In addition, in the case of apnea type detection, the inclusion of respiratory efforts (TE and/or AE) with an AF signal is mandatory in designing an automatic algorithm and (2) incorporating multiple logics into an automatic algorithm. Multiple logics should be designed in such a way that they can accurately detect the apnea changes readily. Inclusion of accurate and multiple logics based on updated scoring rules of respiratory events (Berry et al., 2012) is mandatory to design more efficient automatic algorithms for sleep apnea detection, and (3) by using large clinical datasets for validation of automated system performance.

Some limitations of this review should be mentioned. Firstly, some studies included in this review did not report clearly on the performance metrics used for sleep apnea detection. Secondly, only English-language publications were included.

2.5 Sleep Apnea Diagnosis using EEG

In an attempt to identify existing literature that addressed sleep apnea diagnosis using EEG signals and to inform the timing of EEG arousal and total sleep time, a brief systematic search of the literature was conducted. We found limited studies where the EEG signals were used. Liu, Pang, and Lloyd (2008) reported a neural network method to detect OSA based on the EEG signal with a 91% accuracy. Another study performed by Alvarez, Hornero, Marcos, del Campo, and Lopez (2009) investigated EEG signal in addition to SpO_2 signal to diagnose sleep apnea and reported sensitivity (91%), specificity (83.3%), and accuracy (88.5%). Tagluk and Sezgin (2011) reported an artificial neural network to detect sleep apnea from the EEG signal. The detected global accuracy was 96.15% with a low sample size (n = 20).

Not only a very limited number of studies employed EEG to diagnose sleep apnea, but the performance of the detection approaches was also poor. Whilst one study reported high accuracy (96.15%), the sample size (n = 20) was very small. In addition, no studies reported the detection and incorporation of EEG arousal for the automatic diagnosis of sleep apnea. For the proper diagnosis of sleep apnea, respiratory (especially AF) and oximetry signals are indispensable for apnea and hypopnea detection. In addition, inclusion of an EEG signal permits evaluation of arousal from sleep. Moreover, total sleep time estimation requires the EEG analysis of sleep and wake epochs. The spectral analysis of EEG would be a possible option to link respiratory events (apnea and hypopnea) with its corresponding arousals.

2.6 Summary

The systematic literature review has synthesized and summarized the existing methods based on respiratory and oximetry signals to diagnose sleep apnea. Sixty-two studies were examined and the main findings are summarized as follows. A single respiratory signal, AF or SpO_2, provided good support for binary class decision-making, whereas multiple respiratory signals (AE, TE, and AE) combined with SpO_2 signal resulted in better multi-class decision-making in sleep apnea diagnosis. Several ML techniques, specifically the SVM and KNN, were by far more accurate than other methods and thus selection of appropriate ML approaches with appropriately selected respiratory and oximetry signals would be effective for sleep apnea detection. Despite certain benefits associated with the use of respiratory and oximetry signals, major concerns remained: high accuracy is yet to be achieved with the automated detection technique. In addition, large and/or multiple samples of data should be included especially from a clinical perspective. Moreover, the inclusion of EEG signal along with AF and SpO_2 would result in improved performance by detecting arousals. Thus, the next chapter, Chapter 3, addresses the power spectral analysis of EEG signal during and after apnea termination.

Chapter 3

Sleep Apnea duration and its effect on EEG

3.1 Introduction

The automatic analysis of AF and SpO_2 can detect apnea and hypopnea events but hypopneas associated with arousal cannot be identified without EEG analysis. In addition, the EEG spectral power would vary with the duration of respiratory events, since arousal from sleep usually occurs after an event is terminated. This chapter examined if EEG spectral power was altered with varying apnea durations before and after apnea termination. This study was carried out for the purpose of justifying the usability of EEG for the automatic diagnosis of sleep apnea. The power spectral changes for all apnea duration groups before and after apnea termination were not significantly different. Thus, the inclusion of EEG signals in automatic diagnosis would not be helpful to distinguish apnea from normal epochs.

3.1.1 EEG rhythms/frequency bands

Electroencephalography (EEG) is usually described in terms of rhythmic activity that is divided into frequency bands. These frequency bands are extracted using spectral methods (for instance Welch) as implemented in EEG software. Most of the cerebral signals observed in the scalp EEG fall in the range of 0.5-30 Hz. Activity below or above this range is considered artefacts, under standard clinical recording techniques. EEG is subdivided into bandwidths known as delta, theta, alpha, sigma, beta, and gamma.

Delta is the frequency range up to 4 Hz. It tends to be the highest in amplitude and the slowest waves. It is seen normally in adults in slow-wave sleep (Figure 3.1a). Theta is the frequency range from 4 to 8 Hz. Theta is seen normally in young children. It may be seen in drowsiness or arousal in older children and adults; it can also be seen in meditation (Figure 3.1b). Alpha is the frequency range from 8 to 12 Hz. It emerges with closing of the eyes and with relaxation and attenuates with eye opening or mental exertion (Figure 3.1c). Stage 2 sleep is characterized by sleep spindles (transient runs of rhythmic activity in the 12-14 Hz range). These sleep spindles are sometimes referred to as the sigma band (Figure 3.1d). Beta is the frequency range from 14 to 30 Hz. Beta activity is closely linked to motor behavior and is generally attenuated during active movements. Low-amplitude beta with multiple and varying frequencies is often associated with active, busy, or anxious thinking, and active concentration (Figure 3.1e). Gamma is the frequency range approximately above 30 Hz. Gamma rhythms are thought to represent binding of different

populations of neurons together into a network for the purpose of carrying out a certain cognitive or motor function (Figure 3.1f).

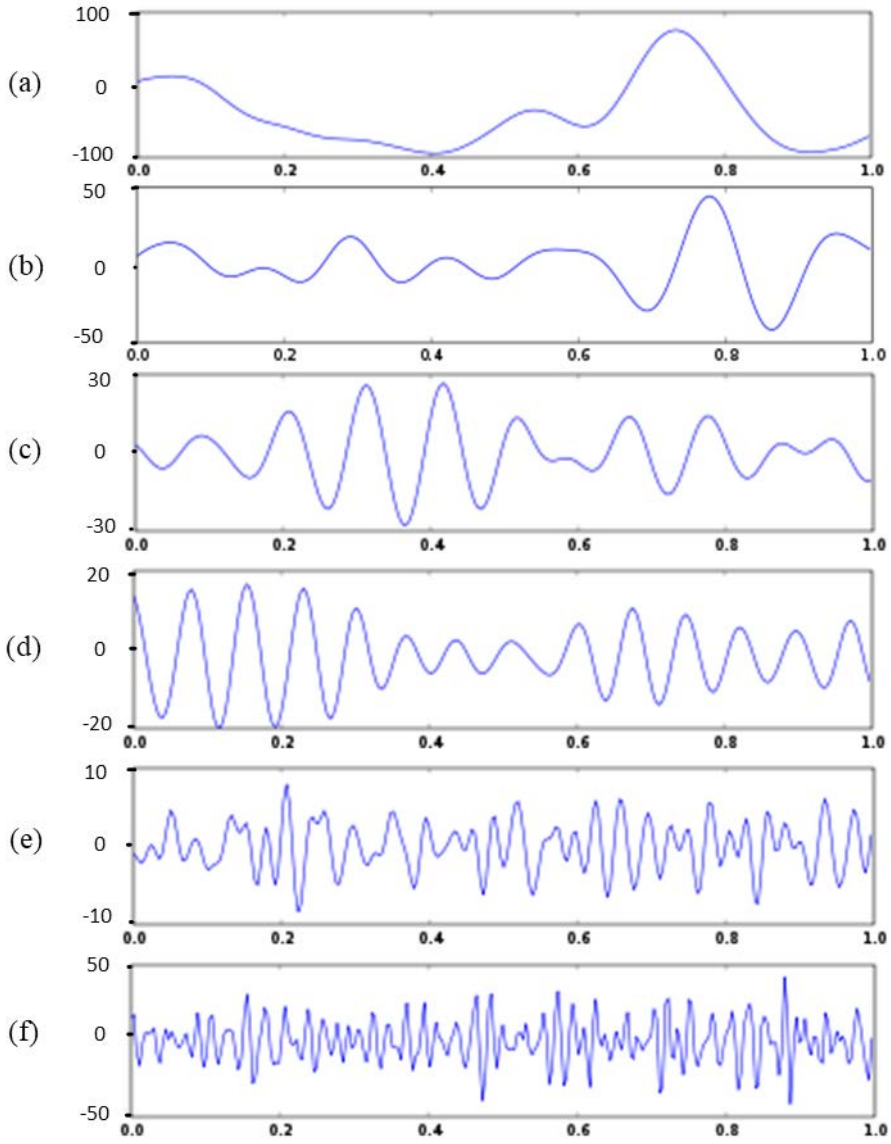

Figure 3.1. EEG rhythms or frequency bands (time in second and amplitude in mV are shown in x and y-axis respectively).

3.1.2 EEG spectral power

EEG, the recording of electrical activity generated by the cortex and thalamus, provides an objective method for detecting dynamic changes in cortical function. The EEG shows different patterns of electrical activity, which is characterized by typical frequency bands. The EEG of a normal human shows activity over the range of 1–30 Hz with amplitude in the range of 20–100 μV (Muthuswamy & Thakor, 1998). The ranges of delta (δ), theta (θ), alpha (α), sigma (σ) and

beta (β) frequency bands are 0.5–4 Hz, 4–8 Hz, 8–12 Hz, 12–14 Hz and 14–30 Hz, respectively (Yang et al., 2010).

Spectral analysis is a very useful tool to assess the EEG power in different frequency bands (Muthuswamy & Thakor, 1998). The delta wave (0.5–4 Hz), a high amplitude brain wave, appears in non-rapid eye movement (NREM) stage N3 slow-wave sleep (SWS) or deep sleep (Schulz, 2008). Theta waves (4–8 Hz) are usually observed at the first stage of sleep (Dement & Kleitman, 1957) when people are mentally fatigued or drowsy (Scher, 2017), whereas sigma waves (12–14 Hz) (known as sleep spindles) appear in NREM stage N2 light sleep and play an essential role in both sensory processing and long-term memory consolidation (Holz et al., 2012). Alpha waves (8–12 Hz) are generally considered the dominant frequency in human adults (Broughton & Hasan, 1995) and observed best during wakeful relaxation with closed eyes (Aminoff, 2012). Beta waves (14–30 Hz) are high-frequency, low-amplitude brain waves that are commonly observed in an awakened state and linked to increased alertness and arousal (Abhang, Gawali, & Mehrotra, 2016).

During an apnea episode, airway obstruction results in a reduced O_2 level with a corresponding rise in CO_2. Respiratory arousal occurs when a certain (threshold) level of inspiratory effort is reached (Gleeson et al., 1990). Thus, an altered degree of chemoreceptor stimulation (reduced O_2 and increased CO_2) has a direct influence on the timing of apnea termination (Kimoff et al., 1994). Respiratory-induced cortical arousal is associated with EEG desynchronization. These cortical arousals often follow rather than precede an airway opening (the resumption of breathing) (Younes, 2004). The changes in the EEG are usually visible in the EEG records. For some apneas, these changes are not visible. Despite the lack of visible changes, cortical activity fluctuates at apnea termination (Dingli et al., 2002). EEG is extremely useful for investigating the dynamic changes of cortical activities, especially at apnea termination.

3.1.3 Previous work and research question

Several studies investigated the changes in EEG power before, during, and after apnea episodes. Dingli et al. (2002) studied the changes in cortical activity at apnea termination in 15 sleep apnea patients (aged 51 ± 9 years). No significant changes were found in spectral bands other than theta between two 10-s EEG epochs before and after apnea termination. Normalized theta power (4–8 Hz) decreased significantly after the termination of apnea. The changes in theta powers were found to be consistent during NREM and rapid eye movement (REM) sleep. In contrast to these findings, (Xavier, Behbehani, Watenpaugh, & Burk, 2007), in 13 subjects (aged 49.08 ± 8.82 years) previously diagnosed with OSA, found a significant decrease in normalized delta power (1–4 Hz) and a significant increase in normalized theta (4–8 Hz), alpha (8–12 Hz) and sigma (12–16 Hz) power after apnea termination. These discrepant findings require further investigation.

In a group of male OSA patients (aged 55 ± 6.10 years, $N = 15$), a significant decrease in delta (<4 Hz) power was observed during OSA compared to before and after OSA (Coito, Belo, Paiva, & Sanches, 2011). In eight children (aged 2–8 years) with OSA, a significant decrease in delta (0.5–4.5 Hz) power was also observed during OSA, but with a rebound increase after OSA termination (Bandla & Gozal, 2000). Finally, Yang et al. (2012) observed a significant fall in delta (0.75–4 Hz) and theta (4.1–8 Hz) powers after event termination in 20 children (aged 7–12 years). These EEG changes were associated with cortical arousals.

The dynamic changes in EEG spectral power are well investigated across apnea events (before, during, and after) as well as at apnea termination (before and after). The apnea duration increases with the progression of the night (Charbonneau et al., 1994). It remains unknown if the dynamic changes that occur in the EEG spectral power at apnea termination vary as the duration of the apnea episode is prolonged. The present study tests the hypothesis that EEG spectral power at apnea termination will vary according to changes in apnea duration. To investigate the changes related to apnea termination, the power spectrum of the EEG signal has been analyzed. The dynamic changes in EEG spectral powers were compared between apnea duration groups.

3.2 Methods

3.2.1 PSG records

The Sleep Heart Health Study (SHHS) is a multi-center cohort study implemented by the National Heart Lung & Blood Institute to determine the consequences of sleep disorders (Quan et al., 1997; G. Q. Zhang et al., 2018). Participants were recruited from nine existing epidemiological studies in which data on cardiovascular risk factors had been collected previously. The participants who met the following inclusion criteria were invited to participate in the examination of the SHHS:

- age 40 years or older
- no history of the treatment of sleep apnea
- no tracheostomy
- no current home oxygen therapy

Polysomnograms (PSG) were obtained in an unattended setting, usually in the homes of the participants, by trained and certified technicians. The recording montage consisted of:

- C3/A2 and C4/A1 electroencephalograms (EEGs), sampled at 125 Hz
- right and left electrooculograms (EOGs), sampled at 50 Hz

- a bipolar submental electromyogram (EMG), sampled at 125 Hz
- thoracic and abdominal excursions, recorded by inductive plethysmography bands and sampled at 10 Hz
- airflow, detected by a nasal-oral thermocouple and sampled at 10 Hz
- finger-tip pulse oximetry sampled at 1 Hz
- electrocardiogram (ECG) from a bipolar lead, sampled at 125 Hz
- Heart rate derived from the ECG and sampled at 1 Hz
- body position

3.2.2 Demographics and apnea scoring

PSG records (anonymous) were collected from freely available, large, and recognized datasets of the SHHS. The present study included nocturnal PSG records of patients who had been diagnosed with sleep apnea and excluded records of patients with tracheostomy and oxygen therapy. The records of patients who had major medical illnesses (e.g., hypertension, diabetes, or neurological disorders) or who had taken medications (e.g., EEG active drugs) were excluded. Thirty PSG records were chosen according to the selection criteria stated above. The mean ± SD (standard deviation) of age and body mass index (BMI) of selected records of corresponding patients (20 male, 10 female) were 68.17 ± 9.95 years and 26.95 ± 4.04 kg m^{-2} respectively.

The University of Technology Sydney Human Research Ethics Committee considered the research Nil/Negligible risk and provided an ethics application number [UTS HREC ETH17-2041] for tracking purposes.

According to the American Academy of Sleep Medicine (AASM) updated scoring rules (Berry et al., 2017; Berry et al., 2012), an experienced sleep physiologist who was blind to the objective of this investigation verified all apnea events scored from each record. The sleep physiologist also reported the event duration for each apnea event. Based on event duration, all apnea events from each record were categorized into three groups: Short (between 10 and 20 s), Moderate (between 20 and 30 s), and Long (between 30 and 40 s). Five apnea events from each duration group were randomly selected, yielding 15 apnea events from each record. This selection process yielded an equal distribution of apnea events for each duration group over the 30 PSG records. Of these, there were two records where the number of apnea events in the Moderate apnea duration group was less than five. Moreover, in seven records, apnea events of Long-duration were not found, resulting in an unequal sample size among the apnea duration groups. Thus, a total of 375 apnea events were selected from all the records for power spectral analysis.

Each selected apnea event from the 375 episodes was further checked for corresponding sleep state and apnea type. For accurate determination of the sleep state and apnea type, the

AASM updated manual (Berry et al., 2017; Berry et al., 2012) was followed. Thus, each selected apnea event was labeled with its corresponding sleep state (i.e., NREM or REM sleep) and apnea type (i.e., obstructive, central, or mixed) for all apnea duration groups (Table 3.1). No mixed apnea event was found in this study.

Table 3.1. Number of apnea events for apnea duration groups, apnea types, and associated sleep states.

Groups	No. of apnea events	No.[a]			No. of apnea events associated with their respective sleep states[b]	
		OSA	*CSA*	*MSA*	*NREM sleep*	*REM sleep*
Short	150	107	43	0	122	28
Moderate	144	116	28	0	102	42
Long	81	81	0	0	52	29
Total	375	304	71	0	276	99

[a]Apnea types: OSA = Obstructive sleep apnea, CSA = Central sleep apnea, MSA = Mixed sleep apnea

[b]Sleep states: NREM = Non-rapid eye movement, REM = Rapid eye movement

3.2.3 EEG processing and spectral power calculation

Using a finite impulse response (FIR) low-pass filter with a cut-off frequency at 32 Hz (Oppenheim, Willsky, & Young, 1983), artefact-free C3/A2 and C4/A1 EEGs were filtered to remove unwanted frequency responses. Two 10-s EEG epochs (immediately before and after the apnea termination) were clipped from all apnea events for power spectral analysis, as shown in Figure 3.2. The power spectral analysis was performed separately for each 10-s epoch using the Welch method of averaged periodograms (Welch, 1967), as shown in Figure 3.3. Using the Simpson's rule (Cartwright, 2016) instead of the trapezoidal rule (Atkinson, 2008) for the better spectral approximation, the areas under the spectral curve that corresponded to the average power of delta (δ: 0.5–4 Hz), theta (θ: 4–8 Hz), alpha (α: 8–12 Hz), sigma (σ: 12–14 Hz) and beta (β: 14–30 Hz) frequency bands were calculated. The relative (percentage) powers of each frequency band were calculated for each 10-s epoch.

3.2.4 Statistical analysis

To determine whether there are any statistically significant differences between the means of two or more independent groups, statistical analysis was performed using SPSS software (Nie, Bent, & Hull, 1970). For the comparison of relative spectral powers between the Short, Moderate and Long apnea duration groups, a Kruskal–Wallis H test (Corder & Foreman, 2009) was applied, satisfying all assumptions. The distribution of relative spectral powers of all spectral bands was similar for all apnea duration groups, as assessed by visual inspection of a boxplot. The Kruskal–

Wallis test was also conducted to compare the proportion of apnea events associated with the sleep states and apnea types between apnea duration groups. A p-value <0.05 was considered statistically significant. The selection procedure for the Kruskal–Wallis H test and the associated statistical analysis are described in ***Appendix A***.

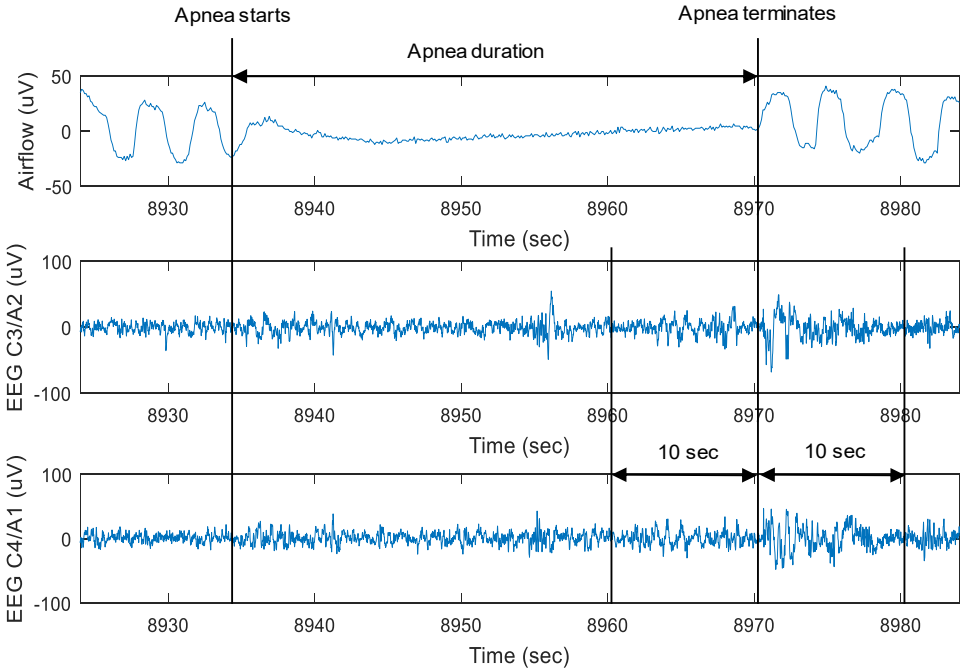

Figure 3.2. Apnea duration with corresponding 10-s EEG epochs at apnea termination.

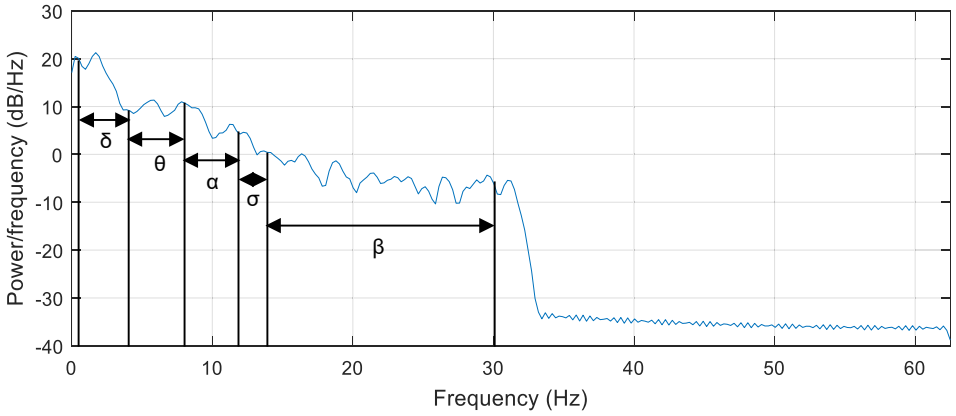

Figure 3.3. Estimating power spectral density of a 10-s EEG epoch using the Welch method.

3.3 Results

3.3.1 Spectral powers

Delta power. Before apnea termination (BAT): the median relative delta powers showed non-significant differences between apnea duration groups. After apnea termination (AAT): a

marginal significance was observed for C3 and C4 EEGs, with non-significant differences between groups (Table 3.2) (Uddin, Su, Chen, & Chow, 2019).

Table 3.2. Statistical findings of different frequency bands with their apnea duration groups.

Frequency bands	EEG channels	Epoch Position[a]	Median spectral powers[b] (%)			Significance	
			Short	*Moderate*	*Long*	$\chi^2(2)$	*p*
Delta	C3	BAT	58.39	59.59	64.72	2.009	0.366
		AAT	60.90	56.66	64.25	5.033	0.081
	C4	BAT	56.60	58.89	62.46	3.407	0.182
		AAT	57.09	55.20	61.29	4.953	0.084
Theta	C3	BAT	18.95	18.37	19.80	0.347	0.841
		AAT	15.64	16.56	15.52	1.440	0.487
	C4	BAT	20.68	18.53	19.86	1.161	0.560
		AAT	17.60	17.49	13.86	10.982	0.004
Alpha	C3	BAT	10.57	9.11	8.47	5.732	0.057
		AAT	9.98	11.60	7.62	6.286	0.043
	C4	BAT	11.03	10.56	8.73	7.941	0.019
		AAT	10.62	11.25	8.86	4.669	0.097
Sigma	C3	BAT	2.91	2.62	2.04	8.052	0.018
		AAT	2.44	2.68	1.95	15.028	0.001
	C4	BAT	2.83	2.77	2.34	1.474	0.479
		AAT	2.80	3.16	2.37	5.828	0.054
Beta	C3	BAT	5.68	5.18	4.42	1.254	0.534
		AAT	6.31	7.71	5.84	1.046	0.593
	C4	BAT	6.70	5.90	6.26	1.814	0.404
		AAT	7.41	8.99	7.96	2.291	0.318

[a]Positions of 10s EEG epochs: BAT = Before apnea termination, AAT = After apnea termination

[b]Spectral powers: median values are expressed instead of the mean for nonparametric analysis.

Theta power. BAT: differences in the median relative theta powers between groups were not statistically significant for C3 and C4 EEGs. AAT: the median relative theta powers were significantly different ($p = 0.004$) between the apnea duration groups for C4 EEG (Table 3.2). Subsequent post hoc analysis (Dunn's test with a Bonferroni correction) revealed statistically significant differences between the Short and Long ($p = 0.009$), and Moderate and Long ($p = 0.007$) groups, but not between the Short and Moderate groups (Figure 3.4b) (Uddin et al., 2019).

Alpha power. BAT: the median relative alpha powers were significantly different ($p = 0.019$) between the apnea duration groups for C4 EEG. Subsequent post hoc analysis revealed statistically significant differences in median relative alpha powers between the Short and Long

(p = 0.016) groups, but not between the Short and Moderate, and Moderate and Long groups (Figure 3.5b). AAT: the median relative alpha powers were significantly different (p = 0.043) between the groups for C3 EEG. Subsequent post hoc analysis revealed statistically significant differences between the Moderate and Long (p = 0.037) groups, but not between the Short and Moderate, and Short and Long groups (Figure 3.5a) (Uddin et al., 2019).

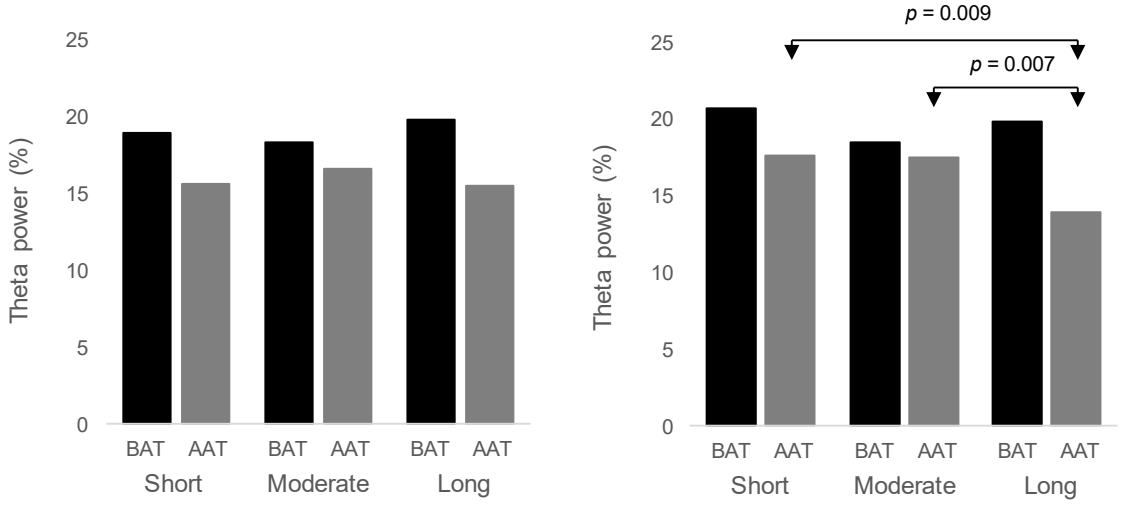

Figure 3.4. Median relative theta powers in apnea duration groups for (a) C3 and (b) C4 EEG.

Sigma power. BAT: the median relative sigma powers were significantly different (p = 0.018) between the apnea duration groups for C3 EEG. Subsequent post hoc analysis revealed statistically significant differences between the Short and Long (p = 0.033), and Moderate and Long (p = 0.028) groups, but not between the Short and Moderate groups (Figure 3.6a). AAT: the median relative sigma powers were significantly different (p = 0.001) between the groups. Subsequent post hoc analysis revealed significant differences between the Short and Long (p = 0.008), and Moderate and Long (p < 0.0005) groups, but not between the Short and Moderate groups (Figure 3.6a) (Uddin et al., 2019).

Beta power. BAT: the median relative beta powers showed non-significant differences between apnea duration groups. AAT: the differences between groups were not significantly different for C3 or C4 EEG (Table 3.2) (Uddin et al., 2019).

Apnea event-wise relative spectral powers (for delta, theta, alpha, sigma, and beta bands) at BAT and AAT for C3 EEG are tabulated in ***Appendix B*** and ***Appendix C*** respectively. Similarly, ***Appendix D*** and ***Appendix E*** respectively indicate the event-wise relative spectral powers at BAT and AAT for C4 EEG.

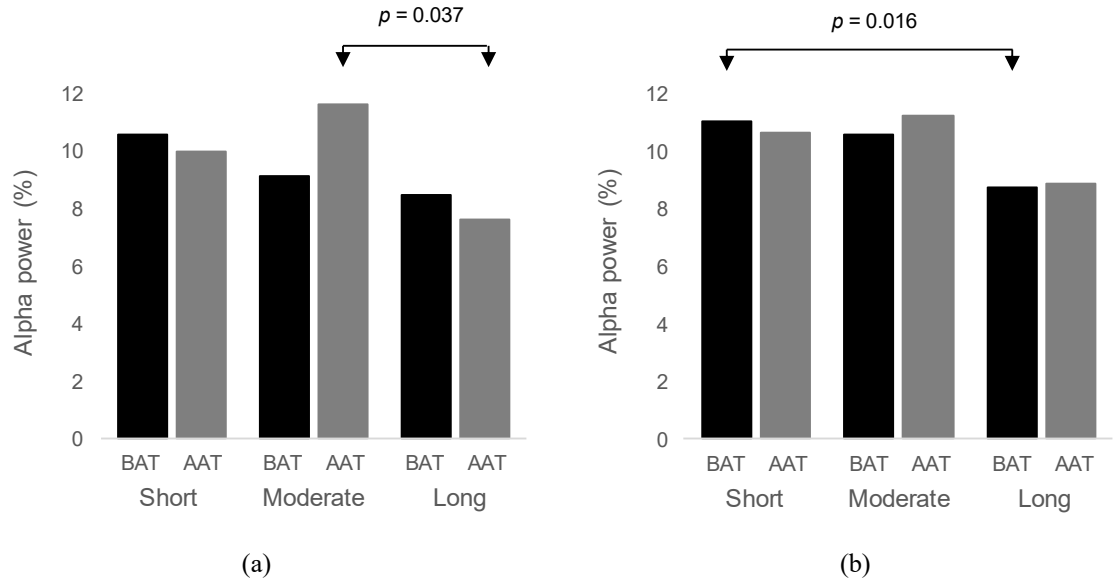

Figure 3.5. Median relative alpha powers in apnea duration groups for (a) C3 and (b) C4 EEG.

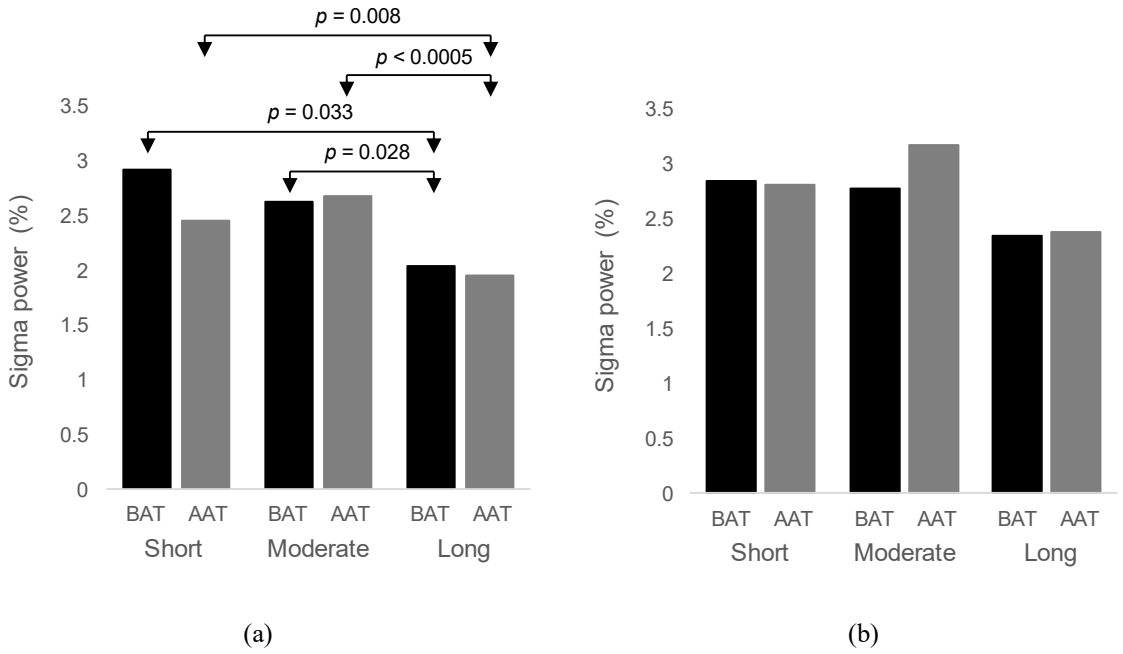

Figure 3.6. Median relative sigma powers in apnea duration groups for (a) C3 and (b) C4 EEG.

3.3.2 Apnea events as a function of sleep state

In NREM sleep, the proportion of apnea events decreased as the apnea duration increased, reflecting a significant linear trend from the Short to Moderate to Long apnea duration groups (p = 0.002), whereas an increased but non-significant trend was observed for REM sleep (p = 0.451) (Figure 3.7a). The differences between apnea duration groups were statistically significant (p = 0.004) for NREM sleep but were not significant (p = 0.483) for REM sleep as shown in Table 3.3. Pairwise comparisons revealed statistically significant differences in the proportion of apnea events between the Short and Long (p = 0.002) groups, but not between the Moderate and Long

(p = 0.134), and Short and Moderate (p = 0.452) groups (Figure 3.7a) (Uddin et al., 2019). Apnea event-wise sleep states are tabulated in ***Appendix F***.

3.3.3 Apnea events as a function of apnea type

The proportion of CSA events decreased as the apnea duration increased, reflecting a significant trend from the Short to Moderate to Long apnea duration groups (p = 0.001) with zero Long apnea episodes found, whereas an increased but non-significant trend was observed for OSA events (p = 0.977) (Figure 3.7b). The differences between apnea duration groups were significant (p = 0.001) for CSA events but were not statistically significant (p = 0.591) for OSA events as shown in Table 3.4. Subsequent post hoc analysis revealed statistically significant differences in the proportion of CSA events between the Short and Long ($p < 0.0005$) groups, but not between the Moderate and Long (p = 0.053), and Short and Moderate (p = 0.342) groups (Figure 3.7b) (Uddin et al., 2019). Apnea event-wise apnea types are tabulated in ***Appendix F***.

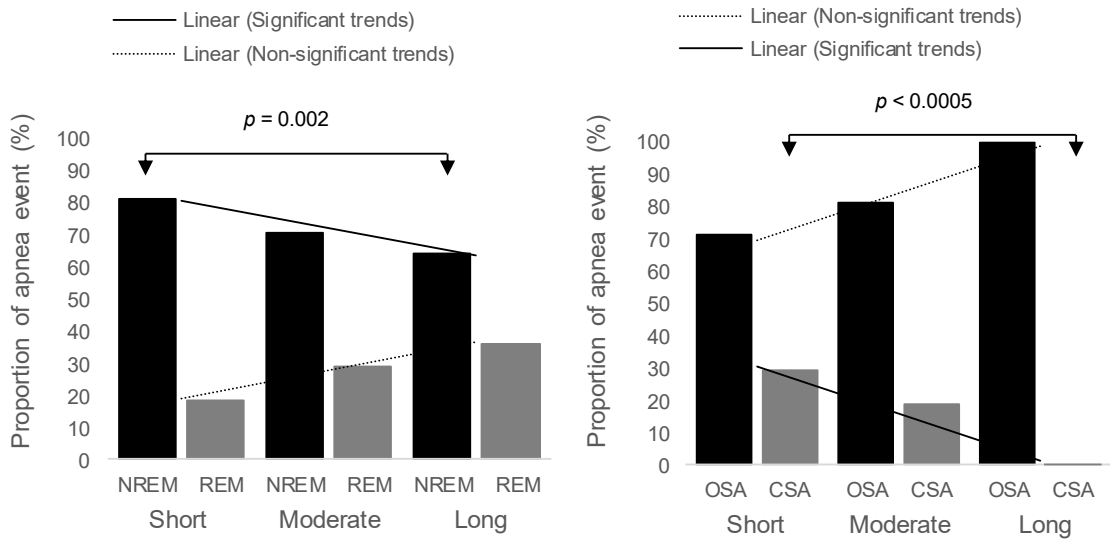

Figure 3.7. The proportion of apnea events as a function of (a) sleep states and (b) apnea types.

Table 3.3. Statistical findings for the analysis of sleep states between apnea duration groups.

Sleep states[a]	Sample size			Significance	
	Short	*Moderate*	*Long*	$\chi^2(2)$	*p*
NREM	122	102	52	11.216	0.004
REM	28	42	29	1.454	0.483

[a]Sleep states: NREM = Non rapid eye movement, REM = Rapid eye movement

Table 3.4. Statistical findings for the analysis of apnea types between apnea duration groups.

Apnea types[a]	Sample size			Significance	
	Short	*Moderate*	*Long*	$\chi^2(2)$	*p*
OSA	107	116	81	1.054	0.591
CSA	43	28	0	14.834	0.001

[a]Apnea types: OSA = Obstructive sleep apnea, CSA = Central sleep apnea

3.4 Discussion

In this study of EEG spectral power as a function of apnea duration, we report two original observations. (a) Changes in apnea duration greatly influenced the relative powers of EEG frequency bands, where the spectral powers differ between brain regions (C3 and C4). Significantly, lower theta, alpha, and sigma powers (low-frequency bands) were observed for the Long compared to the Moderate and Short apnea duration groups. However, no significant differences were found for the lowest (delta) and highest (beta) frequency bands for both EEG channels. (b) The proportion of apnea events showed a significantly decreased trend with increased apnea duration for NREM sleep but not REM sleep. In addition, the proportion of CSA events decreased with increased apnea duration but not OSA (Uddin et al., 2019).

3.4.1 Apnea duration and relative EEG powers

It would be expected that long-duration apneas caused a more marked decrease in end-apnea arterial O_2 saturation and increased CO_2 (Bowes, 1984; Kimoff et al., 1994). These chemical stimuli (hypoxemia and hypercapnia) increased the chemoreceptor drive that led to end-apnea arousal (Bowes, 1984). Thus, the longer the apnea duration, the greater the chemoreceptor stimuli, serving to arouse an individual faster. Our data confirmed that physiological changes were associated with changes in brain EEG.

Our data reported a significant reduction in EEG powers for lower frequency alpha and sigma bands in the Long (between 30 and 40 s) compared to the Moderate (between 20 and 30 s) and Short (between 10 and 20 s) apnea duration groups before apnea termination (BAT), consistent with a greater level of EEG arousal for apneas of longer duration (>30 s). It was not surprising that beta power did not show significant increases. Non-significant changes in beta powers between apnea duration groups indicate that the patients were not in an alert state regardless of apnea duration length, in line with a low level of beta activity observed (Table 3.2). These findings suggest that for longer duration apneas, transient arousals occurred in association with lower alpha and sigma powers than for the shorter duration apneas. Moreover, the low level of beta power

confirmed that awakenings were not experienced before apnea termination. These EEG observations are entirely consistent with theoretical expectations. Additionally, outright awakenings were scored as awake episodes and were not part of the records analyzed in this paper.

In addition to the significantly lower alpha and sigma powers seen in the Long than in the Moderate or the Short apnea duration groups at BAT, a reduction in theta powers was also seen following apnea termination (AAT), which lent support to the previous findings of Dingli et al. (2002) but contrasted with the findings of Xavier et al. (2007). It is clear that at apnea termination, a more extensive EEG arousal had occurred, coincident with a reduction in the EEG powers of all three low-frequency bands of theta, alpha, and sigma.

Notably, non-significant changes were observed for the delta power between apnea duration groups. However, in the present study, a relatively low proportion of apnea events was found in stage N3 (slow-wave sleep/deep sleep), which may explain why delta power was not altered. It is known that sleep apnea severity was reduced markedly during N3 compared to lighter stages (N1 and N2) of NREM sleep (Marcuse, Fields, & Yoo, 2015).

Electroencephalogram (EEG) spectral powers at the left (C3) and right (C4) hemispheres reveal nearly an identical pattern (Schramm et al., 2000). Sometimes, hemispheric asymmetries exist because of the difference in gender (Armitage, 1995) or application of different analysis methods (linear and non-linear) (Cvetkovic, Ubeyli, Holland, & Cosic, 2010). In this study, the changes found between C3 and C4 spectral powers may be due to any of the aforementioned factors.

3.4.2 Apnea duration as a function of sleep state and apnea type

The present study showed that the proportion of apnea events is linked to sleep states and apnea types to the change of apnea du- ration. Long-duration apneas were least found in NREM sleep (Figure 3.7a). On the other hand, long apneas were more common in REM sleep, although the linear trend was not significant. These results confirmed that the threshold for arousal was significantly higher in REM sleep (permitting longer apneas with a greater O_2 desaturation being tolerated) than NREM sleep (Kass, Akers, Bartter, & Pratter, 1996; Series, Cormier, & La Forge, 1990; Younes, 2004). Besides, as the night progressed, the proportion of REM sleep increased (Charbonneau et al., 1994) as a result of circadian timing, along with the appearance of more obstructive episodes. It is conceivable that reduced apnea episodes may be recorded because of truncated REM sleep, if patients wake earlier under the conditions of a clinical laboratory.

Long-duration apneas contained virtually no central apnea events in this sample (Figure 3.7b). Presumably, an absence of the central respiratory drive could mean the cessation of life, if

not restored. Thus, it would be expected that sufficient stimuli (e.g., elevated brain interstitial fluid pH) would be necessary to provide a drive to breathe (Nattie & Li, 2009) in response to breathing cessation of central origin. The absence of CSA events in the Long apnea group contrasted with the highest proportion of OSA, consistent with a previous study (Series et al., 1990).

3.4.3 Study limitations

This study has some limitations. We carried out spectral power calculations in different frequency bands of EEG before and after apnea termination. The incorporation of an additional method, for example, the Hilbert transform, to check instantaneous frequency would be logical and can be addressed in future studies. The sample size among apnea duration groups was unequal. In practical cases, it is almost impossible to get an equal sample size for all groups, because the PSG records or patient data did not contain all three groups of apnea duration, especially the Long group where CSA was absent. The total number of CSA events in all groups was small. Thus, it is not possible to make clear statements about CSA events. Because of the absence of MSA events, this study has failed to make any comparison of MSA events within the apnea duration groups. In addition, the study did not include all apnea events in entirety from each overnight sleep recording. Further studies on the relative spectral powers between apnea duration groups with large datasets are recommended.

3.5 Summary

We examined the EEG spectral power changes, which were not distinguishable with varying apnea durations either before or after apnea termination. Thus, EEG spectral power analysis would not be effective as a method to detect apneic events. Based on these results, the justification was made to exclude the EEG signal for automatic diagnosis of sleep apnea.

Chapter 4

Automatic Diagnosis of Sleep Apnea

4.1 Introduction

An automatic diagnosis is independent of any human effort. Sleep apnea diagnosis using EEG signals is associated with several challenges. The study (Chapter 3) found that the EEG spectral power varied for some frequency bands but not for other bands. The EEG spectral powers were not uniform for all apnea events. In addition, it would be challenging to link hypopnea events with the changes of EEG spectral power or arousal. Moreover, the acquisition and processing of EEG for an automatic diagnosis is challenging. Thus, EEG signals are often excluded from the automatic approach for sleep apnea diagnosis. Airflow and oximetry are the pertinent signals upon which the actual scoring of apnea and hypopnea events is based on. As summarized in our systematic review, respiratory (especially airflow) and oximetry signals are reliable for sleep apnea diagnosis. In addition, these signals can be easily acquired throughout the night and their processing is easy and reliable. This chapter addresses the design and function of an automatic algorithm for the diagnosis of sleep apnea using airflow and oximetry signals.

Sleep apnea, the most common breathing disorder during sleep, is characterized by the complete (apnea) or partial (hypopnea) cessation of breathing (Berry et al., 2017; Berry et al., 2012). The total number of apnea and hypopnea events per hour of sleep is known as the apnea hypopnea index (AHI) that measures the severity of sleep apnea as normal (0≤AHI <5), mild (5≤ AHI <15), moderate (15≤ AHI <30), and severe (AHI ≥30) (Grover & Pittman, 2008; Kryger, 2000).

Sleep apnea significantly decreases the quality of sleep and can lead to respiratory, cardiovascular, and cerebrovascular diseases (Young, Peppard, & Gottlieb, 2002). Early diagnosis of sleep apnea is required for appropriate treatment to reduce long-term health risks. Nocturnal polysomnography (PSG) is considered the gold standard and a reliable method for sleep analysis and sleep apnea diagnosis (Kushida et al., 2005). Skilled personnel in sleep technology monitor and manually review the overnight study for scoring apnea and hypopnea events according to the American Academy of Sleep Medicine (AASM) guidelines (Berry et al., 2017). This manual scoring process, whilst an accepted reference standard, is costly and time-consuming with inter-scorer variability (Rosenberg & Van Hout, 2014).

Automatic processes have been developed obviating the manual process. Different automatic techniques employing different physiological signals have been applied for sleep apnea diagnosis, although not without limitations:

Minute-by-minute annotation and classification: In the period 2000-2019, much sleep apnea classification techniques focus attention on the ECG signal from the Apnea-ECG database. The recordings of this database (Penzel, Moody, Mark, Goldberger, & Peter, 2000) were segmented into minutes and each minute was annotated as 'apnea' or 'normal'. It follows that minute-by-minute annotation was provided as a standard for ECG recordings. Many studies (Al-Angari & Sahakian, 2012; de Chazal et al., 2003; Hassan & Haque, 2017; Mendez et al., 2010; Sharma & Sharma, 2016; Urtnasan, Park, Joo, & Lee, 2018; Zarei & Asl, 2019) that followed used the minute-by-minute annotations as a standard. However, these minute-by-minute annotations yield an AHI that greatly deviates from conventional scoring and reporting. The automated minute-classification approach potentially confuses sleep apnea diagnosis against the established guidelines for scoring and interpretation of AHI and make a difficult comparison of AHI between studies.

Exclusion of airflow or oximetry: Apnea and hypopnea events are required for AHI computation as per AASM scoring guidelines (Berry et al., 2017), and the detection algorithm is based on the recommended signals of airflow (AF) and pulse oximetry (SpO_2) (Uddin et al., 2018). Although several studies (Han et al., 2008; Otero et al., 2012) have reported automatic detection of apnea events, these algorithms are not useful for sleep apnea diagnosis due to exclusion of hypopnea events. In addition to AF reduction criteria, at least 3% oxygen desaturation from pre-event baseline is required for scoring a hypopnea event (Berry et al., 2017). Although several studies (Ciolek et al., 2015; H. Lee et al., 2016; Otero, Felix, & Alvarez, 2011) reported an automated method for detecting apnea and hypopnea events using only AF reduction criteria. Detecting an hypopnea event without satisfying oxygen desaturation criteria is not in alignment with the AASM guidelines. Omission of SpO_2 would correctly detect apnea events, since oxygen desaturation is not included in the AASM criteria for apnea, but would lead to incorrect detection of hypopnea events and raise the question of accuracy of these approaches. In contrast, several studies reported sleep apnea diagnosis using oximetry signal where the AF signal was omitted (Gutiérrez-Tobal, Álvarez, Crespo, Del Campo, & Hornero, 2018; Jung et al., 2018). Oxygen saturation, as a single signal, cannot be reliably used to diagnose sleep apnea since it dissociates from the basic criteria of AF drop.

Lag time in oxygen desaturation: A lag time in oxygen desaturation typically of 10 to 30 s (Otero et al., 2012) is observed with oximetry. Thus, the effective design of an automatic approach using AF and SpO_2 signals requires the adjustment of the time lag. W. Huang et al. (2017) reported

the detection of apnea and hypopnea events using AF and SpO_2 signals from 30 subjects. However, the study did not correct for this lag time. Technically, this lag time may interfere with the accurate detection of hypopnea events, where a ≥30% drop from baseline AF is not aligned with a ≥3% desaturation.

Hypopnea with arousal: The updated AASM guidelines incorporated the arousal criteria for the scoring of hypopnea events (Berry et al., 2017). A hypopnea is scored when the AF reduction criteria is associated with a ≥3% oxygen desaturation or an arousal. Designing an automatic algorithm using AF and SpO_2 signals may be challenging, where hypopnea detection is required to satisfy the above criteria. The study by W. Huang et al. (2017) underestimated the hypopnea event detection by applying ≥3% oxygen desaturation criteria without incorporating events with arousal and thus reported poor agreement between the scored and detected AHI. A reliable method is required that can satisfy the updated criteria for hypopnea detection.

Total sleep time (TST) approximation: In addition to detecting the total number of apnea and hypopnea events, the computation of TST is required for conventional reporting of AHI (total events per hour of TST). Though several studies reported AHI, the TST was manually added (Ciolek et al., 2015; Koley & Dey, 2013; H. Lee et al., 2016). Thus, these approaches were not fully automated. Not surprisingly, most of the single-channel and dual-channel automatic approaches that employed total recording time (TRT) had reported poor AHI agreement (de Almeida et al., 2006; Grover & Pittman, 2008; Nakano, Tanigawa, Furukawa, & Nishima, 2007; Nakano et al., 2008; Ragette, Wang, Weinreich, & Teschler, 2010; Rathnayake, Wood, Abeyratne, & Hukins, 2010; Rofail, Wong, Unger, Marks, & Grunstein, 2010; Shochat et al., 2002; Ward et al., 2015; Wong et al., 2008). However, Erman, Stewart, Einhorn, Gordon, & Casal (2007) reported good performance with an AHI cut-off 15 but the performance greatly decreased with other AHI cut-offs.

Small validating dataset: The reliability of automatic algorithm depends on the validation results with a large dataset. The automatic approaches have been reported with high accuracy, where the performance parameters were extracted from a smaller validation dataset e.g., from 78 to 121 records (Álvarez et al., 2020; Ayappa, Norman, Seelall, & Rapoport, 2008; Chai-Coetzer et al., 2011; de Oliveira et al., 2009; Masdeu, Ayappa, Hwang, Mooney, & Rapoport, 2010; Ward et al., 2015). Machine-learning and other logic-based diagnostic approaches usually shows significantly reduce performance when validated with a different and/or large dataset, and hence most of the automatic studies recommended to validate the designed algorithm with a large dataset (Álvarez et al., 2020).

4.1.1 Research questions

This study reports a fully automatic algorithm for the diagnosis of sleep apnea from the AF and SpO_2 signals. The new technique applied resolved the above-mentioned limitations and addressed three novel concepts: (1) detection of apnea and hypopnea events using AF envelope tracking and a digitization process that aligned with the updated AASM guidelines, (2) application of an estimated TST instead of TRT for the automatic determination of AHI, and (3) validation of the automatic algorithm with an extremely large dataset of 943 recordings.

4.2 Methods

4.2.1 PSG records and demographics

The Sleep Heart Health Study (SHHS) provides a wide range of overnight PSG records (anonymous) with all severity groups of sleep apnea (normal, mild, moderate, and severe) (Quan et al., 1997; G. Q. Zhang et al., 2018). It provides two datasets: shhs1 (5793 records) and shhs2 (2651 records). The SHHS also provides the manually scored AHI of each PSG record according to the updated AASM guideline (Berry et al., 2017; Berry et al., 2012). In short, an apnea event was scored when there was a complete cessation of breathing and the duration of the complete cessation was ≥10 s. A hypopnea event was scored when the AF peak excursion dropped by ≥30% of its baseline (partial cessation of breathing) with a duration of drop ≥10 s and this AF reduction is associated with ≥3% oxygen desaturation from the pre-event baseline or an arousal.

It is obvious that the inclusion of all PSG records from the SHHS is not an affordable task. To avoid bias in the PSG record selection from the SHHS, the present study collected the first one thousand PSG records from the shhs1 dataset (records id: shhs-200001 to shhs-201003 that includes 3 missing records). The SHHS recorded the airflow signal by an oronasal thermocouple, whereas fingertip pulse oximeter was used to detect oxygen saturation. Airflow (AF) and pulse oximetry (SpO_2) signals were extracted from the above mentioned one thousand records. Twelve records were excluded due to the unavailability of AF (i.e., AF was in form of a flat line or random noise throughout the night). Thus, 988 records were included in the current study. Forty five out of 988 records were randomly selected for the development of the automatic algorithm and the remainder 943 records form the validation dataset. No records were excluded due to the poor signal quality or insufficient sleep time (TST <3 h). Table 4.1 shows the summary of demographics and manually scored data reported in the SHHS. The overall and record-wise demographics and scoring details are tabulated in ***Appendix G***.

The University of Technology Sydney Human Research Ethics Committee considered the research Nil/Negligible risk and provided an ethics application number [UTS HREC ETH17-2041] for tracking purposes.

Table 4.1. Demographic and scoring summary of PSG records.

	Development set	Validation set
Subjects (N)	45	943
Males n (% of N)	29 (64.4)	461 (48.9)
Females n (% of N)	16 (35.6)	482 (51.1)
Age (years)	61.3 ± 10.1	57.2 ± 11.3
BMI ($kg.m^{-2}$)	25.7 ± 4.1	27.5 ± 5.1
TRT (h)	8.2 ± 0.7	8.3 ± 0.7
TST (h)	6.0 ± 1.0	6.0 ± 1.1
AHI (events/h)	32.1 (1.7 – 93.5)	16.4 (0 – 121.3)

Data are presented as n (% of N), mean ± standard deviation or mean (range) unless otherwise stated. BMI: Body mass index; TRT: Total recording time; TST: Total sleep time; AHI: Apnea hypopnea index.

4.2.2 Designing an automatic diagnostic algorithm

The design of the automatic algorithm for the diagnosis of sleep apnea was based on AF and SpO_2 signals. The AF and SpO_2 signals were loaded as the inputs to the automated process. Total sleep time (TST) was estimated from the auto-analysis of input signals. Apnea events were detected from AF, whereas hypopnea events were detected from AF and SpO_2 signals. Apnea hypopnea index (AHI) was estimated from the total number of detected apneas and hypopneas divided by estimated TST. The automatic process finally delivered the output in the form of estimated AHI. Thus, the overall automatic process can be divided into the following four parts: (i) TST estimation, (ii) detection of apnea events, (iii) detection of hypopnea events, and (iv) estimation of AHI, as depicted in Figure 4.1. Each part of the automatic process is explained in the next section.

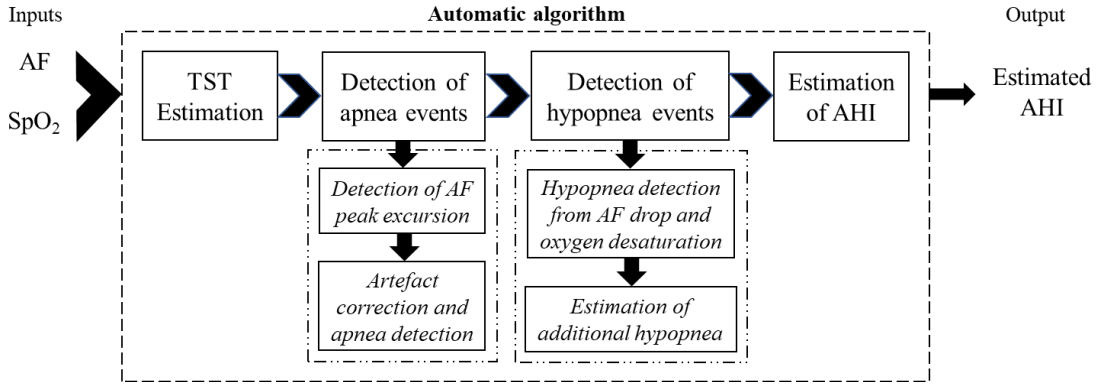

Figure 4.1. Flowchart of the automatic diagnostic process.

(i) **TST estimation**: In this study, an automatic approach is proposed to estimate TST from AF and SpO_2 signals. Rather than using the TRT for calculating AHI per hour, this study determined the timing and duration of major artefact detected in the AF and SpO_2 signals. The awake time was discounted in two ways: 1) where a recording was not terminated (thus prolonging the recorded study time), the potential period of the major artefact was assessed via detection of sensor connections. For example, removal of the oximeter sensor showed oxygen saturation clearly fell to zero (Figure 4.2a), and thus the 'major artefact' was detected and 2) where a signal had dropped out near the end of a study with random noise, e.g., in the AF signal (Figure 4.2b), the entire period of random noise was detected as the 'major artefact'. The combined analysis of AF and SpO_2 signals yielded the total duration of the 'major artefact', which was then subtracted from the TRT to determine the modified recording time (MRT).

For the development set, the mean difference between scored TST (reported in the SHHS) and TRT was found to be -2.2 h (an overestimation is indicated by a negative sign) (Table 4.2). This overestimation was the consequence of incapacity to include in the analysis the awake EEG during the sleep period. In addition, any 'major artefact' was removed from the TRT, yielding the MRT. The mean difference observed between scored TST and MRT was -1.5 h (Table 4.2). The overall overestimation was reduced by approximately 32% (the percentage overestimation was calculated with respect to the initial overestimation of -2.2 h) when MRT was used instead of TRT.

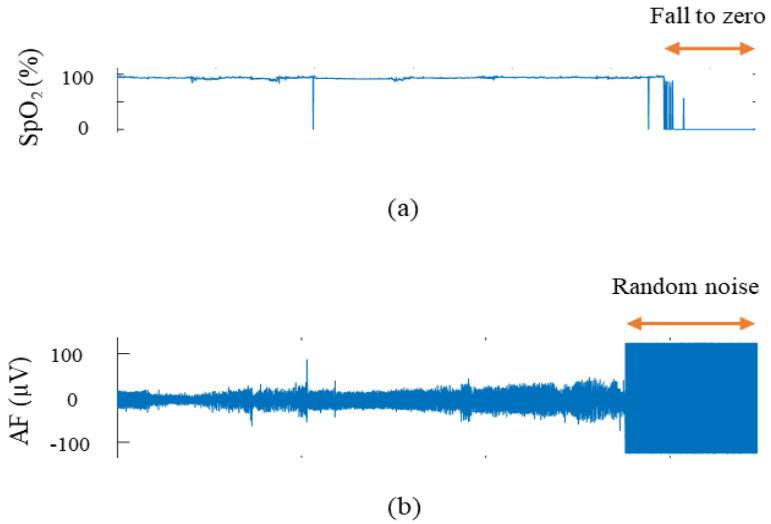

Figure 4.2. Detecting the duration of major artefacts.

This method represented an optimization approach that resulted in improved correlation with the scored TST, since an automatic approach cannot recognize the 'wake' period during sleep and movement arousals. Table 4.2 displays the mean difference between scored TST and %MRT against the percentage of MRT. The lowest mean difference of 0.02 h was observed against 80%MRT, whereas other percentages of MRT resulted in comparatively greater mean differences

(overestimation or underestimation). Thus, an 80%MRT (i.e., 0.8MRT) was finally applied as the estimated TST.

Table 4.2. Estimation of total sleep time from total recording time for the development set.

Parameter	Mean difference between scored TST and parameter (h)	Standard deviation (h)
TRT	-2.2	1.18
MRT	-1.5	1.02
90% of MRT (= 0.9MRT)	-0.75	0.98
80% of MRT (= 0.8MRT)	**+0.02**	**0.95**
70% of MRT (= 0.7MRT)	+0.77	0.93
60% of MRT (= 0.6MRT)	+1.52	0.93

'+' and '-' signs respectively indicate the mean underestimation and overestimation.
TST = total sleep time (scored), MRT = modified recording time (detected).

(ii) **Detection of apnea event**: The raw AF was smoothed using a 3-point moving average filter to produce the smoothed AF as illustrated in Figure 4.3. In time-domain analysis, this smoothing process is very effective in retaining the overall original signal amplitude by reducing the random noise.

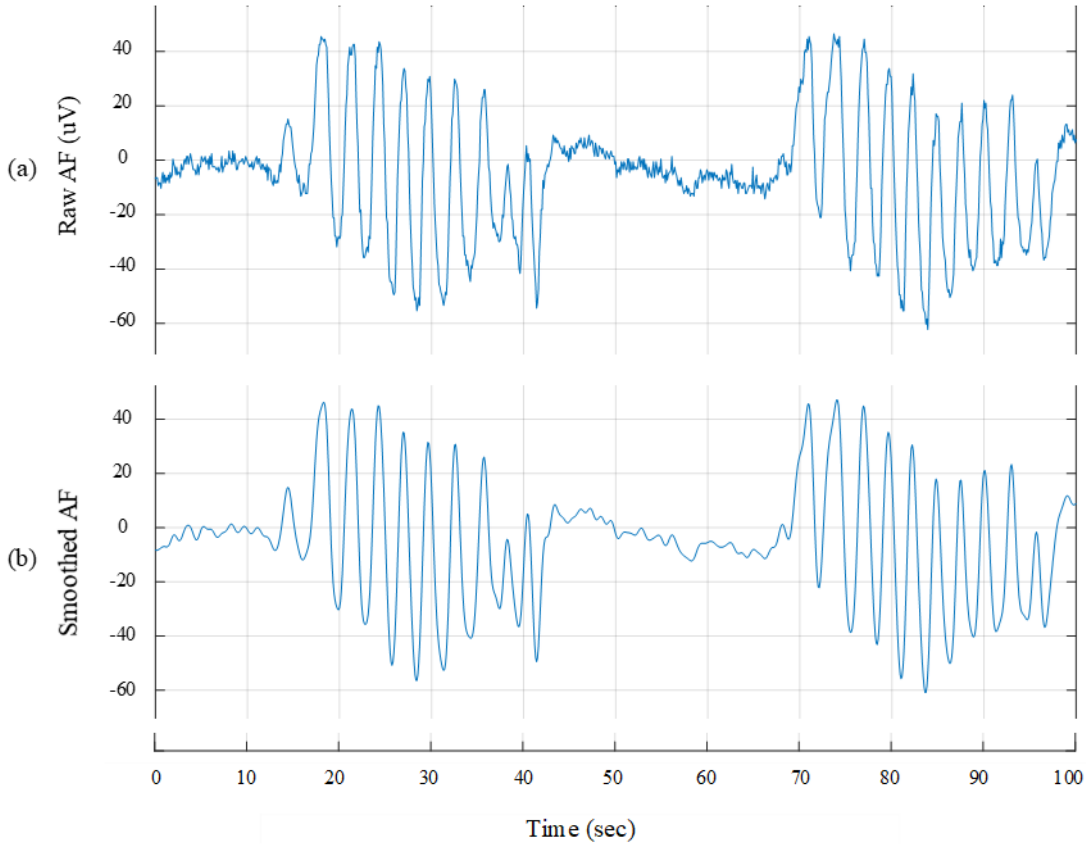

Figure 4.3. Preprocessing of the raw AF signal.

Detection of AF peak excursion: A single breath consists of two phases: inhalation and exhalation as depicted in Figure 4.4a. The maximum amplitude of inhalation is known as peak (top), whereas the minimum amplitude of exhalation is called trough (bottom). The vertical height difference between the peak and trough is called peak-to-trough amplitude or peak excursion. The horizontal distance between the peak and trough is called peak-to-trough distance (Figure 4.4a).

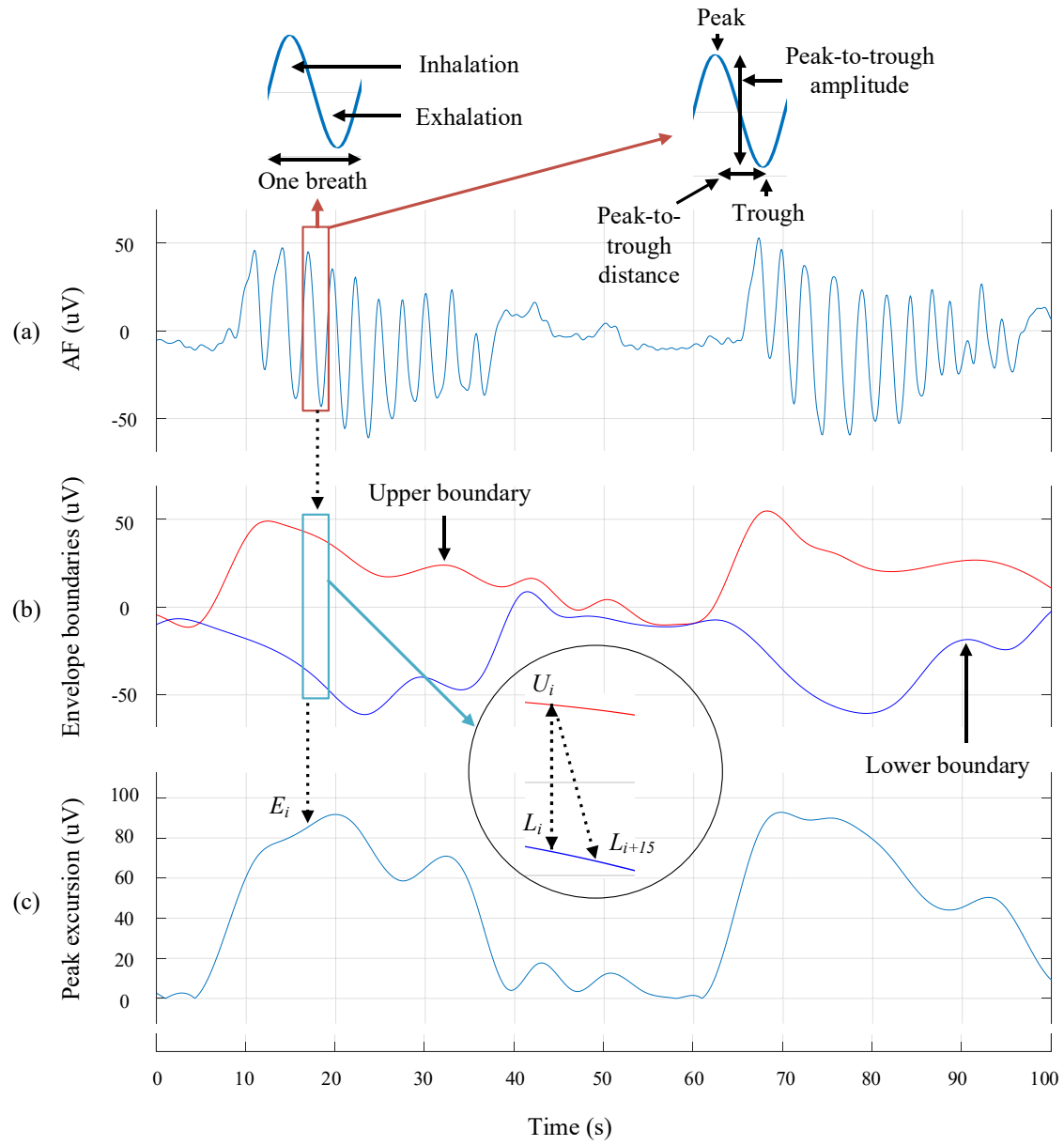

Figure 4.4. Determination of peak signal excursion from the AF signal.

Using a built-in MATLAB command "envelope (AF, 40, 'peak')", the peak envelope of smoothed AF (Figure 4.4a) was created that consisted of the upper and lower boundaries (Figure 4.4b) with the duration of a normal breath being approximately 4 s (i.e., 40 samples; AF sampling rate of 10 Hz). The overall and record-wise analysis of the duration of normal breaths are tabulated in ***Appendix H***.

The nature of the upper and lower peak boundaries with varying the smoothing interval is shown in Figure 4.5. The selection of the smoothing interval was crucial when created the peak envelope, as depicted in Figure 4.5. The best performing envelope was resulted when the smoothing interval was selected approximately equal to the mean duration of the normal breath. Hence, the smoothing interval for creating envelope was selected as 40-samples (4 s) to get optimized performance (Figure 4.5c). The upper and lower boundaries respectively represented the peak and trough amplitudes (Figure 4.4b). Equation (4.1) was used to derive the peak excursion from the boundaries as follows:

$$E_i(t) = |U_i - L_{i+15}| \tag{4.1}$$

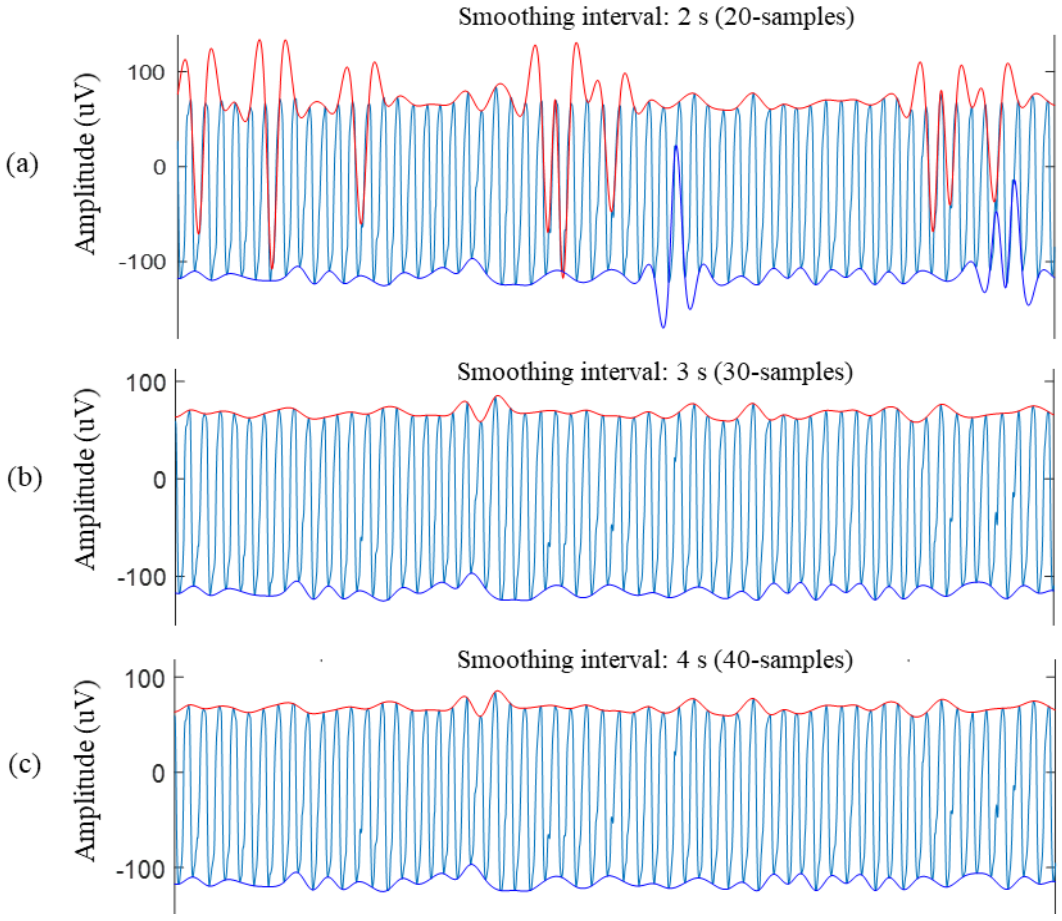

Figure 4.5. Selection of smoothing interval to create envelope of the AF signal.

where, U_i, L_{i+15}, and E_i were the respective magnitudes of the i-th sample of the upper boundary, the (i+15)-th sample of the lower boundary, and the i-th sample of the peak excursion. The direct subtraction of L_i from U_i might not produce accurate peak excursion due to the peak-to-trough distance (Figure 4.4a). This study observed a mean peak-to-trough distance of approximately 1.5 s (15-samples) from the analysis of the development set (***Appendix I***). Thus, in this algorithm,

L_{i+15} was subtracted from U_i to generate an optimal peak excursion, E_i. The derived peak excursion, the absolute difference between the upper and lower boundaries, represented the peak-to-trough amplitude of the detected breath (Figure 4.4c).

Artefact correction and apnea detection: Sudden body movement or sighs (Perez-Padilla, West, & Kryger, 1983) during sleep (as a compensatory breath for inadequate ventilation) may create an unexpectedly large variation in AF signal as shown in Figure 4.6a. These sighs may result in intrusion of "erroneous" large peaks (Figure 4.6b) in the determination of a peak excursion. The location of the sigh and its impact on the peak excursion are represented by the dotted line 'A' (Figure 4.6).

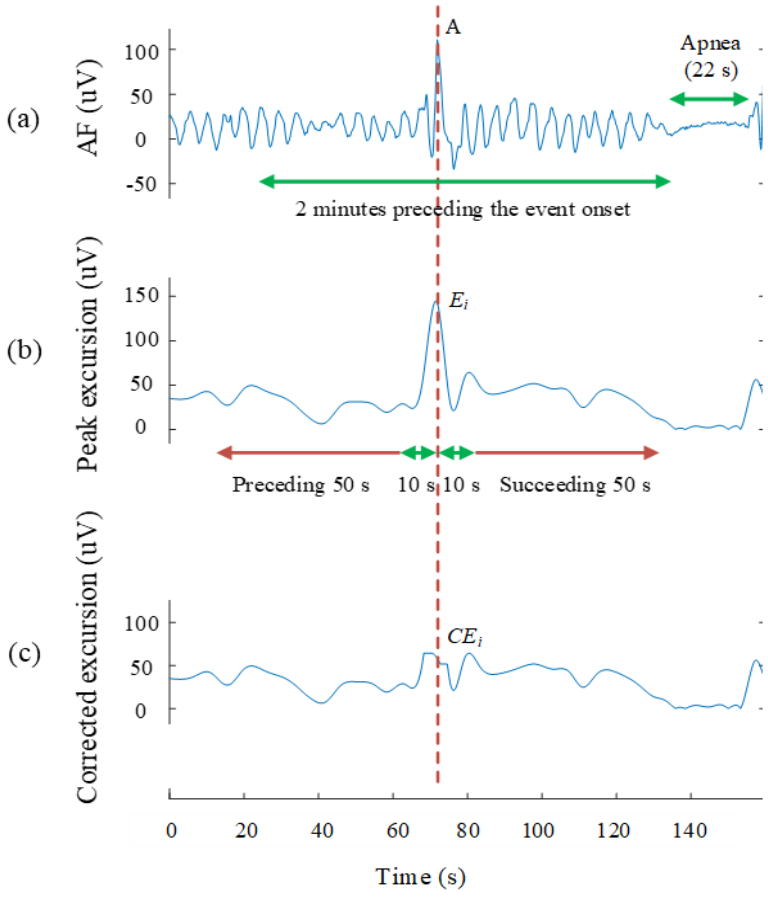

Figure 4.6. Representation of the correction of peak excursion.

The occurrence and impact of sighs were minimized by analyzing the 50 s preceding and succeeding epochs of the peak excursion with 10 s separation on either side of the erroneous peak (Figure 4.6b). In this algorithm, the minimum distance between two successive sighs was estimated to be 60 s and the maximum duration of a single sigh 10 s. Previous study (Huang *et al* 2017) reported the longest duration of a respiratory event (apnea/hypopnea) as approximately 120 s. Thus, sigh correction approach was applied with considering 60 s either side of the sigh. In addition, the duration of sigh is usually longer than the normal breath. Thus, a maximum duration

of sigh of 10 s was set during correction. A corrected peak excursion (CE_i) was generated following peak truncation that was free from artefacts linked to sighs (inter-event artefacts) (Figure 4.6). Though the parameters set during sigh correction are arbitrary, inclusion of such correction may improve the automatic determination of the peak excursion.

A binary digit '1' or '0' was generated against each sample of the corrected peak excursion using (4.2) as follows:

$$BD_i(t) = \begin{cases} 1, & \text{if } CE_i \leq \frac{10}{100} CE_{b,i} \\ 0, & \text{otherwise} \end{cases} \tag{4.2}$$

where, $CE_{b,i}$ and BD_i denote the respective baseline amplitude and binary digit for the sample amplitude, CE_i. The baseline amplitude for i-th sample was determined from the maximum value at 2 minutes preceding the sample as recommended in the updated AASM guidelines (Berry et al., 2012). Thus, a complete binary sequence (Figure 4.7b) was generated where the binary digit '1' represented ≥90% drop in the peak excursion.

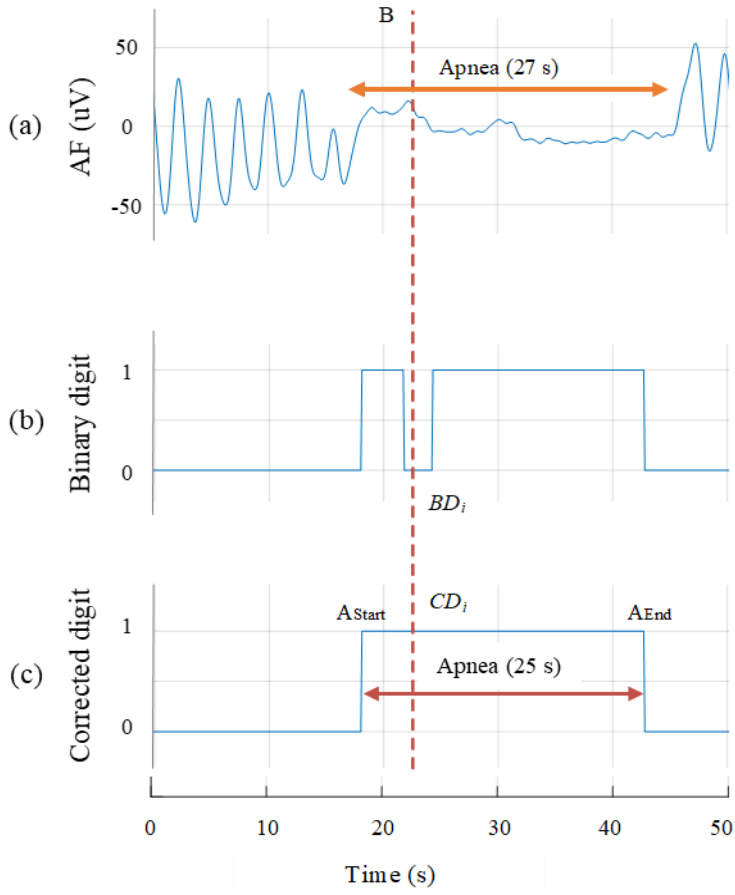

Figure 4.7. Representation of the correction of binary digit.

In ideal cases, an apnea in the AF trace should present as a flat line due to the complete cessation of breathing. In practical cases, there may be some small oscillations (Figure 4.7a), with minor

intra-event fluctuations during an apnea event. Small oscillation in the AF signal and its corresponding binary digit during an apnea event are shown by the dotted line 'B' (Figure 4.7). Thus, the binary sequence of '1's may not be continuous (Figure 4.7b) during an apnea event with such artefacts. An auto-correction step in the binary sequence was applied when two '1's were separated by <4s (i.e., the average duration of a normal breath). Thus, the corrected binary sequence CD_i was generated against the binary sequence BD_i which represented a continuous sequence of '1's against the duration of apnea event (Figure 4.7c). This setting of 4 s during an auto-correction has minimal impact on the detection of apnea events since the sudden fluctuations during an apnea event may not be frequently found. Inclusion of such correction may enhance the detection of apnea events.

The algorithm can identify an apnea start-point (A_{Start}), i.e., from the binary sequence where '0' was detected followed by at least one hundred successive '1's (10 s). Similarly, the apnea end-point (A_{End}) was identified where '0' was detected preceding at least one hundred successive '1's. Thus, the difference in interval between A_{End} and A_{Start} was calculated for the apnea duration (at least 10 s) as depicted in Figure 4.7c. The designed algorithm resulted in a consistent shortening of the detected apnea duration by approximately 2 s. The AF envelope cannot respond to the immediate sharp amplitude changes at the start and end of an apnea event. Thus, the envelope tracking approach is responsible for a consistent shortening of the detected apnea duration and hence could miss-detect some apneas if ≥10 s is set for apnea duration.

Designing an effective and reliable algorithm depends on the process of optimization that can set a specific apnea duration threshold. The SHHS reported the overall AHI against each PSG record and provided the PSG analysis files that contained all scored events. The scoring of apnea was done using ≥75% drop in airflow reduction. In addition, thoracic or abdominal effort was used for scoring apneas where AF was not reliable. Hypopnea was scored using either criteria of ≥3% oxygen desaturation and an arousal. This study required the number of scored apneas and hypopneas against each record in the development set for the optimization process. Since the scoring reported in the SHHS did not completely follow the AASM scoring guidelines, the comparison of these scored events with the detected events was incompatible. In contrast, this study used AF and SpO_2 signals for detecting apnea and hypopnea events. For the reliable and logical optimization of the designed algorithm, this study considered re-scoring of apnea and hypopnea events based on AF and SpO_2 signals. The development set of AF and SpO_2 was re-scored for apnea and hypopnea events by an experienced sleep physiologist. In short, an apnea was re-scored when AF drops ≥90% with a duration ≥10 s, whereas a hypopnea was re-scored when AF drop (≥30% with a duration ≥10 s) associated with ≥3% oxygen desaturation. Hypopneas associated with arousal but <3% oxygen desaturation were not scored due to the exclusion of EEG signal from this study. The re-scoring reported in 3666 apneas and 4069

hypopneas from 45 records of the development set. The overall and record-wise re-scoring is listed in ***Appendix J***. It should be mentioned here that this re-scoring was done for the purpose of developing the algorithm.

To get an optimized apnea duration threshold, the re-scored apneas were compared with detected apneas for the development set. An apnea duration threshold of ≥8 s was established within the algorithm for apnea detection. This optimization process applying a threshold duration of ≥8 s resulted in the highest correlations between re-scored and detected apneas, as indicated in Table 4.3. Other apnea duration thresholds were sub-optimal. Thus, ≥8 s apnea duration threshold was set within the automatic process and the number of detected apnea events was listed with their corresponding duration and timing.

Table 4.3. Selecting apnea duration threshold for the development set.

Detected apneas [duration threshold]	Scored apneas	Difference	*r*	*ICC*	95% *CI*
3839 [≥7 s]	3666	-173	0.990	0.995	0.991 – 0.997
3574 [≥8 s]	3666	**+92**	**0.991**	**0.994**	**0.990 – 0.997**
3340 [≥9 s]	3666	+326	0.989	0.990	0.980 – 0.995
3096 [≥10 s]	3666	+570	0.986	0.983	0.955 – 0.992

'+' and '-' signs respectively indicate the overall number of miss-detected and over-detected apneas; Correlations was resulted from the record-wise analysis of re-scored and detected apneas; *r*, *ICC*, and *CI* respectively represent the Pearson's correlation coefficient, intraclass correlation coefficients, and confidence interval.

(iii) **Detection of hypopnea event**: For hypopnea event detection, AF drop (≥30% that lasts ≥10 s) must be associated with ≥3% oxygen desaturation or an arousal. Initially, the algorithm detected hypopnea event associated with ≥3% oxygen desaturation. Later, the overall number of hypopnea event (associated with ≥3% oxygen desaturation or an arousal) was estimated.

The raw SpO_2 was loaded as the input to the automated process. Due to the setup of the signal recording process, the sample values of the SpO_2 signal may not always be an integer value (A = 93.9) as shown in Figure 4.8a. All the sample values of the raw SpO_2 signal was then converted to its nearest integer value (A = 94) as indicated in Figure 4.8b. After converting to the nearest integer, any sudden unstable peaks (A = 94) were corrected to generate a stabilized signal (Figure 4.8c).

Oximetry signal may sometimes fall to near zero due to body movement or vibration (Figure 4.9a). These artefacts may interfere with the accurate determination of oxygen desaturation. A correction approach was applied, where the faulty sample value (sudden fall to near zero, Figure 4.9b) of the oximetry signal was imputed to its previous stable value as shown in Figure 4.9c. Thus, a preprocessed (rounded, stabilized, and corrected) SpO_2 signal was generated (Figure 4.9c).

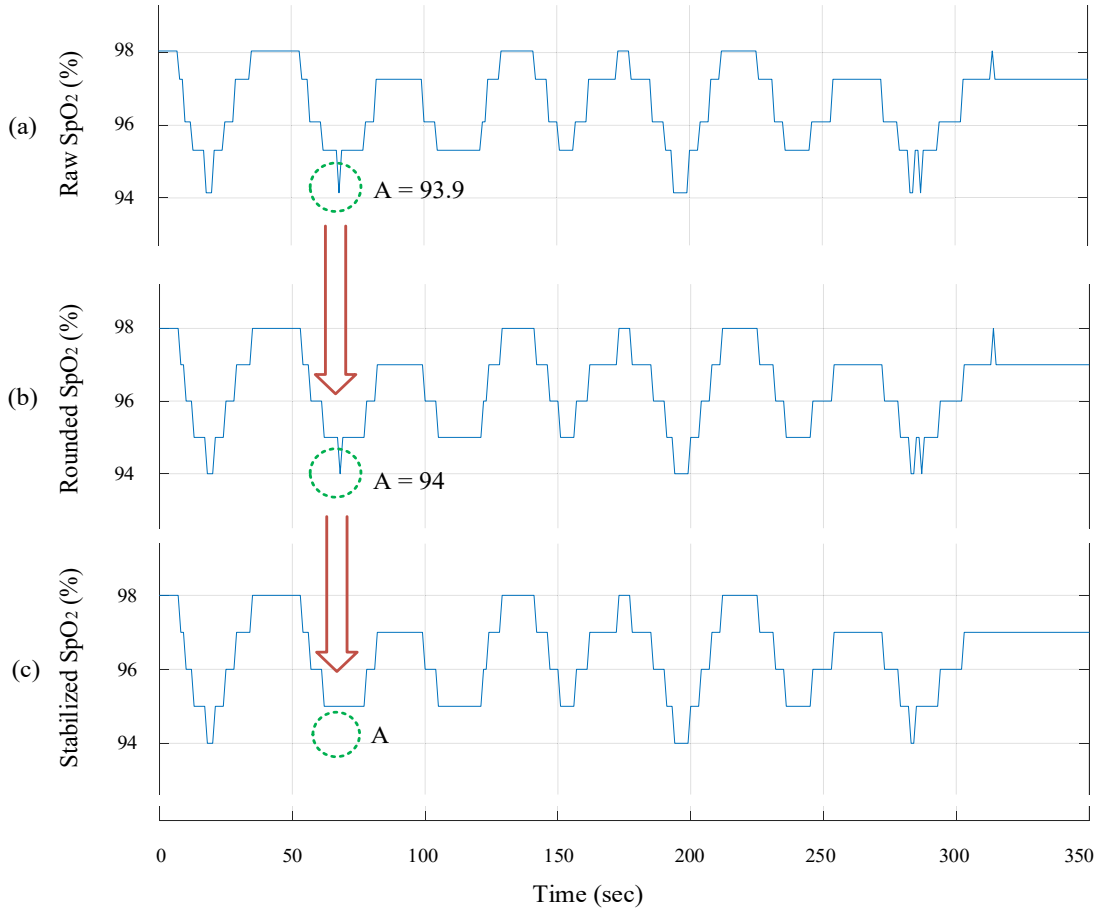

Figure 4.8. Stabilization of oximetry signal.

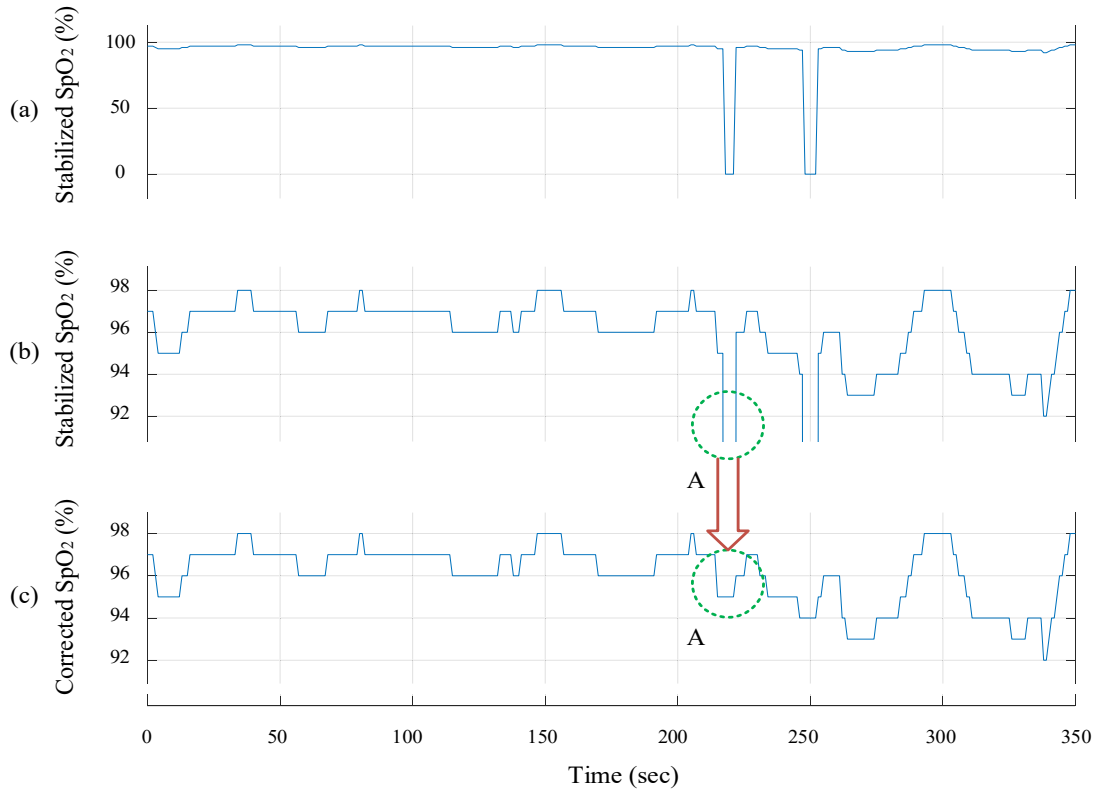

Figure 4.9. Removing sudden fall to zero from oximetry signal.

Hypopnea detection from AF drop and oxygen desaturation: The corrected SpO_2 signal was used for the determination of desaturation (≥3%). For hypopnea event detection, alignment between the AF drop and SpO_2 desaturation was required. To make the alignment, the number of sample points must be same for both signals. The AF signal was recorded with a sampling rate of 10 Hz but the SpO_2 of 1 Hz. Though the duration of each recorded signal was the same, but the sampling rates (or, total number of samples) were different. The SpO_2 signal was converted to 10 Hz to make equal number of sample that the AF signal has.

A 40 s moving window was applied to corrected SpO_2 signal to determine the level of desaturation as shown in Figure 4.10a. The window moved forward by one sample after determining a digital bit linked to the desaturation criteria. For example, to determining a digital bit for the sample 'A' (i.e., *i*-th sample), the location of the window was '*X*' (Figure 4.10a). The maximum value was determined from the window. Thus, the maximum value of 98 was determined from the window for the sample 'A (=94)'. This maximum value (=98) was designed as the 'Baseline' for the sample A (=94). A binary digit was generated against the sample 'A' using (4.3):

$$BD_i(t) = \begin{cases} 1, & \text{if } A \leq (Baseline_i - 3) \\ 0, & \text{otherwise} \end{cases} \tag{4.3}$$

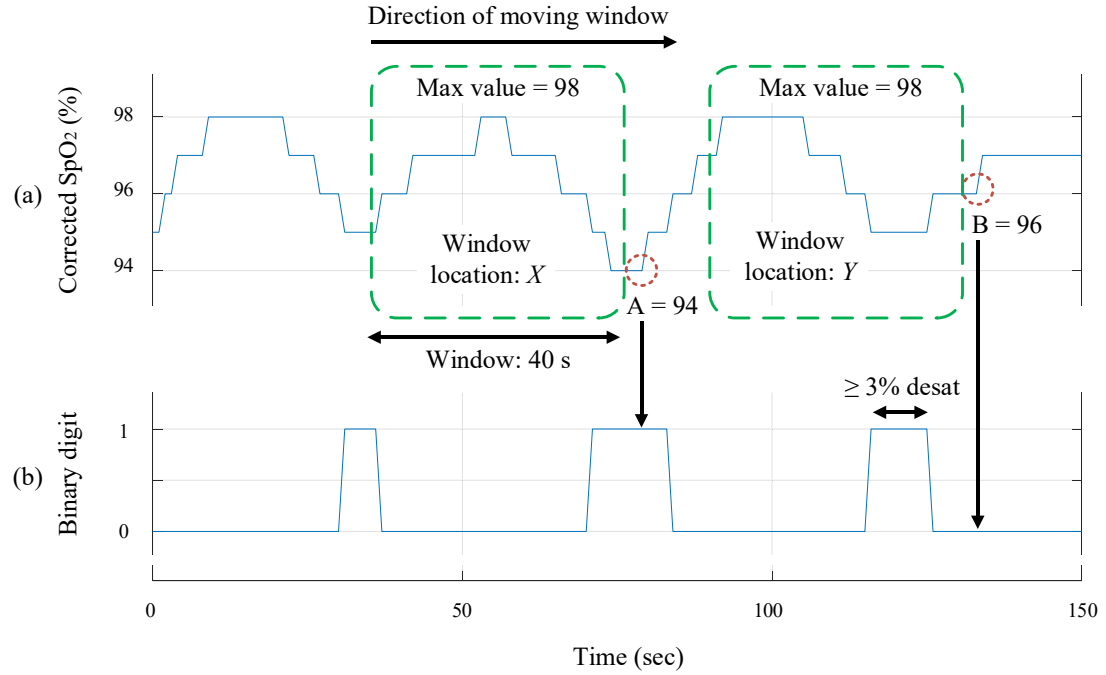

Figure 4.10. Generating digital sequence against SpO_2 signal.

where $BD_i(t)$ denotes the corresponding binary digit for the *i*-th sample value 'A'. The value of $(Baseline_i - 3)$ was found to be 95 which was greater than the value of the *i*-th sample 'A'. This indicated a ≥3% desaturation for the sample 'A'. Thus, a binary digit '1' was generated against the

sample ‘A’ as shown in Figure 4.10a. Similarly, ‘0’ was generated for the sample ‘B’ when the window was in location ‘*Y*’ (Figure 4.10a). Thus, a continuous digital sequence was generated against the corrected SpO_2 signal where ‘1’ and ‘0’ represented ≥3% and <3% desaturations respectively (Figure 4.10b).

A tiny deflection during desaturation (Figure 4.11a, dotted circle ‘A’) may create discrete binary digits (Figure 4.11b, dotted circle ‘A’). Ideally, there should some difference between the start of two successive desaturations. To remove these tiny deflections within the single desaturation phase, binary digits were corrected where two successive desaturations were separated by a small duration (<10 s)**.** Thus, the corrected binary sequence (Figure 4.11c, dotted circle ‘A’) represented a continuous sequence of ‘1’s against the desaturation.

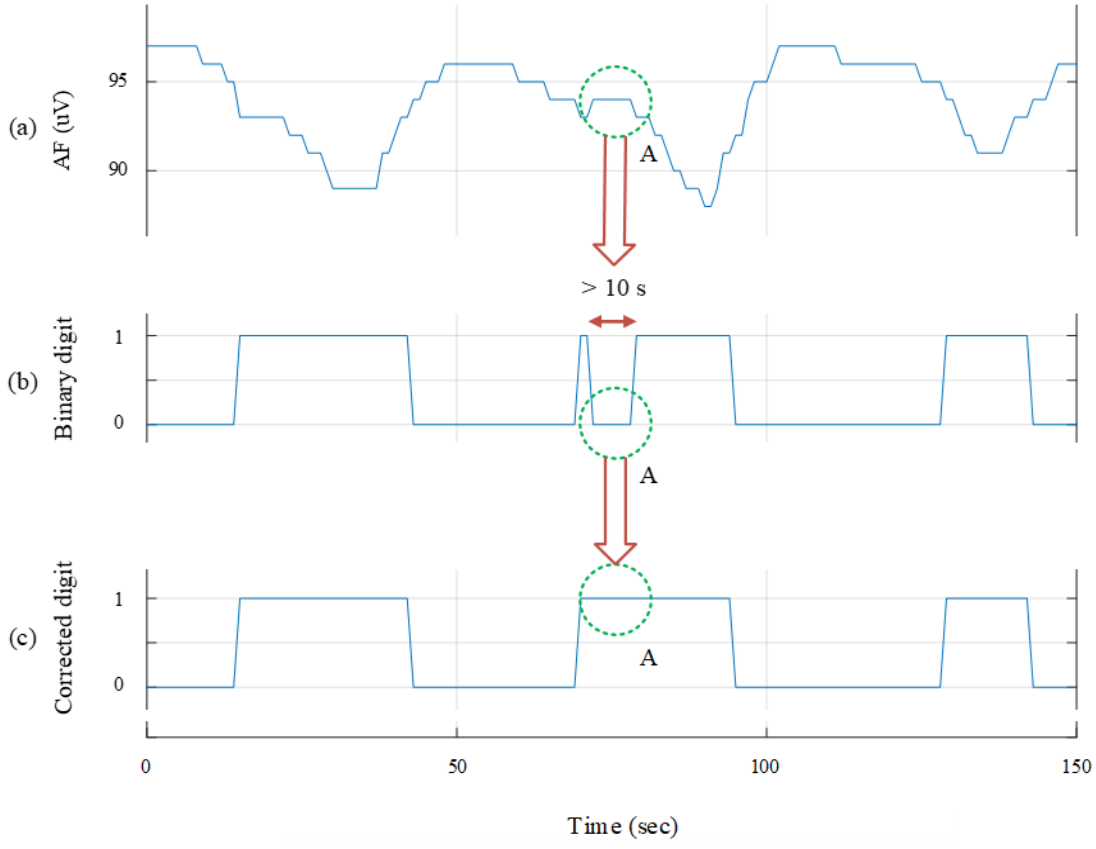

Figure 4.11. Correcting digital sequence of SpO_2 signal.

The duration of desaturation phase should be detected from the start of desaturation to the end of desaturation as shown in Figure 4.12a. The duration of the detected desaturation (23 s, Figure 4.12b) was significantly lower than the actual duration (32 s, Figure 4.12a). The 40 s moving window resulted in displacing the ≥3% oxygen desaturation by ~10 s at start of each desaturation phase, thereby shortening the desaturation duration by an equivalent amount. This problem was resolved by generating an extended binary sequence, where the start of each detected desaturation

was extended backward by 10 s. Thus, the extended sequence depicted a continuous sequence of '1's against the duration of ≥3% oxygen desaturation (Figure 4.12c).

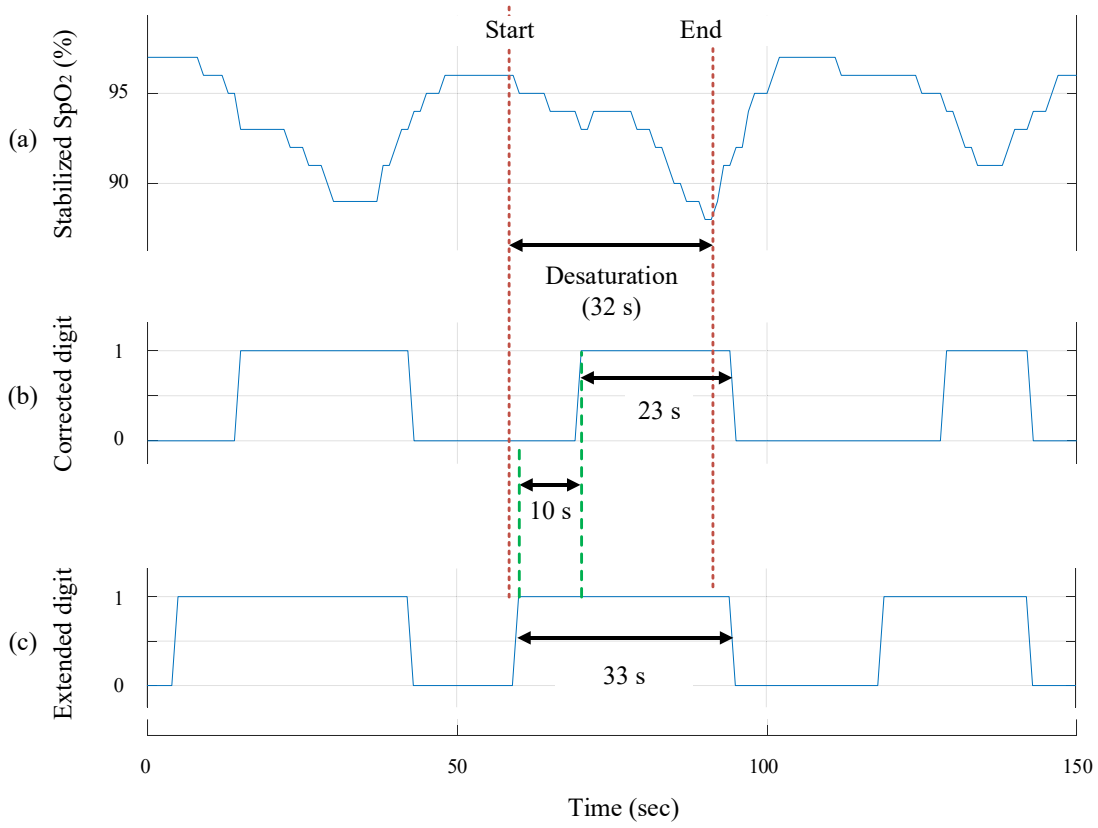

Figure 4.12. Extending digital sequence of SpO_2 signal.

Figure 4.13b shows two sections of ≥3% desaturations (desat A and desat B) resulted from their corresponding ≥30% drops ≥10 s (drop A and drop B). In practice, the SpO_2 signal always showed a lag with respect to the AF signal that may vary approximately from 10 to 30 s (Otero et al., 2012). Thus, a backward time shift of 20 s (i.e., the average time lag) in the oximetry (BS SpO_2) signal was generated (Figure 4.13c).

A binary sequence against the corrected peak excursion was generated using ≥30% drop criterion, as similarly done for apnea event detection. The binary sequence of '1's was converted to '0's where the duration of ≥30% drop was <10 s. Thus, the corrected sequence (i.e., CD_i) represented a continuous sequence of '1's for ≥30% drop with a duration of ≥10 s (Figure 4.14a).

Using a 40 s moving window, an extended binary sequence (Figure 4.12c) was generated as explained above. The extended sequence was backward shifted by 20 s to produce a backward shifted binary sequence (i.e., BSD_i) as illustrated in Figure 4.14b. Technically, the process of a hypopnea event detection mandates a parallel temporal drop in AF signal (≥30%, ≥10 s) and

oxygen saturation (≥3%). The resultant binary sequence was generated by parallel sample-to-sample multiplication using (4.4) as follows:

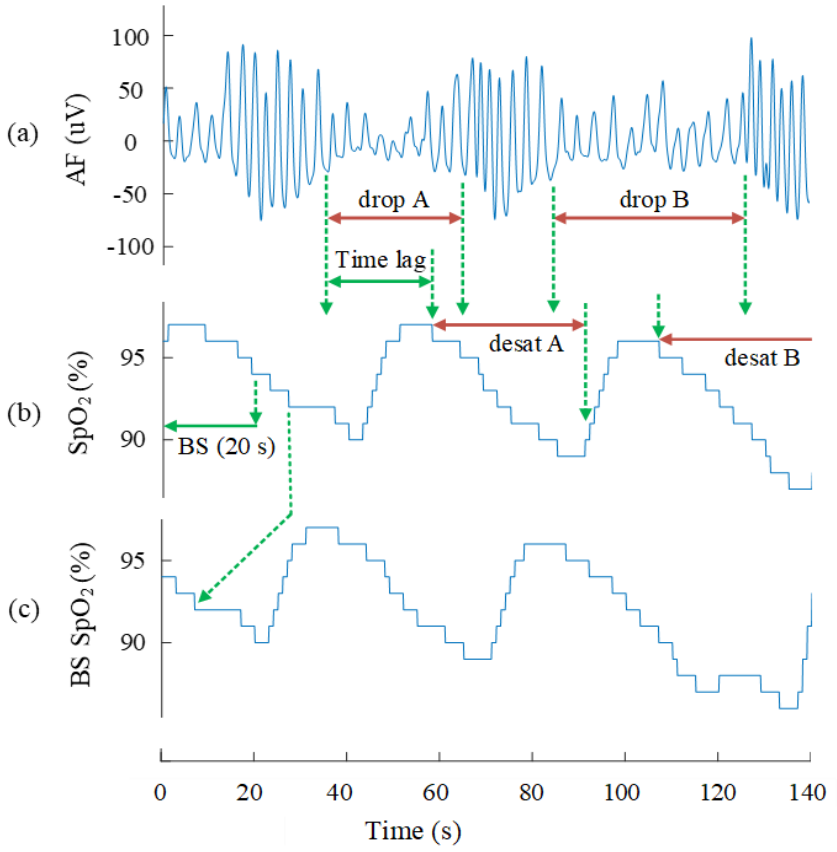

Figure 4.13. Adjustment to the time lag in the SpO_2 signal.

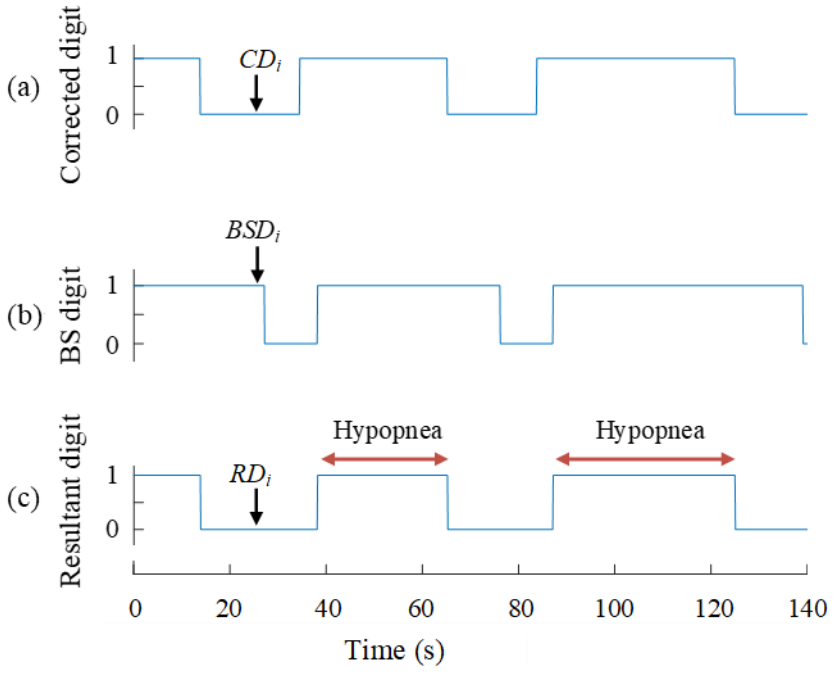

Figure 4.14. Hypopnea detection by multiplication.

$$RD_i(t) = CD_i \times BSD_i \tag{4.4}$$

where, RD_i, CD_i, and BSD_i respectively denote the resultant binary sequence, corrected binary sequence generated from the AF, and backward shifted binary sequence generated from the SpO_2 signal. Thus, two hypopnea events were detected from the resultant binary sequence with their corresponding duration and timing (Figure 4.14c). Hypopnea events that were overlapped with apnea events were removed and the remaining events were finalized as hypopnea events associated with ≥3% oxygen desaturation.

The selection of window length for the accurate determination of ≥3% oxygen desaturation and the duration of backward shifting (time lag) are very crucial for the accurate detection of hypopnea events. An optimization was performed where the window length was varied, and the number of detected hypopnea event was noted as shown in Table 4.4.

Table 4.4. Selecting window length for hypopnea detection.

Detected hypopneas [window length]	Scored hypopneas	Difference	*r*	*ICC*	95% *CI*
3634 [20 s]	4069	+435	0.973	0.980	0.945 – 0.991
4022 [30 s]	4069	**+47**	**0.979**	**0.989**	**0.981 – 0.994**
4234 [40 s]	4069	-165	0.979	0.989	0.980 – 0.994

'+' and '-' signs respectively indicate the overall number of miss-detected and over-detected hypopneas; Correlations was resulted from the re-record-wise analysis of scored and detected hypopneas; *r*, *ICC*, and *CI* respectively represent the Pearson's correlation coefficient, intraclass correlation coefficients, and confidence interval.

Table 4.4 shows that the total number of detected hypopneas with 30 s window length closely approximate to the total number of re-scored hypopneas. In addition, the false detection is minimized, and the highest correlations are achieved with 30 s window length. The optimized window length of 30 s resulted in the highest Pearson's correlation coefficient (r = 0.979) and intraclass correlation coefficient (ICC = 0.989) between the re-scored and detected hypopneas. Other window lengths (20 and 40 s) were responsible for significant false detection and lower correlation coefficients. Thus, a window length of 30 s was finally selected for the accurate detection of ≥3% oxygen desaturation.

During the above optimization process, we set a backward shifting of 20 s to detect hypopneas. An optimization was performed where the window length was fixed to 30 s, but the duration of backward shifting was varied, and the number of detected hypopnea event was noted as shown in Table 4.5.

Table 4.5 shows that the total number of detected hypopneas with 20 s backward shifting closely approximate to the total number of re-scored hypopneas. In addition, the false detection is

minimized, and the highest correlations are achieved with 20 s backward shifting. An optimized adjustment of time lag of 20 s resulted in the highest Pearson's correlation coefficient (r = 0.979) and intraclass correlation coefficient (ICC = 0.989) between the re-scored and detected hypopneas. Other durations of backward shifting (0 s, 10 s, 30 s, and 40 s) were responsible for significant false detection and lower correlation coefficients. Thus, a duration of 20 s backward shifting was finally selected for the accurate detection hypopnea events.

Table 4.5. Selecting the duration of backward shifting for hypopnea detection.

Detected hypopneas [Backward shifting]	Scored hypopneas	Difference	*r*	*ICC*	95% *CI*
3780 [0 s]	4069	+289	0.966	0.980	0.962 – 0.990
3983 [10 s]	4069	+86	0.974	0.987	0.976 – 0.993
4022 [20 s]	4069	**+47**	**0.979**	**0.989**	**0.981 – 0.994**
4017 [30 s]	4069	+52	0.977	0.988	0.979 – 0.994
3835 [40 s]	4069	+234	0.968	0.982	0.967 – 0.990

'+' sign indicates the overall number of miss-detected hypopneas; Correlations was resulted from the record-wise analysis of re-scored and detected hypopneas; *r*, *ICC*, and *CI* respectively represent the Pearson's correlation coefficient, intraclass correlation coefficients, and confidence interval.

The above detected hypopneas (associated with ≥3% oxygen desaturation) may or may not be linked with an arousal. The designed approach will miss-detect some hypopnea events that are associated with arousal but <3% oxygen desaturation. These hypopneas are designated 'additional hypopneas'. Detection of these additional hypopneas from AF and SpO_2 signals is challenging since arousal may occur with any value of oxygen desaturation (≥1% to <3%). Consideration of ≥1% to <3% oxygen desaturation may overestimate additional hypopneas since the SpO_2 often fluctuates by about 1% during normal breathing. Hence, we designed the algorithm to detect the addition hypopneas when AF drop (≥30% for a duration ≥10 s) was associated with ≥2% to <3% oxygen desaturation with a duration ≥20 s.

In setting the duration of ≥2% to <3% oxygen desaturation to ≥20 s, the optimization showed the highest correlations (r = 0.958, ICC = 0.975, and 95% CI = 0.955 to 0.986) between the scored (reported in the SHHS) and detected AHI (Table 4.6). Additional hypopneas that were overlapped with previously detected apneas and hypopneas (with ≥3% oxygen desaturation) were removed. The remaining additional hypopneas were added to previously detected hypopneas to compute the total number of hypopneas.

Table 4.6. Estimating additional hypopneas with changing the duration of desaturations.

Duration of ≥2% to <3% oxygen desaturation	Correlations between actual and estimated AHI		
	r	*ICC*	95% *CI*
≥10 s	0.957	0.967	0.922 – 0.984
≥20 s	**0.958**	**0.975**	**0.955 – 0.986**
≥30 s	0.959	0.974	0.952 – 0.986

AHI: Apnea hypopnea index; Correlations was resulted from the record-wise analysis of actual and estimated AHI; *r*, *ICC*, and *CI* respectively represent the Pearson's correlation coefficient, intraclass correlation coefficients, and confidence interval.

(iv) **Estimation of AHI**: The algorithm is now ready to compute the AHI from automatically detected total number of apneas, total number of hypopneas (associated with ≥3% oxygen desaturation or an arousal), and estimated TST. The algorithm computed the AHI using (4.5) as follows:

$$AHI = \frac{No.of\ detected\ (apneas + hypopneas)}{Estimated\ TST} \tag{4.5}$$

This fully automatic algorithm requires no human input for respiratory event analysis and TST estimation. Once the raw AF and SpO_2 are fed to the algorithm, the automatic process takes over and delivers the AHI.

4.2.3 Parameters for performance evaluation

The designed algorithm reported the estimated AHI from the automatic analysis of AF and SpO_2 signals. Thus, the AHI estimated by the algorithm was compared to the actual AHI reported in the SHHS database for performance evaluation. The parameters used for performance evaluation included correlation coefficient, Bland-Altman plot, sensitivity, specificity, accuracy, area under ROC curve, Cohen's kappa coefficient, and confusion matrix (see definitions in ***Appendix K***).

4.3 Results

4.3.1 Performance in development set

Correlation coefficients: The automatic algorithm was developed with a development set of 45 records. The algorithm detected respiratory events (apneas and hypopneas), sleep period, and finally estimated AHI, which was compared to manual scoring reported in the SHHS (actual AHI). The record-wise actual and estimated AHI are tabulated in ***Appendix L***). Strong correlations were

found between the automatically estimated and actual AHI (r = 0.97, ICC = 0.98, 95% CI = 0.97 to 0.99) as illustrated in Figure 4.15.

Bland-Altman plot: The Bland-Altman plot (difference vs average of the actual and estimated AHI) illustrates good agreement across a whole range of AHI severity (mean bias, 95% CI, and mean bias ± 95% LoA were -1, 0.9 to -2.9, and 11.4 to -13.3 events/h respectively) (Figure 4.16). The record-wise actual and estimated AHI and their differences are tabulated in ***Appendix L***).

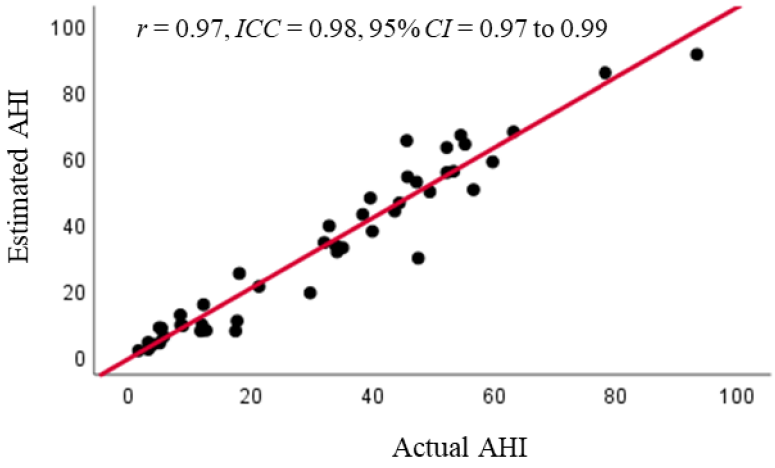

Figure 4.15. Scatter plot of the correlation between actual and estimated AHI.

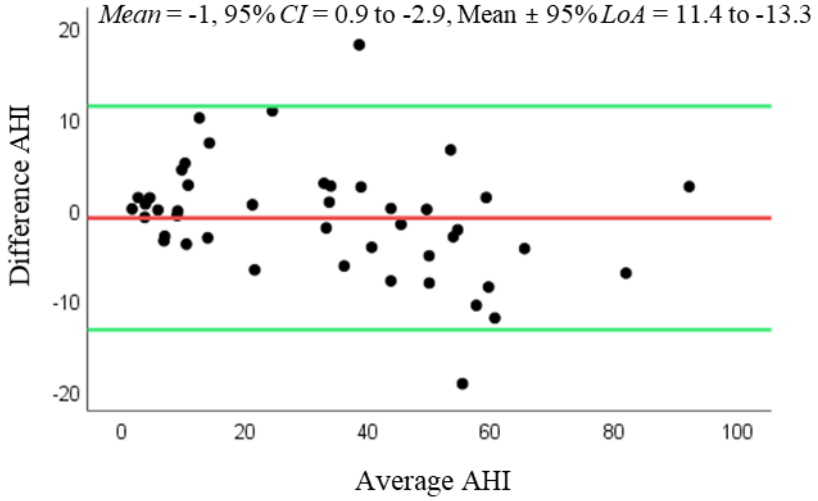

Figure 4.16. Bland-Altman plot of AHI.

Sensitivity, specificity, and accuracy: The confusion matrices for 2 class (binary) diagnosis with commonly used AHI cut-offs are listed in Table 4.7. The overall performance of the automatic algorithm for the development set is listed in Table 4.8. The agreement between the estimated and actual AHI was determined by using three common AHI cut-offs (≥5, ≥15, and

≥30). The overall accuracies of diagnosis were found 97.8%, 95.6%, and 97.8% for AHI cut-offs ≥5, ≥15, and ≥30 events/h respectively (Table 4.8).

Table 4.7. Confusion matrices for 2 class diagnosis.

		Estimated		Estimated		Estimated	
		Positive (AHI ≥5)	*Negative (AHI <5)*	*Positive (AHI ≥15)*	*Negative (AHI <15)*	*Positive (AHI ≥30)*	*Negative (AHI <30)*
Actual	*Positive*	40	1	28	2	24	1
	Negative	0	4	0	15	0	20

AHI: apnea hypopnea index

Table 4.8. Agreement between estimated and actual classes for 2 class diagnosis.

Performance parameters	Cut-offs		
	AHI ≥5	*AHI ≥15*	*AHI ≥30*
TP	40	28	24
TN	4	15	20
FP	0	0	0
FN	1	2	1
PPV (%)	100	100	100
NPV (%)	80	88.2	95.2
Sensitivity (%)	97.6	93.3	96
Specificity (%)	100	100	100
Accuracy (%)	97.8	95.6	97.8
AUC	0.99	0.97	0.98
k	0.88	0.90	0.96

AHI: Apnea hypopnea index, TP: True positives, TN: True negatives, FP: False positives, FN: False negatives, PPV: Positive predictive value, NPV: Negative predictive value, AUC: Area under ROC curve, *k*: Cohen's kappa coefficient. PPV, NPV, sensitivity, specificity, and accuracy were calculated using (*K1*) to (*K5*) respectively, as indicated in ***Appendix K***.

The confusion matrix for 4 classes (normal, mild, moderate, and severe) of diagnosis is listed in Table 4.9. The class-wise and overall performances of the automatic algorithm for the development set is listed in Table 4.10. The agreement between the estimated and actual classes was determined by using the AHI range of the corresponding class. The accuracies of diagnosis were found 97.8%, 93.3%, 93.3%, and 97.8% for normal, mild, moderate, and severe class respectively (Table 4.10). The overall 4 class accuracy and kappa were found 91.1% and 0.86 respectively (Table 4.10).

Table 4.9. Confusion matrix for 4 class diagnosis.

		Estimated			
		Normal	*Mild*	*Moderate*	*Severe*
Actual	*Normal*	4	0	0	0
	Mild	1	10	0	0
	Moderate	0	2	3	0
	Severe	0	0	1	24

Table 4.10. Agreement between estimated and actual classes for 4 class diagnosis.

Performance parameters	AHI classes/groups			
	Normal	*Mild*	*Moderate*	*Severe*
TP	4	10	3	24
TN	40	32	39	20
FP	1	2	1	0
FN	0	1	2	1
PPV (%)	80	83.3	75	100
NPV (%)	100	97	95.1	95.2
Sensitivity (%)	100	91	60	96
Specificity (%)	97.6	94.1	97.5	100
Accuracy (%)	97.8	93.3	93.3	97.8
4 class accuracy (%)	91.1			
4 class kappa	0.86			

AHI: Apnea hypopnea index, TP: True positives, TN: True negatives, FP: False positives, FN: False negatives, PPV: Positive predictive value, NPV: Negative predictive value. TP, FP, FN, and TN of the specific class were calculated using (*K6*) to (*K9*) respectively; PPV, NPV, sensitivity, and specificity of the specific class were calculated using (*K1*) to (*K4*) respectively; 4 class accuracy were calculated using (*K10*), as mentioned in ***Appendix K***.

The overall performance in the development set is outstanding due to the optimizations applied throughout the design process. The actual performance was found by testing the automatic algorithm with an unknown large validation set of 943 records as described below.

4.3.2 Performance in validation set

Correlation coefficient: The automatic algorithm was tested with a large and unknown validation set of 943 records. The algorithm detected respiratory events (apneas and hypopneas), sleep period, and finally estimated AHI, which was compared to manual scoring reported in the SHHS (actual AHI). The record-wise actual and estimated AHI are tabulated in ***Appendix M***). Strong correlations were found between the automatically estimated and actual AHI ($r = 0.91$, $ICC = 0.95$, 95% $CI = 0.94$ to 0.96) as depicted in Figure 4.17.

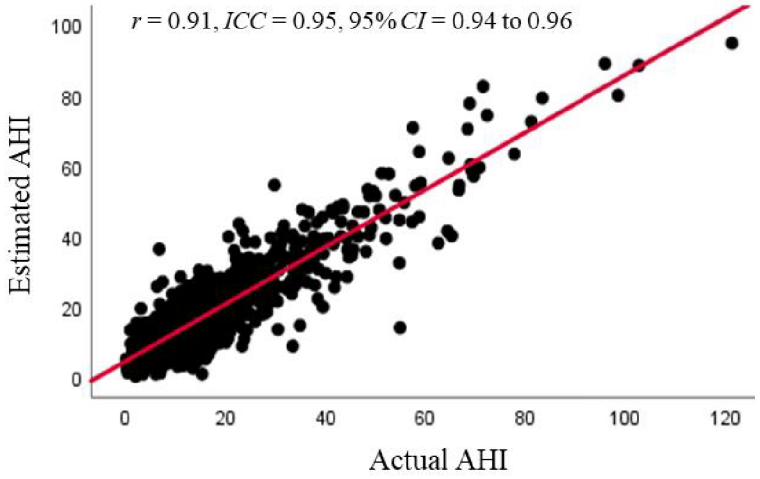

Figure 4.17. Scatter plot of the correlation between actual and estimated AHI.

Bland-Altman plot: Bland-Altman plot (difference vs average of the actual and estimated AHI) illustrates good agreement across a whole range of AHI severity (mean bias, 95% *CI*, and mean bias ± 95% *LoA* were -1.6, -1.2 to -2, and 10.9 to -14.1 events/h respectively) as illustrated in Figure 4.18. The record-wise actual and estimated AHI and their differences are tabulated in ***Appendix M***).

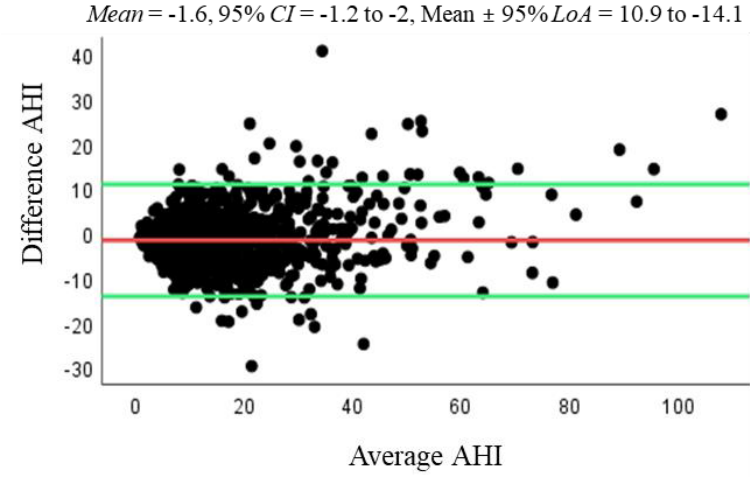

Figure 4.18. Bland-Altman plot of AHI.

Sensitivity, specificity, and accuracy: The confusion matrices for 2 class (binary) diagnosis with commonly used AHI cut-offs are listed in Table 4.11. The overall performance of the automatic algorithm for the validation set is listed in Table 4.12. The agreement between the estimated and actual AHI was determined by using three common AHI cut-offs (≥5, ≥15, and ≥30). The overall accuracies of diagnosis were found 90.7%, 91%, and 96.7% for AHI cut-offs ≥5, ≥15, and ≥30 events/h respectively (Table 4.12).

Table 4.11. Confusion matrices for 2 class diagnosis.

		Estimated		Estimated		Estimated	
		Positive (AHI ≥5)	*Negative (AHI <5)*	*Positive (AHI ≥15)*	*Negative (AHI <15)*	*Positive (AHI ≥30)*	*Negative (AHI <30)*
Actual	*Positive*	735	8	359	20	115	16
	Negative	80	120	65	499	15	797

AHI: Apnea hypopnea index

Table 4.12. Agreement between estimated and actual classes for 2 class diagnosis.

Performance parameters	Cut-offs		
	AHI ≥5	*AHI ≥15*	*AHI ≥30*
TP	735	359	115
TN	120	499	797
FP	80	65	15
FN	8	20	16
PPV (%)	90.2	84.7	88.5
NPV (%)	93.8	96.2	98
Sensitivity (%)	98.9	94.7	87.8
Specificity (%)	60	88.5	98.2
Accuracy (%)	90.7	91	96.7
AUC	0.79	0.92	0.93
k	0.68	0.82	0.86

AHI: Apnea hypopnea index, TP: True positives, TN: True negatives, FP: False positives, FN: False negatives, PPV: Positive predictive value, NPV: Negative predictive value, AUC: Area under ROC curve, *k*: Cohen's kappa coefficient. PPV, NPV, sensitivity, specificity, and accuracy were calculated using (*K1*) to (*K5*) respectively, as indicated in ***Appendix K***.

The automatic algorithm showed strong agreement between actual and estimated AHI for all AHI cut-offs except some special conditions such as- (i) lowest specificity (60%) was observed when the sample size of the normal class (AHI <5) was too small (n = 200) with respect to the total size of the validation set (n = 943), and (ii) too narrow range of AHI for detecting normal class (0≤ AHI <5) was also responsible for the lowest specificity, and hence the lowest kappa of 0.68. The automatic algorithm might often overestimate or underestimate around the narrow range of AHI, thus producing reduced agreement for the normal class.

The confusion matrix for 4 classes (normal, mild, moderate, and severe) of diagnosis is listed in Table 4.13. The class-wise and overall performances of the automatic algorithm for the validation set is listed in Table 4.14. The agreement between the estimated and actual classes was determined by using the AHI range of the corresponding class. The accuracies of diagnosis were found 90.7%, 82%, 88.4%, and 96.7% for normal, mild, moderate, and severe class respectively

(Table 4.14). The overall 4 class accuracy and kappa were found 78.9% and 0.70 respectively (Table 4.14).

Table 4.13. Confusion matrix for 4 class diagnosis.

		Estimated			
		Normal	*Mild*	*Moderate*	*Severe*
Actual	*Normal*	120	80	0	0
	Mild	8	293	61	1
	Moderate	0	19	216	14
	Severe	0	1	15	115

Table 4.14. Agreement between estimated and actual classes for 4 class diagnosis.

Performance parameters	AHI classes/groups			
	Normal	*Mild*	*Moderate*	*Severe*
TP	120	293	216	115
TN	735	480	618	797
FP	8	100	76	15
FN	80	70	33	16
PPV (%)	93.8	74.6	74	88.5
NPV (%)	90.2	87.3	94.9	98
Sensitivity (%)	60	80.7	86.8	87.8
Specificity (%)	98.9	82.8	89.1	98.2
Accuracy (%)	90.7	82	88.4	96.7
4 class accuracy (%)	78.9			
4 class kappa	0.70			

AHI: Apnea hypopnea index, TP: True positives, TN: True negatives, FP: False positives, FN: False negatives, PPV: Positive predictive value, NPV: Negative predictive value. TP, FP, FN, and TN of the specific class were calculated using (*K6*) to (*K9*) respectively; PPV, NPV, sensitivity, and specificity of the specific class were calculated using (*K1*) to (*K4*) respectively; 4 class accuracy were calculated using (*K10*), as mentioned in ***Appendix K***.

The automatic algorithm showed strong agreement between actual and estimated classes except some special conditions such as- (i) lowest sensitivity (60%) was observed for the normal class, where the actual sample size of the normal class was too small (n = 200) with respect to the total size of the validation set (n = 943), and (ii) too narrow range of AHI for the normal class (0≤ AHI <5) was also responsible for the lowest sensitivity. These special conditions might be responsible for the reduced 4 class accuracy (78.9%) and kappa (0.70).

4.4 Discussion

In this study, we reported a novel automatic approach using AF and SpO_2 signals for the diagnosis of sleep apnea. For performance evaluation, the output of the automatic algorithm was compared to the SHHS manually scored data. The automatic algorithm showed strong correlations between estimated and actual AHI (Figure 4.17). In addition, the Bland-Altman plot showed very good agreement between estimated and actual AHI, with small mean bias and narrow limits of agreement (Figure 4.18). The overall accuracies (binary class diagnosis) were found 90.7%, 91%, and 96.7% for AHI cut-offs ≥5, ≥15, and ≥30 events/h respectively (Table 4.12). Moreover, good accuracy (78.9%) and kappa (0.70) were observed for 4 class diagnosis (Table 4.14).

4.4.1 Novelties of the designed algorithm

The current study extensively tested unattended AF and SpO_2 signals with an optimized logic-based automatic algorithm. All the recording included in this study were obtained at patient's home that lay the foundation for an efficient screening process for type 4 portable monitoring. It is important to highlight three main novelties of this study. Firstly, this study used an algorithm that can detect apnea and hypopnea events from AF and SpO_2 signals. AF envelope tracking and subsequent digitization approaches were implemented within the algorithm that can satisfy the updated AASM scoring rules (Berry et al., 2017). Intra-event fluctuations (transient variation during an apnea event) and inter-event abnormalities (sighs) were precisely corrected. In addition, the precise detection of hypopnea events was aligned with the updated AASM guidelines (Berry et al., 2017). The lag-time in SpO_2 was adjusted for the reliable detection of hypopneas. Several logical optimizations were performed throughout the algorithm to detect apneas and hypopneas. Thus, the designed algorithm precisely estimated AHIs, contrasting other studies that used a single channel (AF or SpO_2). It is evidential that the single-channel oximetry cannot be an effective alternative of combined AF and SpO_2 to the accurate diagnosis of sleep apnea (Álvarez et al., 2020). Single-channel oximetry-based approaches (Chung et al., 2012; Gutiérrez-Tobal et al., 2018) are somehow responsible for reduced performance, whereas dual-channel (AF and SpO_2) approaches have been reported with better accuracy (Álvarez et al., 2020). Additionally, most of the conventional single-channel AF-based devices like the SleepStrip (Shochat et al., 2002), SleepCheck (de Almeida et al., 2006), ApneaLink (Rofail et al., 2010) reported poor agreement (sensitivity and specificity) as well as large mean bias and wider limits of agreement (*LoA*). ApneaLink device developed by Erman et al. (2007) reported good performance with an AHI cut-off 15 but not impressive for other AHI cut-offs. The reduced performance was attributed to use of a single signal (AF or SpO_2), whereas both AF and SpO_2 are recommended for sleep apnea automatic diagnosis. Secondly, the current algorithm identified the estimated TST by analyzing the AF and SpO_2 signals. Good agreement was found between the scored TST and estimated EST.

The incorporation of estimated TST instead of TRT resulted in good agreements for sleep apnea diagnosis. Thirdly, the designed algorithm was tested with a large random validation set for performance evaluation.

4.4.2 Comparison with existing methods

Incorporation of the novel features made the designed algorithm robust and reliable compared to other existing approaches. Due to the use of different datasets, number of records, detection methods, and performance parameters, it would not be feasible to directly compare our method with the existing dual-channel (AF and SpO_2) approaches. W. Huang et al. (2017) proposed an automatic approach using AF and SpO_2, where time lag adjustment and detection of additional hypopneas were not estimated. In addition, AHI was estimated using TRT, hence a wider 95% *LoA* (17.8 to -18.6 events/h) resulted. Other similar approaches (Álvarez et al., 2020; Ayappa et al., 2008; Chai-Coetzer et al., 2011; de Oliveira et al., 2009; Masdeu et al., 2010; Ward et al., 2015) shown a wider LoA, where TRT (with or without removing artefact section) was used to estimate AHI. Álvarez et al. (2020) reported *ICC* of 0.93 between scored and detected AHIs, whereas the overall accuracies were found 94.8%, 90.6%, and 95.9% using AHI cut-offs ≥5, ≥15, and ≥30 events/h, respectively. The results indicate the lowest performance (sensitivity 96%, specificity 72.7%) with commonly used AHI cut-off (≥15) to distinguish normal and disease groups. Thus, this approach can significantly underestimate normal group when a cut-off ≥15 events/h is set for 2-class diagnosis. Ayappa et al. (2008) reported sensitivity of 85% and specificity 91% with AHI cut-off ≥15, whereas Masdeu et al. (2010) reported sensitivity of 86%, specificity 84%, and accuracy 85% with AHI cut-off ≥10. These results were based on the comparison of AHIs where both the scoring and detection of hypopneas were performed using 4% oxygen desaturation criteria. Though the approaches implemented simple oxygen desaturation criteria (≥4%) for hypopnea detection, the performance was not significantly improved with the use of different AHI cut-offs. Chai-Coetzer et al. (2011) reported sensitivity of 88% and specificity 82% with a cut-off ≥30, whereas de Oliveira et al. (2009) reported sensitivity of 96% and specificity 64% with a cut-off ≥5. Using a cut-off ≥5, Ward et al. (2015) reported sensitivity of 80% and specificity 83% for the diagnosis of sleep apnea in an unattended home setting.

In addition to binary (2 class) diagnosis using a specific AHI cut-off, a 4-classes (normal, mild, moderate, and severe) of diagnosis is very important to assess the overall performance of the designed algorithm. A recent study (Álvarez et al., 2020) reported a 4-class accuracy of 81.3% and kappa 0.71 from a validation set of 96 AF and SpO_2 records, whereas our method resulted in the 4-class accuracy of 78.9% and kappa 0.70 from a large validation set of 943 records. Machine learning-based diagnostic performance reported by Álvarez et al. (2020) may be significantly reduced with a large validation set.

From the overall comparison with the existing literatures (dual-channel approaches) as mentioned above, it is clearly seen that our proposed algorithm outperformed. Moreover, our reported algorithm performs better than the existing automatic approaches if we considered the following critical issues. Firstly, the number of validation dataset that greatly influence the overall performance of the automatic algorithm. The existing algorithms were validated with a smaller dataset (78 to 121 records) (Álvarez et al., 2020; Ayappa et al., 2008; Chai-Coetzer et al., 2011; de Oliveira et al., 2009; Masdeu et al., 2010; Ward et al., 2015), whereas the present study used 943 records to validate. Secondly, our proposed algorithm was designed to perform reliably even in the presence of noisy signals without unnecessarily discarding valuably collected data. Several correction approaches were implemented that significantly minimized the effects of noise or artefacts, e.g., smoothing to minimizing random noise, inter-event correction of 'erroneous peak' during sighs, intra-event correction of sudden signal fluctuations during an apnea event, and removal of SpO_2 section where O_2 level fell to zero. Thus, the proposed algorithm can manage recordings with noisy signals. In addition, the algorithm can be applied to studies of short recording duration. This contrast existing approaches requiring the exclusion of records of some 8 to 10%, for example, studies with SpO_2 artefact due to patient movement and low quality (noisy) AF signal (Álvarez et al., 2020), and studies with low study recording period (e.g., <4 h, de Oliveira et al. (2009); Ward et al. (2015)).

4.4.3 Applications

The proposed automatic algorithm can report AHI with other parameters (number and indexes for apnea and hypopnea) for detailed diagnosis, where machine-learning based approach fails to report detail diagnosis (Álvarez et al., 2020; Jung et al., 2018). Thus, the current dual-channel based algorithm is suitable for simple type 4 portable sleep screeners for home applications as well as for clinical/laboratory PSG studies.

4.4.4 Study limitations

The presented automatic method has been addressed with some possible limitations. Firstly, the estimated AHI was compared with the standard reported in the SHHS where the apnea event was scored with absent of airflow or ≥75% drop in the peak excursion, whereas the updated AASM recommended ≥90% drop for apnea scoring. The basis for a ≥90% drop is entirely arbitrary but is an attempt to operationalize the requirement of 'absent or nearly absent airflow' (Berry et al., 2012). For noisy and low-amplitude signals, it is almost challenging to score an apnea event with satisfying the '≥90% drop' rule, where the peak excursion during the 'complete cessation of breathing' is often found >10% of its baseline due to intra-event fluctuations. The scoring of apnea

event with ≥75% drop may overestimate some apneas (i.e., some hypopneas are scored as apneas), the overall number of events (apneas + hypopneas) or AHI will not be significantly affected.

Secondly, estimated TST from the analysis of AF and SpO_2 signals may overestimate or underestimate the scored TST. Though the application of estimated TST to execute AHI was found more logical than applying TRT, the estimated TST may deviate from scored TST.

Thirdly, detection of additional hypopnea by applying specific criteria (≥2 to <3% oxygen desaturation with a duration ≥20 s) may overestimate the overall AHI. The dual-channel (AF and SpO_2)-based approaches have no other alternative signals to accurately determine TST and additional hypopneas.

Fourthly, the Sleep Heart Health Study dataset relied on home polysomnograms and used an oronasal thermocouple (thermistor) for recording the airflow signal. According to the updated AASM guidelines, nasal pressure signal is recommended for hypopnea scoring that allows more hypopneas to be detected than with the thermistor.

Finally, the designed algorithm was validated using 943 PSG recording from the SHHS. It would be more reliable if validated with data from other study populations. In addition, the validation of the designed algorithm is recommended with using different PSG recording equipment.

Though the present study outperformed over the existing approaches, the above limitations can influence our results.

Since there are no other alternative signals to assist the diagnostic process, the limitations listed above exist for any dual-channel (AF and SpO_2)-based approach. Thus, our designed algorithm presently cannot address the above limitations.

Chapter 5

Modified Diagnosis of Sleep Apnea

5.1 Introduction

The automatic diagnosis of sleep apnea using the airflow (AF) and oximetry (SpO_2) signals showed reliable performance as described in the earlier chapter. The envelope tracking approach (Chapter 4) can detect an accurate peak excursion for approximately >95% of the total AF duration as depicted in Figure 5.1a. However, the approach does not track closely the upper boundary of fluctuations in breathing, thus inducing an incorrect peak excursion in small sections of the AF signal (e.g., see the dash line black box in Figure 5.1b). The lower boundary appropriately recognized all trough points of AF signal (Figure 5.1b). This phenomenon has some impact on the overall apnea/hypopnea event detection. In addition, the upper boundary falls short of detecting the end point of an apnea event (see the dash line black boxes in Figure 5.1c). Thus, the upper boundary tracking incorrectly tracked the sharp rise in airflow and amplitude change that are usually found at the end of an apnea event (Figure 5.1c). This phenomenon may explain the lower diagnostic performance, as reported in Chapter 4.

Furthermore, for the determination of ≥3% oxygen desaturation for hypopnea detection, decrements in algorithm performance arose when applying a specific window length. In selecting a specific window length of 30 s (albeit optimally estimated) together with a binary sequence may still not precisely detect the exact start and end of each oxygen desaturation occurrence (Chapter 4). Thus, the estimated desaturation duration may not temporally correspond with the AF drop for hypopnea detection, hence contributed to the lower diagnostic performance. Moreover, a specific SpO_2 time-lag adjustment (20 s) may further impact on the overall diagnostic performance (Chapter 4).

A sample-to-sample encoding of AF and SpO_2 signals would have the advantage of minimizing problems associated with the AF envelope tracking and fixed-window based SpO_2 digitization. This chapter addresses the design and function of a modified algorithm for the automatic diagnosis of sleep apnea from AF and SpO_2 signals that can minimize the above-mentioned issues by employing a sample-to-sample encoding process of AF and SpO_2 signals.

This study reports a fully automatic modified algorithm for the diagnosis of sleep apnea from the AF and SpO_2 signals. The new technique aimed to resolve the above-mentioned limitations and addressed a novel concept using per-sample encoding of AF and SpO_2 signals to detect apnea

and hypopnea events, the algorithm aligned with the updated AASM scoring guidelines. Additionally, the algorithm applied an estimated TST (please see Chapter 4, page 57-58) instead of TRT for the automatic determination of AHI. The modified automatic algorithm was validated with a large dataset of 943 recordings.

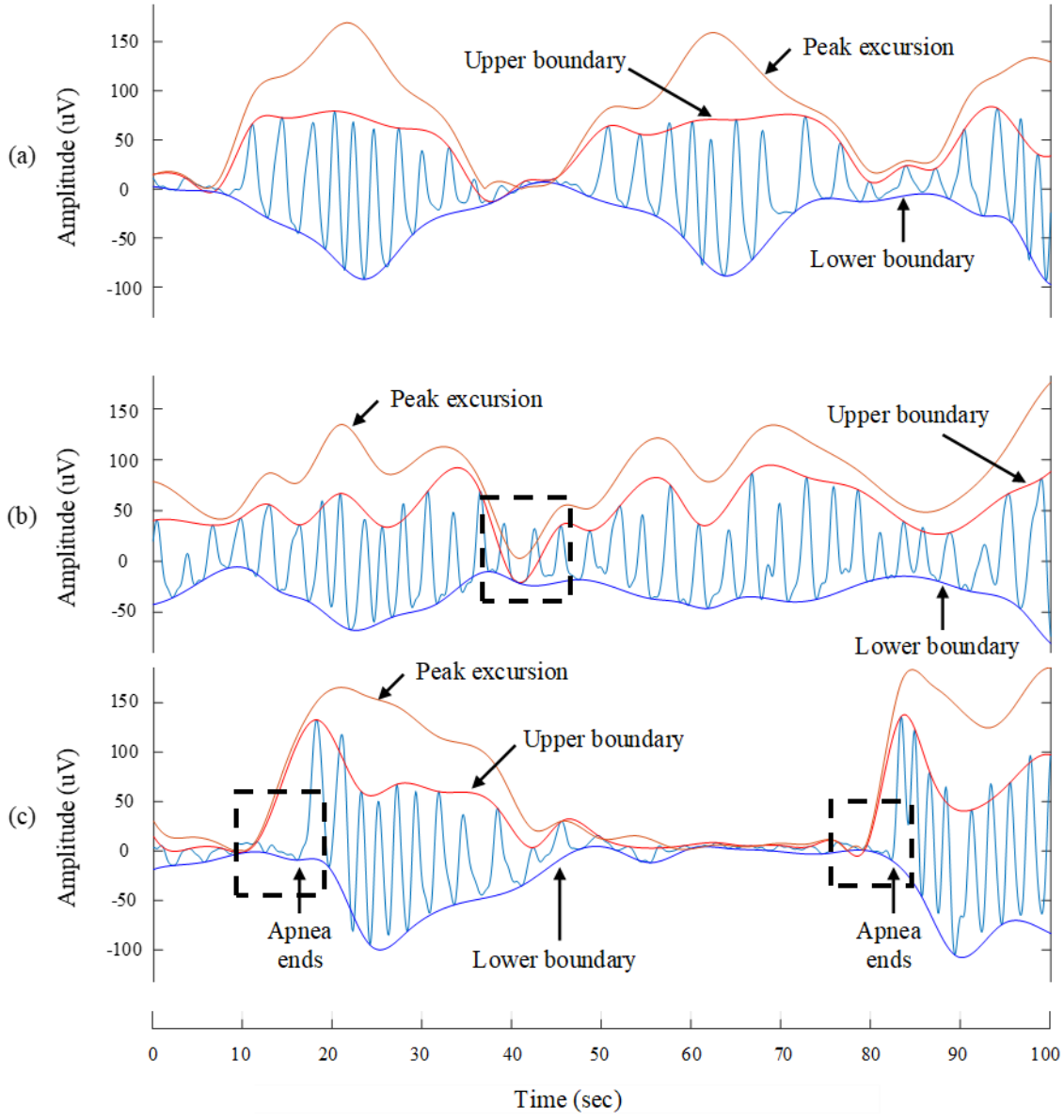

Figure 5.1. Illustration of identified issues with envelope tracking in detecting respiratory events.

5.2 Methods

5.2.1 **PSG records and demographics** (see Section 4.2.1, page 55)

Demographic and scoring summary of PSG records (please see Table 4.1 on page 56)

5.2.2 Designing a modified algorithm

An automatic algorithm for the diagnosis of sleep apnea was designed using multiple steps as shown in Figure 5.2. The algorithm inputs were the raw AF and SpO_2 signals, and gave output information of estimated AHI. A first step was to estimate the total sleep time (TST) from the automatic analysis of AF and SpO_2 signals (as explain in Chapter 4). Apnea events were detected from the per-sample encoding of AF signal. Hypopnea events were detected from the per-sample encoding of AF and SpO_2 signals along with the adjustment of associated SpO_2 time lag. Finally, the algorithm estimated AHI (output) from the total number of detected apnea and hypopnea events divided by the estimated TST. Figure 5.2 depicts the step-by-step design of the automatic algorithm.

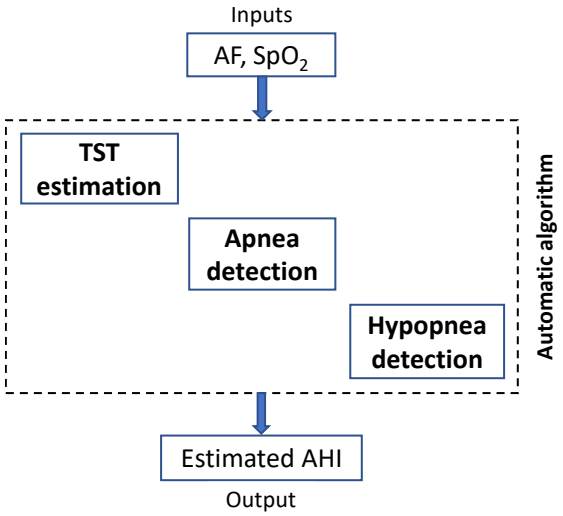

Figure 5.2. Block diagram of the designed automatic algorithm.

TST estimation

The combined analysis of AF and SpO_2 signals and the corresponding optimization process (please see Chapter 4, page 57-58) yielded the estimated TST for the automatic diagnosis.

Apnea detection

The raw AF was smoothed using a 3-point moving average filter to produce the preprocessed AF. A single breath consists of two phases: inhalation and exhalation. The maximum amplitude of inhalation is known as peak, whereas the minimum amplitude of exhalation is called trough (Figure 5.3a). The vertical height difference between the peak and trough is called peak-to-trough amplitude or peak excursion (Figure 5.3a). The horizontal distance between the peak and trough is called peak-to-trough distance.

In practice, a sharp transition to a high amplitude is often found. Due to this sharp transition, the upper boundary envelope tracking incorrectly detected peak excursion for some breaths, as

reported in Chapter 4. We determined the accurate peak excursion by analyzing the peak-to-trough distance of 900 normal breaths and the results showed a mean peak-to-trough distance of approximately 1.5 s, that varies from 1 to 2 s (***Appendix I***). Since a window length of 2 s encompassed both the peak and trough points of each breath, the peak excursion was determined by applying a 2-s sliding window (Figure 5.3a). Additionally, since a window longer than 2 s caused the event boundary to become fuzzy, a duration time window of 2 s was applied as recommended by W. Huang et al. (2017). Thus, applying a 2 s window minimized the limitations associated with the envelope tracking method.

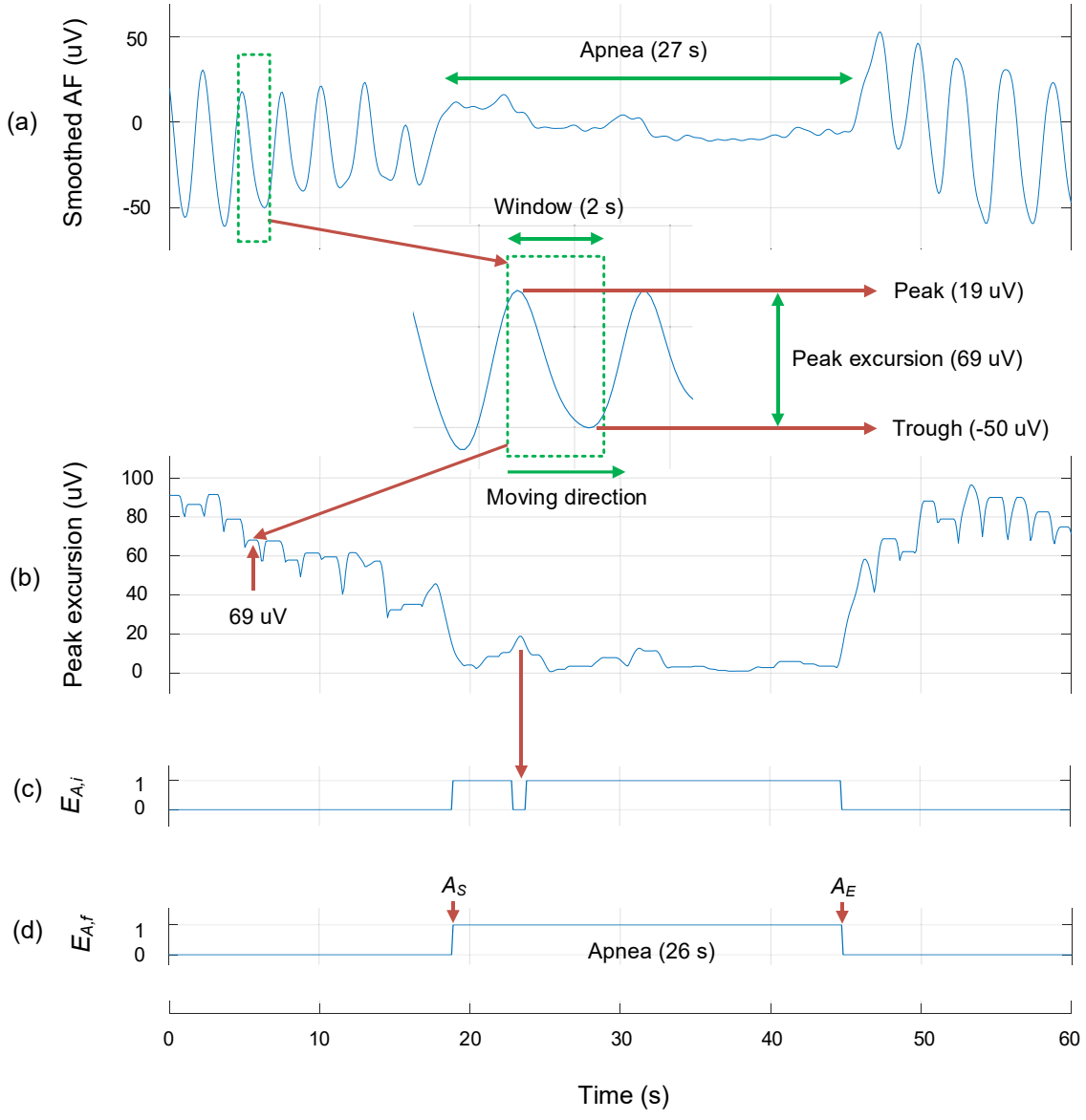

Figure 5.3. Apnea event detection from peak excursion tracking and digitization.

Equation (5.1) was used to derive the peak excursion from the sliding window as follow:

$$(PE)_i = |(W_P)_i - (W_T)_i| \tag{5.1}$$

where, $(W_P)_i$, $(W_T)_i$, and $(PE)_i$ were the peak (maximum), trough (minimum), and peak excursion (resultant) amplitudes. The subscript *i* indicated the current location of the window. Thus, the derived peak excursion (69 μV) determined from the sliding window at *i*-th location was equal to the actual peak-to-trough amplitude (69 μV) of the corresponding AF breath. The sliding window was then moved forward by one sample distance (0.1 s, since the sampling frequency of AF was 10 Hz) of AF and the above calculation using (5.1) executed the peak excursion at (*i*+1)-th location. This process was initiated at the starting sample of the smoothed AF and continue till the ending sample. Thus, per-sample tracking of the AF using a 2-s sliding window resulted in a corresponding continuous peak excursion signal (Figure 5.3b).

Since a peak excursion contains the peak-to-trough amplitude of each breath, the algorithm can pick up sighs, which occur during sleep (Perez-Padilla et al., 1983). A sigh is defined as an abnormal breath (artefact) where the magnitude is excessively higher than the normal breath. These sighs may result in insertion of "erroneous" large peaks in the determination of peak excursions. The erroneous peaks resulted from the sighs were removed from the derived peak excursion (please see Chapter 4, page 57).

Encoding is the process of converting data from one form to another. In this algorithm, each sample amplitude of the peak excursion (after removing the erroneous large peaks) was encoded to a binary digit ('1' or '0', '1' representing ≥90% drop in the peak excursion, whereas '0' for <90% drop) using (5.2) as follows:

$$(BD)_i = \begin{cases} 1, & \text{if } (PE)_i \leq \frac{10}{100}(BA)_i \\ 0, & \text{otherwise} \end{cases} \tag{5.2}$$

where, $(BD)_i$ $(PE)_i$, and $(BA)_i$ denote the binary digit, peak excursion amplitude, and baseline amplitude for the *i*-th location respectively. The baseline amplitude for *i*-th location was determined from the maximum amplitude in the 2 minutes (i.e., 1200 samples) preceding the *i*-th location, as recommended in the updated AASM guidelines (Berry et al., 2012). Thus, an initial encoded sequence for apnea ($E_{A,i}$) was generated against the peak excursion where the binary digit '1' represented ≥90% drop (Figure 5.3c).

In practice, the AF signal usually shows minor fluctuations rather than a flat line during an apnea event (see an example, red arrow, Figure 5.3c). Due to these fluctuations, the algorithm generated a binary digit '0' during an apnea event (Figure 5.3c). An auto-correction step was applied and the final encoded sequence for apnea ($E_{A,f}$) was generated (Figure 5.3d). Thus, the final encoding represented a continuous sequence of '1's against the duration of an apnea event (Figure 5.3d).

From the final encoded sequence for apnea (E_{Af}), the algorithm can identify an apnea start-point (A_S), i.e., from the binary sequence where '0' was detected followed by at least one hundred successive '1's (10 s). Similarly, the apnea end-point (A_E) was identified where '0' was detected preceding at least one hundred successive '1's (Figure 5.3d). Thus, the difference in timing between A_E and A_S was calculated for the apnea duration (at least 10 s). The designed algorithm resulted in a consistent shortening of the detected apnea duration by approximately 1 s (Figure 5.3a and Figure 5.3d). Thus, the per-sample tracking approach with a 2 s sliding window and a consistent shortening of the detected apnea duration could miss-detect some apneas when ≥10 s is set for apnea duration. This miss-detection tendency (due to the consistent shortening of the detected apnea duration) was further analyzed by identifying the optimal apnea duration threshold; the number of apnea detected was then compared with that re-scored (3666 apneas) in the development set as per Chapter 4 (page 63) and data listed in ***Appendix J***.

To arrive at an optimized threshold for apnea duration, varying apnea duration of ≥8 s, ≥9 s, and ≥10 s were tested in the development set. The apnea scores for each threshold duration were compared with the re-scored apneas. Table 5.1 shows that the total number of detected apneas with ≥9 s duration threshold closely approximates the total number of re-scored apneas. In addition, false detection was minimized, and the highest correlations were achieved with ≥9 s apnea duration threshold. The optimized duration threshold (≥9 s) also resulted in the highest Pearson's correlation coefficient (r = 0.995) and intraclass correlation coefficient (ICC = 0.997) between the detected and re-scored apneas. Other duration thresholds (≥8 and ≥10 s) contributed to significant false detection and lower correlation coefficients. Thus, the ≥9 s apnea duration threshold was set within the automatic process and the number of detected apnea events was listed with their corresponding duration and timing (A_S and A_E).

Table 5.1. Selecting apnea duration threshold for the development set.

Detected apneas [duration threshold]	Scored apneas	Difference	*r*	*ICC*	95% *CI*
3830 [8 s]	3666	-164	0.994	0.997	0.994 – 0.999
3527 [9 s]	3666	**+139**	**0.995**	**0.997**	**0.994 – 0.998**
3280 [10 s]	3666	+386	0.993	0.992	0.980 – 0.996

'+' and '-' signs respectively indicate the overall number of miss-detected and over-detected apneas; Correlations was resulted from the record-wise analysis of re-scored and detected apneas; *r*, *ICC*, and *CI* respectively represent the Pearson's correlation coefficient, intraclass correlation coefficients, and confidence interval.

Hypopnea detection

Hypopnea with ≥3% oxygen desaturation: For hypopnea event detection, AF drop (≥30% that lasts ≥10 s) must take place with a ≥3% oxygen desaturation. The automatic algorithm took the AF signal as input and produced the peak excursion (see Apnea detection section). A binary

sequence against the AF peak excursion was generated using ≥30% drop criterion, as similarly done for apnea event detection. The start and end timing of each ≥30% drop was detected from the binary sequence. The difference between the end and start timing represented the duration of ≥30% drop. For hypopnea detection, the duration of ≥30% drop must be ≥10 s. Thus, the start and end timing of ≥30% drop with a duration of ≥10 s were considered for further analysis. These start and end timing of ≥30% drop ≥10 s were represented by H_S and H_E respectively.

The algorithm then took the SpO_2 signal as another input. The raw SpO_2 was preprocessed to remove unwanted artefacts, e.g., a sudden fall to zero. The preprocessed SpO_2 contains two phases: desaturation and resaturation. The timing of desaturation (D_{Start} and D_{End}) was determined from the preprocessed SpO_2 as depicted in Figure 5.4a. At first, the desaturation phase was tracked and sample-to-sample digitization was performed. Each sample saturation value was encoded to a binary digit ('1' or '0') using (5.3) as follows:

$$(E)_i = \begin{cases} 1, & \text{if } [(SpO_2)_{i-1} - (SpO_2)_i] \geq 1 \\ 0, & \text{otherwise} \end{cases} \tag{5.3}$$

where, $(E)_i$ represents the encoded digit for i-th sample saturation. $(SpO_2)_{i-1}$ and $(SpO_2)_i$ respectively indicate the saturation values in percentage for (i-1)-th and i-th sample saturation. Thus, each sample saturation value was represented by a binary digit as shown in Figure 5.4b. The representation of binary digits, corresponding to desaturation and resaturation phases, were respectively indicated by the arrows 'A' and 'B'. The sample-to-sample binary digits ('1's) were not continuous during the desaturation phase (Figure 5.4b). Thus, an appropriate correction was needed for the sample-to-sample binary digits. A 15-s moving window was applied to correct for the binary digits. When two '1's were separated by <15 s, the intermediate '0's between those '1's were converted to '1's. Thus, the corrected digital sequence represents the desaturation phase by a continuous sequence of binary digit '1's (Figure 5.4c). From the corrected digital sequence, the timing (starting: D_{Start} and ending: D_{End}) of the desaturation phase was recorded.

The algorithm returned to the preprocessed SpO_2 to characterize the ≥3% oxygen desaturation level for hypopnea detection and recorded the saturation values in percentage (S_{Start} and S_{End}) for the corresponding timing (D_{Start} and D_{End} respectively). S_{Start} and S_{End} indicated the saturation values in percentage for the respective D_{Start} and D_{End}. The percentage of desaturation (D) was calculated from the difference between S_{Start} and S_{End}. Thus, D_{Start}, D_{End}, and its corresponding %D were considered. For at least 3% desaturation (i.e., D≥3%), D_{Start} and D_{End} were recorded for detecting hypopnea events associated with ≥3% oxygen desaturation.

The SpO_2 signal is always lagged in time to the AF signal. In Chapter 4, we applied a fixed, backward shift of 20 s to account for the time lag. Whilst this duration worked well and captured most hypopnea events, this time lag is not fixed and may vary approximately from 10 to 30 s (Otero

et al., 2012). Thus, in this chapter we resolved this issue by correcting for the time lag by an appropriate backward shift duration as required.

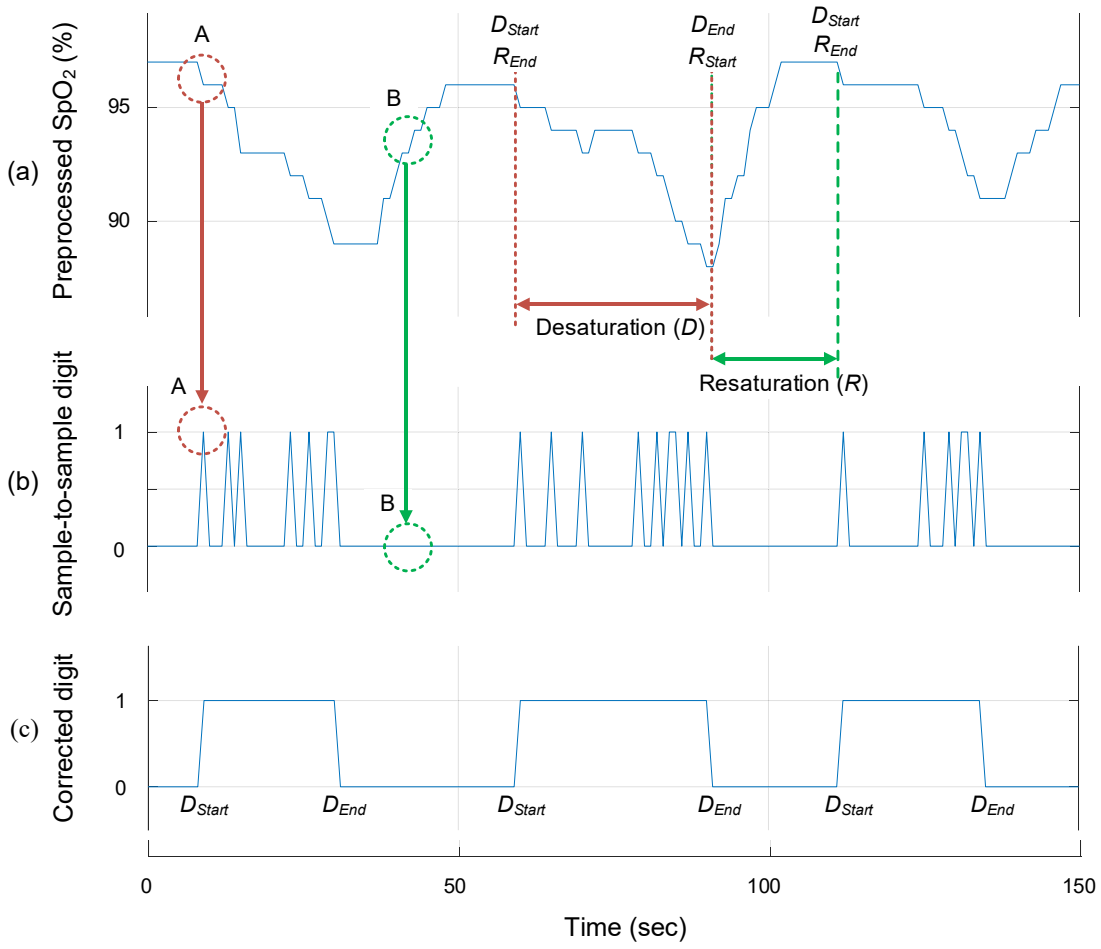

Figure 5.4. Oxygen desaturation phase tracking for generating sample-to-sample binary digit.

Figure 5.5 shows two sections of ≥3% desaturations (desat A and desat B) that resulted from their corresponding ≥30% AF drop of ≥10 s (drop A and drop B). The start and end of ≥3% oxygen desaturation are represented by D_{Start} and D_{End}, whereas H_S and H_E represents the start and end of ≥30% drop of ≥10 s. For both hypopnea events (as shown in Figure 5.5), an approximately 20 s time lag exists between the AF signal drop and oxygen desaturation, where their overlaps are depicted by the blue color boxes. The parallel overlapping between the durations of ≥30% drop ≥10 s and ≥3% oxygen desaturation is represented by blue color boxes.

No backward shifting (BS) was required where overlapping in signals existed between the durations of ≥30% AF drop ≥10 s and ≥3% oxygen desaturation (Figure 5.5). Thus, applying 0 s time lag adjustment (no backward shifting in D_{Start}), the modified algorithm detected hypopneas for these overlapping scenarios, where H_S and H_E were recorded as the start and end timing of hypopnea event.

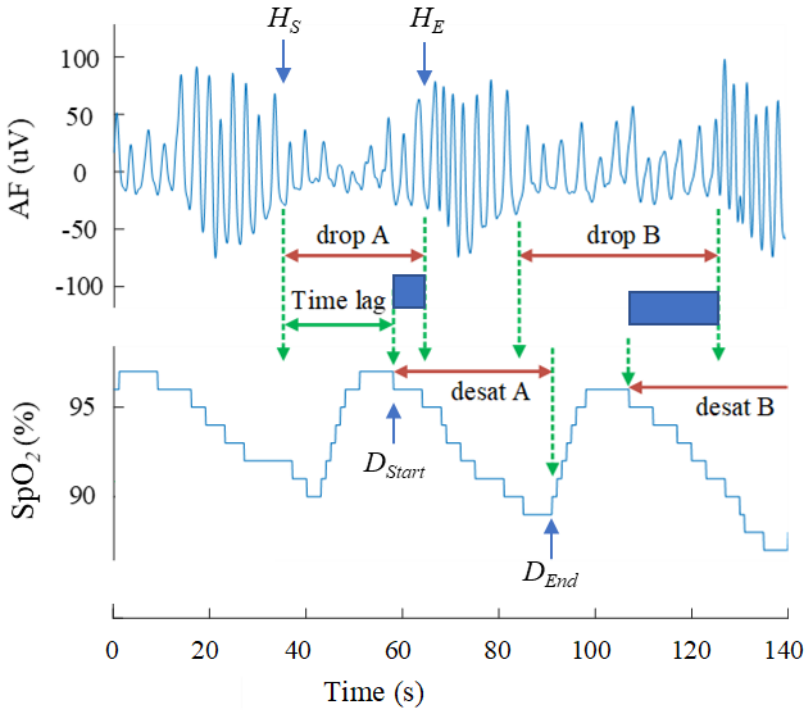

Figure 5.5. Hypopnea detection with overlapping between AF drop and desaturation.

In cases where the time lag in SpO_2 was very long, no overlapping was observed between the durations of ≥30% AF drop ≥10 s and ≥3% oxygen desaturation (Figure 5.6). Thus, no hypopnea was detected when 0 s time lag adjustment (0 s BS) was considered. Applying 10 s BS of SpO_2 signal, an overlapping existed between the durations of ≥30% AF drop ≥10 s and ≥3% oxygen desaturation. Thus, applying 10 s time lag adjustment (10 s backward shifting in D_{Start}), the modified algorithm detected the first and second hypopnea events (hypopnea 1 and hypopneas 2) as shown in Figure 5.6. Similarly, the modified algorithm detected the third hypopnea event by applying a 20 or 30 s BS of SpO_2 signal (Figure 5.6). Thus, the modified algorithm applied 0, 10, 20, and 30 s time lag adjustment in turn (one-by-one) to detect all hypopneas. This process would detect many duplicate hypopneas that were removed and the remaining hypopneas (with their corresponding start and end timing) were recorded. The hypopneas that overlapped with previously detected apneas were removed and the remaining events were finally considered as the number of detected hypopneas associated with ≥3% oxygen desaturation.

Optimization: This algorithm detected hypopneas with considering time lags (0, 10, 20, and 30 s), where the corrected binary digit (Figure 5.4c) was generated from sample-to-sample binary digit (Figure 5.4b) using a 15 s moving window. This window length (15 s) was found optimal (the highest correlations), whereas other lengths of window (10 and 20 s) were sub-optimal (Table 5.2).

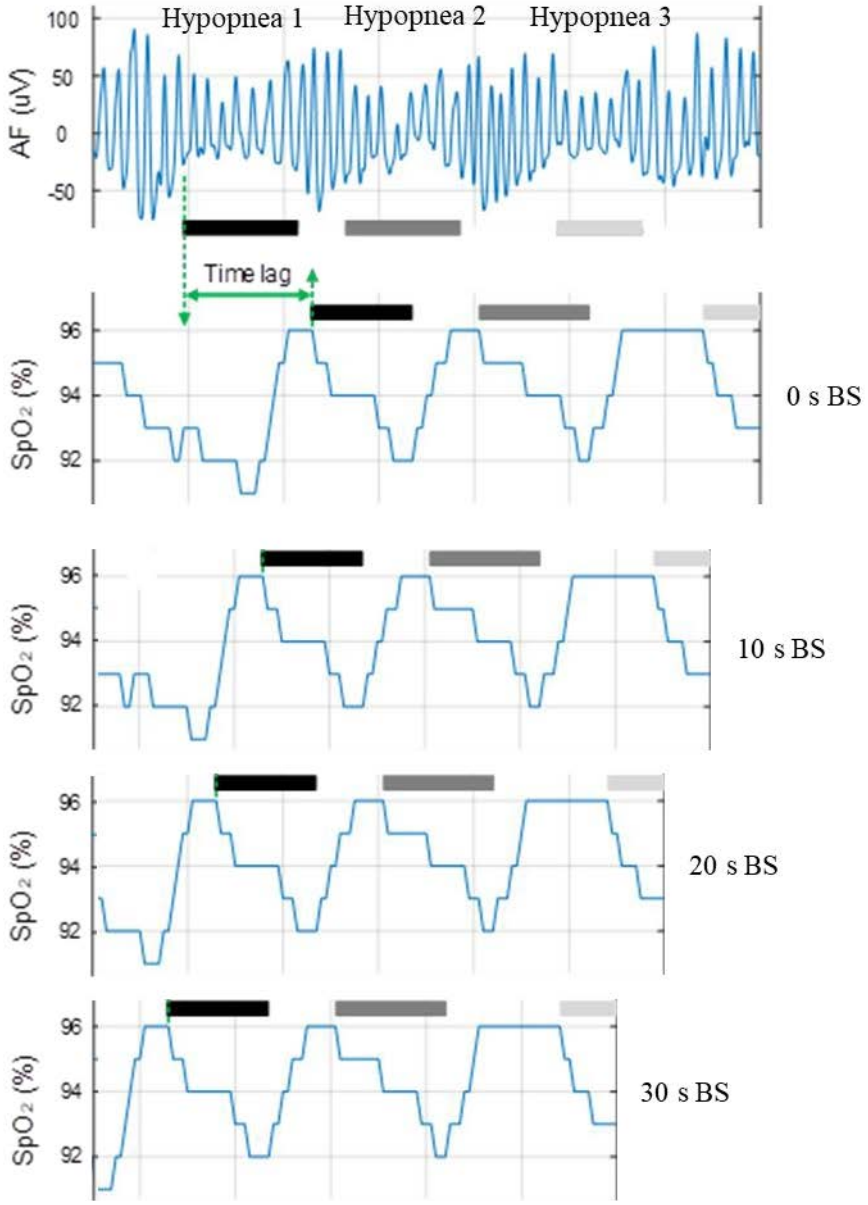

Figure 5.6. Backward shifting (BS) of SpO_2 signal in accordance with varying time lag.

Table 5.2. Selecting window length for binary digit correction.

Detected hypopneas [window length]	Scored hypopneas	Difference	*r*	*ICC*	95% *CI*
3927 [10 s]	4069	+142	0.968	0.983	0.970 – 0.991
4300 [15 s]	4069	**-231**	**0.977**	**0.986**	**0.974 – 0.994**
4155 [20 s]	4069	-86	0.964	0.982	0.967 – 0.990

'+' and '-' signs respectively indicate the overall number of miss-detected and over-detected hypopneas; Correlations was resulted from the re-record-wise analysis of scored and detected hypopneas; *r*, *ICC*, and *CI* respectively represent the Pearson's correlation coefficient, intraclass correlation coefficients, and confidence interval.

Additional hypopnea detection: As per Chapter 4, hypopnea events associated with arousal but <3% oxygen desaturation were detected and designated 'additional hypopneas'. An approximate approach proposed for detecting these hypopneas considered ≥2% to <3% oxygen desaturation, since the SpO_2 often fluctuated by about 1% during normal breathing. In this chapter, we applied backward shifting of 0, 10, 20 and 30 s in sequence to detect additional hypopneas associated with arousal (assumed).

The approximate approach detected the start and end of all desaturations (≥2% to <3%), as similarly done above. An additional hypopnea was detected when a backward shifted D_{Start} and D_{End} were bounded by the boundaries (H_S and H_E) of ≥30% drop with a duration of ≥10 s. Thus, the timing (H_S and H_E) of the additional hypopnea event was recorded when the above criteria were fulfilled. Additional hypopneas that were overlapped with previously detected apneas and hypopneas (with ≥3% oxygen desaturation) were removed. Thus, the remaining hypopneas were counted as the additional hypopneas (assumed as an approximate number of hypopneas associated with arousal but <3% oxygen desaturation). These detected additional hypopneas (n = 1076, from the development set) were added to previously detected hypopneas (with ≥3% oxygen desaturation) to compute the total number of hypopneas (associated with ≥3% oxygen desaturation or an arousal).

The algorithm is now ready to compute the AHI from automatically detected total number of apneas, total number of hypopneas (associated with ≥3% oxygen desaturation or an arousal), and estimated TST. The algorithm computed the AHI using (4.5) as follows:

$$AHI = \frac{No.of\ detected\ (apneas + hypopneas)}{Estimated\ TST} \tag{5.4}$$

This fully automatic algorithm requires no human input for respiratory event analysis and TST estimation. Once the raw AF and SpO_2 are fed to the algorithm, the automatic process takes over and delivers the AHI.

5.3 Results

5.3.1 Performance in development set

Correlation coefficients: The modified automatic algorithm was developed with a development set of 45 records. The modified algorithm detected respiratory events (apneas and hypopneas), sleep period, and finally estimated AHI, which was compared to manual scoring reported in the SHHS (actual AHI). The record-wise actual and estimated AHI are tabulated in

Appendix L). Strong correlations were found between the automatically estimated and actual AHI (r = 0.96, ICC = 0.98, 95% CI = 0.96 to 0.99) as illustrated in Figure 5.7.

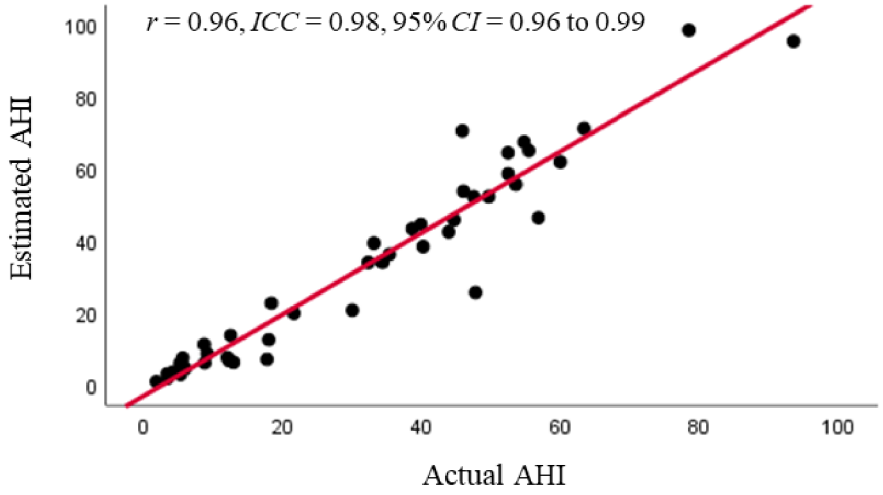

Figure 5.7. Scatter plot of the correlation between actual and estimated AHI.

Bland-Altman plot: The Bland-Altman plot (difference vs average of the actual and estimated AHI) illustrates good agreement across a whole range of AHI severity (mean bias, 95% *CI*, and mean bias ± 95% *LoA* were -1.4, 0.9 to -3.7, and 13.5 to -16.3 events/h respectively) (Figure 5.8). The record-wise actual and estimated AHI and their differences are tabulated in ***Appendix L***).

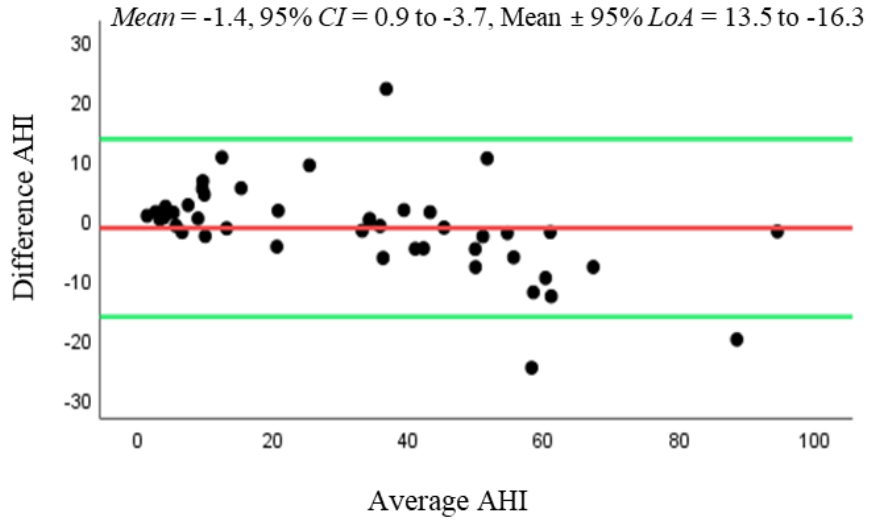

Figure 5.8. Bland-Altman plot of AHI.

Sensitivity, specificity, and accuracy: The confusion matrices for 2 class (binary) diagnosis with commonly used AHI cut-offs are listed in Table 5.3. The overall performance of the automatic algorithm for the development set is listed in Table 5.4. The agreement between the estimated and actual AHI was determined by using three common AHI cut-offs (≥5, ≥15, and

≥30). The overall accuracies of diagnosis were found 97.8%, 95.6%, and 97.8% for AHI cut-offs ≥5, ≥15, and ≥30 events/h respectively (Table 5.4).

Table 5.3. Confusion matrices for 2 class diagnosis.

		Estimated		Estimated		Estimated	
		Positive (AHI ≥5)	*Negative (AHI <5)*	*Positive (AHI ≥15)*	*Negative (AHI <15)*	*Positive (AHI ≥30)*	*Negative (AHI <30)*
Actual	*Positive*	40	1	28	2	24	1
	Negative	0	4	0	15	0	20

AHI: apnea hypopnea index

Table 5.4. Agreement between estimated and actual classes for 2 class diagnosis.

Performance parameters	Cut-offs		
	AHI ≥5	*AHI ≥15*	*AHI ≥30*
TP	40	28	24
TN	4	15	20
FP	0	0	0
FN	1	2	1
PPV (%)	100	100	100
NPV (%)	80	88.2	95.2
Sensitivity (%)	97.6	93.3	96
Specificity (%)	100	100	100
Accuracy (%)	97.8	95.6	97.8
AUC	0.99	0.97	0.98
k	0.88	0.90	0.96

AHI: Apnea hypopnea index, TP: True positives, TN: True negatives, FP: False positives, FN: False negatives, PPV: Positive predictive value, NPV: Negative predictive value, AUC: Area under ROC curve, *k*: Cohen's kappa coefficient. PPV, NPV, sensitivity, specificity, and accuracy were calculated using (*K1*) to (*K5*) respectively, as indicated in ***Appendix K***.

The confusion matrix for 4 classes (normal, mild, moderate, and severe) of diagnosis is listed in Table 5.5. The class-wise and overall performances of the automatic algorithm for the development set is listed in Table 5.6. The agreement between the estimated and actual classes was determined by using the AHI range of the corresponding class. The accuracies of diagnosis were found to be 97.8%, 93.3%, 93.3%, and 97.8% for normal, mild, moderate, and severe class respectively (Table 5.6). The overall 4 class accuracy and kappa were found 91.1% and 0.86 respectively (Table 5.6).

The overall performance in the development set was outstanding due to the optimizations applied throughout the design process. The actual performance was found by testing the automatic algorithm with an unknown large validation set of 943 records as described below.

Table 5.5. Confusion matrix for 4 class diagnosis.

		Estimated			
		Normal	*Mild*	*Moderate*	*Severe*
Actual	*Normal*	4	0	0	0
	Mild	1	10	0	0
	Moderate	0	2	3	0
	Severe	0	0	1	24

Table 5.6. Agreement between estimated and actual classes for 4 class diagnosis.

Performance parameters	AHI classes/groups			
	Normal	*Mild*	*Moderate*	*Severe*
TP	4	10	3	24
TN	40	32	39	20
FP	1	2	1	0
FN	0	1	2	1
PPV (%)	80	83.3	75	100
NPV (%)	100	97	95.1	95.2
Sensitivity (%)	100	90.9	60	96
Specificity (%)	97.6	94.1	97.5	100
Accuracy (%)	97.8	93.3	93.3	97.8
4 class accuracy (%)	91.1			
4 class kappa	0.86			

AHI: Apnea hypopnea index, TP: True positives, TN: True negatives, FP: False positives, FN: False negatives, PPV: Positive predictive value, NPV: Negative predictive value. TP, FP, FN, and TN of the specific class were calculated using (*K6*) to (*K9*) respectively; PPV, NPV, sensitivity, and specificity of the specific class were calculated using (*K1*) to (*K4*) respectively; 4 class accuracy were calculated using (*K10*), as mentioned in ***Appendix K***.

5.3.2 Performance in validation set

Correlation coefficient: The automatic algorithm was tested with a large and unknown validation set of 943 records. The algorithm detected respiratory events (apneas and hypopneas), sleep period, and finally estimated AHI, which was compared to manual scoring reported in the SHHS (actual AHI). The record-wise actual and estimated AHI are tabulated in ***Appendix M***). Strong correlations were found between the automatically estimated and actual AHI ($r = 0.90$, *ICC* = 0.94, 95% *CI* = 0.94 to 0.95) as depicted in Figure 5.9.

Bland-Altman plot: Bland-Altman plot (difference vs average of the actual and estimated AHI) illustrates good agreement across a whole range of AHI severity (mean bias, 95% *CI*, and mean bias ± 95% *LoA* were -0.7, -0.3 to -1.1, and 12.3 to -13.8 events/h respectively) as illustrated

in Figure 5.10. The record-wise actual and estimated AHI and their differences are in ***Appendix M***.

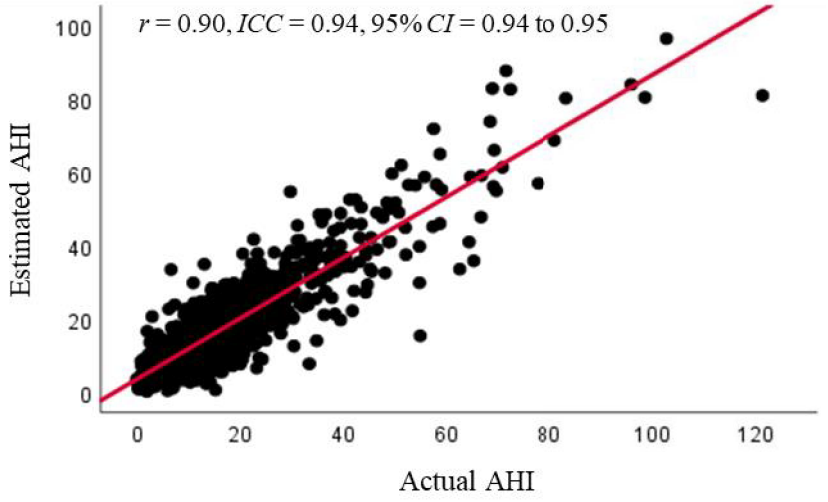

Figure 5.9. Scatter plot of the correlation between actual and estimated AHI.

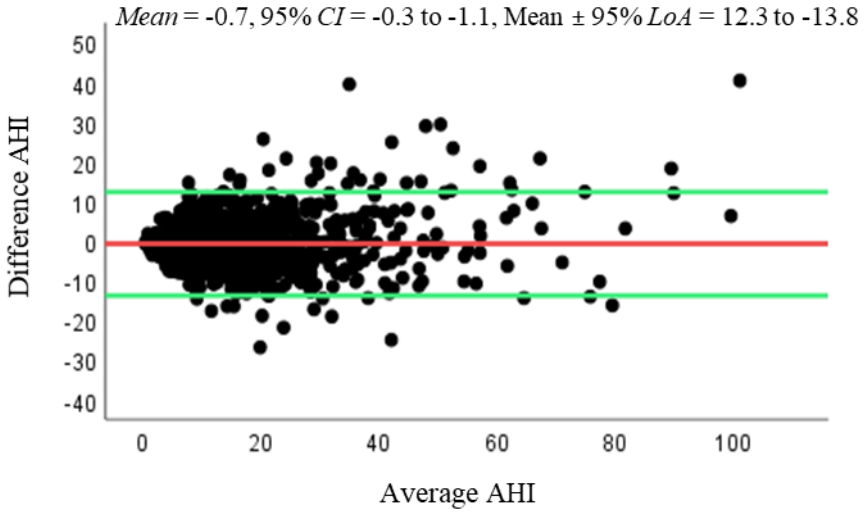

Figure 5.10. Bland-Altman plot of AHI.

Sensitivity, specificity, and accuracy: The confusion matrices for 2 class (binary) diagnosis with commonly used AHI cut-offs are listed in Table 5.7. The overall performance of the automatic algorithm for the validation set is listed in Table 5.8. The agreement between the estimated and actual AHI was determined by using three common AHI cut-offs (≥5, ≥15, and ≥30). The overall accuracies of diagnosis were found 93.5%, 92.4%, and 96.5% for AHI cut-offs ≥5, ≥15, and ≥30 events/h respectively (Table 5.8).

The automatic algorithm showed strong agreement between actual and estimated AHI for all AHI cut-offs except some special conditions such as- (i) lowest specificity (73%) was observed

when the sample size of the normal class (AHI <5) was too small (n = 200) with respect to the total size of the validation set (n = 943), and (ii) too narrow range of AHI for detecting normal class (0≤ AHI <5) was also responsible for the lowest specificity, and hence the lowest kappa of 0.77. The automatic algorithm might often overestimate or underestimate around the narrow range of AHI, thus producing reduced agreement for the normal class.

Table 5.7. Confusion matrices for 2 class diagnosis.

		Estimated		Estimated		Estimated	
		Positive (AHI ≥5)	*Negative (AHI <5)*	*Positive (AHI ≥15)*	*Negative (AHI <15)*	*Positive (AHI ≥30)*	*Negative (AHI <30)*
Actual	*Positive*	752	13	370	30	114	19
	Negative	48	130	42	501	14	796

AHI: Apnea hypopnea index

Table 5.8. Agreement between estimated and actual classes for 2 class diagnosis.

Performance parameters	Cut-offs		
	AHI ≥5	*AHI ≥15*	*AHI ≥30*
TP	752	370	114
TN	130	501	796
FP	48	42	14
FN	13	30	19
PPV (%)	94	89.8	89.1
NPV (%)	90.9	94.4	97.7
Sensitivity (%)	98.3	92.5	85.7
Specificity (%)	73	92.3	98.3
Accuracy (%)	93.5	92.4	96.6
AUC	0.86	0.92	0.92
k	0.77	0.84	0.85

AHI: Apnea hypopnea index, TP: True positives, TN: True negatives, FP: False positives, FN: False negatives, PPV: Positive predictive value, NPV: Negative predictive value, AUC: Area under ROC curve, *k*: Cohen's kappa coefficient. PPV, NPV, sensitivity, specificity, and accuracy were calculated using (*K1*) to (*K5*) respectively, as indicated in ***Appendix K***.

The confusion matrix for 4 classes (normal, mild, moderate, and severe) of diagnosis is listed in Table 5.9. The class-wise and overall performances of the automatic algorithm for the validation set is listed in Table 5.10. The agreement between the estimated and actual classes was determined by using the AHI range of the corresponding class. The accuracies of diagnosis were found 93.5%, 86.7%, 90%, and 96.6% for normal, mild, moderate, and severe class respectively (Table 5.10). The overall 4 class accuracy and kappa were found 83.4% and 0.77 respectively (Table 5.10).

The automatic algorithm showed strong agreement between actual and estimated classes except some special conditions such as- (i) lowest sensitivity (76%) was observed for the normal class, where the actual sample size of the normal class was too small (n = 200) with respect to the total size of the validation set (n = 943), and (ii) too narrow range of AHI for the normal class (0≤ AHI <5) was also responsible for the lowest sensitivity. These special conditions might be responsible for the reduced 4 class accuracy (83.4%) and kappa (0.77).

Table 5.9. Confusion matrix for 4 class diagnosis.

		Estimated			
		Normal	*Mild*	*Moderate*	*Severe*
Actual	*Normal*	152	47	1	0
	Mild	13	311	38	2
	Moderate	0	26	209	13
	Severe	0	1	16	114

Table 5.10. Agreement between estimated and actual classes for 4 class diagnosis.

Performance parameters	AHI classes/groups			
	Normal	*Mild*	*Moderate*	*Severe*
TP	152	311	209	114
TN	730	507	640	797
FP	13	74	55	15
FN	48	51	39	17
PPV (%)	92.1	80.8	79.2	88.4
NPV (%)	93.8	90.9	94.3	97.9
Sensitivity (%)	76	85.9	84.3	87
Specificity (%)	98.3	87.3	92.1	98.2
Accuracy (%)	93.5	86.7	90	96.6
4 class accuracy (%)	83.4			
4 class kappa	0.77			

AHI: Apnea hypopnea index, TP: True positives, TN: True negatives, FP: False positives, FN: False negatives, PPV: Positive predictive value, NPV: Negative predictive value. TP, FP, FN, and TN of the specific class were calculated using (*K6*) to (*K9*) respectively; PPV, NPV, sensitivity, and specificity of the specific class were calculated using (*K1*) to (*K4*) respectively; 4 class accuracy were calculated using (*K10*), as mentioned in ***Appendix K***.

5.3.3 Modified algorithm vs envelope-based algorithm

The performance of the sample-to-sample algorithm was compared to the envelope-based approach (Chapter 4) as shown in Table 5.11. It is clearly seen that the modified algorithm resulted in lower mean bias compared to the envelope-based algorithm. A mean bias of -0.7 events/h was observed with this modified approach, whereas a mean bias of -1.6 events/h was resulted in with envelope method (Chapter 4). In addition, significant percentage increments in overall accuracies (for 2 class and 4 class diagnosis) were observed (Table 5.11). The modified method showed an increment of 1.4% and 2.2% respectively for 2 and 4 class diagnosis accuracies with respect to envelope method (Chapter 4). In addition, an overall 4 class accuracy was significantly improved by 4.5%, whereas 4 class kappa was increased from 0.70 to 0.77 (compared to envelope-based algorithm in Chapter 4).

Table 5.11. Performance comparison (envelope-based approach vs modified approach).

Performance parameters		Envelope-based approach (*Chapter 4*)	Modified approach (*Chapter 5*)
Overall performance	*r*	0.91	0.90
	ICC	0.95	0.94
	Mean bias (event/h)	**-1.6**	**-0.7**
	Mean ± 95% *LoA* (event/h)	10.9 to -14.1	12.3 to -13.8
2 class diagnosis	Average PPV (%)	87.8	91
	Average NPV (%)	96	94.3
	Average sensitivity (%)	93.8	92.2
	Average specificity (%)	82.2	87.9
	Average accuracy (%)	**92.8**	**94.2**
	Average AUC	0.88	0.90
	Average *k*	0.79	0.82
4 class diagnosis	Average PPV (%)	82.7	85.1
	Average NPV (%)	92.6	94.2
	Average sensitivity (%)	78.8	83.3
	Average specificity (%)	92.3	94
	Average accuracy (%)	89.5	91.7
	4 class accuracy (%)	**78.9**	**83.4**
	4 class kappa	**0.70**	**0.77**

r: Pearson's correlation coefficient, *ICC*: Intraclass correlation coefficient, *LoA*: Limits of agreement, PPV: Positive predictive value, NPV: Negative predictive value, AUC: Area under ROC curve, *k*: Cohen's kappa coefficient.

5.4 Discussion

In this study, we reported an improved algorithm employing a sample-to-sample encoding approach using AF and SpO_2 signals for the diagnosis of sleep apnea. For performance evaluation, the output of the automatic algorithm (estimated AHI) was compared to the actual AHI (reported in the SHHS). The overall accuracies (binary class diagnosis) were found 93.5%, 92.4%, and 96.6% for AHI cut-offs ≥5, ≥15, and ≥30 events/h respectively (Table 5.8). Moreover, excellent overall accuracy (83.4%) and kappa (0.77) were observed for the 4 classes of diagnosis (Table 5.10). The modified algorithm resulted in lower mean bias compared to the envelope-based algorithm (Table 5.11). The increment of 1.4% and 4.5% respectively for 2 and 4 class diagnosis accuracies were observed in the modified method compared to the envelope method (Table 5.11). In addition, 4 class kappa increased significantly from 0.70 to 0.77 (Table 5.11).

5.4.1 Novelties of the modified algorithm

The current modified study extensively tested unattended AF and SpO_2 signals with an optimized logic-based automatic algorithm. Applying a 2 s sliding widow instead of using AF envelope (upper and lower boundaries), the current algorithm detected peak excursion from per-sample encoding of AF signal. The 2 s sliding window correctly detected the peak and trough amplitudes of each breath, whereas the envelop tracking method (Chapter 4) incorrectly detected the peak amplitudes of some breaths when applying upper boundary tracking. The sample-to-sample tracking (i.e., the per-sample encoding) of AF signal correctly identified the difference between peak and trough amplitudes, hence accurate detection of peak excursion throughout the recording duration. Thus, the current study corrected for the erroneous peak excursion due to fluctuations in the upper boundary) as seen in Chapter 4. In addition, per-sample encoding method more precisely detected the end-point of an apnea event, whereas the upper boundary (envelope method in Chapter 4) falls short of detecting the end-point of an apnea event. The current method detected the duration of an apnea events of ~9 s against a true duration of 10 s, whereas the envelope tracking detected an apnea duration of ~8 s. Thus, the per-sample encoding method more precisely responded to the sharp rise in airflow and amplitude change that are usually found at the end of an apnea event. Hence, the modified algorithm more precisely detected apnea events from per-sample encoding of AF signal (compared to AF envelope method) that also satisfies the updated AASM scoring rules (Berry et al., 2017).

In addition, the current algorithm applied a sample-to-sample encoding of SpO_2 signal. This per-sample encoding method accurately tracked each desaturation step in the SpO_2 signal and thus, precisely detected the start and end of each oxygen desaturation phase. In contrast, the determination of oxygen desaturation applying a specific window length (30 s) may

overestimate the duration of oxygen desaturations (Chapter 4). Moreover, the current algorithm employed all possible amount of time lag (0, 10, 20, and 30 s) adjustment in SpO_2 signal, whereas the envelope tracking method applied only 20 s backward shifting (Chapter 4). Addressing all possible amount of time lag within the current algorithm made the automatic detection of hypopnea more accurate, logical, and robust with respect to the envelope method. Thus, per-sample encoding of AF and SpO_2 signals vastly improved the diagnostic performance compared to envelope method (Chapter 4).

5.4.2 Comparison with other automatic approaches

Incorporation of the novel features made the modified algorithm robust and reliable compared to other automatic approaches. The estimated AHI (automatic method) was compared to the standard (scored AHI) for performance evaluation of dual-channel (AF and SpO_2)-based approaches. Álvarez et al. (2020) reported the overall accuracies of 94.8%, 90.6%, and 95.9% using AHI cut-offs ≥5, ≥15, and ≥30 events/h respectively. Ayappa et al. (2008) reported sensitivity of 85% and specificity 91% with AHI cut-off ≥15, whereas Masdeu et al. (2010) reported sensitivity of 86%, specificity 84%, and accuracy 85% with AHI cut-off ≥10. Chai-Coetzer et al. (2011) reported sensitivity of 88% and specificity 82% with a cut-off ≥30, whereas de Oliveira et al. (2009) reported sensitivity of 96% and specificity 64% with a cut-off ≥5. Using a cut-off ≥5, Ward et al. (2015) reported sensitivity of 80% and specificity 83% for the diagnosis of sleep apnea in an unattended home setting. The AF envelope tracking and digitization approach (Chapter 4) was reported with overall accuracies (2 class diagnosis) of 90.7%, 91%, and 96.7% for AHI cut-offs ≥5, ≥15, and ≥30 events/h respectively. The current per-sample encoding approach resulted in the overall accuracies (2 class diagnosis) of 93.5%, 92.4%, and 96.6% for AHI cut-offs ≥5, ≥15, and ≥30 events/h respectively. Thus, for 2 class diagnosis, the overall comparison showed that the per-sample encoding method outperformed over other automatic approaches.

In addition to binary (2 class) diagnosis using a specific AHI cut-off, 4 classes (normal, mild, moderate, and severe) of diagnosis is very important to assess the class-wise and overall performance of the designed algorithm. A recent study (Álvarez et al., 2020) reported 4 class accuracy of 81.3% and kappa 0.71 from a validation set of 96 AF and SpO_2 records, whereas our envelope-based method (Chapter 4) resulted in 4 class accuracy of 78.9% and kappa 0.70 from a large validation set of 943 records. In comparison to the above studies, the per-sample encoding method outperformed with a 4 class accuracy of 83.4% and kappa 0.77 for the same validation set of 943 records.

5.4.3 Applications

The proposed automatic algorithm can report AHI with other parameters (number and indexes for apnea and hypopnea) for detailed diagnosis, where machine-learning based approach fails to report detail diagnosis (Álvarez et al., 2020; Jung et al., 2018). Moreover, the presented approach outperformed over the existing approaches. Thus, the current dual-channel-based algorithm is suitable for simple type 4 portable sleep screeners for home applications as well as for clinical/laboratory PSG studies.

5.4.4 Study limitations

The presented modified method has been addressed with some possible limitations. Firstly, the estimated AHI was compared with the standard reported in the SHHS where the apnea event was scored with absent of airflow or ≥75% drop in the peak excursion, whereas the updated AASM recommended ≥90% drop for apnea scoring. Secondly, estimated TST from the analysis of AF and SpO_2 signals may overestimate or underestimate the scored TST. Finally, detection of additional hypopnea by applying a specific criteria (≥2 to <3% oxygen desaturation) may overestimate the overall AHI. Though the present study outperformed over the existing approaches, the above limitations can influence our results.

Chapter 6

Summary, Discussion and Future Works

This thesis represented a series of work that led to a superior algorithm that can be accurately and reliably applied to the automatic diagnosis of sleep apnea.

The systematic literature review has synthesized and summarized the existing automatic algorithms based on respiratory and oximetry signals to diagnose sleep apnea. Sixty-two studies were examined and the main findings reported whereas a single respiratory signal (AF or SpO_2), provided good support for binary class decision-making, multiple respiratory signals (AF, TE, and AE) combined with SpO_2 signal resulted in better in multi-class decision-making in sleep apnea diagnosis. Notably, the inclusion of EEG signals for automatic diagnosis, in addition to those of AF and SpO_2, would be expected to improve algorithm performance by analyzing power spectral changes between apnea duration groups. This notion led to Chapter 3, which addressed the power spectral analysis of EEG signal before and at apnea termination, and subsequent chapters on algorithm approaches to automatic diagnosis of sleep apnea.

The EEG spectral powers for theta, alpha and sigma bands decreased significantly as apnea was prolonged (≥30 s, Chapter 3). This observation suggests that transient EEG arousals, without awakenings, avoided sleep disruptions and therefore were protective of sleep. No significant difference was found when the apnea duration increased from 10 to 20 s. The EEG spectral powers were not uniform for all apnea events. In addition, it would be challenging to link hypopnea events with the changes of EEG spectral power or arousal. Due to the limitations associated with signal acquisition, processing, artefacts, complexity, and non-effective spectral features, it was concluded that EEG were inadequate as signals to be used reliably for sleep apnea diagnosis. The literature review (Chapter 2) suggested that it would be effective to use airflow and oximetry signals with excluding EEG for the diagnosis of sleep apnea. However, there remained many limitations with existing published automatic algorithms (Chapter 4).

This thesis presented a novel automatic algorithm for a reliable diagnosis of sleep apnea from AF and SpO_2 signals. Apnea and hypopnea events were detected by tracking and digitizing the AF envelope and oxygen desaturation. The developed algorithm incorporated the estimation of total sleep time from the combined analysis of AF and SpO_2, an approach not previously carried out (Chapter 4). Though the envelope-based approach showed good diagnostic performance, there were some possible limitations. The thesis advanced this by developing a modified algorithm that

overcome the limitations of the envelope-based approach. In the modified approach, apnea and hypopnea events were detected by per-sample encoding of AF and SpO_2 signals. This sample-to-sample encoding represented an approach that outperformed over the envelope-based approach. An increment of 1.4% and 4.5% respectively for 2 and 4 class diagnostic accuracies were resulted with the modified method compared to envelope method (Chapter 5). The modified algorithm also outperformed over the existing automatic approaches for sleep apnea diagnosis. The designed algorithm can provide significant ease of computational implication in event scoring and applicable for user-friendly home diagnosis of sleep apnea.

Despite the enhanced algorithm for sleep apnea diagnosis, there remains future work that could refine the current developed algorithm to produce a penultimate algorithm.

- A precise and accurate method for estimating TST without using EEG remains a target for future investigation, given that the estimated TST from the analysis of AF and SpO_2 signals may overestimate or underestimate the scored TST. A more sophisticated way to estimate TST would be the inclusion of cardiorespiratory signals (electrocardiogram and pulse plethysmogram). The above-mentioned cardiorespiratory signals are easy to collect and the end-used may not face any trouble during overnight acquisition. The inclusion of such additional signals with AF-SpO_2 may enhance the accuracy of the automatic diagnosis.

- Novel algorithms are required to reliably detect apnea event types, i.e., central, obstructive, and mixed apneas. For the detailed diagnosis of sleep apnea, the number of central, obstructive, and mixed apnea events and their indexes (e.g., central apnea index: number of central apnea events per hour of sleep) may add additional information for proper treatment. The future work will include the automatic detection of event types (central, obstructive, and mixed) for the detailed diagnosis of sleep apnea.

- Incorporation of newly developed machine learning method (deep learning) may be applied to design a robust diagnostic algorithm for sleep apnea diagnosis. The conventional classification approaches have been already developed and tested in numerous published articles, where the associated limitations and lower accuracy of the classification approaches were the big concerns. Newly developed deep learning approaches would be a good option to try in future.

- The confirmation of results with different dataset is very important. The current study used the first 1000 PSG records form shhs1 dataset for testing and validating the designed algorithm. Inclusion of the whole dataset of shhs1 would have been good for confirming

the results. In addition, other PSG-based datasets can be used for the justification of the algorithm's output.

Appendix A

Statistical analysis

To determine whether there are any statistically significant differences between the means of two or more independent groups, a one-way analysis of variance (ANOVA) (Howell, 2009) can be used. A one-way ANOVA can be used to evaluate EEG relative spectral power changes (dependent variable, measured from 0-100) based on apnea duration (independent variable with three levels: 'Short', 'Moderate', and 'Long').

Basic requirements of one-way ANOVA

To run a one-way ANOVA, six assumptions need to be considered. The first three assumptions relate to the choice of study design and the measurements, whilst the second three assumptions relate to how data fits the one-way ANOVA model. These assumptions are:

- *Assumption 1*: Must have one dependent variable that is measured at a continuous level. For the present study, one dependent variable was found (EEG relative spectral power).
- *Assumption 2*: Must have one independent variable that consists of three or more categorical**,** independent groups. For the present study found one independent variable (apnea duration) that consists of three independent groups (Short, Moderate, and Long).
- *Assumption 3*: Must have the independence of observations, which means that there is no relationship between the observations in each group of the independent variable or between the groups themselves. This study had 375 apnea events categorized into three groups. There was no relationship between the apnea events in each group or between the groups themselves.
- *Assumption 4*: There should be no significant outliers in the groups of the independent variable in terms of the dependent variable.
- *Assumption 5*: The dependent variable should be approximately normally distributed for each group of the independent variable.
- *Assumption 6*: Must have homogeneity of variances (i.e., the variance is equal in each group of the independent variable).

The present study design met assumptions 1, 2, and 3. This study tested the remaining main three assumptions as follows:

Testing for outliers

Outliers were tested in SPSS software (IBM SPSS Statistics 25) (Nie, Bent, & Hull, 1975) using the graphical user interface (GUI). The boxplots for the relative delta powers for C3 EEG before apnea termination (BAT) is shown in Figure A1. The simple boxplots enabled the determination of whether there were any outliers in the current data.

Any data points (e.g., any spectral powers) that were more than 1.5 box-lengths from the edge of their box were classified by Stata (SPSS software) as outside values (outliers). Those outliers were labeled with their case number for easy identification. No outliers were found for delta band (Figure A1). Two outliers with more extreme values were found for sigma band (Figure A2). Stata highlighted a data point with the star symbol in the 'Long' group (i.e., case number 334) as a potential outlier (i.e., case number 334 had an unusually large power of 11.41) and a data point in the 'Moderate' group (i.e., case number 227) as a potential outlier (i.e., case number 227 had an unusually large power of 14.59).

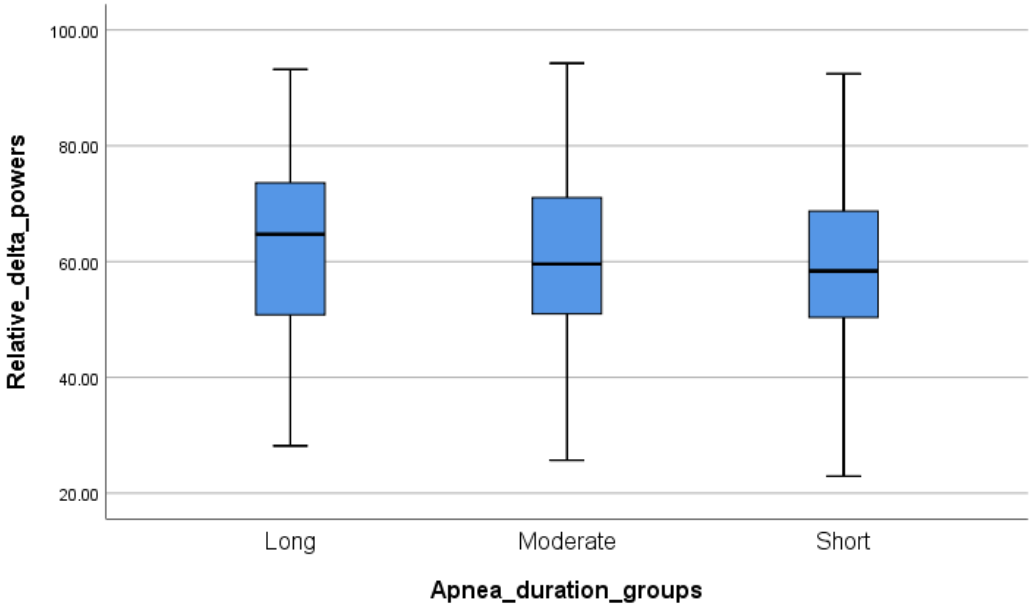

Figure A1. Boxplots for testing outliers (delta band)

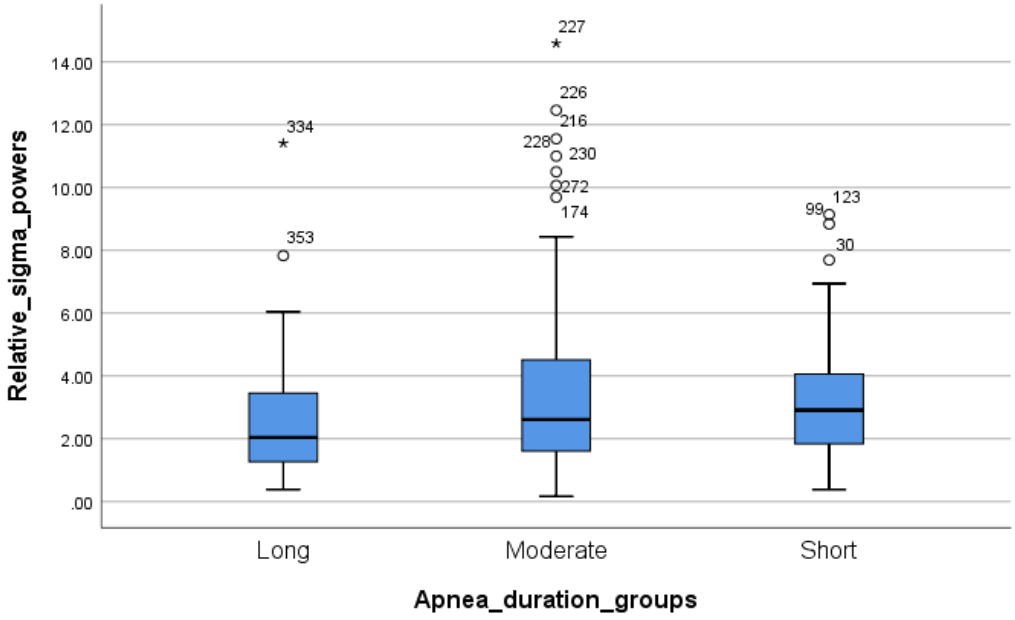

Figure A2. Boxplots for testing outliers (sigma band)

In this way, boxplots were generated for all spectral bands (delta, theta, alpha, sigma, and beta) with their corresponding channels (C3 and C4) and positions (before and after apnea termination). The summary of boxplots analysis is tabulated in Table A1.

There were no outliers in delta powers, but had many outliers for other bands (theta, alpha, sigma, and beta), as assessed by inspection of a boxplot. The total numbers of outliers/extreme outliers in the 'Short', 'Moderate', and 'Long' apnea duration groups were respectively 79/6, 71/10, and 33/6). Overall, the total number of outliers in the present study dataset was 183 out of 7500 data point, which indicated 2.44% outliers in the study dataset.

Table A1. Summary of testing for outliers

Frequency bands	EEG channels	Epoch Position[a]	No. of outliers (extreme/total)		
			Short	*Moderate*	*Long*
Delta	C3	BAT	0/0	0/0	0/0
		AAT	0/0	0/0	0/0
	C4	BAT	0/0	0/0	0/0
		AAT	0/0	0/0	0/0
Theta	C3	BAT	0/3	0/4	0/0
		AAT	0/4	0/3	0/1
	C4	BAT	1/5	0/4	0/1
		AAT	0/4	0/2	0/2
Alpha	C3	BAT	0/7	0/1	0/0
		AAT	0/3	0/2	1/3
	C4	BAT	0/5	0/3	0/0
		AAT	0/1	0/2	2/7
Sigma	C3	BAT	0/3	1/7	1/2
		AAT	2/5	0/2	1/4
	C4	BAT	0/2	6/8	1/5
		AAT	1/5	1/7	0/1
Beta	C3	BAT	1/5	1/8	0/1
		AAT	1/6	0/2	0/0
	C4	BAT	0/6	1/3	0/0
		AAT	0/9	0/3	0/0

[a]Positions of 10s EEG epochs: BAT = Before apnea termination, AAT = After apnea termination

Testing for normality

The Shapiro-Wilk test for normality (Shapiro & Francia, 1972) is a numerical method, but other methods can be used to determine normality, such as skewness/kurtosis values, or histograms. While it is most common to run only one type of normality test for a given analysis. The Shapiro-Wilk test is

recommended when the sample sizes are small (< 50) and are not confident visually interpreting Normal Q-Q Plots or other graphical methods used to test for normality. In this study, the sample sizes were more than 50. Thus, we choose Normal Q-Q Plots instead of the Shapiro-Wilk test for testing normality. The relative delta powers for the 'Long' group were normally distributed, as assessed by Normal Q-Q Plots (Figure A3), whereas the 'Long' group of sigma powers was not normally (or approximately normally) distributed (Figure A4).

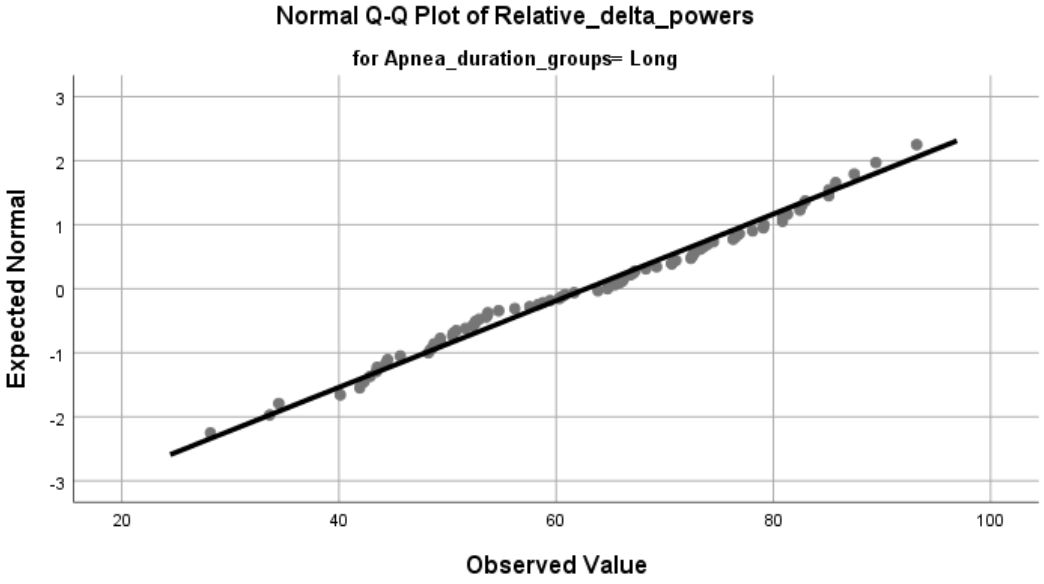

Figure A3. Testing normality for the 'Long' group of delta band

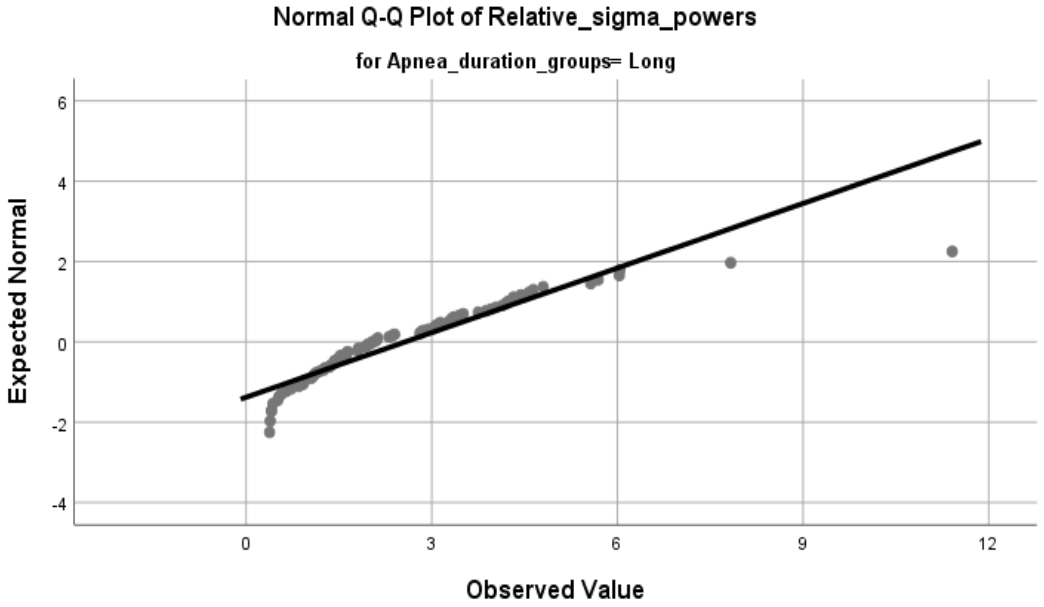

Figure A4. Testing normality for the 'Long' group of sigma band

In this way, we generated Normal Q-Q Plots for all spectral bands (delta, theta, alpha, sigma, and beta) with their corresponding channels (C3 and C4), positions (before and after apnea termination), and groups

(Short, Moderate, and Long). The summary of Normal Q-Q Plots analysis is tabulated in Table A2. Overall, the data were not normally distributed except for some groups of the delta band.

Table A2. Summary of testing for normality

Frequency bands	EEG channels	Epoch Position[a]	Normality[b]		
			Short	*Moderate*	*Long*
Delta	C3	BAT	N	N	N
		AAT	AN	AN	AN
	C4	BAT	AN	AN	AN
		AAT	NN	AN	AN
Theta	C3	BAT	NN	NN	AN
		AAT	NN	NN	NN
	C4	BAT	NN	NN	AN
		AAT	NN	NN	NN
Alpha	C3	BAT	NN	NN	NN
		AAT	NN	NN	NN
	C4	BAT	NN	NN	NN
		AAT	NN	NN	NN
Sigma	C3	BAT	NN	NN	NN
		AAT	NN	NN	NN
	C4	BAT	NN	NN	NN
		AAT	NN	NN	NN
Beta	C3	BAT	NN	NN	NN
		AAT	NN	NN	NN
	C4	BAT	NN	NN	NN
		AAT	NN	NN	NN

[a]Positions of 10s EEG epochs: BAT = Before apnea termination, AAT = After apnea termination

[b]Normality status: N = Normal, AN = Approximately normal, NN = Not normal

Testing for homogeneity of variance

This study used Levene's test for homogeneity of variances (Glass, 1966) in Stata using the graphical user interface (GUI). Table A3 shows the test results of homogeneity of variance for all bands for C3 EEG before apnea termination (BAT).

Levene's test for the sigma band returned a statistically significant result ($p < 0.05$) (Table A3). Therefore, the assumption of homogeneity of variances was violated for the sigma band. Levene's test was performed for all bands (delta, theta, alpha, sigma, and beta) with their corresponding channels (C3 and C4), and positions (BAT and AAT). The summary of Levene's test is tabulated in Table A4. Overall, the assumption of homogeneity of variances was not violated (i.e., the groups' variances are equal).

Table A3. Test of homogeneity of variance

Bands	Analysis	Levene statistic	df1	df2	*p*
Delta	Based on Mean	0.713	2	372	0.491
	Based on Median	0.663	2	372	0.516
	Based on Median and with adjusted df	0.663	2	368.049	0.516
	Based on trimmed mean	0.707	2	372	0.494
Theta	Based on Mean	0.442	2	372	0.643
	Based on Median	0.438	2	372	0.646
	Based on Median and with adjusted df	0.438	2	369.727	0.646
	Based on trimmed mean	0.454	2	372	0.635
Alpha	Based on Mean	1.346	2	372	0.262
	Based on Median	1.230	2	372	0.294
	Based on Median and with adjusted df	1.230	2	348.687	0.294
	Based on trimmed mean	1.262	2	372	0.284
Sigma	Based on Mean	7.047	2	372	0.001
	Based on Median	4.401	2	372	0.013
	Based on Median and with adjusted df	4.401	2	296.989	0.013
	Based on trimmed mean	5.971	2	372	0.003
Beta	Based on Mean	0.850	2	372	0.428
	Based on Median	0.514	2	372	0.599
	Based on Median and with adjusted df	0.514	2	368.110	0.599
	Based on trimmed mean	0.790	2	372	0.454

Table A4. Levene's test of homogeneity of variance

Frequency bands	EEG channels	Epoch Position[a]	Homogeneity of variance between groups
Delta	C3	BAT	Yes
		AAT	Yes
	C4	BAT	Yes
		AAT	Yes
Theta	C3	BAT	Yes
		AAT	Yes
	C4	BAT	Yes
		AAT	Yes
Alpha	C3	BAT	Yes
		AAT	Yes
	C4	BAT	Yes

		AAT	Yes
Sigma	C3	BAT	No
		AAT	No
	C4	BAT	Yes
		AAT	Yes
Beta	C3	BAT	Yes
		AAT	Yes
	C4	BAT	Yes
		AAT	Yes

[a]Positions of 10s EEG epochs: BAT = Before apnea termination, AAT = After apnea termination

The three main assumptions (4, 5, and 6) for one-way ANOVA were checked. The study data did not meet the requirements of outliers (assumption 4) and normality (assumption 5) but fulfilled assumption 6 (homogeneity of variance). Thus, One-way ANOVA was not appropriate for the present study data.

Kruskal-Wallis H test

The Kruskal-Wallis H test (sometimes also called the "one-way ANOVA on ranks") (Corder & Foreman, 2011; Kruskal & Wallis, 1952) is a rank-based nonparametric test that can be used to determine if there are statistically significant differences between two or more groups of an independent variable on a continuous or ordinal dependent variable. The Kruskal-Wallis H test is generally considered the nonparametric alternative to the one-way ANOVA, which can be used when the study data fail the assumptions of the one-way ANOVA. However, it should be noted that the Kruskal-Wallis H test cannot simply be considered an alternative to the one-way ANOVA. It has four assumptions that must be considered to accurately interpret the results.

- *Assumption 1*: Must have one dependent variable that is measured at a continuous level. For the present study, one dependent variable was found (EEG relative spectral power).
- *Assumption 2*: Must have one independent variable that consists of three or more categorical**,** independent groups. For the present study found one independent variable (apnea duration) that consists of three independent groups (Short, Moderate, and Long).
- *Assumption 3*: Must have the independence of observations, which means that there is no relationship between the observations in each group of the independent variable or between the groups themselves. This study had 375 apnea events categorized into three groups. There was no relationship between the apnea events in each group or between the groups themselves.
- *Assumption 4*: Must determine whether the distribution of spectral powers for each group of our independent variable have the same shape or a different shape. Having the same shape also means having the same variability. This will determine how we can interpret the results of the Kruskal-Wallis H test.

Test for similarly shaped distributions

By visually inspecting the boxplots, the distributions of spectral powers for the different apnea duration groups were analyzed. To view the boxplots, the Hypothesis Test Summary and Model Viewer window for the delta powers (C3 at BAT) were generated, as shown in Figure A5 and Figure A6 respectively.

Hypothesis Test Summary

	Null Hypothesis	Test	Sig.	Decision
1	The distribution of Relative_delta_powers is the same across categories of Apnea_duration_groups.	Independent-Samples Kruskal-Wallis Test	.366	Retain the null hypothesis.

Asymptotic significances are displayed. The significance level is .05.

Figure A5. Hypothesis test summary for delta band

Hypothesis Test Summary

	Null Hypothesis	Test	Sig.	Decision
1	The distribution of Relative_delta_powers is the same across categories of Apnea_duration_groups.	Independent-Samples Kruskal-Wallis Test	.366	Retain the null hypothesis.

Asymptotic significances are displayed. The significance level is .05.

Independent-Samples Kruskal-Wallis Test

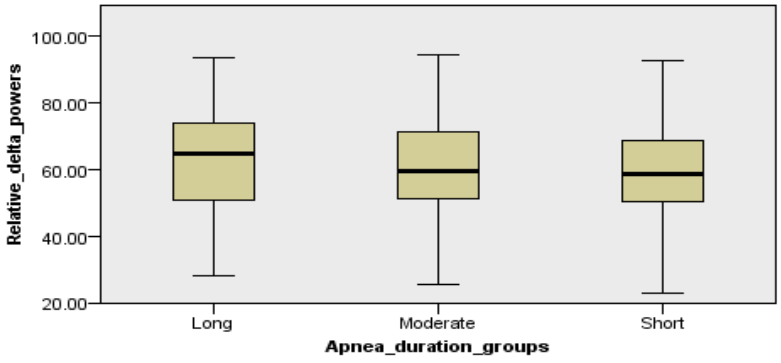

Total N	375
Test Statistic	2.009
Degrees of Freedom	2
Asymptotic Sig. (2-sided test)	.366

1. The test statistic is adjusted for ties.
2. Multiple comparisons are not performed because the overall test does not show significant differences across samples.

Figure A6. Model Viewer window

By visually inspecting the shapes of these distributions (boxplot), some differences were found in the distribution in delta powers (C3 at BAT) especially for the 'Long' apnea duration group (Figure A7).

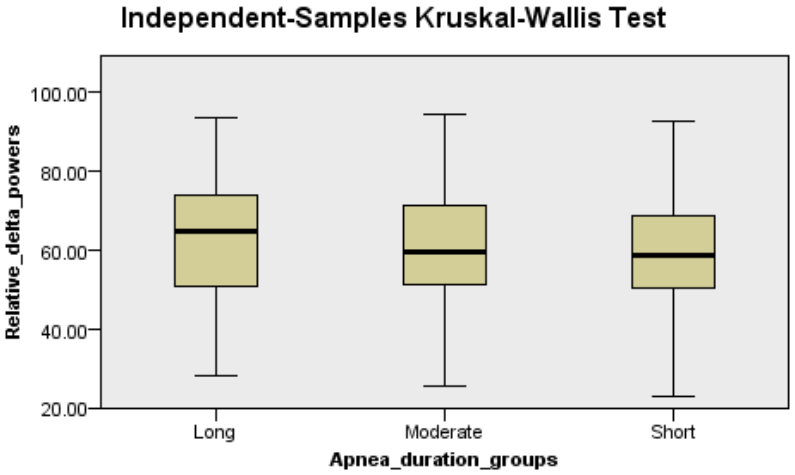

Total N	375
Test Statistic	2.009
Degrees of Freedom	2
Asymptotic Sig. (2-sided test)	.366

1. The test statistic is adjusted for ties.
2. Multiple comparisons are not performed because the overall test does not show significant differences across samples.

Figure A7. Boxplot and test statistic for delta band

The visual inspection of the boxplots showed that the delta powers (C3 at BAT) had similarly shaped distribution. This process was repeated to check the similarly shaped distributions for all spectral bands (delta, theta, alpha, sigma, and beta) with their corresponding channels (C3 and C4), and positions (BAT and AAT). The summary of this analysis is indicated in Table A5. Overall, the distributions of spectral powers were similar for all groups, as assessed by visual inspection of boxplots (Table A5).

Table A5. Summary for similarly shaped distributions

Frequency bands	EEG channels	Epoch Position[a]	Similarly shaped distributions between groups
Delta	C3	BAT	Yes
		AAT	Yes
	C4	BAT	Yes
		AAT	Yes
Theta	C3	BAT	Yes

		AAT	Yes
	C4	BAT	Yes
		AAT	Yes
Alpha	C3	BAT	Yes
		AAT	Yes
	C4	BAT	Yes
		AAT	Yes
Sigma	C3	BAT	Yes
		AAT	Yes
	C4	BAT	Yes
		AAT	Yes
Beta	C3	BAT	Yes
		AAT	Yes
	C4	BAT	Yes
		AAT	Yes

[a]Positions of 10s EEG epochs: BAT = Before apnea termination, AAT = After apnea termination

Summarizing test results

The distributions of spectral powers were found to be similar for the 'Short', 'Moderate', and 'Long' apnea duration groups. The Hypothesis Test Summary table (Figure A5) was revisited. The null hypothesis was retained since the result was not statistically significant ($p = 0.366$). The statistically not significant result ($p = 0.366$) indicated that median delta power (C3 at BAT) was different between the apnea duration groups. The overall result can be expressed as follows:

A Kruskal-Wallis H test was run to determine if there were differences in spectral powers between three groups of durations with different levels: the 'Short', 'Moderate', and 'Long' apnea duration groups. Distributions of spectral powers were similar for all groups, as assessed by visual inspection of a boxplot. Median relative spectral powers for delta band (C3 at BAT) were not statistically significantly different between groups, $\chi^2(2) = 2.009$, $p = 0.366$.

To report the results, the median values of the apnea duration groups and the number of apnea events (i.e., sample size) in each group were required. These values were found in the Report table under the 'Median' and 'N' columns, respectively, as shown in Table A6. The overall result can be expressed as follows:

A Kruskal-Wallis H test was conducted to determine if there were differences in delta powers (C3 at BAT) between groups that differed in their level of apnea duration: the 'Short' (n = 150), 'Moderate' (n = 144), and 'Long' (n = 81) apnea duration groups. Distributions of spectral powers were similar for all groups, as assessed by visual inspection of a boxplot. Median spectral powers increased from the Short

(58.385) to Moderate (59.585), to Long (64.720) apnea duration groups, but the differences were not statistically significant, $\chi^2(2) = 2.009$, $p = 0.366$.

Table A6. Reporting with relative spectral powers for delta band (C3 at BAT)

Apnea duration groups	N	Median
Long	81	64.720
Moderate	144	59.585
Short	150	58.385
Total	375	59.840

Post hoc test

When the Kruskal-Wallis H test was statistically significant (i.e., $p < 0.05$), a post hoc test was required to determine where the differences lied. According to the above-mentioned process, the Hypothesis Test Summary table for the sigma powers (C3 at BAT) was generated as shown in Figure A8. This test showed that the Kruskal-Wallis H test was statistically significant (i.e., $p < 0.05$) indicating that the median of at least one group was different from the median of another group. To discover which group(s) were different to which another groups, a post hoc test is required. In the case of the Kruskal-Wallis H test, all pairwise comparisons using Dunn (1964) procedure with a Bonferroni adjustment (Dunn, 1961) were run and interpreted.

Hypothesis Test Summary

	Null Hypothesis	Test	Sig.	Decision
1	The distribution of Relative_sigma_powers is the same across categories of Apnea_duration_groups.	Independent-Samples Kruskal-Wallis Test	.018	Reject the null hypothesis.

Asymptotic significances are displayed. The significance level is .05.

Figure A8. Hypothesis test summary for sigma band

The pairwise comparisons were run by SPSS Statistics as shown in Figure A9 and the overall results of all these pairwise comparisons can be expressed as follows:

Pairwise comparisons were performed using Dunn's procedure with a Bonferroni correction for multiple comparisons. Adjusted *p*-values are presented. This post hoc analysis revealed statistically significant differences in median relative spectral powers between the Long (2.040) and Short (2.910) ($p = 0.033$), and Long and Moderate (2.615) ($p = 0.028$) apnea duration groups, but not between the Short and Moderate apnea duration groups. It is perfectly possible to have a statistically significant Kruskal-Wallis H test but not statistically significant pairwise comparisons.

Using all the information from the Kruskal-Wallis H test and pairwise comparisons results, the overall results can be expressed as follows:

A Kruskal-Wallis H test was conducted to determine if there were differences in sigma powers (C3 at BAT) between groups that differed in their level of apnea duration: the 'Short' (n = 150), 'Moderate' (n = 144), and 'Long' (n = 81) apnea duration groups. Distributions of spectral powers were similar for all groups, as assessed by visual inspection of a boxplot. Median spectral powers were statistically significantly different between the different apnea duration groups, $\chi^2(2) = 8.052$, $p = 0.018$. Subsequently, pairwise comparisons were performed using Dunn's procedure with a Bonferroni correction for multiple comparisons. Adjusted *p*-values are presented. This post hoc analysis revealed statistically significant differences in median relative spectral powers between the Long (2.040) and Short (2.910) ($p = 0.033$), and Long and Moderate (2.615) ($p = 0.028$) apnea duration groups, but not between the Short and Moderate apnea duration groups.

Pairwise Comparisons of Apnea_duration_groups

Each node shows the sample average rank of Apnea_duration_groups.

Sample1-Sample2	Test Statistic	Std. Error	Std. Test Statistic	Sig.	Adj.Sig.
Long-Short	-38.044	14.946	-2.545	.011	.033
Long-Moderate	-39.139	15.055	-2.600	.009	.028
Short-Moderate	1.096	12.646	.087	.931	1.000

Each row tests the null hypothesis that the Sample 1 and Sample 2 distributions are the same.
Asymptotic significances (2-sided tests) are displayed. The significance level is .05.
Significance values have been adjusted by the Bonferroni correction for multiple tests.

Figure A9. Pairwise comparisons (post hoc test) for sigma band

In this way, using the Kruskal–Wallis H test, the statistical analysis was summarised for the relative spectral powers for all spectral bands (delta, theta, alpha, sigma, and beta) with their corresponding channels (C3 and C4), and positions (BAT and AAT), which was represented in the result section). Similar statistical investigations mentioned above were performed for the analysis of apnea event types (OSA, CSA, and MSA) and sleep states (NREM and REM) between different apnea duration groups. The Kruskal–Wallis H test was also qualified for those analysis and the summary analysis was represented in the result section.

Appendix B

Relative spectral powers at before apnea termination (BAT) for C3 EEG

Apnea event number	Apnea duration groups	Relative spectral powers				
		Delta	*Theta*	*Alpha*	*Sigma*	*Beta*
1	Short	63.79	20.69	9.60	2.42	3.50
2	Short	61.46	18.99	14.32	2.13	3.10
3	Short	53.99	30.02	10.74	1.96	3.29
4	Short	51.57	25.36	15.39	3.03	4.65
5	Short	59.97	24.23	6.94	3.37	5.49
6	Short	57.92	18.15	8.80	2.43	12.70
7	Short	45.43	28.80	9.52	4.84	11.41
8	Short	44.07	28.83	9.31	4.63	13.16
9	Short	53.64	23.38	8.41	4.55	10.02
10	Short	61.30	18.79	8.47	4.60	6.84
11	Short	61.09	17.44	14.08	3.47	3.92
12	Short	55.01	20.44	14.34	3.66	6.55
13	Short	56.53	17.95	15.95	3.99	5.58
14	Short	47.83	20.43	20.49	4.53	6.72
15	Short	46.94	20.42	20.92	4.25	7.47
16	Short	79.07	12.66	4.88	1.05	2.34
17	Short	75.35	12.76	5.70	1.55	4.64
18	Short	68.71	19.66	3.89	1.63	6.11
19	Short	58.11	23.47	7.69	2.55	8.18
20	Short	65.68	18.19	8.83	2.66	4.64
21	Short	47.99	13.82	24.11	6.94	7.14
22	Short	48.84	12.86	28.78	2.96	6.56
23	Short	62.08	16.57	14.79	3.84	2.72
24	Short	55.67	8.93	27.70	4.66	3.04
25	Short	56.19	16.12	18.40	3.06	6.23
26	Short	63.27	19.13	7.69	3.61	6.30
27	Short	52.63	19.87	14.62	6.10	6.78
28	Short	70.84	14.24	7.43	4.06	3.43
29	Short	61.97	21.19	7.00	2.97	6.87
30	Short	56.30	15.37	11.49	7.69	9.15
31	Short	90.49	5.62	2.49	.42	.98
32	Short	50.64	20.70	13.84	4.75	10.07
33	Short	54.39	12.56	17.01	5.90	10.14
34	Short	56.88	19.25	10.67	3.11	10.09
35	Short	54.45	15.09	13.44	6.80	10.22
36	Short	63.35	29.33	4.61	.95	1.76
37	Short	50.27	35.69	8.15	1.58	4.31
38	Short	62.81	25.68	5.91	2.42	3.18
39	Short	83.09	9.66	3.32	1.45	2.48
40	Short	85.50	10.61	1.67	.77	1.45
41	Short	84.82	9.51	3.70	.61	1.36
42	Short	48.61	19.89	14.39	5.10	12.01
43	Short	50.57	22.81	11.42	4.16	11.04
44	Short	54.60	21.66	11.00	3.79	8.95
45	Short	57.21	24.37	6.40	3.14	8.88
46	Short	85.96	7.84	4.79	.76	.65
47	Short	85.11	8.89	4.92	.46	.62
48	Short	57.31	30.87	8.14	1.92	1.76
49	Short	29.96	44.58	16.63	3.55	5.28
50	Short	49.24	31.69	14.80	1.59	2.68
51	Short	55.51	27.73	9.39	2.50	4.87

52	Short	73.91	18.06	5.12	1.23	1.68
53	Short	75.90	15.73	4.75	1.18	2.44
54	Short	65.86	24.18	5.37	1.86	2.73
55	Short	67.52	19.16	6.39	3.47	3.46
56	Short	76.73	18.80	2.27	.65	1.55
57	Short	69.99	23.05	3.76	.84	2.36
58	Short	84.46	10.35	3.03	.54	1.62
59	Short	88.29	9.83	1.05	.38	.45
60	Short	69.13	25.66	2.99	.73	1.49
61	Short	58.36	21.94	8.05	2.93	8.72
62	Short	58.43	22.87	11.00	1.93	5.77
63	Short	53.90	25.05	13.83	2.22	5.00
64	Short	44.56	31.95	16.98	1.73	4.78
65	Short	47.32	27.68	16.17	3.04	5.79
66	Short	50.73	23.35	8.20	6.66	11.06
67	Short	57.73	23.51	10.24	2.37	6.15
68	Short	62.01	18.86	11.26	3.52	4.35
69	Short	59.07	22.60	9.57	3.22	5.54
70	Short	47.18	23.98	9.98	5.16	13.70
71	Short	43.63	22.20	22.31	4.40	7.46
72	Short	30.17	20.16	32.95	5.96	10.76
73	Short	33.87	22.56	31.08	3.20	9.29
74	Short	45.48	15.49	25.80	6.05	7.18
75	Short	32.93	17.65	34.03	5.23	10.16
76	Short	55.12	15.49	16.61	4.59	8.19
77	Short	63.42	16.73	9.30	2.35	8.20
78	Short	62.51	15.92	11.60	3.99	5.98
79	Short	66.98	11.90	9.40	3.18	8.54
80	Short	41.45	15.12	15.24	4.80	23.39
81	Short	83.86	10.91	3.04	.38	1.81
82	Short	81.37	10.83	4.38	1.17	2.25
83	Short	71.53	15.11	7.84	1.95	3.57
84	Short	66.63	13.41	13.35	3.09	3.52
85	Short	65.19	12.82	13.12	4.67	4.20
86	Short	46.51	25.49	17.76	3.09	7.15
87	Short	50.57	19.93	17.76	5.19	6.55
88	Short	58.77	19.55	13.90	2.83	4.95
89	Short	40.17	30.60	19.41	3.54	6.28
90	Short	66.55	18.08	10.32	1.56	3.49
91	Short	81.80	9.30	4.39	2.16	2.35
92	Short	60.52	20.96	11.81	2.64	4.07
93	Short	78.43	10.14	8.73	.98	1.72
94	Short	72.34	16.27	7.81	1.84	1.74
95	Short	68.18	18.16	7.61	1.96	4.09
96	Short	49.23	20.73	18.17	3.24	8.63
97	Short	73.62	9.38	8.60	2.86	5.54
98	Short	47.08	26.59	11.40	3.73	11.20
99	Short	22.94	21.49	35.78	8.84	10.95
100	Short	66.46	16.05	8.14	2.69	6.66
101	Short	58.41	23.47	12.28	1.87	3.97
102	Short	62.02	14.75	9.66	2.96	10.61
103	Short	67.39	13.63	13.86	1.14	3.98
104	Short	64.70	18.81	8.13	1.53	6.83
105	Short	67.24	17.70	8.68	1.45	4.93
106	Short	59.84	23.88	8.32	2.41	5.55
107	Short	72.47	10.99	10.53	2.19	3.82
108	Short	88.71	5.51	3.53	.63	1.62
109	Short	57.29	18.41	12.85	4.53	6.92
110	Short	92.44	3.87	1.84	.53	1.32
111	Short	36.69	39.70	13.59	3.07	6.95

112	Short	38.78	38.65	14.52	1.80	6.25
113	Short	57.91	25.88	9.51	2.49	4.21
114	Short	79.36	12.43	4.49	1.94	1.78
115	Short	62.04	21.56	8.30	2.05	6.05
116	Short	50.37	19.22	12.68	5.37	12.36
117	Short	39.63	17.47	17.19	3.50	22.21
118	Short	36.25	25.02	16.82	6.01	15.90
119	Short	34.40	16.83	19.72	5.88	23.17
120	Short	40.71	24.12	11.87	6.11	17.19
121	Short	30.38	21.81	29.83	4.73	13.25
122	Short	49.30	19.68	17.61	6.08	7.33
123	Short	56.11	15.27	10.60	9.14	8.88
124	Short	43.05	26.53	19.46	3.29	7.67
125	Short	79.50	9.13	6.72	2.74	1.91
126	Short	54.54	18.09	11.55	2.60	13.22
127	Short	56.94	19.98	11.75	2.47	8.86
128	Short	87.34	6.07	2.95	1.34	2.30
129	Short	67.23	15.08	4.89	1.07	11.73
130	Short	83.29	7.87	3.23	1.11	4.50
131	Short	78.85	10.63	5.37	2.89	2.26
132	Short	70.50	18.76	5.60	2.59	2.55
133	Short	70.67	22.24	3.28	1.27	2.54
134	Short	79.09	12.30	4.22	2.28	2.11
135	Short	69.56	21.56	5.17	1.55	2.16
136	Short	70.86	16.61	6.85	1.23	4.45
137	Short	65.24	14.18	11.23	2.50	6.85
138	Short	54.90	24.48	10.68	2.49	7.45
139	Short	80.75	12.78	2.84	.94	2.69
140	Short	68.40	17.22	7.82	2.28	4.28
141	Short	55.35	18.91	12.79	5.62	7.33
142	Short	55.11	23.09	13.56	3.63	4.61
143	Short	54.07	27.34	10.77	3.10	4.72
144	Short	44.59	22.42	18.15	6.84	8.00
145	Short	54.88	22.65	13.94	3.53	5.00
146	Short	38.99	24.60	17.43	3.91	15.07
147	Short	38.34	15.88	12.86	6.10	26.82
148	Short	62.57	14.61	12.14	3.79	6.89
149	Short	51.70	17.29	18.71	3.94	8.36
150	Short	47.72	23.95	17.49	2.87	7.97
151	Moderate	72.33	17.61	5.07	1.77	3.22
152	Moderate	67.08	18.50	8.98	2.40	3.04
153	Moderate	74.73	12.23	9.70	1.57	1.77
154	Moderate	73.62	18.28	5.76	.98	1.36
155	Moderate	76.38	13.76	5.24	1.64	2.98
156	Moderate	45.69	19.03	10.85	5.20	19.23
157	Moderate	82.87	12.52	2.50	.56	1.55
158	Moderate	51.21	20.79	6.43	6.73	14.84
159	Moderate	58.18	18.81	8.01	3.73	11.27
160	Moderate	52.29	30.87	6.78	2.57	7.49
161	Moderate	54.52	19.77	14.60	3.33	7.78
162	Moderate	47.23	23.25	17.47	5.36	6.69
163	Moderate	51.88	16.78	22.34	4.44	4.56
164	Moderate	44.79	26.13	18.15	4.23	6.70
165	Moderate	38.38	23.10	26.51	4.50	7.51
166	Moderate	88.54	6.30	1.95	.65	2.56
167	Moderate	74.25	11.60	4.09	1.49	8.57
168	Moderate	71.53	15.51	6.39	2.29	4.28
169	Moderate	74.94	14.96	5.67	1.28	3.15
170	Moderate	60.96	20.03	10.58	2.45	5.98
171	Moderate	73.07	9.20	10.35	5.39	1.99

172	Moderate	71.26	13.38	9.78	3.51	2.07
173	Moderate	63.21	10.45	20.24	3.47	2.63
174	Moderate	50.62	17.27	18.94	9.69	3.48
175	Moderate	56.34	9.84	22.35	8.21	3.26
176	Moderate	73.66	9.85	8.01	1.80	6.68
177	Moderate	54.19	19.99	14.79	2.10	8.93
178	Moderate	37.66	27.91	16.01	5.38	13.04
179	Moderate	57.37	16.61	10.17	4.35	11.50
180	Moderate	55.35	22.56	10.42	3.73	7.94
181	Moderate	53.13	25.35	11.76	3.65	6.11
182	Moderate	66.51	16.48	9.07	2.55	5.39
183	Moderate	54.31	19.01	10.17	5.50	11.01
184	Moderate	52.77	21.72	9.10	3.70	12.71
185	Moderate	60.54	17.58	13.50	2.32	6.06
186	Moderate	59.99	24.69	11.32	1.56	2.44
187	Moderate	50.36	36.65	8.08	1.68	3.23
188	Moderate	65.88	23.46	5.91	1.51	3.24
189	Moderate	65.17	26.30	4.00	1.21	3.32
190	Moderate	63.48	26.19	6.38	1.30	2.65
191	Moderate	42.81	24.09	11.51	6.67	14.92
192	Moderate	56.87	15.29	13.97	4.26	9.61
193	Moderate	42.58	24.66	16.62	4.94	11.20
194	Moderate	59.47	24.31	7.87	1.05	7.30
195	Moderate	70.29	18.11	3.93	1.52	6.15
196	Moderate	69.83	17.25	7.18	1.55	4.19
197	Moderate	30.68	38.65	19.76	3.30	7.61
198	Moderate	63.29	22.25	8.71	2.42	3.33
199	Moderate	44.01	36.05	14.58	2.18	3.18
200	Moderate	36.84	31.44	24.39	1.20	6.13
201	Moderate	76.60	16.37	3.74	2.04	1.25
202	Moderate	70.81	18.24	5.95	2.26	2.74
203	Moderate	65.24	25.60	4.67	2.64	1.85
204	Moderate	83.19	10.90	3.45	.93	1.53
205	Moderate	81.73	12.51	3.99	.70	1.07
206	Moderate	77.00	19.01	2.52	.67	.80
207	Moderate	75.05	19.09	3.85	.97	1.04
208	Moderate	79.18	15.00	3.96	.80	1.06
209	Moderate	78.84	15.89	3.65	.69	.93
210	Moderate	73.43	21.65	3.03	.68	1.21
211	Moderate	64.84	23.11	8.09	1.29	2.67
212	Moderate	52.64	29.09	12.59	1.88	3.80
213	Moderate	48.79	26.13	15.86	2.90	6.32
214	Moderate	56.02	24.17	13.15	2.26	4.40
215	Moderate	47.59	30.21	15.20	2.38	4.62
216	Moderate	47.85	22.23	8.66	11.55	9.71
217	Moderate	58.76	24.42	9.22	2.69	4.91
218	Moderate	57.72	18.23	9.28	7.96	6.81
219	Moderate	59.26	20.12	8.83	6.52	5.27
220	Moderate	72.67	16.10	4.83	2.41	3.99
221	Moderate	39.55	22.34	22.08	5.84	10.19
222	Moderate	46.65	15.87	24.10	5.81	7.57
223	Moderate	69.03	11.06	15.18	1.39	3.34
224	Moderate	67.78	18.28	7.24	3.04	3.66
225	Moderate	50.87	16.30	20.27	4.47	8.09
226	Moderate	57.43	15.62	10.41	12.46	4.08
227	Moderate	63.81	9.93	8.53	14.59	3.14
228	Moderate	42.07	19.51	21.24	11.00	6.18
229	Moderate	65.92	11.02	8.67	8.43	5.96
230	Moderate	62.52	11.57	8.90	10.07	6.94
231	Moderate	73.82	15.58	4.89	1.99	3.72

232	Moderate	56.90	13.13	13.90	3.71	12.36
233	Moderate	67.55	14.84	5.14	2.15	10.32
234	Moderate	59.70	16.72	7.02	2.76	13.80
235	Moderate	67.35	14.24	4.39	2.34	11.68
236	Moderate	75.41	10.52	7.50	1.84	4.73
237	Moderate	54.18	20.13	13.85	4.99	6.85
238	Moderate	59.25	14.99	10.49	2.98	12.29
239	Moderate	58.99	18.89	14.25	2.46	5.41
240	Moderate	37.37	28.93	21.45	2.54	9.71
241	Moderate	64.31	18.08	12.79	1.70	3.12
242	Moderate	64.56	22.01	8.40	1.34	3.69
243	Moderate	70.30	19.91	6.22	1.02	2.55
244	Moderate	54.49	28.01	11.32	1.68	4.50
245	Moderate	55.47	32.65	8.27	.89	2.72
246	Moderate	57.57	16.96	17.64	2.78	5.05
247	Moderate	55.97	21.12	11.29	5.29	6.33
248	Moderate	67.96	18.25	6.61	1.85	5.33
249	Moderate	59.08	26.85	6.26	1.67	6.14
250	Moderate	46.34	22.46	18.85	3.65	8.70
251	Moderate	61.20	21.95	9.88	1.80	5.17
252	Moderate	57.12	18.97	8.83	2.48	12.60
253	Moderate	66.36	21.02	6.06	.98	5.58
254	Moderate	48.52	37.50	7.90	1.65	4.43
255	Moderate	66.90	19.66	5.56	2.59	5.29
256	Moderate	89.43	5.81	2.46	.75	1.55
257	Moderate	83.61	8.61	4.75	.90	2.13
258	Moderate	79.53	8.39	9.35	.97	1.76
259	Moderate	78.41	12.71	5.39	1.17	2.32
260	Moderate	94.24	3.87	1.13	.17	.59
261	Moderate	25.67	25.76	30.37	4.92	13.28
262	Moderate	70.10	18.46	5.03	2.70	3.71
263	Moderate	62.03	22.57	5.71	4.50	5.19
264	Moderate	69.25	16.47	6.21	3.75	4.32
265	Moderate	77.59	11.26	4.19	1.57	5.39
266	Moderate	45.51	15.71	15.76	5.98	17.04
267	Moderate	61.30	13.98	8.47	2.96	13.29
268	Moderate	36.81	17.32	16.02	7.37	22.48
269	Moderate	36.20	19.71	18.41	5.42	20.26
270	Moderate	55.71	17.15	9.56	3.48	14.10
271	Moderate	54.06	16.00	19.67	6.38	3.89
272	Moderate	57.40	12.83	16.31	10.50	2.96
273	Moderate	62.23	15.18	13.10	6.46	3.03
274	Moderate	42.39	26.87	17.29	5.95	7.50
275	Moderate	79.64	8.30	7.16	1.64	3.26
276	Moderate	66.87	16.49	7.91	2.41	6.32
277	Moderate	58.20	21.30	9.11	8.31	3.08
278	Moderate	74.92	12.07	7.14	4.17	1.70
279	Moderate	72.28	14.05	5.94	4.53	3.20
280	Moderate	78.01	10.86	6.84	2.50	1.79
281	Moderate	58.28	17.94	14.18	4.09	5.51
282	Moderate	89.00	5.81	2.88	.60	1.71
283	Moderate	86.00	8.73	3.06	.57	1.64
284	Moderate	81.48	10.45	4.87	.94	2.26
285	Moderate	47.35	29.05	13.86	3.91	5.83
286	Moderate	49.18	27.00	11.86	4.48	7.48
287	Moderate	41.50	27.96	17.82	5.37	7.35
288	Moderate	32.94	38.31	18.20	3.51	7.04
289	Moderate	47.69	28.24	15.05	4.19	4.83
290	Moderate	40.61	22.01	17.85	4.91	14.62
291	Moderate	51.04	16.55	16.46	5.15	10.80

292	Moderate	44.99	19.76	14.71	4.57	15.97
293	Moderate	48.38	20.54	10.12	3.70	17.26
294	Moderate	44.16	22.54	19.05	3.10	11.15
295	Long	80.84	12.91	4.23	.93	1.09
296	Long	76.56	16.56	3.93	1.05	1.90
297	Long	58.80	24.10	11.24	2.04	3.82
298	Long	61.66	23.89	10.31	1.13	3.01
299	Long	66.33	21.99	5.75	2.13	3.80
300	Long	82.93	7.77	5.59	1.08	2.63
301	Long	82.60	11.18	3.68	.85	1.69
302	Long	52.30	22.66	11.99	4.30	8.75
303	Long	50.80	22.45	14.73	2.31	9.71
304	Long	44.48	23.07	15.96	3.75	12.74
305	Long	72.55	16.83	6.78	1.35	2.49
306	Long	52.91	35.55	7.05	1.63	2.86
307	Long	67.26	22.82	4.96	2.40	2.56
308	Long	73.60	17.19	5.04	1.42	2.75
309	Long	81.30	12.69	4.32	.73	.96
310	Long	51.65	27.15	8.84	3.14	9.22
311	Long	63.84	14.99	8.60	4.04	8.53
312	Long	42.31	29.75	13.02	2.95	11.97
313	Long	71.03	15.79	6.42	1.92	4.84
314	Long	68.26	15.39	6.72	2.11	7.52
315	Long	73.28	16.89	6.43	1.80	1.60
316	Long	70.64	25.46	2.59	.43	.88
317	Long	76.87	18.57	3.08	.57	.91
318	Long	72.64	23.76	1.76	.65	1.19
319	Long	85.10	11.69	2.05	.41	.75
320	Long	85.12	11.76	2.09	.39	.64
321	Long	34.46	25.42	19.99	4.57	15.56
322	Long	50.45	33.86	11.00	1.62	3.07
323	Long	79.08	14.54	4.67	.53	1.18
324	Long	65.40	24.59	6.38	1.26	2.37
325	Long	48.70	31.95	13.98	1.19	4.18
326	Long	43.52	20.86	14.34	4.23	17.05
327	Long	53.71	27.47	8.48	2.86	7.48
328	Long	57.56	21.90	9.08	3.07	8.39
329	Long	72.40	13.48	6.50	1.42	6.20
330	Long	48.44	19.10	16.36	3.36	12.74
331	Long	49.33	14.50	24.43	2.36	9.38
332	Long	93.20	3.41	2.06	.38	.95
333	Long	49.31	23.41	18.48	1.97	6.83
334	Long	64.72	11.00	8.60	11.41	4.27
335	Long	76.29	9.73	3.30	1.82	8.86
336	Long	79.12	9.22	3.28	1.10	7.28
337	Long	69.24	15.83	4.05	2.10	8.78
338	Long	74.48	11.23	3.21	1.50	9.58
339	Long	66.12	15.15	4.01	1.96	12.76
340	Long	73.92	13.94	7.40	1.43	3.31
341	Long	72.81	14.26	9.00	1.37	2.56
342	Long	82.44	10.06	5.26	.51	1.73
343	Long	60.53	20.14	11.68	1.64	6.01
344	Long	85.74	7.67	4.88	.96	.75
345	Long	41.91	23.90	16.25	5.57	12.37
346	Long	60.27	18.73	10.20	1.82	8.98
347	Long	44.31	22.56	13.15	2.83	17.15
348	Long	67.11	19.22	8.47	1.48	3.72
349	Long	59.44	24.34	8.43	1.51	6.28
350	Long	66.13	21.01	7.24	1.27	4.35
351	Long	70.64	14.70	7.04	3.96	3.66

352	Long	65.83	19.42	8.76	3.11	2.88
353	Long	48.23	24.57	14.95	7.83	4.42
354	Long	64.81	21.51	7.15	3.04	3.49
355	Long	78.09	12.05	4.86	2.81	2.19
356	Long	45.65	21.62	12.24	4.44	16.05
357	Long	42.86	25.64	14.53	3.06	13.91
358	Long	28.16	24.50	16.98	6.04	24.32
359	Long	54.71	23.60	13.67	3.32	4.70
360	Long	58.35	25.99	9.05	3.88	2.73
361	Long	52.58	17.85	16.79	6.03	6.75
362	Long	66.84	15.05	7.58	3.51	7.02
363	Long	56.19	21.56	12.13	4.14	5.98
364	Long	60.83	22.61	9.78	3.45	3.33
365	Long	80.85	9.48	5.76	1.53	2.38
366	Long	53.67	25.45	10.56	4.80	5.52
367	Long	87.45	7.34	2.17	.92	2.12
368	Long	89.44	5.54	3.30	.41	1.31
369	Long	53.56	28.88	8.16	3.28	6.12
370	Long	52.50	19.80	14.69	4.64	8.37
371	Long	40.12	31.43	19.40	4.20	4.85
372	Long	48.76	30.62	10.79	2.03	7.80
373	Long	43.44	33.01	15.81	3.33	4.41
374	Long	50.53	18.72	14.67	4.32	11.76
375	Long	33.62	21.34	22.77	5.69	16.58

Appendix C

Relative spectral powers at after apnea termination (AAT) for C3 EEG

Apnea event number	Apnea duration groups	Relative spectral powers				
		Delta	*Theta*	*Alpha*	*Sigma*	*Beta*
1	Short	76.46	12.07	7.77	1.25	2.45
2	Short	75.16	16.82	5.82	.95	1.25
3	Short	61.07	23.23	10.58	2.20	2.92
4	Short	77.11	14.32	4.61	.88	3.08
5	Short	64.58	21.36	8.26	1.90	3.90
6	Short	54.51	19.39	6.35	5.12	14.63
7	Short	43.17	21.45	11.42	6.73	17.23
8	Short	66.63	12.78	6.22	2.16	12.21
9	Short	60.36	20.47	9.50	3.28	6.39
10	Short	62.03	19.88	9.66	2.57	5.86
11	Short	62.25	21.17	10.53	2.07	3.98
12	Short	27.56	25.23	31.88	4.02	11.31
13	Short	44.93	19.46	21.34	4.51	9.76
14	Short	71.20	5.79	10.47	4.43	8.11
15	Short	79.15	7.77	7.57	2.26	3.25
16	Short	34.61	27.43	19.41	5.05	13.50
17	Short	40.66	16.07	19.37	2.44	21.46
18	Short	69.77	18.20	6.70	1.12	4.21
19	Short	58.66	22.59	7.57	1.60	9.58
20	Short	83.07	7.83	5.41	1.04	2.65
21	Short	42.44	21.97	17.60	3.49	14.50
22	Short	81.62	5.40	4.91	1.91	6.16
23	Short	50.56	17.61	24.88	3.44	3.51
24	Short	73.15	10.35	11.67	2.39	2.44
25	Short	79.78	10.63	4.96	2.00	2.63
26	Short	50.16	22.72	9.66	7.34	10.12
27	Short	69.66	12.69	8.16	4.08	5.41
28	Short	85.94	6.28	3.78	1.74	2.26
29	Short	70.25	12.71	9.52	3.14	4.38
30	Short	52.32	18.54	13.89	7.45	7.80
31	Short	76.11	10.61	9.87	1.33	2.08
32	Short	28.99	14.17	24.26	6.07	26.51
33	Short	27.77	20.91	21.70	9.13	20.49
34	Short	44.96	23.49	14.06	3.28	14.21
35	Short	32.00	11.08	20.44	9.70	26.78
36	Short	28.17	39.58	14.33	3.00	14.92
37	Short	52.75	34.33	6.88	2.82	3.22
38	Short	47.56	37.91	7.15	1.58	5.80
39	Short	79.25	15.02	3.46	.81	1.46
40	Short	90.06	7.31	1.51	.33	.79
41	Short	84.45	11.85	2.05	.41	1.24
42	Short	44.15	24.35	17.59	4.74	9.17
43	Short	59.89	16.81	8.53	4.27	10.50
44	Short	45.18	29.65	12.64	3.40	9.13
45	Short	27.72	31.02	21.44	5.01	14.81
46	Short	77.11	15.71	4.69	.96	1.53
47	Short	83.64	8.39	6.38	.67	.92
48	Short	67.33	15.66	13.42	1.17	2.42
49	Short	42.73	36.55	13.66	3.24	3.82
50	Short	53.34	20.48	16.89	2.35	6.94
51	Short	65.32	14.76	10.09	2.03	7.80

52	Short	70.71	16.66	6.62	2.83	3.18
53	Short	78.63	12.77	5.01	.88	2.71
54	Short	72.02	14.51	8.32	2.38	2.77
55	Short	74.66	16.06	5.47	1.61	2.20
56	Short	75.40	16.69	3.97	1.08	2.86
57	Short	63.37	19.58	7.40	2.67	6.98
58	Short	76.06	14.77	4.62	1.36	3.19
59	Short	85.95	8.23	2.70	.75	2.37
60	Short	55.37	28.54	7.36	2.27	6.46
61	Short	22.00	29.19	33.87	3.68	11.26
62	Short	29.27	19.49	18.02	3.99	29.23
63	Short	55.54	24.56	10.57	3.62	5.71
64	Short	45.42	21.23	13.03	1.63	18.69
65	Short	31.17	36.65	22.38	2.56	7.24
66	Short	35.10	18.36	17.01	14.02	15.51
67	Short	41.01	27.42	14.73	5.28	11.56
68	Short	49.24	24.65	13.74	3.45	8.92
69	Short	46.06	25.58	10.79	7.33	10.24
70	Short	54.52	17.93	12.74	5.18	9.63
71	Short	33.65	21.04	36.92	2.78	5.61
72	Short	37.76	16.11	30.01	3.85	12.27
73	Short	37.11	26.98	21.49	6.30	8.12
74	Short	35.90	20.87	32.07	4.14	7.02
75	Short	39.31	16.27	31.72	3.81	8.89
76	Short	80.45	8.46	5.93	2.30	2.86
77	Short	49.53	14.01	11.01	17.95	7.50
78	Short	73.83	5.70	7.53	3.36	9.58
79	Short	74.24	7.47	7.58	2.92	7.79
80	Short	43.28	15.29	15.44	9.11	16.88
81	Short	46.15	15.15	10.90	6.65	21.15
82	Short	56.36	11.81	10.72	4.57	16.54
83	Short	54.40	14.23	9.06	2.30	20.01
84	Short	60.03	13.09	16.67	3.57	6.64
85	Short	53.79	5.73	5.45	3.69	31.34
86	Short	61.37	5.96	9.52	4.65	18.50
87	Short	73.08	8.37	3.72	.85	13.98
88	Short	68.37	4.60	2.56	1.30	23.17
89	Short	82.85	6.72	4.17	1.30	4.96
90	Short	62.13	10.94	14.47	5.12	7.34
91	Short	64.23	11.91	16.88	2.97	4.01
92	Short	83.35	7.56	5.55	1.38	2.16
93	Short	83.25	9.49	4.35	1.14	1.77
94	Short	85.59	8.62	3.60	.97	1.22
95	Short	54.38	15.02	17.49	3.39	9.72
96	Short	38.54	24.98	25.95	4.52	6.01
97	Short	75.09	10.66	8.00	2.51	3.74
98	Short	62.08	18.97	8.57	1.59	8.79
99	Short	71.23	10.04	8.61	2.14	7.98
100	Short	49.68	22.26	12.17	4.35	11.54
101	Short	60.72	31.74	4.45	1.03	2.06
102	Short	86.23	6.50	4.29	.79	2.19
103	Short	78.98	11.54	5.65	1.06	2.77
104	Short	25.98	45.62	20.75	2.08	5.57
105	Short	82.49	10.92	4.09	.57	1.93
106	Short	73.18	12.17	8.51	1.57	4.57
107	Short	81.76	9.16	5.94	.94	2.20
108	Short	89.00	5.00	3.81	1.05	1.14
109	Short	87.16	8.08	2.63	.57	1.56
110	Short	76.61	13.44	4.66	1.39	3.90
111	Short	47.60	17.38	22.04	2.01	10.97

112	Short	29.10	42.85	17.70	3.09	7.26
113	Short	46.53	17.66	27.44	2.35	6.02
114	Short	74.23	13.22	8.16	1.46	2.93
115	Short	61.28	12.88	19.53	2.74	3.57
116	Short	53.75	18.98	12.61	3.55	11.11
117	Short	70.65	9.07	6.49	2.18	11.61
118	Short	43.30	16.75	17.46	5.53	16.96
119	Short	41.35	22.96	16.01	4.04	15.64
120	Short	60.50	15.60	10.36	3.06	10.48
121	Short	41.08	32.47	12.02	1.47	12.96
122	Short	17.51	19.21	30.90	2.21	30.17
123	Short	12.37	32.91	34.07	7.01	13.64
124	Short	31.47	9.82	13.62	4.56	40.53
125	Short	27.90	17.18	28.43	3.86	22.63
126	Short	35.74	21.10	18.25	3.23	21.68
127	Short	36.87	29.71	14.61	2.48	16.33
128	Short	79.02	9.76	4.64	2.44	4.14
129	Short	56.78	17.16	7.17	1.79	17.10
130	Short	66.43	13.91	5.13	2.23	12.30
131	Short	89.88	4.28	2.32	1.20	2.32
132	Short	92.14	4.02	1.91	.60	1.33
133	Short	82.95	7.98	4.21	1.43	3.43
134	Short	92.31	3.46	2.39	.60	1.24
135	Short	93.51	2.08	2.53	.55	1.33
136	Short	91.48	5.50	1.55	.51	.96
137	Short	89.81	4.84	3.09	.75	1.51
138	Short	92.53	3.81	2.62	.32	.72
139	Short	93.88	3.47	1.39	.37	.89
140	Short	93.26	4.16	1.62	.24	.72
141	Short	56.70	17.99	13.38	6.12	5.81
142	Short	48.21	26.27	16.17	4.30	5.05
143	Short	41.35	24.89	24.27	4.41	5.08
144	Short	67.16	14.21	13.69	1.87	3.07
145	Short	68.04	15.41	12.97	1.30	2.28
146	Short	35.86	26.99	20.36	3.03	13.76
147	Short	34.33	26.45	14.15	3.50	21.57
148	Short	43.71	15.62	21.08	4.78	14.81
149	Short	62.55	17.08	14.10	1.47	4.80
150	Short	60.14	14.07	15.97	3.59	6.23
151	Moderate	69.39	17.37	9.20	1.13	2.91
152	Moderate	66.46	16.98	9.94	2.38	4.24
153	Moderate	83.15	9.78	5.01	.88	1.18
154	Moderate	82.08	12.12	3.82	.76	1.22
155	Moderate	66.95	18.38	7.84	1.82	5.01
156	Moderate	37.95	20.69	10.35	5.37	25.64
157	Moderate	84.07	12.22	1.59	.40	1.72
158	Moderate	54.18	24.15	7.14	3.28	11.25
159	Moderate	46.23	12.82	13.11	8.16	19.68
160	Moderate	48.21	16.34	14.44	5.03	15.98
161	Moderate	61.91	15.23	13.71	3.56	5.59
162	Moderate	75.81	5.93	11.45	2.01	4.80
163	Moderate	70.25	8.49	15.54	2.22	3.50
164	Moderate	39.26	19.34	21.98	6.25	13.17
165	Moderate	43.58	19.80	22.49	5.65	8.48
166	Moderate	46.42	27.52	8.12	2.14	15.80
167	Moderate	44.06	14.53	15.14	5.99	20.28
168	Moderate	82.18	7.82	4.92	1.25	3.83
169	Moderate	21.25	24.51	13.55	7.96	32.73
170	Moderate	34.60	20.68	14.78	5.84	24.10
171	Moderate	70.82	10.53	12.89	3.56	2.20

172	Moderate	71.11	9.57	13.97	3.24	2.11
173	Moderate	58.25	17.42	15.09	4.37	4.87
174	Moderate	71.16	12.28	12.76	1.51	2.29
175	Moderate	69.77	15.42	10.05	2.53	2.23
176	Moderate	92.38	3.74	2.60	.51	.77
177	Moderate	20.87	17.92	45.03	5.58	10.60
178	Moderate	94.82	1.51	2.46	.45	.76
179	Moderate	19.79	13.99	38.65	10.80	16.77
180	Moderate	28.76	21.89	24.61	2.61	22.13
181	Moderate	48.76	10.41	15.21	7.74	17.88
182	Moderate	53.49	9.68	22.04	3.04	11.75
183	Moderate	26.19	18.70	26.09	5.59	23.43
184	Moderate	34.94	9.41	20.87	7.89	26.89
185	Moderate	43.18	14.54	13.37	6.76	22.15
186	Moderate	38.15	44.90	9.32	1.71	5.92
187	Moderate	25.24	49.40	11.70	1.73	11.93
188	Moderate	40.49	36.67	10.77	2.28	9.79
189	Moderate	45.11	32.91	9.03	2.80	10.15
190	Moderate	64.11	21.90	9.09	1.71	3.19
191	Moderate	22.95	27.10	28.25	6.32	15.38
192	Moderate	13.95	39.81	30.45	3.54	12.25
193	Moderate	18.80	32.29	30.68	4.08	14.15
194	Moderate	42.01	22.69	19.33	3.12	12.85
195	Moderate	58.12	21.15	8.64	2.37	9.72
196	Moderate	18.06	46.74	15.38	5.70	14.12
197	Moderate	10.87	30.19	28.24	8.91	21.79
198	Moderate	22.23	38.14	27.26	4.66	7.71
199	Moderate	15.35	32.94	29.40	8.78	13.53
200	Moderate	25.77	28.60	26.16	6.58	12.89
201	Moderate	66.92	16.67	11.21	1.78	3.42
202	Moderate	85.24	7.81	3.53	1.12	2.30
203	Moderate	71.36	19.35	4.67	1.21	3.41
204	Moderate	84.50	7.44	4.89	.52	2.65
205	Moderate	81.61	11.49	4.28	.96	1.66
206	Moderate	66.37	23.48	5.57	1.64	2.94
207	Moderate	64.96	20.03	7.53	2.32	5.16
208	Moderate	76.91	16.47	3.22	1.44	1.96
209	Moderate	73.69	14.74	6.36	2.29	2.92
210	Moderate	82.34	11.94	3.66	.70	1.36
211	Moderate	30.40	22.81	11.86	1.78	33.15
212	Moderate	33.35	26.90	14.37	3.35	22.03
213	Moderate	41.25	33.62	13.93	3.93	7.27
214	Moderate	46.41	28.87	17.50	1.75	5.47
215	Moderate	60.12	22.14	10.32	2.80	4.62
216	Moderate	49.93	15.05	17.89	7.43	9.70
217	Moderate	41.55	19.25	22.90	7.03	9.27
218	Moderate	51.84	17.43	18.64	3.64	8.45
219	Moderate	64.61	12.72	11.94	4.66	6.07
220	Moderate	43.19	20.27	22.81	6.35	7.38
221	Moderate	49.11	12.43	21.67	3.51	13.28
222	Moderate	47.44	16.15	26.95	2.98	6.48
223	Moderate	42.01	25.08	17.78	7.27	7.86
224	Moderate	41.56	22.40	22.97	4.54	8.53
225	Moderate	63.07	8.73	17.34	2.62	8.24
226	Moderate	81.84	7.16	7.57	1.85	1.58
227	Moderate	87.67	5.94	3.43	.89	2.07
228	Moderate	75.01	8.53	7.11	4.56	4.79
229	Moderate	67.60	6.90	11.24	10.56	3.70
230	Moderate	56.68	16.64	12.33	8.98	5.37
231	Moderate	62.18	19.76	7.77	2.63	7.66

232	Moderate	64.80	13.65	8.26	4.99	8.30
233	Moderate	45.15	30.68	4.67	5.02	14.48
234	Moderate	52.33	16.66	7.82	2.53	20.66
235	Moderate	43.51	26.26	6.72	3.54	19.97
236	Moderate	79.47	3.46	4.23	1.30	11.54
237	Moderate	74.12	4.49	3.96	1.15	16.28
238	Moderate	60.23	6.05	3.36	1.70	28.66
239	Moderate	58.69	10.01	12.11	4.24	14.95
240	Moderate	94.16	1.54	2.23	.32	1.75
241	Moderate	77.39	12.71	6.86	.79	2.25
242	Moderate	61.08	18.47	13.08	1.88	5.49
243	Moderate	55.39	17.76	19.55	1.58	5.72
244	Moderate	34.18	28.49	25.50	2.21	9.62
245	Moderate	56.64	23.21	12.23	1.85	6.07
246	Moderate	53.36	17.18	19.16	3.74	6.56
247	Moderate	55.37	9.44	19.97	4.32	10.90
248	Moderate	45.94	17.31	18.06	4.81	13.88
249	Moderate	43.65	27.34	12.22	5.99	10.80
250	Moderate	43.98	24.70	17.53	3.68	10.11
251	Moderate	64.69	17.29	10.02	1.99	6.01
252	Moderate	84.36	7.14	4.64	1.33	2.53
253	Moderate	55.21	17.05	7.39	3.31	17.04
254	Moderate	87.51	5.02	3.59	.48	3.40
255	Moderate	29.86	17.28	20.16	4.99	27.71
256	Moderate	97.31	1.06	.97	.21	.45
257	Moderate	95.39	2.07	1.61	.28	.65
258	Moderate	96.29	1.78	1.28	.22	.43
259	Moderate	96.58	1.98	.92	.14	.38
260	Moderate	81.76	13.27	2.88	.62	1.47
261	Moderate	35.69	32.51	19.52	3.27	9.01
262	Moderate	56.21	26.75	8.96	2.96	5.12
263	Moderate	70.43	17.43	5.26	1.20	5.68
264	Moderate	64.35	14.57	10.02	2.04	9.02
265	Moderate	64.66	18.62	6.72	1.65	8.35
266	Moderate	51.24	16.36	10.72	4.68	17.00
267	Moderate	57.17	11.08	11.77	5.13	14.85
268	Moderate	67.02	12.35	8.89	2.42	9.32
269	Moderate	46.67	16.12	12.37	5.89	18.95
270	Moderate	62.08	12.15	8.53	2.72	14.52
271	Moderate	39.22	14.29	30.40	4.85	11.24
272	Moderate	56.60	13.31	19.19	1.87	9.03
273	Moderate	57.96	21.38	15.12	2.59	2.95
274	Moderate	39.21	26.76	23.16	3.17	7.70
275	Moderate	54.40	13.76	10.67	2.39	18.78
276	Moderate	58.16	13.60	17.40	3.70	7.14
277	Moderate	81.51	6.13	5.34	2.53	4.49
278	Moderate	88.66	3.39	4.19	1.36	2.40
279	Moderate	95.22	2.13	1.23	.56	.86
280	Moderate	94.18	3.27	1.57	.29	.69
281	Moderate	93.98	4.05	1.19	.26	.52
282	Moderate	87.67	6.39	2.96	1.15	1.83
283	Moderate	85.60	5.84	4.70	1.33	2.53
284	Moderate	94.81	3.00	1.08	.47	.64
285	Moderate	46.09	18.22	14.52	2.22	18.95
286	Moderate	34.26	35.87	21.34	3.37	5.16
287	Moderate	84.60	9.43	3.76	.50	1.71
288	Moderate	58.51	29.05	9.79	.77	1.88
289	Moderate	40.88	28.98	21.18	3.27	5.69
290	Moderate	52.15	18.75	11.50	4.22	13.38
291	Moderate	31.73	17.99	23.30	7.44	19.54

292	Moderate	54.46	16.35	11.83	4.22	13.14
293	Moderate	42.24	16.43	16.68	5.96	18.69
294	Moderate	38.63	24.36	17.13	4.86	15.02
295	Long	72.96	15.58	8.80	1.01	1.65
296	Long	53.27	28.97	12.45	2.26	3.05
297	Long	62.79	24.68	6.93	1.11	4.49
298	Long	41.28	37.62	14.27	2.15	4.68
299	Long	58.05	21.38	14.38	2.13	4.06
300	Long	68.85	8.23	13.92	2.16	6.84
301	Long	56.89	15.52	11.23	4.59	11.77
302	Long	87.04	3.41	4.37	.61	4.57
303	Long	50.76	20.08	15.03	2.78	11.35
304	Long	91.22	1.06	2.12	.78	4.82
305	Long	46.13	36.30	9.19	1.29	7.09
306	Long	36.56	40.30	12.91	2.39	7.84
307	Long	71.88	15.91	5.63	2.09	4.49
308	Long	66.96	19.87	7.06	1.74	4.37
309	Long	71.56	13.98	7.22	1.95	5.29
310	Long	46.35	25.40	10.01	4.62	13.62
311	Long	62.18	24.37	3.47	2.34	7.64
312	Long	27.72	25.72	19.03	6.51	21.02
313	Long	24.23	34.85	23.65	2.57	14.70
314	Long	48.11	23.55	16.11	3.19	9.04
315	Long	90.16	4.80	2.70	.43	1.91
316	Long	62.89	23.19	5.73	1.43	6.76
317	Long	63.86	21.65	7.18	2.17	5.14
318	Long	68.53	18.15	6.94	2.54	3.84
319	Long	78.68	11.59	5.20	1.61	2.92
320	Long	77.02	10.31	7.68	1.55	3.44
321	Long	45.41	17.69	13.45	2.66	20.79
322	Long	44.71	25.81	16.18	2.79	10.51
323	Long	70.00	12.19	7.41	2.88	7.52
324	Long	46.62	29.32	12.65	2.01	9.40
325	Long	42.94	29.04	10.95	2.38	14.69
326	Long	37.21	20.23	22.25	2.16	18.15
327	Long	30.33	23.78	19.08	6.10	20.71
328	Long	40.66	16.05	17.81	3.27	22.21
329	Long	26.08	14.05	42.18	4.56	13.13
330	Long	21.88	13.71	43.30	2.73	18.38
331	Long	43.80	17.08	30.33	3.43	5.36
332	Long	58.73	16.49	17.28	1.79	5.71
333	Long	79.06	8.08	7.62	1.40	3.84
334	Long	85.88	5.90	3.57	1.03	3.62
335	Long	60.23	18.45	6.73	1.55	13.04
336	Long	76.07	6.81	4.66	2.24	10.22
337	Long	94.96	1.77	.86	.41	2.00
338	Long	67.54	12.45	4.83	1.17	14.01
339	Long	53.98	15.05	5.36	2.88	22.73
340	Long	60.86	19.77	11.42	2.11	5.84
341	Long	62.57	17.61	13.43	1.50	4.89
342	Long	50.15	25.90	15.76	2.06	6.13
343	Long	97.24	1.44	.65	.11	.56
344	Long	81.32	10.66	5.83	.84	1.35
345	Long	35.48	17.93	19.60	10.57	16.42
346	Long	87.21	3.34	4.03	1.49	3.93
347	Long	84.01	7.42	4.16	.71	3.70
348	Long	70.54	17.76	6.93	1.30	3.47
349	Long	91.51	4.07	2.39	.65	1.38
350	Long	83.47	8.83	5.56	.84	1.30
351	Long	69.50	13.49	6.25	2.30	8.46

352	Long	81.27	9.52	5.37	.69	3.15
353	Long	75.25	10.85	7.74	1.24	4.92
354	Long	70.30	9.85	6.84	1.72	11.29
355	Long	63.30	20.14	10.56	2.22	3.78
356	Long	41.54	15.09	18.12	5.66	19.59
357	Long	41.34	20.81	15.95	5.24	16.66
358	Long	43.78	21.66	17.50	3.51	13.55
359	Long	48.81	19.49	12.53	3.23	15.94
360	Long	80.20	2.40	2.33	.78	14.29
361	Long	88.82	1.45	2.95	.68	6.10
362	Long	75.27	9.58	9.50	1.84	3.81
363	Long	92.54	3.27	2.24	.49	1.46
364	Long	93.33	3.34	1.91	.31	1.11
365	Long	90.77	4.26	2.30	.66	2.01
366	Long	96.05	1.30	1.15	.41	1.09
367	Long	93.45	2.10	.55	.57	3.33
368	Long	88.55	5.96	3.11	.89	1.49
369	Long	64.25	12.91	9.69	1.64	11.51
370	Long	38.87	20.75	14.73	3.06	22.59
371	Long	72.24	9.14	7.42	1.83	9.37
372	Long	86.49	5.87	5.65	.50	1.49
373	Long	85.70	9.36	3.56	.40	.98
374	Long	40.08	26.73	15.92	2.71	14.56
375	Long	60.19	16.79	8.86	3.60	10.56

Appendix D

Relative spectral powers at before apnea termination (BAT) for C4 EEG

Apnea event number	Apnea duration groups	Relative spectral powers				
		Delta	*Theta*	*Alpha*	*Sigma*	*Beta*
1	Short	57.40	23.04	12.03	2.99	4.54
2	Short	57.55	23.90	12.64	2.17	3.74
3	Short	51.60	26.38	11.51	2.80	7.71
4	Short	56.57	22.06	10.84	2.98	7.55
5	Short	59.12	25.71	8.03	3.14	4.00
6	Short	64.51	17.28	6.96	2.73	8.52
7	Short	47.62	23.21	7.36	7.53	14.28
8	Short	53.12	21.88	9.85	3.19	11.96
9	Short	50.32	24.47	9.55	4.00	11.66
10	Short	53.01	24.92	11.09	3.26	7.72
11	Short	62.13	23.52	7.52	2.48	4.35
12	Short	51.81	23.80	13.62	3.34	7.43
13	Short	42.27	26.62	19.90	3.55	7.66
14	Short	49.93	18.70	18.70	5.98	6.69
15	Short	54.43	21.91	14.64	2.36	6.66
16	Short	63.14	19.26	9.48	1.98	6.14
17	Short	75.39	15.33	3.91	1.04	4.33
18	Short	73.13	14.27	4.50	1.55	6.55
19	Short	70.91	14.25	5.39	1.96	7.49
20	Short	66.61	19.71	6.85	1.28	5.55
21	Short	63.96	10.12	16.79	4.45	4.68
22	Short	52.70	12.88	24.55	3.56	6.31
23	Short	66.31	16.61	10.27	3.30	3.51
24	Short	63.17	12.43	17.46	3.84	3.10
25	Short	69.20	9.56	15.35	1.95	3.94
26	Short	53.03	20.70	11.46	3.61	11.20
27	Short	42.30	22.48	15.46	6.98	12.78
28	Short	64.38	13.98	10.33	4.60	6.71
29	Short	57.89	19.80	9.02	3.79	9.50
30	Short	41.42	21.95	16.50	6.24	13.89
31	Short	90.00	5.54	3.05	.69	.72
32	Short	43.17	22.55	13.30	3.51	17.47
33	Short	62.00	10.97	14.39	2.61	10.03
34	Short	45.85	12.41	10.00	6.13	25.61
35	Short	57.20	17.74	13.47	4.15	7.44
36	Short	72.11	18.64	6.19	.99	2.07
37	Short	67.72	18.23	6.33	2.30	5.42
38	Short	65.36	20.30	8.67	1.34	4.33
39	Short	83.67	9.77	3.15	1.23	2.18
40	Short	85.51	7.75	3.44	1.17	2.13
41	Short	77.22	14.88	4.76	.60	2.54
42	Short	42.38	28.91	12.04	6.86	9.81
43	Short	48.73	24.33	13.03	3.52	10.39
44	Short	56.78	20.80	12.02	3.51	6.89
45	Short	61.13	16.63	9.42	2.79	10.03
46	Short	83.53	9.07	5.98	.75	.67
47	Short	86.28	8.53	3.97	.53	.69
48	Short	63.30	29.44	5.07	.85	1.34
49	Short	24.88	57.59	11.03	2.48	4.02
50	Short	51.13	31.12	10.38	2.79	4.58
51	Short	52.93	30.96	10.13	1.82	4.16

52	Short	67.97	22.60	5.99	1.69	1.75
53	Short	71.46	18.18	6.65	.94	2.77
54	Short	56.88	28.97	8.23	2.63	3.29
55	Short	59.21	25.32	8.40	3.95	3.12
56	Short	74.21	16.82	4.79	1.08	3.10
57	Short	62.06	24.38	6.05	.92	6.59
58	Short	67.55	24.79	3.12	1.35	3.19
59	Short	87.32	9.54	2.04	.45	.65
60	Short	61.90	29.10	5.57	.94	2.49
61	Short	43.12	38.75	7.72	2.36	8.05
62	Short	63.33	23.33	7.72	1.80	3.82
63	Short	50.47	29.80	13.09	2.57	4.07
64	Short	49.64	24.70	18.32	2.37	4.97
65	Short	58.02	24.72	9.69	1.82	5.75
66	Short	46.94	25.75	10.63	6.05	10.63
67	Short	52.11	24.34	12.54	2.41	8.60
68	Short	51.45	18.65	16.19	3.20	10.51
69	Short	45.84	25.46	14.44	3.13	11.13
70	Short	38.18	24.88	12.73	4.80	19.41
71	Short	34.75	26.85	22.27	8.15	7.98
72	Short	42.08	14.43	30.94	4.18	8.37
73	Short	40.23	17.35	25.80	6.43	10.19
74	Short	31.69	18.89	36.03	5.45	7.94
75	Short	31.18	19.65	34.29	4.54	10.34
76	Short	47.84	17.69	16.29	6.18	12.00
77	Short	53.17	19.40	13.73	2.60	11.10
78	Short	72.03	9.90	8.21	4.71	5.15
79	Short	60.72	12.08	11.48	3.82	11.90
80	Short	34.98	17.45	21.21	5.23	21.13
81	Short	72.06	20.21	3.52	.81	3.40
82	Short	68.49	19.25	6.61	1.99	3.66
83	Short	61.17	23.09	7.09	3.40	5.25
84	Short	67.41	16.87	8.21	1.53	5.98
85	Short	58.42	22.49	10.96	3.78	4.35
86	Short	48.23	21.65	18.74	2.66	8.72
87	Short	51.01	19.73	17.49	4.47	7.30
88	Short	44.69	30.21	13.85	3.44	7.81
89	Short	41.34	32.09	16.32	2.61	7.64
90	Short	67.59	15.17	11.75	2.21	3.28
91	Short	85.07	7.61	3.42	2.19	1.71
92	Short	53.34	16.69	17.06	7.73	5.18
93	Short	52.31	25.51	17.91	1.51	2.76
94	Short	67.67	15.84	12.69	1.12	2.68
95	Short	53.05	21.52	14.88	4.13	6.42
96	Short	43.37	24.55	18.88	2.67	10.53
97	Short	53.92	18.35	13.28	4.28	10.17
98	Short	43.09	22.57	14.98	4.89	14.47
99	Short	25.25	22.66	34.78	7.13	10.18
100	Short	56.31	16.57	13.06	2.48	11.58
101	Short	48.37	33.03	11.22	1.47	5.91
102	Short	44.00	17.58	12.05	4.39	21.98
103	Short	70.20	15.24	8.88	1.73	3.95
104	Short	59.58	21.04	12.14	1.20	6.04
105	Short	46.68	21.05	14.98	3.07	14.22
106	Short	45.26	27.09	18.39	2.38	6.88
107	Short	67.77	13.33	11.28	1.80	5.82
108	Short	89.57	3.62	4.37	.88	1.56
109	Short	59.60	22.13	10.30	3.04	4.93
110	Short	94.18	3.37	1.19	.32	.94
111	Short	42.15	35.96	10.35	3.33	8.21

112	Short	55.37	23.91	10.60	2.10	8.02
113	Short	58.38	21.55	9.91	3.27	6.89
114	Short	77.50	14.76	4.19	1.10	2.45
115	Short	56.62	22.24	12.52	2.40	6.22
116	Short	45.03	19.98	11.02	4.19	19.78
117	Short	46.50	23.59	10.74	4.81	14.36
118	Short	27.45	27.49	19.82	5.93	19.31
119	Short	35.72	20.70	17.82	5.89	19.87
120	Short	37.53	24.52	12.72	7.09	18.14
121	Short	29.16	20.65	28.44	4.38	17.37
122	Short	51.71	21.30	16.75	2.86	7.38
123	Short	46.32	21.68	16.81	3.89	11.30
124	Short	45.85	20.21	17.74	5.29	10.91
125	Short	77.69	9.66	7.89	2.43	2.33
126	Short	57.13	17.89	11.13	1.76	12.09
127	Short	60.68	18.54	10.69	1.60	8.49
128	Short	78.21	10.42	5.61	1.78	3.98
129	Short	61.32	16.59	4.63	1.25	16.21
130	Short	50.32	22.73	8.48	3.41	15.06
131	Short	73.37	12.12	5.13	6.14	3.24
132	Short	71.10	16.79	6.30	2.12	3.69
133	Short	74.43	10.64	7.19	4.40	3.34
134	Short	82.34	8.85	3.89	2.42	2.50
135	Short	50.36	26.76	9.20	6.41	7.27
136	Short	63.16	23.35	7.94	1.81	3.74
137	Short	63.91	22.25	7.31	1.80	4.73
138	Short	34.62	43.84	10.27	2.00	9.27
139	Short	79.24	14.71	3.19	.87	1.99
140	Short	60.82	24.62	10.26	1.55	2.75
141	Short	43.84	24.22	15.68	6.62	9.64
142	Short	64.68	19.82	9.61	1.95	3.94
143	Short	50.39	18.37	20.01	3.12	8.11
144	Short	48.51	17.70	18.59	5.41	9.79
145	Short	41.35	23.99	20.18	5.97	8.51
146	Short	39.95	15.34	23.58	5.29	15.84
147	Short	31.49	15.56	22.94	8.17	21.84
148	Short	54.52	21.79	14.36	3.54	5.79
149	Short	60.69	15.14	12.48	3.48	8.21
150	Short	37.79	29.65	22.85	3.22	6.49
151	Moderate	67.65	18.93	6.93	2.55	3.94
152	Moderate	78.15	11.62	6.08	1.57	2.58
153	Moderate	70.55	14.19	10.37	2.59	2.30
154	Moderate	84.45	8.81	4.25	.68	1.81
155	Moderate	73.38	13.98	5.19	1.55	5.90
156	Moderate	46.19	22.40	10.36	3.94	17.11
157	Moderate	67.67	24.72	3.97	.92	2.72
158	Moderate	50.36	23.73	7.37	5.14	13.40
159	Moderate	60.29	15.51	9.07	3.78	11.35
160	Moderate	52.69	28.88	5.81	2.03	10.59
161	Moderate	38.69	23.60	23.02	4.92	9.77
162	Moderate	40.90	28.31	22.87	2.82	5.10
163	Moderate	41.33	24.63	20.96	5.56	7.52
164	Moderate	50.46	23.27	15.13	3.75	7.39
165	Moderate	44.92	24.88	21.00	2.68	6.52
166	Moderate	88.47	6.63	1.75	.62	2.53
167	Moderate	67.85	14.08	6.84	1.20	10.03
168	Moderate	53.79	24.03	9.42	2.86	9.90
169	Moderate	78.17	14.97	2.88	.71	3.27
170	Moderate	48.29	29.20	11.42	4.21	6.88
171	Moderate	63.39	16.24	12.40	4.04	3.93

172	Moderate	65.11	18.35	10.63	3.28	2.63
173	Moderate	75.68	8.67	10.74	2.62	2.29
174	Moderate	56.22	16.05	18.61	5.62	3.50
175	Moderate	48.72	13.90	27.42	4.74	5.22
176	Moderate	44.82	15.39	16.21	5.31	18.27
177	Moderate	47.50	16.89	13.41	7.93	14.27
178	Moderate	38.77	26.94	12.17	4.76	17.36
179	Moderate	46.23	20.11	12.06	7.72	13.88
180	Moderate	20.69	13.29	16.89	10.35	38.78
181	Moderate	59.25	20.50	8.41	3.72	8.12
182	Moderate	53.00	18.63	14.26	3.06	11.05
183	Moderate	57.35	13.21	9.08	4.12	16.24
184	Moderate	57.12	17.79	10.28	3.14	11.67
185	Moderate	57.38	19.04	10.39	3.09	10.10
186	Moderate	52.20	28.82	12.40	2.59	3.99
187	Moderate	64.29	20.58	8.40	3.21	3.52
188	Moderate	58.58	28.77	6.68	2.54	3.43
189	Moderate	73.56	14.45	8.24	1.35	2.40
190	Moderate	67.65	16.52	9.87	2.71	3.25
191	Moderate	39.12	22.86	15.81	6.44	15.77
192	Moderate	54.86	16.80	11.60	5.00	11.74
193	Moderate	45.25	21.21	16.26	4.57	12.71
194	Moderate	61.52	21.63	6.04	2.37	8.44
195	Moderate	65.07	21.11	6.69	2.05	5.08
196	Moderate	68.16	17.71	7.83	1.86	4.44
197	Moderate	23.96	45.66	18.65	4.17	7.56
198	Moderate	65.42	17.66	13.15	1.46	2.31
199	Moderate	57.26	27.50	11.34	1.02	2.88
200	Moderate	40.37	33.76	17.15	2.83	5.89
201	Moderate	72.48	18.88	6.12	.90	1.62
202	Moderate	71.52	18.74	4.60	2.59	2.55
203	Moderate	50.61	39.45	5.27	2.74	1.93
204	Moderate	63.71	24.67	7.50	1.33	2.79
205	Moderate	76.04	15.50	5.19	1.85	1.42
206	Moderate	76.59	18.41	2.69	.80	1.51
207	Moderate	68.69	24.63	4.02	1.14	1.52
208	Moderate	76.84	16.91	3.94	.75	1.56
209	Moderate	78.41	14.83	4.70	.77	1.29
210	Moderate	63.84	25.03	7.39	1.42	2.32
211	Moderate	56.66	27.24	9.02	2.63	4.45
212	Moderate	54.85	24.04	13.52	3.62	3.97
213	Moderate	46.22	26.03	20.49	2.21	5.05
214	Moderate	59.65	25.38	9.71	1.84	3.42
215	Moderate	52.71	26.73	14.93	1.82	3.81
216	Moderate	47.10	23.76	11.57	4.78	12.79
217	Moderate	48.55	25.71	11.41	7.90	6.43
218	Moderate	62.04	16.65	11.02	3.25	7.04
219	Moderate	60.56	24.50	7.16	2.96	4.82
220	Moderate	53.27	27.50	6.73	5.18	7.32
221	Moderate	34.16	18.03	32.52	6.14	9.15
222	Moderate	39.73	15.69	29.16	7.36	8.06
223	Moderate	59.49	12.17	22.12	1.96	4.26
224	Moderate	69.86	13.32	7.96	3.81	5.05
225	Moderate	49.95	13.59	23.17	5.07	8.22
226	Moderate	46.04	12.09	13.82	23.60	4.45
227	Moderate	58.95	12.30	8.97	15.90	3.88
228	Moderate	42.44	13.91	16.03	20.56	7.06
229	Moderate	53.58	11.98	12.20	12.41	9.83
230	Moderate	48.75	13.11	11.31	14.47	12.36
231	Moderate	74.81	15.72	5.53	1.13	2.81

232	Moderate	36.28	34.44	8.72	5.45	15.11
233	Moderate	41.19	24.48	11.84	2.41	20.08
234	Moderate	42.97	28.25	8.05	4.86	15.87
235	Moderate	38.47	33.15	9.72	2.89	15.77
236	Moderate	63.16	16.74	12.33	2.63	5.14
237	Moderate	55.57	18.92	13.53	4.24	7.74
238	Moderate	65.51	12.82	7.50	4.03	10.14
239	Moderate	59.79	13.85	15.05	4.10	7.21
240	Moderate	35.66	23.30	25.98	3.92	11.14
241	Moderate	67.05	15.05	10.96	1.98	4.96
242	Moderate	64.97	21.09	8.31	1.06	4.57
243	Moderate	79.05	12.18	5.39	.80	2.58
244	Moderate	67.06	16.28	11.77	1.51	3.38
245	Moderate	37.85	40.80	11.88	4.05	5.42
246	Moderate	49.76	21.28	17.86	4.66	6.44
247	Moderate	58.82	17.65	10.72	5.76	7.05
248	Moderate	61.02	16.71	11.69	2.47	8.11
249	Moderate	46.96	23.34	13.49	2.67	13.54
250	Moderate	48.89	22.83	15.88	2.22	10.18
251	Moderate	63.05	19.74	9.66	1.41	6.14
252	Moderate	62.48	20.85	9.12	2.01	5.54
253	Moderate	71.26	16.77	4.90	1.81	5.26
254	Moderate	39.16	37.72	16.50	1.65	4.97
255	Moderate	66.72	18.19	7.10	2.37	5.62
256	Moderate	75.62	12.40	7.38	.98	3.62
257	Moderate	59.36	21.14	11.07	2.27	6.16
258	Moderate	61.07	18.06	14.80	1.84	4.23
259	Moderate	79.41	10.85	5.68	1.59	2.47
260	Moderate	92.70	4.52	1.47	.34	.97
261	Moderate	23.45	40.77	20.69	2.91	12.18
262	Moderate	49.70	31.20	11.65	1.55	5.90
263	Moderate	64.87	19.08	7.83	2.54	5.68
264	Moderate	70.52	15.56	4.23	2.68	7.01
265	Moderate	85.32	6.79	4.15	1.00	2.74
266	Moderate	36.66	23.19	15.69	7.54	16.92
267	Moderate	59.35	13.94	10.92	3.51	12.28
268	Moderate	32.76	24.81	14.72	7.00	20.71
269	Moderate	39.92	20.29	16.66	5.05	18.08
270	Moderate	63.01	12.51	8.77	4.06	11.65
271	Moderate	42.37	22.49	18.31	13.03	3.80
272	Moderate	50.18	16.52	16.30	11.09	5.91
273	Moderate	47.19	16.06	23.01	11.06	2.68
274	Moderate	46.81	23.36	16.61	3.81	9.41
275	Moderate	66.94	15.01	10.01	2.70	5.34
276	Moderate	66.90	18.42	6.01	1.71	6.96
277	Moderate	72.74	12.51	9.16	2.20	3.39
278	Moderate	79.88	8.44	6.30	3.29	2.09
279	Moderate	85.08	7.85	3.34	1.89	1.84
280	Moderate	75.50	12.68	7.49	2.16	2.17
281	Moderate	60.80	20.74	8.13	2.80	7.53
282	Moderate	91.14	5.95	1.45	.40	1.06
283	Moderate	82.08	13.14	2.95	.57	1.26
284	Moderate	73.55	17.08	5.76	1.31	2.30
285	Moderate	35.21	25.62	23.50	6.29	9.38
286	Moderate	40.89	28.05	15.05	6.63	9.38
287	Moderate	33.71	33.96	20.98	4.02	7.33
288	Moderate	34.12	39.23	16.80	3.99	5.86
289	Moderate	43.69	34.16	13.81	2.32	6.02
290	Moderate	71.31	12.80	7.09	1.60	7.20
291	Moderate	73.38	12.69	6.50	2.13	5.30

292	Moderate	57.75	17.80	11.14	3.56	9.75
293	Moderate	61.19	16.78	10.49	2.87	8.67
294	Moderate	58.12	19.07	13.16	2.71	6.94
295	Long	81.91	10.78	3.72	1.27	2.32
296	Long	73.74	16.36	4.15	.88	4.87
297	Long	66.64	18.24	9.76	1.76	3.60
298	Long	52.90	22.52	11.26	2.34	10.98
299	Long	64.76	17.79	7.71	2.25	7.49
300	Long	69.20	17.17	8.08	1.43	4.12
301	Long	65.19	22.41	5.99	2.25	4.16
302	Long	49.76	20.80	10.45	4.83	14.16
303	Long	46.00	15.50	16.15	7.48	14.87
304	Long	44.62	19.86	16.71	4.70	14.11
305	Long	69.86	19.69	6.08	1.50	2.87
306	Long	68.10	22.48	5.92	1.43	2.07
307	Long	67.18	17.95	6.55	3.61	4.71
308	Long	64.89	24.51	5.49	1.63	3.48
309	Long	69.48	20.71	6.05	1.66	2.10
310	Long	60.09	22.91	6.39	2.41	8.20
311	Long	71.54	15.26	4.60	1.81	6.79
312	Long	48.85	25.83	9.76	4.67	10.89
313	Long	84.99	7.05	3.73	1.24	2.99
314	Long	65.00	15.60	8.73	3.23	7.44
315	Long	58.69	30.68	7.19	1.99	1.45
316	Long	74.12	15.89	7.16	.91	1.92
317	Long	74.11	19.59	3.25	1.50	1.55
318	Long	69.81	23.66	3.91	.75	1.87
319	Long	71.57	21.48	4.36	1.20	1.39
320	Long	83.91	9.32	4.24	.83	1.70
321	Long	39.74	29.52	13.31	3.39	14.04
322	Long	36.46	43.33	13.60	1.82	4.79
323	Long	73.46	19.21	5.32	.55	1.46
324	Long	65.55	23.46	6.17	1.38	3.44
325	Long	49.43	26.77	18.85	1.48	3.47
326	Long	33.88	25.19	19.00	7.51	14.42
327	Long	53.78	25.97	8.00	2.47	9.78
328	Long	45.91	21.28	15.22	4.16	13.43
329	Long	57.42	16.13	13.49	3.52	9.44
330	Long	48.64	24.20	13.81	1.97	11.38
331	Long	41.65	23.38	23.40	3.98	7.59
332	Long	89.52	3.76	3.85	1.08	1.79
333	Long	58.91	13.69	15.99	3.51	7.90
334	Long	51.41	12.66	13.05	19.07	3.81
335	Long	77.43	9.76	3.43	1.34	8.04
336	Long	69.54	16.68	5.16	1.65	6.97
337	Long	54.34	24.10	5.90	1.59	14.07
338	Long	49.23	30.22	5.61	2.08	12.86
339	Long	62.91	20.29	4.89	1.37	10.54
340	Long	67.34	18.50	9.01	1.30	3.85
341	Long	66.49	18.46	9.78	1.50	3.77
342	Long	72.94	14.35	8.47	1.33	2.91
343	Long	75.44	9.80	9.71	.94	4.11
344	Long	71.44	15.77	7.33	2.80	2.66
345	Long	32.91	31.04	14.36	8.54	13.15
346	Long	38.07	28.62	16.86	4.00	12.45
347	Long	58.06	24.18	9.31	2.23	6.22
348	Long	70.15	15.73	7.94	1.53	4.65
349	Long	55.40	24.27	9.01	3.60	7.72
350	Long	63.95	23.40	6.81	1.14	4.70
351	Long	56.67	19.22	11.75	5.85	6.51

352	Long	58.18	21.39	11.65	3.63	5.15
353	Long	53.61	20.93	12.99	4.79	7.68
354	Long	54.85	24.17	8.66	5.07	7.25
355	Long	76.50	12.60	5.81	2.07	3.02
356	Long	42.39	18.75	14.27	6.74	17.85
357	Long	43.51	19.62	15.05	6.77	15.05
358	Long	45.34	22.21	14.33	3.88	14.24
359	Long	57.67	21.61	12.15	3.78	4.79
360	Long	66.95	16.68	10.92	3.05	2.40
361	Long	53.00	17.49	18.01	4.76	6.74
362	Long	62.46	15.45	6.79	7.52	7.78
363	Long	66.27	9.59	9.78	8.56	5.80
364	Long	53.44	21.40	9.62	9.28	6.26
365	Long	74.38	11.03	7.01	2.63	4.95
366	Long	49.86	20.14	10.35	11.04	8.61
367	Long	86.78	8.03	2.91	.50	1.78
368	Long	83.32	10.60	4.66	.38	1.04
369	Long	50.33	24.35	11.45	6.41	7.46
370	Long	42.79	24.64	13.59	6.34	12.64
371	Long	38.67	26.86	20.67	4.42	9.38
372	Long	38.61	33.00	14.59	4.02	9.78
373	Long	42.44	35.55	13.53	3.18	5.30
374	Long	65.99	18.45	6.65	2.12	6.79
375	Long	62.64	19.52	6.83	2.84	8.17

Appendix E

Relative spectral powers at after apnea termination (AAT) for C4 EEG

Apnea event number	Apnea duration groups	Relative spectral powers				
		Delta	*Theta*	*Alpha*	*Sigma*	*Beta*
1	Short	67.57	18.54	8.55	1.69	3.65
2	Short	61.20	23.59	9.25	2.79	3.17
3	Short	53.35	20.98	14.10	2.42	9.15
4	Short	75.38	15.83	4.16	1.06	3.57
5	Short	80.97	11.72	4.28	.83	2.20
6	Short	51.31	21.13	9.54	6.23	11.79
7	Short	52.21	21.24	9.55	4.50	12.50
8	Short	45.92	20.40	7.74	3.08	22.86
9	Short	61.61	17.51	9.73	4.15	7.00
10	Short	62.10	19.18	12.08	2.48	4.16
11	Short	48.47	24.02	19.45	2.80	5.26
12	Short	36.01	18.56	24.26	6.22	14.95
13	Short	39.60	27.53	18.25	4.79	9.83
14	Short	41.55	14.74	23.66	7.02	13.03
15	Short	81.18	8.03	5.74	1.53	3.52
16	Short	37.02	23.89	20.56	5.32	13.21
17	Short	39.15	18.44	21.95	3.25	17.21
18	Short	68.37	17.24	5.93	2.85	5.61
19	Short	70.34	14.52	6.92	2.40	5.82
20	Short	78.76	7.67	6.87	3.13	3.57
21	Short	83.75	7.97	4.50	1.60	2.18
22	Short	88.76	5.26	3.40	.93	1.65
23	Short	91.79	3.72	3.31	.51	.67
24	Short	90.71	4.73	3.07	.66	.83
25	Short	90.65	5.22	2.45	.50	1.18
26	Short	49.42	16.20	14.48	9.44	10.46
27	Short	54.22	16.00	14.54	5.44	9.80
28	Short	63.42	15.37	11.89	3.29	6.03
29	Short	56.43	17.59	12.77	3.95	9.26
30	Short	42.54	28.59	12.87	6.19	9.81
31	Short	68.73	15.97	10.44	1.71	3.15
32	Short	26.30	14.43	22.79	9.65	26.83
33	Short	28.59	13.53	22.59	6.21	29.08
34	Short	33.57	14.21	17.51	6.66	28.05
35	Short	24.84	10.40	30.42	9.10	25.24
36	Short	56.00	14.06	12.27	3.70	13.97
37	Short	64.46	23.76	5.55	2.84	3.39
38	Short	40.20	36.40	12.18	2.79	8.43
39	Short	74.13	16.54	6.24	1.10	1.99
40	Short	88.28	7.70	2.14	.68	1.20
41	Short	83.80	10.67	3.11	.88	1.54
42	Short	42.92	23.65	16.74	3.74	12.95
43	Short	62.23	17.64	8.07	2.11	9.95
44	Short	43.40	25.75	16.12	4.11	10.62
45	Short	16.08	32.32	30.14	7.64	13.82
46	Short	68.67	23.44	5.73	.89	1.27
47	Short	77.11	12.27	8.87	.77	.98
48	Short	68.29	14.55	13.94	1.29	1.93
49	Short	25.50	50.88	16.26	3.42	3.94
50	Short	66.24	20.39	9.24	1.02	3.11
51	Short	67.40	14.39	4.84	2.98	10.39

52	Short	66.85	20.02	7.47	2.26	3.40
53	Short	71.48	18.79	6.38	1.28	2.07
54	Short	73.84	14.94	6.86	1.89	2.47
55	Short	78.21	14.28	3.76	1.82	1.93
56	Short	54.43	28.22	7.42	2.79	7.14
57	Short	57.77	29.22	5.20	2.38	5.43
58	Short	58.02	22.13	8.97	2.78	8.10
59	Short	79.17	11.83	4.80	.96	3.24
60	Short	68.49	17.05	8.21	2.04	4.21
61	Short	25.57	30.66	30.54	3.21	10.02
62	Short	26.65	27.37	21.83	5.67	18.48
63	Short	48.79	29.78	13.94	2.52	4.97
64	Short	33.88	25.87	22.72	2.57	14.96
65	Short	35.79	40.41	16.41	1.49	5.90
66	Short	32.86	28.16	16.66	5.69	16.63
67	Short	43.00	23.27	13.68	3.16	16.89
68	Short	49.77	19.01	12.60	3.83	14.79
69	Short	33.68	33.36	13.82	7.84	11.30
70	Short	46.65	23.32	13.63	4.94	11.46
71	Short	37.46	23.51	29.42	3.79	5.82
72	Short	38.59	20.12	27.96	3.38	9.95
73	Short	38.45	20.35	26.36	4.67	10.17
74	Short	31.83	26.71	29.65	4.94	6.87
75	Short	38.79	18.49	25.27	4.50	12.95
76	Short	63.74	18.71	7.96	3.49	6.10
77	Short	59.73	10.11	8.68	13.17	8.31
78	Short	57.74	9.14	10.67	6.41	16.04
79	Short	82.88	5.25	4.66	2.30	4.91
80	Short	43.77	13.42	18.39	7.07	17.35
81	Short	34.95	21.02	12.16	7.18	24.69
82	Short	50.95	7.95	12.11	5.21	23.78
83	Short	37.73	15.80	7.52	2.19	36.76
84	Short	36.28	17.61	27.35	6.60	12.16
85	Short	33.01	16.72	5.57	4.10	40.60
86	Short	52.67	17.83	12.26	4.18	13.06
87	Short	50.11	10.40	13.34	2.25	23.90
88	Short	47.36	7.46	7.88	3.72	33.58
89	Short	81.65	8.45	5.39	1.52	2.99
90	Short	47.59	22.76	16.56	4.01	9.08
91	Short	69.73	8.19	14.78	2.49	4.81
92	Short	72.53	13.64	9.38	1.42	3.03
93	Short	84.24	9.20	4.37	.74	1.45
94	Short	66.94	19.28	9.47	1.12	3.19
95	Short	51.04	12.23	13.19	6.66	16.88
96	Short	48.43	18.53	15.75	8.09	9.20
97	Short	58.42	14.93	15.10	1.99	9.56
98	Short	60.94	12.23	15.23	2.64	8.96
99	Short	61.16	14.82	9.55	5.84	8.63
100	Short	37.76	19.68	18.12	5.76	18.68
101	Short	49.67	35.55	9.54	1.32	3.92
102	Short	77.18	10.72	6.54	1.69	3.87
103	Short	63.92	21.02	7.03	2.02	6.01
104	Short	23.42	39.91	28.89	1.51	6.27
105	Short	79.59	10.12	6.55	.75	2.99
106	Short	66.49	19.12	7.84	1.74	4.81
107	Short	65.29	14.57	12.37	1.68	6.09
108	Short	79.89	9.90	5.42	1.87	2.92
109	Short	69.65	19.08	5.42	1.31	4.54
110	Short	78.52	13.00	4.54	1.11	2.83
111	Short	49.64	21.17	18.73	1.87	8.59

112	Short	32.03	38.33	15.87	3.38	10.39
113	Short	31.44	33.90	28.03	2.03	4.60
114	Short	74.84	10.90	7.26	1.67	5.33
115	Short	65.49	15.17	11.93	2.32	5.09
116	Short	59.67	17.08	8.32	2.97	11.96
117	Short	66.12	7.99	5.80	3.64	16.45
118	Short	38.37	18.14	18.85	4.82	19.82
119	Short	51.24	18.81	12.12	3.85	13.98
120	Short	58.37	18.81	9.36	2.80	10.66
121	Short	10.16	21.80	21.45	5.99	40.60
122	Short	15.34	19.74	29.36	2.99	32.57
123	Short	23.14	24.68	36.43	4.67	11.08
124	Short	29.99	12.18	17.88	5.23	34.72
125	Short	16.70	11.39	29.63	6.10	36.18
126	Short	50.74	21.66	8.55	3.33	15.72
127	Short	52.27	21.61	9.02	2.37	14.73
128	Short	74.30	11.24	6.84	2.52	5.10
129	Short	63.70	11.43	6.99	2.03	15.85
130	Short	50.09	21.94	7.12	3.45	17.40
131	Short	73.08	8.47	7.27	2.67	8.51
132	Short	88.03	5.08	2.76	.98	3.15
133	Short	74.79	8.50	5.65	3.78	7.28
134	Short	86.42	4.00	3.25	1.09	5.24
135	Short	74.81	8.50	6.83	2.62	7.24
136	Short	92.50	4.69	1.68	.41	.72
137	Short	82.75	7.75	5.08	2.15	2.27
138	Short	93.38	4.65	1.07	.20	.70
139	Short	94.35	3.00	1.68	.31	.66
140	Short	92.91	5.16	.95	.42	.56
141	Short	45.21	26.46	16.63	5.12	6.58
142	Short	58.60	20.62	12.89	3.44	4.45
143	Short	33.76	35.62	20.17	3.03	7.42
144	Short	65.59	14.41	10.62	1.99	7.39
145	Short	55.03	28.57	10.62	2.41	3.37
146	Short	42.92	18.53	22.43	4.05	12.07
147	Short	36.84	19.88	21.54	3.91	17.83
148	Short	53.27	15.72	18.92	2.10	9.99
149	Short	62.86	19.91	10.76	2.14	4.33
150	Short	54.07	18.74	17.76	3.99	5.44
151	Moderate	69.58	16.24	10.06	1.05	3.07
152	Moderate	56.12	26.21	10.93	1.90	4.84
153	Moderate	74.36	18.18	4.13	1.29	2.04
154	Moderate	82.81	8.86	5.41	1.22	1.70
155	Moderate	51.40	24.71	10.16	2.21	11.52
156	Moderate	64.46	13.15	6.86	2.80	12.73
157	Moderate	76.23	17.77	2.54	.78	2.68
158	Moderate	51.88	23.95	8.82	3.37	11.98
159	Moderate	40.96	15.22	11.75	7.79	24.28
160	Moderate	48.89	13.75	12.57	4.38	20.41
161	Moderate	42.50	26.96	17.96	3.64	8.94
162	Moderate	38.95	20.37	25.85	5.47	9.36
163	Moderate	40.89	19.47	23.34	5.21	11.09
164	Moderate	46.58	22.08	19.15	3.28	8.91
165	Moderate	40.65	30.83	18.29	3.07	7.16
166	Moderate	43.59	27.35	11.05	1.68	16.33
167	Moderate	33.42	23.16	18.89	4.78	19.75
168	Moderate	63.97	15.91	8.73	3.33	8.06
169	Moderate	20.86	17.16	19.09	11.64	31.25
170	Moderate	33.02	25.48	14.03	3.88	23.59
171	Moderate	83.71	6.54	7.07	1.07	1.61

172	Moderate	78.11	8.68	8.84	2.40	1.97
173	Moderate	71.43	13.12	10.67	1.75	3.03
174	Moderate	77.81	10.51	7.42	1.66	2.60
175	Moderate	86.00	6.85	4.04	1.28	1.83
176	Moderate	88.95	3.43	4.50	.58	2.54
177	Moderate	26.34	18.37	31.25	4.79	19.25
178	Moderate	88.78	3.14	4.08	1.09	2.91
179	Moderate	26.90	16.21	31.26	7.77	17.86
180	Moderate	28.19	24.65	19.35	6.56	21.25
181	Moderate	30.76	17.57	22.82	10.20	18.65
182	Moderate	47.47	11.63	19.88	5.44	15.58
183	Moderate	29.85	11.36	26.15	10.48	22.16
184	Moderate	36.03	9.21	24.19	7.19	23.38
185	Moderate	35.19	11.67	22.31	8.60	22.23
186	Moderate	35.50	37.27	12.97	3.52	10.74
187	Moderate	31.02	26.96	16.57	4.72	20.73
188	Moderate	39.94	28.40	13.81	3.24	14.61
189	Moderate	37.93	30.52	14.74	3.38	13.43
190	Moderate	64.62	22.63	6.87	2.27	3.61
191	Moderate	39.04	22.51	18.68	6.32	13.45
192	Moderate	38.66	21.23	20.73	3.93	15.45
193	Moderate	25.31	19.79	32.04	3.64	19.22
194	Moderate	48.08	15.60	18.62	3.09	14.61
195	Moderate	69.25	15.01	6.15	1.50	8.09
196	Moderate	10.10	51.61	16.82	3.64	17.83
197	Moderate	9.94	29.45	37.19	6.50	16.92
198	Moderate	15.73	42.49	28.34	4.13	9.31
199	Moderate	14.65	44.08	23.66	4.35	13.26
200	Moderate	8.13	31.57	42.00	3.95	14.35
201	Moderate	62.67	24.19	6.82	2.47	3.85
202	Moderate	82.16	8.82	5.17	1.10	2.75
203	Moderate	81.94	12.17	3.31	1.02	1.56
204	Moderate	82.76	6.58	4.28	.44	5.94
205	Moderate	80.04	13.00	3.63	1.24	2.09
206	Moderate	62.34	19.60	7.62	3.56	6.88
207	Moderate	67.76	15.99	7.75	2.20	6.30
208	Moderate	56.54	23.42	10.46	3.14	6.44
209	Moderate	63.57	20.54	8.52	2.63	4.74
210	Moderate	67.74	19.86	6.26	2.23	3.91
211	Moderate	31.53	25.88	13.95	3.18	25.46
212	Moderate	24.57	31.30	23.35	3.36	17.42
213	Moderate	45.41	33.36	11.56	3.44	6.23
214	Moderate	56.35	17.41	16.70	1.47	8.07
215	Moderate	55.24	24.53	13.46	2.00	4.77
216	Moderate	39.89	22.37	18.31	5.45	13.98
217	Moderate	39.71	20.29	23.13	5.45	11.42
218	Moderate	31.83	27.98	23.83	4.98	11.38
219	Moderate	36.35	27.44	16.27	7.56	12.38
220	Moderate	28.61	33.21	18.49	9.81	9.88
221	Moderate	55.80	8.50	17.47	3.27	14.96
222	Moderate	31.01	27.72	32.92	2.31	6.04
223	Moderate	46.31	22.55	19.35	4.55	7.24
224	Moderate	47.24	19.34	17.11	5.51	10.80
225	Moderate	58.97	12.37	14.74	3.67	10.25
226	Moderate	84.76	5.50	4.73	2.06	2.95
227	Moderate	71.84	6.17	7.16	2.32	12.51
228	Moderate	69.39	8.52	9.79	3.28	9.02
229	Moderate	54.83	10.21	9.16	17.08	8.72
230	Moderate	59.95	17.12	9.73	6.37	6.83
231	Moderate	57.20	21.05	9.39	1.64	10.72

232	Moderate	59.70	17.13	7.06	6.35	9.76
233	Moderate	58.41	14.86	6.92	3.94	15.87
234	Moderate	47.36	17.83	10.76	5.20	18.85
235	Moderate	29.20	38.40	8.78	4.58	19.04
236	Moderate	64.72	7.38	6.74	3.67	17.49
237	Moderate	77.23	4.54	3.71	2.37	12.15
238	Moderate	73.92	6.13	4.59	1.77	13.59
239	Moderate	85.13	4.66	5.14	1.35	3.72
240	Moderate	53.19	8.25	7.42	3.68	27.46
241	Moderate	42.96	33.42	13.67	3.57	6.38
242	Moderate	66.19	13.87	13.18	2.10	4.66
243	Moderate	64.78	16.39	10.77	2.17	5.89
244	Moderate	55.11	20.32	16.91	1.62	6.04
245	Moderate	41.16	27.54	22.42	1.97	6.91
246	Moderate	39.15	17.24	20.44	3.60	19.57
247	Moderate	45.67	20.83	16.53	2.15	14.82
248	Moderate	29.81	22.45	26.18	5.21	16.35
249	Moderate	47.70	20.83	12.58	7.28	11.61
250	Moderate	48.37	21.32	16.83	3.53	9.95
251	Moderate	60.27	14.91	14.19	3.48	7.15
252	Moderate	80.18	6.40	5.91	2.32	5.19
253	Moderate	49.35	18.16	7.34	2.60	22.55
254	Moderate	84.72	7.95	4.12	.89	2.32
255	Moderate	26.44	12.65	23.78	4.84	32.29
256	Moderate	55.33	12.52	16.66	4.68	10.81
257	Moderate	72.60	16.22	6.71	.88	3.59
258	Moderate	81.18	8.46	7.07	1.03	2.26
259	Moderate	84.38	7.34	5.80	.78	1.70
260	Moderate	67.66	23.55	4.74	1.55	2.50
261	Moderate	35.92	31.18	20.00	2.99	9.91
262	Moderate	55.15	24.34	8.71	3.75	8.05
263	Moderate	69.87	16.59	7.26	2.55	3.73
264	Moderate	72.09	8.05	9.00	1.17	9.69
265	Moderate	61.74	20.33	9.29	2.84	5.80
266	Moderate	50.55	17.74	12.73	4.56	14.42
267	Moderate	61.68	13.35	8.85	3.78	12.34
268	Moderate	68.37	16.36	5.69	2.77	6.81
269	Moderate	42.57	14.74	21.10	5.62	15.97
270	Moderate	80.32	6.28	3.55	1.44	8.41
271	Moderate	40.30	25.39	15.88	3.39	15.04
272	Moderate	38.69	11.73	26.13	5.23	18.22
273	Moderate	62.83	18.21	13.26	1.87	3.83
274	Moderate	30.49	30.23	27.47	3.51	8.30
275	Moderate	25.83	8.20	21.22	9.38	35.37
276	Moderate	70.75	11.50	11.10	1.72	4.93
277	Moderate	82.08	6.69	4.43	2.28	4.52
278	Moderate	86.04	3.79	3.70	2.39	4.08
279	Moderate	84.75	5.32	4.45	1.44	4.04
280	Moderate	88.81	3.92	1.87	1.16	4.24
281	Moderate	90.76	5.18	2.29	.65	1.12
282	Moderate	75.68	13.27	5.95	2.16	2.94
283	Moderate	83.54	7.81	4.93	1.02	2.70
284	Moderate	90.88	4.17	2.37	.90	1.68
285	Moderate	83.20	8.98	5.93	.69	1.20
286	Moderate	45.77	28.70	19.35	1.71	4.47
287	Moderate	54.86	18.97	16.67	2.06	7.44
288	Moderate	54.92	25.73	14.75	1.61	2.99
289	Moderate	46.05	28.39	17.55	2.62	5.39
290	Moderate	57.17	19.39	10.64	2.82	9.98
291	Moderate	67.29	9.34	8.72	2.85	11.80

292	Moderate	63.81	18.15	5.88	3.39	8.77
293	Moderate	56.98	16.40	11.40	3.32	11.90
294	Moderate	54.49	19.00	14.11	3.44	8.96
295	Long	59.25	23.32	12.43	1.81	3.19
296	Long	64.09	14.27	11.98	1.29	8.37
297	Long	72.08	15.85	7.90	1.31	2.86
298	Long	49.23	27.87	10.37	2.40	10.13
299	Long	61.29	16.04	13.38	2.49	6.80
300	Long	61.78	11.02	14.83	3.03	9.34
301	Long	57.64	11.18	15.02	4.47	11.69
302	Long	81.54	6.38	5.99	1.41	4.68
303	Long	32.26	21.30	21.63	5.43	19.38
304	Long	48.69	6.52	10.47	3.19	31.13
305	Long	34.66	35.15	14.56	3.48	12.15
306	Long	36.69	34.67	10.66	4.22	13.76
307	Long	64.78	20.87	7.54	1.65	5.16
308	Long	54.77	26.80	7.25	3.29	7.89
309	Long	68.44	16.31	6.61	2.37	6.27
310	Long	57.27	20.40	8.55	3.85	9.93
311	Long	64.65	18.91	6.63	2.32	7.49
312	Long	41.65	13.58	23.31	4.87	16.59
313	Long	50.58	18.53	15.21	2.09	13.59
314	Long	69.33	13.86	7.01	3.31	6.49
315	Long	83.41	10.55	2.94	.94	2.16
316	Long	66.62	17.99	7.18	1.96	6.25
317	Long	45.57	23.34	18.47	3.10	9.52
318	Long	66.15	18.51	9.09	2.33	3.92
319	Long	76.01	11.35	6.96	2.51	3.17
320	Long	66.47	14.60	11.74	2.77	4.42
321	Long	50.17	11.41	7.82	2.87	27.73
322	Long	39.31	26.53	16.03	2.96	15.17
323	Long	70.26	11.36	8.43	1.58	8.37
324	Long	63.93	11.18	10.74	1.82	12.33
325	Long	55.35	17.26	10.33	3.48	13.58
326	Long	19.12	20.55	28.79	5.10	26.44
327	Long	23.20	16.63	25.36	6.58	28.23
328	Long	32.88	15.53	24.55	2.20	24.84
329	Long	26.09	13.02	36.58	5.12	19.19
330	Long	12.69	21.80	39.62	5.13	20.76
331	Long	34.68	24.64	28.71	4.30	7.67
332	Long	45.66	16.34	28.56	2.52	6.92
333	Long	53.55	13.53	19.61	4.78	8.53
334	Long	81.14	5.77	5.70	2.37	5.02
335	Long	39.08	22.21	11.96	5.35	21.40
336	Long	57.27	14.57	10.88	3.07	14.21
337	Long	60.35	5.85	7.51	7.28	19.01
338	Long	60.64	12.06	8.86	4.37	14.07
339	Long	86.66	3.42	1.61	1.20	7.11
340	Long	79.86	10.35	6.60	.58	2.61
341	Long	74.96	9.39	10.67	1.68	3.30
342	Long	50.19	29.00	14.59	1.06	5.16
343	Long	51.19	11.83	14.78	3.58	18.62
344	Long	81.98	8.88	6.51	.82	1.81
345	Long	46.92	21.10	11.78	6.07	14.13
346	Long	59.80	5.43	7.93	3.65	23.19
347	Long	76.81	8.08	6.16	1.35	7.60
348	Long	74.68	14.21	7.51	1.28	2.32
349	Long	91.88	1.46	1.52	1.17	3.97
350	Long	85.77	9.81	2.94	.39	1.09
351	Long	73.85	14.54	6.50	1.64	3.47

352	Long	83.25	8.10	3.58	1.06	4.01
353	Long	67.60	9.17	4.40	1.66	17.17
354	Long	63.69	11.78	6.35	1.39	16.79
355	Long	49.10	31.18	11.34	3.21	5.17
356	Long	46.34	14.58	13.29	5.62	20.17
357	Long	51.84	16.99	11.95	4.80	14.42
358	Long	49.13	12.52	13.17	4.17	21.01
359	Long	31.40	18.69	21.00	5.77	23.14
360	Long	56.43	3.68	5.37	3.50	31.02
361	Long	60.61	9.86	6.32	.92	22.29
362	Long	74.18	9.65	8.19	1.94	6.04
363	Long	92.49	3.64	1.63	.50	1.74
364	Long	89.64	3.94	3.67	.61	2.14
365	Long	88.59	4.12	3.44	.72	3.13
366	Long	85.09	4.45	4.12	1.58	4.76
367	Long	77.16	8.48	2.14	.78	11.44
368	Long	87.05	5.51	4.10	1.52	1.82
369	Long	83.70	7.03	4.38	.77	4.12
370	Long	89.55	6.39	2.47	.29	1.30
371	Long	53.26	21.52	16.21	1.65	7.36
372	Long	53.68	13.21	11.22	2.36	19.53
373	Long	74.02	14.48	8.24	.92	2.34
374	Long	67.73	14.14	7.88	2.29	7.96
375	Long	67.49	13.90	9.19	2.68	6.74

Appendix F

Sleep states and apnea types with varying apnea duration

Apnea event number	Apnea duration groups	Sleep states		Apnea types		
1	Short	NREM	-	OSA	-	-
2	Short	NREM	-	-	CSA	-
3	Short	NREM	-	-	CSA	-
4	Short	NREM	-	-	CSA	-
5	Short	NREM	-	-	CSA	-
6	Short	-	REM	-	CSA	-
7	Short	-	REM	-	CSA	-
8	Short	-	REM	-	CSA	-
9	Short	-	REM	-	CSA	-
10	Short	NREM	-	-	CSA	-
11	Short	NREM	-	OSA	-	-
12	Short	-	REM	OSA	-	-
13	Short	-	REM	OSA	-	-
14	Short	-	REM	OSA	-	-
15	Short	NREM	-	-	CSA	-
16	Short	NREM	-	OSA	-	-
17	Short	NREM	-	OSA	-	-
18	Short	NREM	-	OSA	-	-
19	Short	NREM	-	OSA	-	-
20	Short	NREM	-	OSA	-	-
21	Short	NREM	-	OSA	-	-
22	Short	NREM	-	OSA	-	-
23	Short	NREM	-	-	CSA	-
24	Short	NREM	-	OSA	-	-
25	Short	NREM	-	-	CSA	-
26	Short	NREM	-	OSA	-	-
27	Short	NREM	-	OSA	-	-
28	Short	NREM	-	OSA	-	-
29	Short	NREM	-	OSA	-	-
30	Short	-	REM	OSA	-	-
31	Short	NREM	-	OSA	-	-
32	Short	NREM	-	-	CSA	-
33	Short	NREM	-	-	CSA	-
34	Short	NREM	-	-	CSA	-
35	Short	NREM	-	-	CSA	-
36	Short	NREM	-	-	CSA	-
37	Short	NREM	-	-	CSA	-
38	Short	NREM	-	-	CSA	-
39	Short	NREM	-	-	CSA	-
40	Short	NREM	-	-	CSA	-
41	Short	NREM	-	OSA	-	-
42	Short	-	REM	OSA	-	-
43	Short	-	REM	OSA	-	-
44	Short	-	REM	OSA	-	-
45	Short	NREM	-	OSA	-	-
46	Short	NREM	-	OSA	-	-
47	Short	NREM	-	OSA	-	-
48	Short	NREM	-	OSA	-	-
49	Short	NREM	-	OSA	-	-
50	Short	NREM	-	OSA	-	-
51	Short	NREM	-	OSA	-	-
52	Short	NREM	-	OSA	-	-

53	Short	NREM	-	OSA	-	-
54	Short	NREM	-	OSA	-	-
55	Short	NREM	-	OSA	-	
56	Short	NREM	-	OSA	-	-
57	Short	NREM	-	OSA	-	-
58	Short	NREM	-	OSA	-	-
59	Short	NREM	-	OSA	-	-
60	Short	NREM	-	OSA	-	-
61	Short	NREM	-	OSA	-	-
62	Short	NREM	-	-	CSA	-
63	Short	NREM	-	-	CSA	-
64	Short	NREM	-	-	CSA	-
65	Short	NREM	-	-	CSA	-
66	Short	NREM	-	OSA	-	-
67	Short	NREM	-	OSA	-	-
68	Short	NREM	-	OSA	-	-
69	Short	NREM	-	OSA	-	-
70	Short	NREM	-	OSA	-	-
71	Short	-	REM	OSA	-	-
72	Short	-	REM	OSA	-	-
73	Short	-	REM	OSA	-	-
74	Short	-	REM	OSA	-	-
75	Short	-	REM	OSA	-	-
76	Short	NREM	-	OSA	-	-
77	Short	NREM	-	-	CSA	-
78	Short	NREM	-	-	CSA	-
79	Short	NREM	-	-	CSA	-
80	Short	NREM	-	-	CSA	-
81	Short	NREM	-	OSA	-	-
82	Short	NREM	-	OSA	-	-
83	Short	NREM	-	OSA	-	-
84	Short	NREM	-	OSA	-	-
85	Short	NREM	-	OSA	-	-
86	Short	NREM	-	-	CSA	-
87	Short	NREM	-	-	CSA	-
88	Short	NREM	-	-	CSA	-
89	Short	NREM	-	OSA	-	-
90	Short	NREM	-	OSA	-	-
91	Short	NREM	-	OSA	-	-
92	Short	NREM	-	OSA	-	-
93	Short	NREM	-	OSA	-	-
94	Short	NREM	-	OSA	-	-
95	Short	NREM	-	OSA	-	-
96	Short	NREM	-	OSA	-	-
97	Short	NREM	-	OSA	-	-
98	Short	-	REM	OSA	-	-
99	Short	-	REM	OSA	-	-
100	Short	-	REM	-	CSA	-
101	Short	NREM	-	-	CSA	-
102	Short	NREM	-	-	CSA	-
103	Short	NREM	-	OSA	-	-
104	Short	NREM	-	-	CSA	-
105	Short	NREM	-	-	CSA	-
106	Short	NREM	-	-	CSA	-
107	Short	NREM	-	OSA	-	-
108	Short	NREM	-	OSA	-	-
109	Short	NREM	-	-	CSA	-
110	Short	-	REM	-	CSA	-
111	Short	NREM	-	-	CSA	-
112	Short	NREM	-	OSA	-	-

113	Short	NREM	-	OSA	-	-
114	Short	NREM	-	OSA	-	-
115	Short	NREM	-	OSA	-	-
116	Short	NREM	-	-	CSA	-
117	Short	NREM	-	OSA	-	-
118	Short	-	REM	OSA	-	-
119	Short	NREM	-	OSA	-	-
120	Short	NREM	-	OSA	-	-
121	Short	NREM	-	OSA	-	-
122	Short	-	REM	OSA	-	-
123	Short	-	REM	OSA	-	-
124	Short	-	REM	OSA	-	-
125	Short	NREM	-	OSA	-	-
126	Short	-	REM	OSA	-	-
127	Short	-	REM	OSA	-	-
128	Short	NREM	-	-	CSA	-
129	Short	-	REM	OSA	-	-
130	Short	-	REM	OSA	-	-
131	Short	NREM	-	OSA	-	-
132	Short	NREM	-	OSA	-	-
133	Short	NREM	-	OSA	-	-
134	Short	NREM	-	OSA	-	-
135	Short	NREM	-	OSA	-	-
136	Short	NREM	-	OSA	-	-
137	Short	NREM	-	OSA	-	-
138	Short	NREM	-	OSA	-	-
139	Short	NREM	-	OSA	-	-
140	Short	NREM	-	OSA	-	-
141	Short	NREM	-	OSA	-	-
142	Short	NREM	-	OSA	-	-
143	Short	NREM	-	OSA	-	-
144	Short	NREM	-	OSA	-	-
145	Short	NREM	-	OSA	-	-
146	Short	NREM	-	OSA	-	-
147	Short	NREM	-	OSA	-	-
148	Short	NREM	-	OSA	-	-
149	Short	NREM	-	OSA	-	-
150	Short	NREM	-	OSA	-	-
151	Moderate	NREM	-	-	CSA	-
152	Moderate	NREM	-	-	CSA	-
153	Moderate	NREM	-	-	CSA	-
154	Moderate	NREM	-	OSA	-	-
155	Moderate	NREM	-	OSA	-	-
156	Moderate	-	REM	-	CSA	-
157	Moderate	-	REM	-	CSA	-
158	Moderate	-	REM	-	CSA	-
159	Moderate	-	REM	-	CSA	-
160	Moderate	-	REM	-	CSA	-
161	Moderate	-	REM	OSA	-	-
162	Moderate	-	REM	OSA	-	-
163	Moderate	-	REM	OSA	-	-
164	Moderate	-	REM	OSA	-	-
165	Moderate	NREM		OSA	-	-
166	Moderate	-	REM	OSA	-	-
167	Moderate	-	REM	OSA	-	-
168	Moderate	NREM	-	OSA	-	-
169	Moderate	NREM	-	OSA	-	-
170	Moderate	NREM	-	OSA	-	-
171	Moderate	NREM	-	-	CSA	-
172	Moderate	NREM	-	OSA	-	-

173	Moderate	NREM	-	OSA	-	-
174	Moderate	NREM	-	OSA	-	-
175	Moderate	NREM	-	OSA	-	-
176	Moderate	-	REM	OSA	-	-
177	Moderate	-	REM	OSA	-	-
178	Moderate	-	REM	OSA	-	-
179	Moderate	-	REM	OSA	-	-
180	Moderate	-	REM	OSA	-	-
181	Moderate	NREM	-	-	CSA	-
182	Moderate	NREM	-	OSA	-	-
183	Moderate	NREM	-	-	CSA	-
184	Moderate	NREM	-	-	CSA	-
185	Moderate	NREM	-	-	CSA	-
186	Moderate	NREM	-	-	CSA	-
187	Moderate	NREM	-	-	CSA	-
188	Moderate	NREM	-	OSA	-	-
189	Moderate	NREM	-	-	CSA	-
190	Moderate	NREM	-	OSA	-	-
191	Moderate	-	REM	OSA	-	-
192	Moderate	-	REM	-	CSA	-
193	Moderate	-	REM	OSA	-	-
194	Moderate	-	REM	OSA	-	-
195	Moderate	-	REM	OSA	-	-
196	Moderate	-	REM	OSA	-	-
197	Moderate	-	REM	OSA	-	-
198	Moderate	NREM	-	OSA	-	-
199	Moderate	NREM	-	OSA	-	-
200	Moderate	NREM	-	OSA	-	-
201	Moderate	NREM	-	OSA	-	-
202	Moderate	NREM	-	OSA	-	-
203	Moderate	NREM	-	OSA	-	-
204	Moderate	NREM	-	OSA	-	-
205	Moderate	NREM	-	OSA	-	-
206	Moderate	NREM	-	OSA	-	-
207	Moderate	NREM	-	OSA	-	-
208	Moderate	NREM	-	OSA	-	-
209	Moderate	NREM	-	OSA	-	-
210	Moderate	NREM	-	OSA	-	-
211	Moderate	NREM	-	-	CSA	-
212	Moderate	NREM	-	-	CSA	-
213	Moderate	NREM	-	-	CSA	-
214	Moderate	NREM	-	-	CSA	-
215	Moderate	NREM	-	-	CSA	-
216	Moderate	NREM	-	OSA	-	-
217	Moderate	NREM	-	OSA	-	-
218	Moderate	NREM	-	OSA	-	-
219	Moderate	NREM	-	OSA	-	-
220	Moderate	NREM	-	OSA	-	-
221	Moderate	-	REM	OSA	-	-
222	Moderate	-	REM	OSA	-	-
223	Moderate	-	REM	OSA	-	-
224	Moderate	-	REM	OSA	-	-
225	Moderate	-	REM	OSA	-	-
226	Moderate	NREM	-	-	CSA	-
227	Moderate	NREM	-	-	CSA	-
228	Moderate	NREM	-	-	CSA	-
229	Moderate	NREM	-	-	CSA	-
230	Moderate	NREM	-	-	CSA	-
231	Moderate	NREM	-	OSA	-	-
232	Moderate	-	REM	OSA	-	-

233	Moderate	-	REM	OSA	-	-
234	Moderate	-	REM	OSA	-	-
235	Moderate	-	REM	OSA	-	-
236	Moderate	NREM	-	-	CSA	-
237	Moderate	NREM	-	OSA	-	-
238	Moderate	NREM	-	OSA	-	-
239	Moderate	NREM	-	OSA	-	-
240	Moderate	NREM	-	OSA	-	-
241	Moderate	-	REM	OSA	-	-
242	Moderate	-	REM	OSA	-	-
243	Moderate	-	REM	OSA	-	-
244	Moderate	-	REM	OSA	-	-
245	Moderate	NREM	-	OSA	-	-
246	Moderate	NREM	-	OSA	-	-
247	Moderate	NREM	-	OSA	-	-
248	Moderate	-	REM	OSA	-	-
249	Moderate	-	REM	OSA	-	-
250	Moderate	NREM	-	OSA	-	-
251	Moderate	NREM	-	OSA	-	-
252	Moderate	NREM	-	OSA	-	-
253	Moderate	NREM	-	OSA	-	-
254	Moderate	NREM	-	OSA	-	-
255	Moderate	-	REM	OSA	-	-
256	Moderate	NREM	-	OSA	-	-
257	Moderate	NREM	-	OSA	-	-
258	Moderate	NREM	-	OSA	-	-
259	Moderate	NREM	-	OSA	-	-
260	Moderate	NREM	-	OSA	-	-
261	Moderate	NREM	-	OSA	-	-
262	Moderate	NREM	-	OSA	-	-
263	Moderate	NREM	-	OSA	-	-
264	Moderate	NREM	-	OSA	-	-
265	Moderate	NREM	-	OSA	-	-
266	Moderate	-	REM	OSA	-	-
267	Moderate	NREM	-	OSA	-	-
268	Moderate	NREM	-	OSA	-	-
269	Moderate	-	REM	OSA	-	-
270	Moderate	NREM	-	OSA	-	-
271	Moderate	NREM	-	OSA	-	-
272	Moderate	NREM	-	OSA	-	-
273	Moderate	NREM	-	OSA	-	-
274	Moderate	NREM	-	OSA	-	-
275	Moderate	NREM	-	OSA	-	-
276	Moderate	NREM	-	OSA	-	-
277	Moderate	NREM	-	OSA	-	-
278	Moderate	NREM	-	OSA	-	-
279	Moderate	NREM	-	OSA	-	-
280	Moderate	NREM	-	OSA	-	-
281	Moderate	NREM	-	OSA	-	-
282	Moderate	NREM	-	OSA	-	-
283	Moderate	NREM	-	OSA	-	-
284	Moderate	NREM	-	OSA	-	-
285	Moderate	NREM	-	OSA	-	-
286	Moderate	-	REM	OSA	-	-
287	Moderate	NREM	-	OSA	-	-
288	Moderate	NREM	-	OSA	-	-
289	Moderate	NREM	-	OSA	-	-
290	Moderate	NREM	-	OSA	-	-
291	Moderate	NREM	-	OSA	-	-
292	Moderate	NREM	-	OSA	-	-

293	Moderate	NREM	-	OSA	-	-
294	Moderate	NREM	-	OSA	-	-
295	Long	NREM	-	OSA	-	-
296	Long	NREM	-	OSA	-	-
297	Long	NREM	-	OSA	-	-
298	Long	NREM	-	OSA	-	-
299	Long	NREM	-	OSA	-	-
300	Long	NREM	-	OSA	-	-
301	Long	NREM	-	OSA	-	-
302	Long	-	REM	OSA	-	-
303	Long	-	REM	OSA	-	-
304	Long	-	REM	OSA	-	-
305	Long	NREM	-	OSA	-	-
306	Long	NREM	-	OSA	-	-
307	Long	NREM	-	OSA	-	-
308	Long	NREM	-	OSA	-	-
309	Long	NREM	-	OSA	-	-
310	Long	-	REM	OSA	-	-
311	Long	-	REM	OSA	-	-
312	Long	-	REM	OSA	-	-
313	Long	NREM	-	OSA	-	-
314	Long	-	REM	OSA	-	-
315	Long	NREM	-	OSA	-	-
316	Long	NREM	-	OSA	-	-
317	Long	NREM	-	OSA	-	-
318	Long	NREM	-	OSA	-	-
319	Long	NREM	-	OSA	-	-
320	Long	NREM	-	OSA	-	-
321	Long	-	REM	OSA	-	-
322	Long	NREM	-	OSA	-	-
323	Long	NREM	-	OSA	-	-
324	Long	NREM	-	OSA	-	-
325	Long	NREM	-	OSA	-	-
326	Long	NREM	-	OSA	-	-
327	Long	NREM	-	OSA	-	-
328	Long	NREM	-	OSA	-	-
329	Long	NREM	-	OSA	-	-
330	Long	NREM	-	OSA	-	-
331	Long	-	REM	OSA	-	-
332	Long	-	REM	OSA	-	-
333	Long	-	REM	OSA	-	-
334	Long	NREM	-	OSA	-	-
335	Long	-	REM	OSA	-	-
336	Long	-	REM	OSA	-	-
337	Long	-	REM	OSA	-	-
338	Long	-	REM	OSA	-	-
339	Long	-	REM	OSA	-	-
340	Long	-	REM	OSA	-	-
341	Long	-	REM	OSA	-	-
342	Long	-	REM	OSA	-	-
343	Long	-	REM	OSA	-	-
344	Long	NREM	-	OSA	-	-
345	Long	-	REM	OSA	-	-
346	Long	NREM	-	OSA	-	-
347	Long	NREM	-	OSA	-	-
348	Long	NREM	-	OSA	-	-
349	Long	NREM	-	OSA	-	-
350	Long	NREM	-	OSA	-	-
351	Long	NREM	-	OSA	-	-
352	Long	NREM	-	OSA	-	-

353	Long	NREM	-	OSA	-	-
354	Long	NREM	-	OSA	-	-
355	Long	NREM	-	OSA	-	-
356	Long	-	REM	OSA	-	-
357	Long	-	REM	OSA	-	-
358	Long	-	REM	OSA	-	-
359	Long	NREM	-	OSA	-	-
360	Long	NREM	-	OSA	-	-
361	Long	-	REM	OSA	-	-
362	Long	NREM	-	OSA	-	-
363	Long	NREM	-	OSA	-	-
364	Long	NREM	-	OSA	-	-
365	Long	NREM	-	OSA	-	-
366	Long	NREM	-	OSA	-	-
367	Long	-	REM	OSA	-	-
368	Long	NREM	-	OSA	-	-
369	Long	-	REM	OSA	-	-
370	Long	-	REM	OSA	-	-
371	Long	NREM	-	OSA	-	-
372	Long	NREM	-	OSA	-	-
373	Long	NREM	-	OSA	-	-
374	Long	NREM	-	OSA	-	-
375	Long	-	REM	OSA	-	-

NREM: Non-rapid eye movement, REM: Rapid eye movement, OSA: Obstructive sleep apnea, CSA: Central sleep apnea.

Appendix G

Demographics and scoring details of the mentioned one thousand PSG records

Record ID	Age (years)	BMI (kg/m^2)	Gender	TRT (min)	TST (min)	AHI (event/h)
200001	55	21.78	1	542	375.5	6.23
200002	78	32.95	1	540	182	38.24
200003	77	24.11	2	525	358.5	9.37
200004	48	20.19	1	438	301	5.18
200005	66	23.31	2	542	370	7.46
200006	63	27.15	1	542	387	6.67
200007	52	29.98	1	460	332.5	15.88
200008	63	25.23	2	480	335	4.12
200009	69	25.82	1	543	351.5	37.55
200010	40	27.84	1	542	415.5	2.02
200011	53	29.00	2	495	371.5	9.53
200012	68	25.40	1	482	311.5	28.70
200013	66	27.14	1	543	238.5	18.36
200014	75	30.80	1	543	367.5	24.16
200015	58	23.94	2	480	251	38.49
200016	60	29.48	1	543	367.5	12.24
200017	58	25.42	1	475	367.5	4.08
200018	57	26.58	1	542	305.5	19.05
200019	65	24.14	1	543	229.5	2.88
200020	62	37.03	1	539	289	44.64
200021	81	20.31	1	536	337	6.41
200022	62	29.90	1	540	307.5	21.66
200023	59	22.23	2	474	368	7.34
200024	48	34.58	1	465	264.5	26.99
200025	67	39.99	1	455	296.5	19.22
200026	78	25.78	2	540	326.5	24.81
200027	61	27.40	1	510	327.5	12.82
200028	56	34.03	1	462	368.5	19.38
200029	56	23.29	1	541	350.5	12.15
200030	66	27.47	2	543	243	17.04
200031	60	23.59	1	470	407	12.38
200032	67	23.08	1	483	307	43.78
200033	56	22.85	1	180	147	6.94
200034	71	22.94	2	435	315	7.62
200035	60	25.93	1	542	373	51.96
200036	67	29.19	1	495	397.5	1.21
200037	60	25.70	1	469	412	35.24
200038	70	28.40	1	421	264.5	56.71
200039	69	20.70	2	480	386	1.87
200040	53	29.59	1	480	327	25.87
200041	63	20.34	2	508	262.5	7.54
200042	69	23.09	2	543	362	11.27
200043	48	20.23	1	420	385.5	17.90
200044	58	18.00	2	542	341	1.76
200045	71	25.53	1	523	332	14.28
200046	53	25.55	1	542	400	5.55
200047	47	28.79	2	480	447.5	11.93
200048	53	29.67	2	543	301.5	2.99
200049	53	26.26	2	542	409	10.42
200050	66	23.11	1	543	380	20.37
200051	73	24.13	2	480	357.5	7.72

200052	57	22.58	2	510	424.5	1.70
200053	68	25.68	2	543	382	4.55
200054	58	28.07	1	475	353	14.96
200055	71		1	543	210.5	5.42
200056	67	24.64	2	508	431.5	6.40
200057	49	37.52	1	542	310.5	27.25
200058	59	24.98	1	542	362.5	5.96
200059	66	28.74	1	374	278	50.72
200060	68	30.59	1	543	332	27.47
200061	60	22.58	2	442	398	17.64
200062	60		1	419	320.5	8.99
200063	64	27.01	2	542	337.5	21.87
200064	73	25.59	1	487	254	22.44
200065	75	23.41	1	543	380	17.53
200066	53	33.83	2	521	180	6.33
200067	71	25.16	1	480	288.5	9.15
200068	57	28.16	2	480	325	1.66
200069	67	23.43	1	543	459.5	1.57
200070	70	26.73	1	542	308.5	52.32
200071	50	31.17	1	542	333.5	11.69
200072	66	23.64	1	543	363	13.06
200073	53	22.27	2	542	375	5.12
200074	43	39.61	1	510	360.5	64.58
200075	68	29.67	2	430	273.5	13.38
200076	83	23.00	1	535	200	12.30
200077	41	23.66	1	535	398.5	19.42
200078	54	28.28	1	480	265	19.02
200079	56	32.29	2	480	305	11.61
200080	54	33.96	1	488	429.5	29.90
200081	40	25.40	2	534	393.5	2.13
200082	40	29.07	1	535	415.5	5.49
200083	54	34.16	1	420	395.5	12.59
200084	51	35.94	2	527	448	13.93
200085	67	33.59	2	360	173.5	17.29
200086	68	26.13	1	255	187.5	6.72
200087	67	26.80	2	450	369	6.02
200088	44	24.90	1	457	426.5	5.49
200089	42	28.13	2	457	405.5	9.03
200090	40	31.01	1	480	363	12.40
200091						
200092	53	26.46	1	451	384.5	4.68
200093	47	21.70	2	494	395.5	16.54
200094	79	25.17	1	510	169.5	29.73
200095	54	29.39	1	462	385	9.35
200096	61	35.22	1	525	376	57.29
200097	41	24.42	2	528	404	0.89
200098	78	26.90	2	526	136.5	18.90
200099	83	24.18	1	453	310	15.10
200100						
200101	53	32.78	1	421	368.5	31.42
200102	47	29.66	2	528	410.5	11.84
200103	51	31.31	1	520	412	18.79
200104	71	28.31	2	481	199.5	6.62
200105	53	25.98	1	304	256	2.11
200106	54	21.73	1	525	383	3.29
200107	66	21.89	1	480	446	20.31
200108						
200109	71	24.16	2	526	393	3.51
200110	58	27.58	1	450	388	13.76
200111	65	23.80	2	480	197.5	9.11

200112	48	26.42	1	535	364.5	2.63
200113	69	33.71	1	510	367	81.09
200114	76	26.03	2	510	446	10.63
200115	44	22.09	2	450	351.5	8.53
200116	83	23.05	2	527	446.5	28.22
200117	43	23.36	2	534	421.5	5.41
200118	70	26.99	1	542	291.5	58.66
200119	64	23.13	1	432	287.5	3.55
200120	68	34.24	2	428	253	12.33
200121	51	30.00	2	489	388	10.98
200122	43	21.41	2	530	445.5	0.67
200123	49	22.13	2	534	371	6.31
200124	77	29.14	1	527	280.5	24.60
200125	48	26.40	2	535	432	18.47
200126	40	20.93	2	510	362.5	8.94
200127	77	22.29	2	450	127.5	7.06
200128	72	28.44	1	511	397.5	21.13
200129	40	22.68	2	535	350.5	3.42
200130	52	40.72	2	534	462.5	19.07
200131	55	25.39	1	535	449	22.58
200132	74	26.78	1	464	298.5	6.43
200133	74	36.03	2	527	375	16.00
200134	58	22.47	1	535	339	13.98
200135	53	26.64	2	535	346	2.43
200136	51	36.95	1	527	468	58.97
200137	45	42.90	2	500	392	18.06
200138	57	29.32	1	480	352	44.32
200139	69	26.54	1	515	409.5	4.69
200140	72	29.48	2	480	295	20.54
200141	54	21.23	2	460	362	0.33
200142	40	19.72	2	467	432	14.44
200143	43	24.78	1	525	450.5	12.52
200144	63	29.07	1	535	360	20.50
200145	69	20.21	2	463	391.5	14.25
NR						
200147	51	30.71	1	535	357.5	7.05
200148	41	24.38	1	535	392	10.56
200149	45	24.38	2	509	301.5	1.79
200150	75	24.00	2	527	351	14.02
200151	49	22.17	2	535	383.5	8.92
200152	43	27.96	2	535	438.5	2.87
200153	46	22.39	1	535	193	22.69
200154	50	25.88	2	534	373.5	16.39
200155	49	25.76	1	535	128	54.84
200156	43	28.02	1	425	346	13.87
200157	40	31.02	2	535	364	12.86
200158						
200159	75	32.08	2	523	285.5	10.93
200160	59	22.51	2	510	452	5.84
200161	68	29.79	1	527	215	17.02
200162	69	25.52	2	526	243.5	3.20
200163	66	45.83	2	535	375.5	21.89
200164	40	28.28	2	480	387.5	4.03
200165	48	26.42	1	445	379.5	9.64
200166	43	20.20	1	525	423	2.84
200167	40	39.62	1	534	414	15.07
200168	62	18.89	2	510	476	1.01
200169	49	23.95	2	534	485	5.32
200170	52	23.05	2	510	292.5	9.44
200171	51	29.75	1	390	310.5	21.06

200172	49	23.17	2	390	353	15.81
200173						
200174	45	21.07	2	535	454	2.64
200175						
200176	47	27.51	2	535	387	11.32
200177	47	30.83	1	535	346	7.98
200178	51	26.80	2	535	452.5	1.72
200179	73	24.77	2	525	444.5	15.66
200180	57	29.07	1	522	435	12.83
200181	54	25.39	2	493	344	9.77
200182	48	25.52	1	405	300.5	14.98
200183	67	31.25	1	535	340.5	57.44
200184	66	25.64	2	535	381.5	8.65
200185	50	33.58	1	480	175.5	20.51
200186	50	18.00	2	479	342	2.28
200187	45	50.00	2	535	387	9.77
200188	72	29.26	2	535	427.5	16.00
200189	63	34.02	1	513	318	77.74
200190	78	18.97	2	480	202	23.17
200191	80	22.94	2	490	272.5	12.11
200192	78	27.49	1	489	206.5	40.10
200193	54	28.13	1	500	406	39.46
200194	41	26.72	2	469	409	8.80
200195	45	33.80	1	535	322.5	20.28
200196	41	23.35	1	535	382	3.30
200197	40	26.79	1	535	307.5	17.17
200198	40	22.77	2	532	376	6.70
200199	55	40.88	2	480	393.5	34.31
200200	69	31.82	1	510	143.5	8.36
200201	62	28.60	2	480	291	9.90
200202	78	24.08	2	535	292.5	9.23
200203	61	26.88	1	540	361	5.65
200204	71	27.47	1	466	292	13.77
200205	49	22.06	2	542	346.5	8.83
200206	73	25.97	2	444	361.5	32.20
200207	64	26.08	1	480	318.5	5.27
200208	61	27.33	2	480	289.5	14.92
200209	68	31.21	1	450	348	55.69
200210	65	21.27	2	450	289	2.28
200211	40	28.00	1	510	375.5	28.92
200212	50	26.52	1	495	320.5	26.02
200213	47	24.91	1	510	416	5.19
200214	44	24.77	2	534	467	1.80
200215	47	25.07	2	484	409	1.76
200216	48	27.63	1	535	462.5	12.06
200217	52	24.24	2	535	404.5	7.86
200218	51	22.94	1	420	366.5	7.37
200219	51	29.55	2	420	276	8.70
200220	84	26.64	2	535	327	44.22
200221	66	29.90	1	463	367	28.94
200222	43	24.91	1	512	249.5	21.64
200223	49	22.40	1	480	325	4.43
200224	50	30.76	2	480	277	1.52
200225	55	40.35	1	510	310	25.16
200226	47	41.31	2	510	392.5	19.11
200227	47	25.07	2	519	440.5	13.08
200228	67	27.78	1	525	367	3.60
200229	54	31.47	2	480	331.5	24.25
200230	57	29.68	1	447	340	54.71
200231	44	25.34	1	450	299.5	11.82

200232	51	34.53	2	450	311	65.21
200233						
200234	58	42.30	2	450	272	34.85
200235	76	23.46	1	542	201.5	47.64
200236	78	24.11	2	542	344	24.94
200237	60	33.23	1	454	314	42.04
200238	76	25.22	1	543	323.5	27.26
200239	52	19.57	2	543	322.5	0.74
200240	70	24.14	1	537	391	11.36
200241	75	24.53	2	480	337.5	14.76
200242	55	27.77	1	437	341	21.29
200243	54	31.25	2	525	412	19.37
200244	57	25.39	1	514	400.5	10.34
200245	69	26.46	1	538	478	33.51
NR						
200247	64	30.09	1	511	453.5	53.45
200248	64	23.60	1	540	332.5	34.29
200249	62	21.95	2	480	315	1.90
200250	59	25.26	2	543	408.5	35.40
200251	60	23.40	2	473	432	3.89
200252	65	32.12	2	542	154	14.81
200253	57	26.94	1	533	313	14.38
200254	71	30.22	2	491	325.5	11.24
200255	64	25.72	1	519	226.5	48.74
200256	67	25.38	1	540	349.5	8.58
200257	68	25.27	1	495	259.5	7.40
200258	58	24.87	2	543	421.5	0.57
200259	47	23.80	1	542	464.5	39.78
200260	67	25.58	1	452	396	24.39
200261	60	18.00	1	414	251.5	3.82
200262	76	27.51	1	503	354.5	22.34
200263	53	30.76	1	543	389.5	17.72
200264	62	31.45	1	510	328.5	27.03
200265	73		1	543	293.5	10.63
200266	67	22.85	2	543	415	14.17
200267	74	29.23	1	543	317.5	17.01
200268	59	22.24	2	500	334.5	93.45
200269	69	26.20	1	486	275.5	55.32
200270	70	24.54	2	462	262	13.51
200271	47	29.52	1	491	343.5	36.33
200272	70	20.51	2	420	363	1.82
200273	51	25.26	1	528	234.5	2.05
200274	65	31.23	1	541	450	14.00
200275	46	30.96	1	526	310.5	9.47
200276	69	33.67	1	506	294	30.82
200277	70	28.37	1	488	377	23.71
200278	48	27.02	1	543	369	7.15
NR						
200280	61	28.73	1	543	376	22.98
200281	61	27.90	1	543	288	32.08
200282	70	23.71	1	446	339	37.35
200283	57	24.58	2	542	428	59.86
200284	63	26.84	1	540	395.5	32.31
200285	65	22.99	1	542	426	34.23
200286	55	32.65	1	528	405.5	38.77
200287	76	25.21	1	542	372.5	9.18
200288	70	26.74	1	542	314.5	38.35
200289	64	29.16	2	502	331	28.10
200290	63	22.96	2	542	342.5	10.34
200291	55	25.30	2	480	451.5	45.32

200292	61	26.88	1	450	407.5	72.29
200293	40	27.78	2	535	317.5	12.66
200294	72	40.55	2	515	390.5	54.70
200295	66	28.18	1	454	392	26.33
200296	72	30.96	2	501	390.5	21.97
200297	76	26.78	1	481	326	20.98
200298	76	33.57	1	480	316.5	22.94
200299	74	28.20	1	510	284.5	29.74
200300	73	24.14	2	480	373	34.42
200301	69	33.07	2	535	367	4.58
200302	60	23.44	1	480	385.5	21.48
200303	56	23.04	2	480	434	18.80
200304	77	18.00	2	534	237.5	6.06
200305	63	25.26	2	494	350	34.11
200306	42	25.74	1	535	403	4.47
200307	70	29.20	1	480	243	22.22
200308	63	29.05	2	480	328.5	17.17
200309	41	28.20	1	535	397	3.32
200310	71	27.38	1	420	290.5	29.33
200311	69	23.58	2	480	403.5	15.76
200312	60	30.04	1	495	331	23.20
200313	69	25.60	1	535	401.5	17.78
200314	40	29.48	1	535	382.5	50.04
200315	69	26.74	1	480	290.5	13.01
200316	71	28.06	1	496	353	31.61
200317	67	23.58	2	534	320.5	7.49
200318	42	23.85	1	445	295.5	7.92
200319	40	19.54	2	484	391	3.53
200320	44	29.86	1	470	377.5	14.30
200321	42	28.44	2	480	365	18.41
200322	75	20.20	2	534	365	1.48
200323	67	28.93	1	360	271	25.02
200324	67	35.08	2	360	339	20.35
200325	64	40.47	2	480	420.5	18.26
200326	47	24.95	1	535	366	6.39
200327	80	27.04	2	534	334	69.16
200328	40	21.64	2	510	431	7.66
200329	54	36.36	2	535	385.5	16.03
200330	51	20.64	2	503	386.5	7.14
200331	47	26.72	2	543	330.5	13.43
200332	49	26.88	1	480	355	19.10
200333	46	46.67	2	523	305	41.70
200334	46	36.31	1	534	175.5	18.80
200335	66	22.28	1	535	380.5	2.21
200336	57	18.82	2	535	404	3.86
200337	44	28.26	2	420	399.5	30.19
200338	44	27.57	1	446	285	49.05
200339	68	26.29	2	535	346	24.10
200340	69	26.92	1	480	348.5	13.26
200341	80	27.90	1	457	273	12.97
200342	41	32.73	2	510	411.5	13.85
200343	40	28.73	1	510	250	9.12
200344	60	23.65	1	543	363	25.29
200345	44	31.67	1	534	394	28.78
200346	52	21.52	2	535	387.5	1.86
200347	59	28.28	1	484	369	15.77
200348	58	26.11	2	480	411.5	1.46
200349	50	36.63	1	480	400.5	4.04
200350	53	20.45	2	526	347	14.01
200351	51	23.24	1	440	344	14.13

200352	46	22.30	2	461	429.5	5.45
200353	67	24.44	1	501	403	32.90
200354	66	23.46	2	495	430	14.23
200355	55	26.15	1	472	380	23.21
200356	73	23.69	2	495	409	27.58
200357	55	31.00	2	508	290.5	17.56
200358	64	29.83	1	467	360	51.17
200359	66	22.36	2	515	370	9.24
200360	63	19.36	2	534	310	12.19
200361	71	24.38	1	535	358.5	22.26
200362	70	24.00	2	431	336	1.96
200363	45	29.60	1	495	397.5	13.13
200364	76	29.62	2	345	227	12.42
200365	77	30.48	2	534	400.5	16.33
200366	68	26.50	2	510	401.5	26.60
200367	54	30.30	2	542	389	19.90
200368	67	22.72	1	456	384	16.41
200369	71	32.37	1	543	301	16.15
200370	57	37.81	1	444	353	8.50
200371	62	24.77	1	531	358	20.78
200372	58	27.78	1	492	356.5	19.52
200373	66	29.68	2	480	374	14.28
200374	72	37.78	2	534	359	11.36
200375	59	24.88	2	526	463	21.64
200376	61	24.84	1	535	357.5	21.99
200377	80	29.55	1	464	434	14.38
200378	57	29.31	2	535	348	9.14
200379	76	29.75	1	543	327.5	40.49
200380	70	28.77	1	481	338	14.56
200381	71	30.75	2	526	378.5	4.76
200382	57	29.58	1	535	409.5	13.04
200383	42	23.26	2	480	378.5	4.44
200384	74	23.46	2	543	308	18.70
200385	78	26.99	2	423	346.5	8.83
200386	52	24.99	2	511	414	19.86
200387	65	23.67	1	510	385	33.82
200388	58	29.64	2	479	418.5	33.55
200389	48	25.26	1	535	315	1.90
200390	46	25.78	2	534	425.5	4.65
200391	47	35.34	1	542	482	11.33
200392	79	27.54	1	390	307.5	17.95
200393	60	23.98	2	388	319.5	0.19
200394	45	28.39	1	534	367.5	4.41
200395	45	34.09	1	480	337.5	17.07
200396	46	24.64	2	520	296.5	11.94
200397	85	18.37	2	511	402	24.48
200398	46	23.95	2	495	415.5	4.48
200399	54	22.89	2	479	427.5	5.89
200400	51	29.17	1	543	346.5	12.64
200401	89	24.12	2	390	358	45.75
200402	44	30.09	1	332	274.5	7.87
200403	43	22.77	2	480	411	16.50
200404	77	34.30	2	527	405.5	3.40
200405	56	27.65	1	535	404.5	14.83
200406	50	32.66	1	444	394	23.76
200407	51	26.99	1	491	337.5	1.42
200408	41	24.52	2	535	479	3.13
200409	51	21.26	2	525	427.5	3.93
200410	78	25.15	2	511	369	0.98
200411	81	25.98	2	510	422.5	17.33

200412	66	31.98	1	450	387	24.65
200413	58	29.88	1	502	408.5	5.73
200414	53	26.59	2	525	425.5	14.24
200415	72	26.67	1	542	356	16.01
200416	79	32.05	2	535	333	30.27
200417	48	26.49	1	526	362	7.96
200418	44	25.83	1	535	461	21.87
200419	44	24.21	1	535	373.5	3.21
200420	47	32.08	1	510	390.5	36.26
200421	47	26.43	2	510	420.5	11.27
200422	54	33.30	2	480	327	14.86
200423	74	22.54	1	535	261	57.93
200424	57	25.25	1	420	185.5	39.46
200425	80	26.51	1	525	332.5	11.73
200426	74	29.21	2	525	337	1.42
200427	63	24.19	1	420	392.5	12.38
200428	53	22.42	2	419	382.5	4.86
200429	73	37.59	1	494	332.5	28.87
200430	60	31.38	1	535	360	14.17
200431	57	22.73	2	510	272	6.84
200432						
200433	62	29.74	2	497	362	12.43
200434	51	21.56	1	525	376	5.11
200435						
200436	83	29.83	2	534	242	12.64
200437	58	28.16	1	472	419.5	3.15
200438	41	25.55	2	420	372.5	1.93
200439	44	31.93	1	535	384.5	8.43
200440	49	23.78	1	535	509	5.66
200441	49	24.89	2	480	406	1.63
200442	52	24.09	1	519	284	2.96
200443	74	26.48	2	521	252	22.62
200444	70	19.07	2	525	440	24.95
200445	60	26.25	1	535	437	8.24
200446	59	29.30	2	534	397	16.93
200447	48	42.08	2	490	401	11.52
200448	69	22.09	2	428	332.5	2.89
200449	73	26.99	1	450	378	17.30
200450	70	50.00	2	534	359	13.37
200451	71	24.59	1	480	301	25.71
200452	76	25.52	2	535	380	12.00
200453	70	29.54	1	360	261.5	19.04
200454	55	26.78	2	480	330	15.64
200455	75	21.85	1	451	379	28.65
200456	75	28.96	2	451	228	20.53
200457	70	19.65	1	535	299	23.28
200458	81	21.94	2	535	280	23.36
200459	69	22.07	2	510	405	12.15
200460	56	25.05	1	534	450.5	35.16
200461	68	27.58	2	510	297	3.03
200462	62	31.06	2	440	358	24.80
200463	81	23.20	2	525	287	2.30
200464	70	26.04	1	390	333.5	5.94
200465	67	27.77	1	465	339.5	14.14
200466	49	27.23	1	498	415	4.05
200467	45	21.20	2	531	401	2.54
200468	85	31.20	1	480	270	13.33
200469	70	22.43	2	535	194.5	16.66
200470	40		1	535	396.5	11.20
200471	75	28.20	1	527	336.5	18.01

200472	73	24.32	2	526	354	9.32
200473	70	35.94	2	480	420	7.00
200474	89	25.09	1	525	271	9.74
200475	84	21.41	2	525	388.5	4.63
200476	55	27.50	2	534	361	12.13
200477	53	30.11	2	480	426.5	2.53
200478	77	24.11	2	510	306	8.63
200479	77	32.94	2	510	376.5	21.67
200480	76	30.59	1	535	283.5	47.62
200481	75	24.02	2	534	171	9.82
200482	55	24.39	2	527	414	5.94
200483	49	26.59	1	535	351.5	15.87
200484	46	25.67	2	534	369	18.86
200485	81	25.30	2	535	431	10.86
200486	50	20.64	2	510	312	6.73
200487	81	23.44	2	535	401	32.92
200488	58	29.77	2	542	298	17.32
200489	67	21.49	2	533	104.5	8.04
200490	66	28.65	1	465	317.5	24.00
200491	62	22.74	2	488	244.5	1.72
200492	76	22.10	1	480	378.5	4.44
200493	74	21.19	2	480	305	4.92
200494	42	27.11	2	510	456	12.37
200495	52	23.49	1	420	271.5	21.22
200496	43	23.26	2	526	464	1.42
200497	62	30.67	1	450	339.5	22.62
200498	59	24.10	2	465	381.5	5.50
200499	67	23.98	1	480	364	17.14
200500	52	22.33	2	517	392.5	1.53
200501	77	26.97	1	495	367	42.34
200502	73	31.96	2	525	312.5	5.57
200503	47		1	542	339	10.09
200504	77	23.47	2	510	386.5	21.27
200505	58	22.89	1	534	375	10.72
200506	42	20.48	2	535	312	8.08
200507	69	31.72	2	510	245.5	14.91
200508	50	32.40	2	510	378.5	6.82
200509	81	28.43	1	535	408.5	21.30
200510	48	27.29	1	535	409.5	12.60
200511	46	24.31	2	510	437.5	6.31
200512	51	21.94	2	480	428.5	5.60
200513	49	27.80	1	534	398.5	20.03
200514	69	25.80	1	447	339.5	14.85
200515	78	29.17	2	527	423	17.45
200516	44	32.95	2	535	466.5	4.24
200517	55	27.96	1	510	409	14.96
200518	50	35.91	1	534	353.5	48.71
200519	73	22.43	1	510	385	33.19
200520	71	25.82	2	510	187	30.16
200521	80	25.79	2	480	387	23.10
200522	52	27.94	1	510	455.5	12.65
200523	52	25.79	2	527	374	0.00
200524	66	23.59	2	520	340	37.76
200525	69	22.05	2	542	420.5	38.53
200526	58	31.89	1	450	365	78.41
200527	51	26.60	2	542	350.5	6.85
200528	76	22.02	1	519	342.5	28.20
200529	68	26.31	2	525	401.5	14.65
200530	70	21.78	2	524	439.5	10.24
200531	59	27.90	1	543	341	1.94

200532	53	22.30	2	465	398	2.71
200533	43	29.64	2	543	426.5	1.69
200534	63	24.67	1	542	445	16.45
200535	47	27.07	2	480	350	5.14
200536	60	21.45	2	543	415	3.47
200537	47	27.02	1	534	331.5	7.06
200538	67	25.77	1	542	448	9.24
200539	68	24.82	1	450	229	44.28
200540	70	29.44	1	542	443.5	5.41
200541	59	22.82	1	503	420	22.14
200542	52	27.58	2	465	345.5	20.49
200543	70	28.04	1	506	394.5	6.39
200544	46	29.15	1	401	291.5	14.20
200545	62	30.10	2	510	368	10.94
200546	68	22.96	1	543	389.5	4.57
200547	68	29.93	1	540	485	15.34
200548	51	27.29	1	542	415	34.55
200549	74	26.69	2	495	356	12.30
200550	52	30.06	2	402	338	3.55
200551	73	24.67	2	465	375.5	5.11
200552	57	29.88	1	485	295	29.49
200553	69	26.26	1	451	319.5	27.23
200554	63	20.90	2	542	412.5	6.84
200555	47	28.09	1	480	419.5	13.44
200556	61	28.50	1	450	361	25.76
200557	55	22.13	2	441	374	5.13
200558	62	22.10	1	480	413	4.94
200559	69	22.73	2	480	423.5	35.28
200560	43	23.95	1	525	319.5	10.89
200561	44	28.28	1	445	366.5	38.14
200562	50	25.84	1	477	392.5	43.41
200563	45	24.55	1	510	383	8.62
200564	42	23.21	2	510	431.5	11.54
200565	55	28.65	1	385	300	7.20
200566	64	29.40	1	535	329.5	54.63
200567	66	32.91	2	543	257.5	32.85
200568	44	25.02	1	435	368	7.99
200569	40		2	487	413.5	1.02
200570	50	29.32	1	535	362.5	34.43
200571	54	21.68	1	420	349	7.91
200572						
200573	57	44.42	1	390	324	83.33
200574	63	26.72	2	542	287	23.00
200575	50	26.62	1	534	392.5	8.10
200576	66	37.06	1	435	315	46.48
200577	45	25.28	2	535	402	11.49
200578	46	33.33	1	534	368	27.88
200579	52	26.26	1	511	361	3.99
200580	40	24.16	1	535	460	19.30
200581	43	25.08	2	439	335	8.24
200582	43	24.24	2	510	422.5	13.21
200583						
200584	47	26.15	1	535	398	18.24
200585	59	28.73	1	535	397.5	16.00
200586	41	25.72	1	450	375.5	10.39
200587	41	30.39	2	525	496	8.71
200588	46	29.00	2	439	282	18.30
200589	48	21.54	1	393	355	2.54
200590	49	21.71	1	535	478	18.45
200591	47	27.10	1	535	433	7.76

200592	51	22.68	2	510	488	7.62
200593	56	22.09	1	418	293.5	9.40
200594	47	25.47	1	535	300.5	21.16
200595	55	29.95	1	534	346.5	18.87
200596	49	22.51	2	535	420.5	9.42
200597	49	27.07	1	439	360.5	27.96
200598	55		1	510	384.5	33.39
200599	58		2	505	447.5	10.19
200600	48	46.48	2	480	346	71.45
200601	65	37.71	2	534	283.5	12.49
200602	49	36.14	2	450	288	18.54
200603	57	28.54	2	479	352.5	24.34
200604	71	27.07	2	456	303.5	5.93
200605	62	24.66	1	480	421	6.41
200606	58	32.34	2	480	379.5	2.37
200607	66	36.82	1	450	386	62.49
200608	68	23.66	1	495	371.5	17.60
200609	59	33.35	2	527	355.5	2.70
200610	65	33.40	1	453	323.5	31.53
200611	58	24.79	2	453	372	3.23
200612	65	24.42	1	535	387	15.19
200613	69	30.90	1	535	295	7.93
200614	45	24.11	1	420	341	9.50
200615	42	24.61	2	535	381.5	2.99
200616	54	35.94	1	520	452	19.78
200617	65	25.64	2	527	434.5	9.11
200618	43	22.88	1	480	423	8.23
200619	44	30.38	2	480	423	8.37
200620	52	24.33	1	534	382.5	6.12
200621	43	28.24	1	534	390.5	23.66
200622	42	23.24	2	534	423	3.40
200623	50	26.45	2	527	483	8.94
200624	50	29.04	1	476	300.5	20.57
200625	59	33.13	2	534	355	13.01
200626	56	39.97	1	534	437	14.69
200627	52	27.89	2	535	362	0.83
200628	65	39.90	1	438	244.5	28.71
200629	65	26.70	2	450	402	1.79
200630	66	20.83	2	535	303	15.25
200631	59	28.04	2	527	454.5	2.38
200632	72	25.32	2	510	439	31.03
200633	54	28.28	1	525	393	27.18
200634	53	24.52	2	525	354.5	9.31
200635	59	24.37	2	482	341	16.54
200636	77	25.14	1	481	423	8.09
200637	44	28.52	2	480	432.5	6.38
200638	47	37.39	1	510	390.5	53.93
200639	51	23.88	1	456	379	13.77
200640	45	27.89	2	510	347	3.11
200641	43	26.99	1	525	276	6.96
200642	53	25.49	2	535	358	7.71
200643	46	27.39	2	473	343	2.45
200644	42	18.36	2	535	497	10.62
200645	40	19.17	2	525	484	2.23
200646	46	21.92	1	527	398.5	20.78
200647	41	23.05	2	535	396.5	4.54
200648	40	25.35	2	444	401	7.33
200649	45	22.28	1	365	295	5.49
200650	46	32.86	2	528	265.5	11.07
200651	48	38.92	1	534	320	33.56

200652	69	18.15	1	511	289	21.80
200653	73	18.03	2	421	323.5	33.01
200654	70	22.22	2	480	342	8.25
200655	79	29.41	1	480	255.5	37.57
200656	58	37.42	2	506	366.5	10.15
200657	59	29.86	1	480	137	25.84
200658	43	26.47	2	510	420	5.43
200659	55	32.70	1	390	351	41.20
200660	47	28.48	2	419	376	3.19
200661	43	29.62	2	507	337	4.81
200662	55	32.56	1	440	285.5	69.56
200663	47	26.97	2	525	340.5	6.17
200664	42	24.57	1	510	431	26.59
200665	40	20.45	2	510	449	0.94
200666	42	43.79	2	535	324.5	11.65
200667	45	32.39	1	535	377.5	33.38
200668	57	31.83	1	513	411.5	8.60
200669	44	25.08	2	510	352	2.56
200670	52	28.37	1	450	396.5	13.92
200671	50	29.22	2	535	389	3.86
200672	69	22.79	2	534	402	6.87
200673	76	25.77	1	510	213.5	48.06
200674	70	27.02	2	511	382	33.46
200675	43	21.45	2	435	392.5	9.32
200676	58	36.13	2	535	310	6.19
200677	50	42.11	2	495	385.5	10.12
200678	40	25.55	2	516	395	1.06
200679	53	26.98	1	465	279	9.46
200680	47	34.30	2	390	363.5	69.00
200681	47	27.53	1	480	327.5	28.58
200682	64	22.16	2	535	285.5	27.11
200683	42	20.58	2	510	416	5.77
200684	48	22.40	1	535	385.5	11.83
200685	48	21.16	2	510	368.5	6.68
200686	41	39.32	1	527	474.5	95.97
200687	54	33.90	1	531	455.5	18.31
200688	46	26.25	1	510	334	29.10
200689	47	27.94	2	510	371	9.70
200690	45	24.90	1	510	452.5	12.33
200691	42	23.20	2	535	484	3.47
200692	63	24.88	1	525	409.5	44.54
200693	64	32.08	1	480	336.5	33.52
200694	51	30.90	1	535	336.5	6.60
200695	45	26.25	1	480	416.5	14.84
200696	58	24.48	1	420	327	49.54
200697	52	26.50	2	480	446.5	9.41
200698	60	22.85	1	495	431	52.34
200699	53	28.59	1	534	340	14.47
200700	49	23.33	2	525	470	2.04
200701	53	22.53	2	472	424.5	3.11
200702	43	23.69	1	480	418.5	2.29
200703	43	29.54	2	390	376.5	22.15
200704	66	26.57	1	420	374.5	4.33
200705	69	25.05	1	508	398	15.98
200706	67	38.37	2	477	379	12.51
200707	48	31.75	1	420	212	12.45
200708	64	33.92	1	535	370.5	23.32
200709	57	34.06	2	535	415.5	21.52
200710	43	20.51	1	435	335	4.66
200711	50	29.45	1	534	442.5	52.61

200712	41	30.48	1	510	300	30.40
200713	42	33.14	1	480	353	45.89
200714	51	28.21	1	534	410.5	16.37
200715	56	24.76	2	535	281.5	1.92
200716	53	19.17	1	535	383	4.54
200717	48	18.00	2	535	269.5	11.58
200718	56	28.24	2	502	279.5	3.43
200719	51	42.10	1	542	285	28.21
200720	49	20.87	2	527	457	3.02
200721	61	30.56	1	420	302	17.28
200722	58	33.67	2	419	299	7.63
200723	66	22.39	1	534	310	5.81
200724	58	27.61	2	535	351.5	35.50
200725	69	23.06	2	542	447	2.68
200726	54	24.31	1	465	341.5	0.70
200727	68	26.36	1	510	309.5	39.35
200728	55	32.20	2	535	413.5	5.95
200729	78	26.93	2	481	296.5	23.68
200730	58	32.64	2	535	450.5	10.52
200731	61	30.04	1	412	390	43.08
200732	54	30.69	2	511	402.5	8.35
200733	74	28.04	2	542	296.5	34.81
200734	50	24.84	1	535	383.5	5.32
200735	61	30.86	2	425	281	16.87
200736	53	28.91	1	420	324.5	3.51
200737	46	20.73	2	535	407	3.69
200738	48	29.14	1	520	447.5	15.02
200739	46	41.43	2	297	224.5	35.81
200740	65	20.98	2	535	353	9.35
200741	68	23.20	2	495	390	0.92
200742	65	40.93	2	450	312.5	13.25
200743	67	32.72	2	505	344.5	52.08
200744	74	27.43	1	507	384	22.66
200745	54	32.02	2	527	469	15.48
200746	73	24.36	2	534	297.5	4.84
200747	72	25.26	1	543	249.5	19.96
200748	57	34.01	2	535	377.5	39.42
200749	60	23.49	2	510	328	1.28
200750	54	24.43	2	535	455.5	8.30
200751	55	44.69	2	535	427	45.11
200752	59	30.64	2	535	409	12.18
200753	60	27.31	1	534	409.5	12.16
200754	40		1	535	401	6.73
200755	40	34.29	2	495	436	10.87
200756	72	34.43	1	468	375	30.24
200757	65	25.61	2	497	295	6.71
200758	66	35.77	1	535	52.5	36.57
200759	44	23.94	2	360	319	13.92
200760	50	24.09	1	510	440	18.14
200761	45	21.90	2	510	446.5	13.17
200762	45	21.34	2	390	319.5	0.38
200763	69	18.99	1	480	336.5	12.84
200764	66	25.38	2	535	388.5	2.47
200765	52	25.47	2	535	430	3.07
200766	45	39.82	2	534	437.5	9.05
200767	48	36.61	2	535	381	4.09
200768	53	22.15	2	518	442.5	5.29
200769	69	29.21	2	480	211.5	19.57
200770	68	25.09	1	527	326.5	4.04
200771	51	19.80	2	510	405.5	2.22

200772	58	23.10	1	480	344.5	24.21
200773	39	22.48	2	509	395.5	8.80
200774	41	27.28	1	475	394.5	9.58
200775	57	19.67	2	535	476	12.61
200776	47	40.11	2	534	385.5	4.05
200777	43	29.59	1	411	340.5	66.61
200778	42	31.03	1	420	356.5	14.81
200779	45	28.41	1	535	484	15.62
200780	74	20.61	2	534	450.5	4.93
200781	43	32.21	1	381	269.5	17.81
200782	42	30.04	2	480	422	8.96
200783	50	24.16	2	480	416	4.18
200784	45	29.07	2	535	492	6.59
200785	50	25.80	2	535	436.5	2.34
200786	59	24.15	1	535	260	13.62
200787	50	27.90	2	525	425	3.53
200788	54	23.21	2	480	342.5	2.45
200789	60	38.87	2	535	395	15.34
200790	40	48.04	2	534	377.5	14.15
200791	44	24.48	1	543	413	98.64
200792	44	22.56	1	514	448	10.71
200793	40	22.72	2	510	438	1.64
200794	60	29.39	1	543	385	21.82
200795	61	24.28	1	525	248.5	33.80
200796	69	32.31	2	501	429	12.59
200797	68	24.77	1	500	419.5	10.30
200798	45	20.52	2	510	360	9.17
200799	55	24.80	2	540	455	7.78
200800	52	25.86	1	542	385.5	13.07
200801	74	24.96	1	480	402	58.66
200802	41	38.82	2	450	324.5	23.48
200803	50	30.69	1	480	375.5	48.42
200804	64	20.70	2	482	331	35.71
200805	51	27.89	2	480	429.5	1.26
200806	49	26.13	1	527	318.5	6.03
200807	72	25.63	1	405	303.5	13.05
200808	65	27.89	2	510	398.5	22.74
200809	53	29.51	1	535	257	24.28
200810	52	36.58	2	535	382	1.88
200811						
200812	61	30.93	1	450	340.5	64.32
200813	58	31.33	1	480	333	10.63
200814	55		2	534	420	7.14
200815	56	28.89	2	510	278	11.65
200816	65	27.35	1	535	180.5	16.29
200817	59	21.79	2	535	342.5	15.24
200818	46	21.49	2	535	382	4.24
200819	43	27.80	1	450	389.5	15.56
200820	45	25.42	2	420	394.5	9.43
200821	41	18.00	2	534	174.5	25.10
200822	47	25.85	1	467	297.5	23.60
200823	57	29.60	2	535	449	2.41
200824	48	26.89	1	480	369	19.35
200825	48	29.61	2	480	382	16.96
200826	70	34.40	2	527	350	16.97
200827	50	30.17	1	520	337	25.46
200828	47	42.45	2	494	379	11.56
200829	42	26.82	2	405	362	0.33
200830	42	28.28	1	510	405.5	6.07
200831	46		1	535	391	16.42

200832	44	24.38	1	513	314.5	2.29
200833	51	27.05	2	535	438	10.14
200834	43	23.14	2	525	457.5	1.31
200835	59	24.88	1	473	396.5	4.99
200836	52	25.66	1	465	429	68.81
200837	51	46.23	2	510	323.5	45.44
200838	53	27.82	1	510	411.5	34.70
200839	48	24.84	2	402	314	10.70
200840	50	24.29	1	535	301.5	8.56
200841	50	25.94	2	510	445	9.17
200842	53	31.55	1	510	474.5	6.83
200843	44	23.19	1	456	378.5	1.74
200844	39	26.82	2	480	330	2.55
200845	71	26.72	2	465	173	1.39
200846	71	25.40	2	543	231	23.12
200847	51	27.27	1	535	363	2.98
200848	57	35.15	1	512	344	8.90
200849	54	26.40	2	480	321.5	11.76
200850	57	28.73	1	390	355.5	28.52
200851	64	31.12	1	520	468.5	18.83
200852	47	21.55	2	535	442.5	2.85
200853	46	19.07	2	499	392.5	2.14
200854	45	26.47	1	495	378.5	29.64
200855	58	31.56	1	543	329	43.40
200856	61	22.81	2	535	355.5	4.22
200857	71	31.70	1	534	440	39.95
200858	66	32.90	1	510	270.5	41.48
200859	63	27.50	2	527	399	7.67
200860	52	24.31	2	480	437	6.18
200861	47	26.35	1	420	361	22.44
200862	58	37.75	1	534	353.5	22.91
200863	66	34.09	1	527	334.5	17.40
200864	52	32.49	1	510	393.5	12.05
200865	48	22.71	2	492	388	5.10
200866	47	24.02	2	527	481	12.85
200867	52	30.31	1	527	390.5	36.57
200868	70	25.69	2	510	420	23.71
200869	47		2	534	495	3.15
200870	46	18.00	2	535	420.5	1.43
200871	48	25.58	1	465	365.5	15.43
200872	46	28.65	2	438	353	4.93
200873	72	23.19	1	510	359	17.05
200874	45	27.19	2	394	341	12.84
200875	69	29.24	1	526	331	66.71
200876	65	31.09	2	527	422	3.41
200877	48	24.84	2	535	395	19.29
200878	45	30.55	1	533	474.5	28.32
200879	44	19.96	2	535	446	4.17
200880	71	29.54	1	480	374	8.50
200881	49	32.43	1	510	438	13.01
200882	57	22.28	1	535	409.5	14.95
200883	54	33.58	2	450	382	19.95
200884	49	32.70	2	510	426	4.51
200885	50	28.58	1	535	265	15.17
200886	48	23.12	2	510	427.5	4.77
200887	48	23.25	1	480	416	2.02
200888	55	21.99	2	480	312	12.12
200889	48	28.84	1	535	407	13.12
200890	48	23.39	2	510	426.5	5.35
200891	40	20.81	2	521	371.5	2.10

200892	47	19.81	2	535	361.5	3.65
200893	58	24.73	1	535	370.5	5.67
200894	49	26.37	1	534	475	14.15
200895	51		2	535	407.5	2.94
200896	66	22.08	2	422	323.5	4.82
200897	47	26.47	2	480	402.5	3.88
200898	48	40.45	1	450	238.5	5.53
200899	44	21.87	2	512	396	9.55
200900	57	25.47	1	535	411	5.69
200901	54	25.22	2	535	438	7.12
200902	42	19.50	2	480	389.5	0.92
200903	43	24.51	1	510	255	10.35
200904	53	24.98	1	510	428.5	31.09
200905	54	31.79	1	480	363.5	47.37
200906	45	23.74	1	479	421.5	7.69
200907	72	28.33	1	534	323.5	40.06
200908	59	20.73	2	462	413	3.20
200909	41	25.69	1	535	369.5	14.61
200910	52	35.78	2	535	423	6.24
200911	48	27.89	2	535	456	5.92
200912	49	29.51	1	435	355.5	102.78
200913	50	35.43	1	405	330.5	43.03
200914	43	32.32	2	435	358	2.18
200915	69	23.28	1	527	446	3.77
200916	54	25.78	2	526	412.5	8.58
200917	58	26.26	2	512	435	5.52
200918	65	29.40	1	450	360	22.33
200919	62	31.84	1	510	373	9.17
200920	49	20.35	2	535	429.5	1.82
200921	50	26.00	1	480	392	10.41
200922	52	25.67	2	535	409.5	3.37
200923	70	20.81	2	534	313	3.45
200924	40	27.22	1	535	465.5	3.48
200925	51	37.83	2	535	275.5	14.81
200926	43	34.74	2	532	376.5	30.60
200927	49	44.28	2	455	315	30.86
200928	62	43.20	2	535	454	23.92
200929	58	25.94	2	465	305	6.49
200930	56	23.62	2	527	398.5	36.89
200931	51	21.20	1	535	411	23.07
200932	44	28.52	2	535	425	3.81
200933	44	28.63	1	535	374	25.99
200934	67	25.30	2	525	316	21.65
200935	67	26.74	2	535	401.5	10.76
200936	69	25.67	1	535	247	6.80
200937	63	29.77	2	525	340	1.76
200938	72	27.74	1	535	358	21.28
200939	68	22.46	2	534	298.5	3.62
200940	71	25.56	1	543	312	15.00
200941	66	33.87	1	534	398.5	49.39
200942	51	26.77	1	535	380.5	26.49
200943	47	22.92	2	535	363.5	6.77
200944	66	26.70	2	527	389	10.95
200945	45	29.41	1	535	416.5	19.74
200946	62	29.62	2	480	304	12.43
200947	46	34.35	2	535	445.5	5.39
200948	67	19.77	2	480	306.5	3.33
200949	49	24.63	1	510	379.5	11.70
200950	69	28.37	2	510	448	24.78
200951	74	30.52	1	527	245.5	46.44

200952	67	23.25	1	479	328.5	14.61
200953	66	24.45	2	480	435.5	2.20
200954	47	19.68	2	535	365.5	12.64
200955	43	24.45	1	535	320.5	21.45
200956	54	39.87	2	534	447.5	6.74
200957	79	27.71	1	535	393	19.85
200958	75	18.00	2	465	384.5	7.65
200959	45	29.42	2	534	413	4.36
200960	44	30.79	2	535	475	5.43
200961	41	30.00	1	535	470.5	13.90
200962	64	31.73	1	535	361.5	27.22
200963	61	37.81	2	535	375	19.36
200964	51	27.47	2	535	456	4.87
200965	47	23.09	1	535	450.5	121.33
200966	55	28.72	2	435	320.5	30.70
200967	55	29.86	2	492	356	1.18
200968	66	23.78	2	527	463	41.47
200969	66	34.02	2	535	343.5	13.97
200970	50	28.59	1	471	316	18.42
200971	42	25.72	2	534	240.5	3.24
200972	55	25.61	1	535	364.5	3.79
200973	56		2	525	434	13.27
200974	51	21.38	1	510	458.5	12.43
200975	48	19.29	2	535	506.5	2.25
200976	71	29.16	1	480	377	29.12
200977	63	32.20	1	497	354	20.00
200978	63	22.96	2	535	399.5	14.27
200979	51	27.65	2	390	332.5	3.79
200980	53	30.80	1	390	372	24.19
200981	50	32.18	1	389	324.5	16.64
200982	62	29.46	1	499	401.5	14.79
200983	62	24.98	2	527	443.5	2.98
200984	56	32.52	1	525	430	68.37
200985	54	36.18	1	510	388.5	32.28
200986	50	29.18	2	533	382.5	17.73
200987	54	26.06	1	374	323.5	13.35
200988	53	27.40	2	528	354	1.02
200989	50	31.23	1	462	362	15.25
200990	60	25.31	2	535	403.5	1.93
200991	57	21.41	2	480	336.5	2.32
200992	46	24.91	2	534	231	12.99
200993	40	22.99	2	420	390.5	7.22
200994	40	26.90	2	535	215	15.63
200995	45	35.46	2	480	415.5	3.61
200996	68	29.58	1	465	307.5	10.93
200997	62	27.34	2	534	439	11.75
200998	47	40.27	2	479	348.5	70.76
200999	68	29.20	1	535	265.5	63.28
201000	53	33.37	2	448	216	3.06
201001	77	32.12	2	526	450.5	24.11
201002	48	29.76	1	479	345.5	11.11
201003	42	29.76	2	524	312	14.81
Mean	**57.4**	**27.4**	**M = 490**	**500**	**361**	**17.1**
SD	**11.3**	**5.1**	**F = 498**	**44**	**67**	**15.9**

BMI: Body mass index, TRT: Total recording time, TST: Total sleep time, AHI: Apnea hypopnea index, SD: Standard deviation, 1 = Male (M), 2 = Female (F), NR: No record found with the corresponding serial number, Blank rows with serial numbers indicate the records with AF corrupted (i.e., AF was found as a flat line or random noise throughout the night).

Appendix H

Duration of normal breath for the development of an automatic algorithm

Record No.	Duration of normal breath (s)																				Mean (s)
	1	*2*	*3*	*4*	*5*	*6*	*7*	*8*	*9*	*10*	*11*	*12*	*13*	*14*	*15*	*16*	*17*	*17*	*19*	*20*	
1	5.1	5.1	5.4	4.7	5.2	5.1	5	5	5.1	5.2	4.5	5	5.6	5	4.7	5.4	4.8	4.3	4.6	5	5
2	3.8	3.8	3.8	3.8	4.1	3.5	3.6	4.2	4.1	4.6	3.8	3.7	4.4	3.7	3.4	3.4	3.7	4.3	3.7	4.3	3.9
3	4.3	4.4	4.5	5.7	5.2	4.9	5.7	4.8	5.7	4.9	4.6	4.7	4.9	5.4	3.9	4.3	4.6	5.1	5.2	5.5	4.9
4	2.8	3.4	3	3.4	3.2	3	3.3	3.2	3.1	3.3	3	3.1	3.1	3	3.1	3.1	3	3.2	3.1	3.4	3.1
5	4.5	4.5	4.7	4.4	4.8	4.5	3.9	4.2	4.6	4.5	4.4	4.7	4.7	5.2	4.1	4.4	4.2	3.9	4.3	4.5	4.5
6	5.1	4.9	5	5	5.3	5.6	5.4	5	4.9	4.6	4.6	5.1	5	5.2	5.3	5	5.2	4.9	5.3	5	5.1
7	2.9	3.1	2.9	2.8	3	3.2	3.2	3.3	3.4	3.1	3.4	3.3	2.7	2.7	2.8	3.1	3.3	3.3	3.2	3.3	3.1
8	4.8	5	4.7	4.5	5.3	4.8	6	4.1	4.7	5.1	4.7	4.7	5.5	4.2	4.4	4.7	5.4	4.6	4.9	5.2	4.9
9	4.8	3.8	4.5	4.9	4.7	4.1	4	3.6	4.5	4.4	4.1	4.7	4.3	4.9	4.6	4.1	4.2	3.9	4	4.6	4.4
10	3.4	3.4	2.6	3.4	3	3.2	3.2	3.6	3.5	4	3.6	3.7	3.5	3.6	3.5	3.7	3.7	4	3	3.5	3.5
11	3.3	3.6	3.5	3.3	3.4	3.6	3.7	3.6	3.6	3.9	3.7	3.5	3.6	3.1	3.6	2.9	3.3	4.2	3.8	4	3.6
12	4.9	5.8	5.8	4.6	4.9	5.2	5.5	5.5	5.5	5.1	5.6	5.6	5.9	4.3	4.8	5.2	5.5	4.2	5.5	5.3	5.2
13	3.4	3.4	3.1	3.8	3.4	3.8	3.9	3.4	3.6	3.2	3.1	3.4	3.5	3.7	3.7	3.5	3.5	3.8	3.3	3.1	3.5
14	3.5	3.6	4.1	3.9	3.8	4.3	3.9	4.3	3.7	3.5	4.3	3.7	4.9	4.2	4.8	4.1	3.6	4	4.6	3.4	4
15	4.4	5	5.7	5	4.8	4.3	3.9	4.2	4.9	5.4	5.4	4.4	3.5	4.1	3.8	4.8	4.7	4.4	4.7	4.9	4.6
16	3.2	3.3	3.8	3.4	3.7	3.1	3.8	2.9	3.5	3	3.4	3.8	3.5	3.1	3.3	3.5	3.4	3.1	3.4	3.4	3.4
17	2.7	2	2.5	2.4	2.7	2.7	2.7	3.1	3	3.5	2.9	3.2	2.8	2.8	2.2	2.6	2.4	2.5	2.6	2.7	2.7
18	3.5	4.2	4.3	3.5	4.5	2.3	3.9	2.8	3.7	4	4.5	3.5	4.1	3.9	3.5	3.9	4.2	4.6	3.3	4.8	4
19	5.8	4.6	4.2	3.3	6.1	6.2	5	4.8	5.2	5.1	6.1	5.8	5	5.6	5.2	4.9	4.7	5	4.9	5.9	5.2
20	4.1	5.7	4.4	5.7	5.1	3.9	6.2	4.8	5.4	3.2	5.1	4.4	5.8	4.6	5.2	5	4.4	5	5.2	3.9	4.9
21	4.4	4.4	4.9	5.3	5.5	4.9	5.2	4.5	4.7	5.4	5.7	4.6	5.7	3.9	5.5	3.9	4.4	4.8	6.5	4.1	4.9
22	3.7	3.2	3.5	3.7	3.6	4	3.8	3	3.8	4	3.8	3.6	3.3	3.7	4.1	4.5	3.4	3.8	3.6	4	3.7
23	3.8	3.7	3.6	3.2	3.3	3.1	3.4	3	3.4	2.5	2.8	3.3	2.8	2.7	3.1	3	3.6	3.3	3	3.2	3.1
24	3.7	3.1	3.5	3.5	3.5	3.1	3	3.2	3	3.2	3.3	3.1	2.7	3.1	3	3.1	2.9	3	2.9	3.1	3.2
25	3.6	4	3.7	2.9	5.3	5.4	5.4	4.8	4.7	5.4	6.2	5	5.6	5.4	6.2	5.6	5.7	5.4	6.1	5.6	5.1
26	4.1	3.8	3.5	4.4	4.3	4.4	4.4	4.6	4.4	4.5	4.1	4.2	4.2	4.5	4.6	4.7	3.4	4.8	4.4	4.4	4.3
27	5	4.1	5.7	4.1	5.3	4.4	4	4.8	4.2	4.8	3.9	4.9	4.7	4.9	5	3.5	4.8	5.4	4.6	5.8	4.7
28	5.6	5	6.1	5.1	5.4	4.9	5.6	5.9	6.2	6	5.6	4.5	6.3	5.9	5.4	5.1	6.1	5.1	5.5	5.5	5.5

29	3	2.7	2.6	2.5	3.1	3.2	2.9	2.8	2.4	2.8	3.2	2.9	3	3.1	3.6	2.6	2.7	3.7	3.1	3.7	3
30	3.4	4.3	3.9	4	3.3	4.5	3.6	3.9	3.4	5	4.5	4.4	3.5	4.2	3	4.3	4.5	4.2	3.5	4.9	4
31	4.4	4	4.4	5.2	4	4.4	4.6	6.5	4.5	4.5	6.1	5.1	4.6	3.2	4.7	4.6	4.7	4.6	5.9	5.7	4.8
32	4.9	5	4.9	4.6	5	4.5	5	4.7	4	4.3	5.4	5.1	4.9	4.3	5.2	4.5	4.9	4.8	4.1	4.6	4.7
33	4.4	5.2	5.7	5	5.3	4.9	5.3	5.3	5.2	4.4	4.5	5.1	5.2	4.7	4.8	5.4	5.6	5	5	5	5.1
34	3.3	3.2	3.6	2.9	3.4	3.4	3.2	3.2	3.4	3.2	3.3	3.5	3.4	3.3	3.6	3.2	3.1	3.1	3.6	3.7	3.3
35	4.4	4.2	4.4	4.0	4.2	3.9	4.1	3.8	4	3.5	3.5	3.6	3.5	3.6	3.9	4	4	3.6	3.6	3.2	3.9
36	4.5	4.3	4.4	3.8	3.5	4.1	3.6	4.8	4.8	4.8	3.6	4.6	4.6	4.7	4.8	4.8	4.8	4.9	4.4	5.2	4.5
37	5.1	6	5.8	5.3	4.5	6.4	6	6.1	5.1	5.9	5.4	5.7	5.3	5	4.5	5.2	5	4.5	4.8	4.8	5.3
38	3.4	3	3.2	3.4	3.4	3.5	3.7	3.6	3.8	3.8	3.5	3.7	3.4	3.2	3.9	3.6	3.6	3.2	3.9	3.7	3.5
39	4.9	4.6	4.7	5.2	5	4.9	5.8	5	5.3	5.3	5.1	5.5	5.6	5	4.5	5.2	5	5.5	5.6	5.4	5.2
40	5	4.9	5	5	5.4	5.3	4.8	5.6	5	5.2	6	5	5.3	4.8	5	4.5	5.1	4.6	5	5	5
41	3.5	3.3	2.9	3.2	3	3.1	3.1	3	3.1	2.9	3.4	3.5	4.1	3.7	3.9	4	3.7	3.5	3.2	3.2	3.4
42	4.6	4.9	4.2	4.1	4.6	4.7	4.8	4.3	5.4	4.3	4.9	5.1	5.0	4.6	4.8	4.8	5.2	4.6	4.9	4.9	4.7
43	3.7	3.5	4.4	3.9	3.5	3.6	4.2	3.6	3.8	4	4.2	4	4.1	3.7	3.6	4	3.8	2.8	3.8	3.5	3.8
44	5.4	4.9	4.8	4.9	5.8	4.9	5.4	5	5	4.9	5.4	4.9	5.9	5.9	4.4	4.9	5	5.5	4.7	4.6	5.1
45	4.6	3.7	4.4	4	4.2	4.9	5.4	4.2	4.3	3.8	4.6	4.8	4.5	4.4	4.4	5.8	3.4	4.4	3.5	4.4	4.4
Mean																					**4.2**

Appendix I

Duration of peak-to-trough excursion of normal breath for the development of an automatic algorithm

Record No.	Duration of peak-to-through excursion of normal breath (s)																				Mean (s)
	1	*2*	*3*	*4*	*5*	*6*	*7*	*8*	*9*	*10*	*11*	*12*	*13*	*14*	*15*	*16*	*17*	*17*	*19*	*20*	
1	1.5	1.4	1.7	2.3	1.8	1.7	2	1.3	1.6	1.4	2	1.7	1.4	1.5	2	1.5	1.6	1.6	1.6	1.1	1.6
2	1.4	1.3	1.6	1.6	1.6	1.3	1.8	1.5	1.6	2	1.3	1.1	1.5	1.6	1.4	1.5	1.6	1.7	1.6	1.7	1.5
3	1.9	2	1.8	2.1	1.7	1.9	2	1.9	1.9	1.6	1.7	1.7	2.1	1.7	1.7	1.3	2	2.4	1.9	1.9	1.9
4	1.6	1.9	1.8	2	1.8	1.6	1.7	1.8	1.7	1.9	1.6	1.6	1.8	1.6	1.7	1.7	1.5	1.7	1.8	1.9	1.7
5	1.9	1.7	1.2	1.6	1.4	1.8	1.3	1.4	1.3	1	1.5	1.5	1.8	1.5	1.8	1.6	1.5	1.5	1.8	1.9	1.6
6	1.9	1.8	1.9	1.8	2	2	2	1.9	1.9	1.9	1.8	2.1	2.1	2	2	1	1.6	1.9	2.1	2	1.9
7	1.1	1.3	1.3	1.3	1.4	1.4	1.5	1.5	1.6	1.4	1.6	1.6	1.4	1.4	1.4	1.5	1.6	1.7	1.6	1.7	1.5
8	1.8	1.9	1.5	1.3	1.4	1	1.8	1.1	1.4	1.4	1.3	1.6	1.5	1.6	1.9	1.9	1.7	1.5	1.5	1.7	1.5
9	1.8	1.5	1.6	2.3	1.6	1.4	1.6	1.9	1.8	1.3	1.3	1.3	1.5	2	2.1	1.7	1.5	1.2	1.7	1.6	1.6
10	1.6	1.7	1.2	1.6	1.4	1.4	1.6	1.5	1.7	1.8	1.4	1.5	1.7	1.4	1.4	1.4	1.6	1.8	1.6	1.5	1.5
11	1.3	1.3	1.3	1.6	1.4	1.5	1.5	1.5	1.5	1.5	1.6	1.2	1.1	1.3	1.4	1.3	1.4	1.8	1.9	1.5	1.5
12	1.5	2.2	1.9	1.2	1.9	1.8	1.9	1.3	1.4	1.8	2	1.7	2.1	1.2	1.9	2.1	2.1	1.5	2.3	1.1	1.8
13	1.5	1.2	1.3	1.8	1.4	1.5	1.6	1.3	1.6	1.8	1.5	1.6	1.4	1.5	1.3	1.5	1.8	1.7	1.5	1.4	1.5
14	1.2	1.1	1.5	1.5	1.4	1.5	1.3	1.2	1.2	1.3	1.5	1.5	2.1	1.5	1.4	1.4	1.4	1.5	2	1.5	1.5
15	1.7	1.5	2	1.9	2	2	2.2	1.6	1.6	2	1.3	1.4	1.9	2	1.5	1.4	1.5	1.6	2	2.2	1.8
16	1.3	1.5	1.5	1.2	1.8	1.1	1.4	1.3	1.5	1.1	1.5	1.5	1.4	1.1	1.3	1.2	1.3	1.2	1.3	1.1	1.3
17	1.6	1.1	1.3	1.3	1.5	1.6	1.3	1.5	1.6	1.7	1.5	1.6	1.5	1.3	1.2	1.1	1	1.1	1.2	1.3	1.4
18	1.6	1.2	1.4	1.7	1.5	1.8	1.6	1.5	1.3	1.5	1.5	1.3	1.2	1.4	1.4	1.8	1.6	1.4	1.3	1.4	1.5
19	1.7	1.5	2	1.9	2	2	2.2	1.6	1.6	2	1.3	1.4	1.9	2	1.5	1.4	1.5	1.6	2	2.2	1.8
20	1.4	1.7	1.7	2.5	1.7	1.7	2.9	1.5	1.9	1.3	2.5	2.2	2.2	1.6	1.6	1.6	1.8	1.4	2	1.7	1.9
21	1.5	1.5	1.6	1.7	1.5	1.5	1.7	1.9	2.2	2.6	1.9	1.8	2.3	1.5	3.1	1.8	1.7	1.8	2.1	1.1	1.8
22	1.5	1.4	1.4	1.3	1.4	1.4	1.4	1.2	1.4	1.4	1.4	1.2	1.4	1.4	1.3	1.5	1.4	1.4	1.3	1.5	1.4
23	1.5	1	1.3	1.2	1.2	1.3	1.3	1.2	1.5	1.4	1.4	1.4	1.2	1.1	1.2	1.3	1.6	1.2	1.1	1.4	1.3
24	1.5	1.1	1.4	1.7	1.4	1.2	1.2	1.5	1.3	1.3	1.5	1	1.2	1.2	1.1	1.3	1.3	1.4	1.3	1	1.3
25	1.7	1.8	2	1.8	2.2	2.2	2	1.7	1.9	2	2.1	1.8	2.1	2.2	2.1	2.1	1.8	2	2	1.9	2
26	1.6	1.7	1.3	1.8	1.6	1.8	1.7	1.7	1.9	2.1	1.4	1.5	1.5	1.7	1.8	1.8	1.3	1.7	1.7	1.8	1.7
27	2	1.8	1.9	2.3	1.8	2	1.6	1.6	2.2	1.7	1.7	1.9	1.7	1.9	1.8	1.5	1.7	1.9	1.9	2	1.9
28	1.6	1.9	1.2	1.8	2.1	1.6	1.6	1.8	1.7	1.7	2.2	1.6	1.8	1.9	1.4	1.9	2.1	1.9	1.7	2.2	1.8

29	1.1	1.4	1.1	1.2	1.7	1.1	1.1	1.7	1.2	1.2	1.1	1.2	1.2	1.1	1	1	1.1	1.3	1.1	1.3	1.2
30	1	1.4	1.3	1.4	1	1.5	1	1.2	1.5	2.2	1.6	1.4	1.2	1.7	1	2.2	1.5	0.9	1	2.1	1.4
31	1.1	2	2	1.9	1.5	1.8	1.4	1.5	1.6	1.5	1.6	1.8	1.9	1.5	1.4	2.3	1.5	1.5	1.6	1.8	1.7
32	1.8	1.6	1.8	1.4	1.9	1.6	1.7	2.1	1.8	1.3	1.3	2	1.5	1.7	1.8	1.3	2.1	1.9	1.5	1.7	1.7
33	2	1.7	1.9	2.1	2	2.2	1.4	2	2.3	1.9	1.7	1.9	2.2	2.5	2.1	2.1	2.3	1.7	2.1	1.9	2
34	1.5	1.4	1.7	1.3	1.7	1.3	1.4	1.5	1.4	1.5	1.6	1.7	1.6	1.4	1.6	1.5	1.9	1.3	1.6	1.2	1.5
35	1.6	1.7	1.5	1.2	1.3	1.3	1.3	1.4	1.6	1.3	1.2	1.1	1.2	1	1.4	1.5	1.3	1.4	0.9	1	1.3
36	1.5	1.8	2.1	1.1	1.2	2.2	2.3	2	1.8	2.1	1.5	2	2	2	1.7	2.1	2.2	2.3	2.1	1.7	1.9
37	1.4	1.7	1.1	1.3	1.4	2.1	1.5	1.6	1.2	1.6	1.5	1.8	1.5	1.3	1.2	1.6	1.5	1.1	2.1	1.7	1.5
38	1	1	1.1	1	1.4	1.8	1.5	1.3	1.6	1.2	1.2	1.4	1.2	1	1.6	1.2	1.6	2.3	2.3	1.8	1.4
39	2	2.1	2.2	1.6	1.7	1.5	1.4	1.6	1.7	1.6	1.5	1.7	1.9	2.1	1.6	1.4	1.7	2.4	1.7	1.7	1.8
40	1.9	2	2.1	2	2.3	1.8	2.1	1.8	2.3	1.7	2.2	2.1	2.2	1.7	2.3	2	1.7	1.7	1.9	1.6	2
41	1.3	1.4	1.1	1.4	1.2	1.3	1.3	1.2	1.3	1.2	1.5	1.3	1.5	1	1.4	1.4	1.6	1.5	1.3	1.2	1.3
42	1.8	2	1.5	1.4	1.9	1.9	1.8	1.6	2.1	1.5	1.9	1.9	1.9	1.8	1.8	2	2.4	2	1.9	2.4	1.9
43	1.6	2.3	2.7	1.7	2.2	2.1	1.8	1.6	1.6	2.2	1.9	2.2	2.3	1.7	2.2	2.4	2.5	1.4	1.7	1.8	2
44	1.2	1.6	1.5	1.8	1.6	1.2	1.5	1.5	1.3	1.3	1.4	1.7	2.1	1.9	1.8	1.6	1.3	1.7	1.4	1.8	1.6
45	1.8	1.8	1.5	1.3	1.5	1.8	1.9	2.1	1.7	1.7	2.3	1.7	2.3	2.1	1.7	1.9	1.9	2.5	2.4	1.8	1.9
Mean																					**1.6**

Appendix J

Re-scored and detected events from the development set

Record No.	Re-scored (Sleep physiologist)			Detection (Chapter 4)			Detection (Chapter 5)		
	A	*H*	*A+H*	*A*	*H*	*A+H*	*A*	*H*	*A+H*
1	6	8	14	7	10	17	5	6	11
2	4	15	19	2	14	16	2	14	16
3	17	15	32	22	15	37	15	21	36
4	3	70	73	5	62	67	3	59	62
5	98	88	186	97	80	177	100	83	183
6	17	159	176	20	144	164	20	162	182
7	60	187	247	57	184	241	64	173	237
8	6	36	42	4	33	37	5	34	39
9	10	35	45	9	30	39	10	31	41
10	6	2	8	2	2	4	4	2	6
11	2	31	33	2	35	37	2	30	32
12	3	41	44	5	37	42	2	38	40
13	236	61	297	236	58	294	229	75	304
14	2	43	45	1	43	44	2	31	33
15	6	97	103	2	95	97	4	105	109
16	8	18	26	7	20	27	6	23	29
17	1	17	18	1	20	21	1	18	19
18	15	8	23	16	10	26	15	7	22
19	9	35	44	7	34	41	7	23	30
20	0	34	34	5	31	36	3	31	34
21	45	62	107	46	56	102	47	64	111
22	1	11	12	0	10	10	1	11	12
23	83	85	168	70	88	158	79	84	163
24	12	142	154	10	137	147	12	129	141
25	184	165	349	152	195	347	167	178	345
26	52	90	142	51	90	141	60	96	156
27	35	20	55	37	22	59	36	23	59
28	94	161	255	131	145	276	89	172	261
29	504	85	589	485	88	573	495	103	598
30	187	146	333	155	183	338	151	194	345
31	112	254	366	120	225	345	127	250	377
32	16	75	91	17	75	92	17	81	98
33	30	132	162	40	122	162	39	133	172
34	12	108	120	14	106	120	11	108	119
35	66	187	253	97	143	240	55	205	260
36	188	73	261	192	61	253	200	61	261
37	342	76	418	284	113	397	297	143	440
38	230	118	348	235	107	342	223	141	364
39	137	59	196	133	55	188	139	46	185
40	110	141	251	121	135	256	118	137	255
41	164	89	253	134	105	239	143	117	260
42	81	249	330	94	224	318	97	244	341
43	201	79	280	191	100	291	178	114	292
44	48	211	259	57	222	279	51	217	268
45	223	251	474	201	258	459	196	283	479
Total	**3666**	**4069**	**7735**	**3574**	**4022**	**7596**	**3527**	**4300**	**7827**

A: Number of apnea event, *H*: Number of hypopnea event.

Appendix K

Parameters for performance evaluation

Correlation coefficient: The Pearson correlation coefficient (*r*), also known as Pearson's *r*, the Pearson product-moment correlation coefficient, or the bivariate correlation, is a statistic that measures the linear correlation between two variables. It has a value between +1 and -1. A value of +1 is a total positive linear correlation, 0 is no linear correlation, and -1 is a total negative linear correlation. Intraclass correlation coefficient (*ICC*) is a descriptive statistic that can be used when quantitative measurements are made on units that are organized into groups. It describes how strongly units in the same group resemble each other. While it is viewed as a type of correlation, unlike most other correlation measures it operates on data structured as groups, rather than data structured as paired observations. A value of *ICC* of less than 0.50 indicates poor agreement, 0.50 to 0.75 is considered moderate, 0.75 to 0.90 is considered good, and more than 0.90 is considered excellent (Koo & Li, 2016). 95% confidence interval (*CI*) provides additional information about the agreement between scoring and detection.

Bland-Altman plot: A method of data plotting to analyze the agreement between two different methods (designed method vs gold standard). In this plot, the differences between the two methods are plotted against their means. Thus, this is also known as a difference plot. A high correlation does not necessarily imply that there is good agreement between the two methods. The mean difference (i.e., fixed bias) is the estimated bias and the standard deviation (SD) of the differences measures the random fluctuations around the mean. If the mean value of the difference differs significantly from 0, this indicates the presence of fixed bias. It is common to compute 95% limits of agreement (*LoA*) for each comparison (average difference ± 1.96 standard deviation of the differences), which tells us how far apart measurements by two methods were more likely to be for most individuals. If the differences within mean ± 1.96 SD are not clinically important, the two methods may be used interchangeably.

Sensitivity, specificity, and accuracy: Sensitivity is also known as the true positive rate (TPR). It measures the proportion of actual positives that are correctly identified as such. Specificity is known as the true negative rate (TNR) that measures the proportion of actual negatives that are correctly identified as such. In addition, positive predictive value (PPV) and negative predictive value (NPV) are considered as other performance parameters. These are defined using (*K1*) to (*K5*) as follows–

$$\text{PPV} = \frac{TP}{TP + FP} \times 100\% \qquad (K1)$$

$$\text{NPV} = \frac{TN}{TN + FN} \times 100\% \qquad (K2)$$

$$\text{Sensitivity} = TPR = \frac{TP}{TP + FN} \times 100\% \qquad (K3)$$

$$\text{Specificity} = TNR = \frac{TN}{TN + FP} \times 100\% \quad (K4)$$

$$\text{Accuracy} = \frac{TP + TN}{TP + FN + TN + FP} \times 100\% \quad (K5)$$

True positive (*TP*) is the number of sick people (sleep apnea patient/record) correctly identified as sick. True negative (*TN*) is the number of healthy people (normal patient/record) correctly identified as healthy. False positive (*FP*) is the number of healthy people incorrectly identified as sick. False negative (*FN*) is the number of sick people incorrectly identified as healthy.

For 2 class (binary) diagnosis, the confusion matrix is shown in Table K1. Sensitivity reflects the percentage of sick people who are correctly identified as having the condition. Similarly, specificity represents the percentage of healthy people who are correctly identified as not having the condition. Accuracy is the overall performance of the designed method calculated from sensitivity and specificity.

Table K1. Confusion matrix for 2 class diagnosis.

		Estimated	
		Positive	*Negative*
Actual	*Positive*	TP	FN
	Negative	FP	TN

TP: true positive, TN: true negative, FP: false positive, FN: false negative

The estimation of performance parameters is quite different when 4 classes (normal, mild, moderate, and severe) are considered with their corresponding ranges of AHI. In practice, 4 class diagnosis results in lower performance compared to 2 class diagnosis. Confusion matrix for 4 class diagnosis is shown in Table K2.

Table K2. Confusion matrix for 4 class diagnosis.

		Estimated			
		Normal (1)	*Mild (2)*	*Moderate (3)*	*Severe (4)*
Actual	*Normal (1)*	**N_{11}**	N_{12}	N_{13}	N_{14}
	Mild (2)	N_{21}	**N_{22}**	N_{23}	N_{24}
	Moderate (3)	N_{31}	N_{32}	**N_{33}**	N_{34}
	Severe (4)	N_{41}	N_{42}	N_{43}	**N_{44}**

For a specific class (for example, Mild class (2)),

$$TP\ (2) = N_{22} \quad (K6)$$

$$FP\ (2) = N_{12} + N_{32} + N_{42} \quad (K7)$$

$$FN\ (2) = N_{21} + N_{23} + N_{24} \tag{K8}$$

$$TN\ (2) = N_{11} + N_{13} + N_{14} + N_{31} + N_{33} + N_{34} + N_{41} + N_{43} + N_{44} \tag{K9}$$

Thus, the performance parameters (PPV, NPV, sensitivity, and specificity) for the mild class are calculated using (*K6* to *K9* respectively). Similar calculations are used to estimate the performance parameters for the other classes (normal, moderate, and severe). The overall accuracy (4 class accuracy) is calculated using (*K10*) as mentioned below:

$$\text{4 Class Accuracy} = \frac{Sum\ of\ diagonal\ elements}{Sum\ of\ all\ elements\ except\ diagonal} \times 100\%$$

$$= \frac{N_{11} + N_{22} + N_{33} + N_{44}}{N_{12} + N_{13} + N_{14} + N_{21} + N_{23} + N_{24} + N_{31} + N_{32} + N_{34} + N_{41} + N_{42} + N_{43}} \times 100\% \tag{K10}$$

Area under ROC curve (AUC): The receiver operating characteristic (ROC) curve is the graphical representation of the connection between sensitivity and specificity for every possible cut-off for a test or a combination of tests. False positive rate is abbreviated as FPR. A ROC curve plots sensitivity vs. 1-specificity (i.e., TPR vs. FPR) at different thresholds. In addition, the area under the ROC curve (AUC or AUROC) is a measure of the usefulness of a test, where a greater area means a more useful test. The area under ROC curves is an effective way to summarize the overall diagnostic accuracy of the test. The values of AUC vary from 0 to 1, where a value of 0 indicates a perfectly inaccurate test and a value of 1 represents a perfectly accurate test. In general, an AUC of 0.5 suggests no discrimination, 0.7 to 0.8 is considered acceptable, 0.8 to 0.9 is considered excellent, and more than 0.9 is considered outstanding (Mandrekar, 2010).

***Cohen's kappa coefficient* (*k*)**: Cohen's kappa coefficient (*k*) is an effective measure for inter-scorer reliability. It is extensively used to analyze the agreement between two different methods (designed method vs gold standard). In general, *k* of 0 to 0.2 suggests no agreement, 0.2 to 0.4 is considered minimal, 0.4 to 0.6 is considered weak, 0. 6 to 0.8 is considered moderate, 0.8 to 0.9 is considered strong, and more than 0.9 is considered almost perfect (McHugh, 2012).

Appendix L

Actual and estimated AHI with their differences for the development set

Record No.	Actual AHI (event/h)	Estimated AHI (event/h)		Difference (event/h)	
		Chapter 4	*Chapter 5*	*Chapter 4*	*Chapter 5*
1	5.18	3.92	3.03	1.26	2.15
2	4.12	3.56	3.73	0.56	0.39
3	12.82	7.76	6.39	5.06	6.43
4	12.38	15.53	13.88	-3.15	-1.49
5	43.78	43.70	42.56	0.08	1.22
6	35.24	32.69	36.34	2.55	-1.10
7	56.71	50.19	46.48	6.52	10.23
8	17.90	10.61	12.66	7.29	5.24
9	11.93	7.60	7.76	4.33	4.17
10	1.70	1.67	1.06	0.03	0.63
11	17.64	7.59	7.24	10.05	10.40
12	8.99	9.19	8.81	-0.20	0.17
13	52.32	62.70	64.52	-10.58	-12.20
14	5.12	8.46	6.17	-3.48	-1.05
15	29.90	19.07	20.82	10.83	9.08
16	5.49	8.47	7.62	-2.98	-2.13
17	3.29	4.18	3.25	-0.89	0.04
18	5.84	5.92	4.71	-0.08	1.13
19	8.65	9.36	6.24	-0.71	2.41
20	12.11	9.29	6.96	2.65	5.15
21	40.10	37.64	38.51	2.46	1.58
22	3.30	2.02	2.02	1.28	1.28
23	32.20	34.07	34.07	-2.06	-1.87
24	47.64	29.54	25.77	18.10	21.87
25	53.45	55.57	55.72	-2.27	-2.27
26	34.29	31.43	34.19	2.86	0.09
27	8.58	12.42	11.36	-3.84	-2.78
28	39.78	47.24	44.62	-7.89	-4.84
29	93.45	90.81	95.45	2.49	-2.00
30	55.32	63.88	65.12	-8.56	-9.80
31	59.86	58.42	61.98	1.29	-2.12
32	21.48	20.99	20.01	0.49	1.47
33	34.11	32.86	34.28	0.78	-0.16
34	18.26	24.95	22.81	-6.69	-4.55
35	45.75	65.17	70.59	-19.22	-24.83
36	38.53	42.57	43.43	-4.18	-4.90
37	78.41	84.51	98.51	-7.04	-20.10
38	54.63	83.51	67.50	-11.98	-12.87
39	33.01	39.27	39.45	-6.26	-6.44
40	44.54	46.06	45.92	-1.67	-1.37
41	49.54	49.56	52.37	-0.02	-2.83
42	52.34	55.39	58.68	-3.05	-6.34
43	45.89	53.86	53.86	-8.14	-7.97
44	47.37	52.50	52.33	-5.13	-4.95
45	63.28	67.33	71.24	-4.34	-7.96
Mean	**32.14**	**33.10**	**33.56**	**-0.97**	**-1.42**
SD	**22.29**	**24.36**	**26.13**	**6.28**	**7.59**

AHI: Apnea hypopnea index, SD: Standard deviation, Estimated AHI was subtracted from actual AHI to calculate the differences, Positive (+) and negative (-) differences indicate underestimation and overestimation respectively.

Appendix M

Actual and estimated AHI with their differences for the validation set

Record No.	Actual AHI (event/h)	Estimated AHI (event/h)		Difference (event/h)	
		Chapter 4	*Chapter 5*	*Chapter 4*	*Chapter 5*
1	6.23	8.91	6.89	-2.68	-0.66
2	38.24	37.33	34.19	0.92	4.06
3	9.37	13.73	11.81	-4.36	-2.44
4	7.46	10.12	9.70	-2.66	-2.24
5	6.67	11.86	9.00	-5.19	-2.33
6	15.88	26.26	25.06	-10.38	-9.18
7	37.55	33.21	35.08	4.34	2.47
8	2.02	4.44	3.72	-2.42	-1.70
9	9.53	10.98	11.30	-1.45	-1.77
10	28.70	33.67	35.00	-4.97	-6.30
11	18.36	19.12	19.57	-0.76	-1.21
12	24.16	30.43	30.00	-6.27	-5.84
13	38.49	30.68	32.95	7.80	5.53
14	12.24	13.66	11.39	-1.42	0.86
15	4.08	3.28	3.44	0.81	0.64
16	19.05	11.86	12.34	7.19	6.71
17	2.88	15.25	14.00	-12.38	-11.12
18	44.64	34.09	29.29	10.55	15.34
19	6.41	6.07	5.35	0.34	1.06
20	21.66	21.80	19.50	-0.14	2.16
21	7.34	27.14	23.85	-19.80	-16.51
22	26.99	20.93	20.76	6.07	6.24
23	19.22	26.84	25.00	-7.61	-5.78
24	24.81	22.30	19.49	2.51	5.32
25	19.38	19.22	17.69	0.16	1.69
26	12.15	16.71	10.79	-4.55	1.37
27	17.04	13.53	14.25	3.51	2.79
28	6.94	5.49	5.03	1.46	1.91
29	7.62	8.29	5.59	-0.67	2.03
30	51.96	45.32	44.88	6.63	7.08
31	1.21	4.25	3.31	-3.05	-2.10
32	1.87	4.20	2.75	-2.34	-0.88
33	25.87	15.87	18.14	10.00	7.73
34	7.54	12.70	8.72	-5.16	-1.18
35	11.27	6.27	5.85	5.00	5.42
36	1.76	3.60	3.02	-1.84	-1.26
37	14.28	9.70	9.70	4.58	4.58
38	5.55	8.30	9.04	-2.75	-3.49
39	2.99	15.18	15.34	-12.20	-12.35
40	10.42	5.29	3.14	5.13	7.27
41	20.37	22.56	22.41	-2.19	-2.05
42	7.72	8.75	7.78	-1.03	-0.06
43	4.55	6.72	5.96	-2.17	-1.40
44	14.96	14.87	14.54	0.09	0.42
45	5.42	12.38	9.81	-6.97	-4.40
46	6.40	13.93	14.39	-7.53	-7.99
47	27.25	18.59	19.86	8.66	7.38
48	5.96	13.12	10.27	-7.16	-4.31
49	50.72	47.51	49.01	3.21	1.71
50	27.47	27.99	27.40	-0.52	0.07
51	21.87	17.83	20.33	4.04	1.53

52	22.44	19.83	16.15	2.61	6.29
53	17.53	26.99	24.09	-9.47	-6.56
54	6.33	12.52	10.14	-6.19	-3.81
55	9.15	7.22	6.56	1.93	2.59
56	1.66	7.92	6.47	-6.26	-4.80
57	1.57	2.57	2.29	-1.00	-0.72
58	11.69	11.23	9.98	0.47	1.71
59	13.06	17.40	16.40	-4.34	-3.34
60	64.58	62.15	58.75	2.42	5.82
61	13.38	15.22	11.19	-1.84	2.20
62	12.30	15.41	15.57	-3.11	-3.27
63	19.42	15.53	14.91	3.89	4.52
64	19.02	20.83	15.72	-1.81	3.30
65	11.61	7.75	6.24	3.85	5.37
66	2.13	7.11	4.79	-4.97	-2.65
67	12.59	11.72	8.56	0.87	4.03
68	13.93	6.46	4.99	7.47	8.94
69	17.29	19.46	21.65	-2.17	-4.36
70	6.72	7.56	5.36	-0.84	1.36
71	6.02	7.26	6.39	-1.24	-0.38
72	5.49	13.64	13.13	-8.15	-7.64
73	9.03	10.47	10.64	-1.44	-1.61
74	12.40	9.33	8.84	3.06	3.55
75	4.68	6.82	5.38	-2.14	-0.70
76	16.54	6.53	5.52	10.01	11.01
77	29.73	54.55	54.71	-24.81	-24.97
78	9.35	20.73	18.21	-11.38	-8.86
79	57.29	44.14	45.17	13.15	12.11
80	0.89	4.26	2.79	-3.37	-1.90
81	18.90	15.03	12.39	3.87	6.51
82	15.10	24.71	24.20	-9.62	-9.10
83	31.42	33.13	33.87	-1.70	-2.45
84	11.84	15.67	14.65	-3.83	-2.81
85	18.79	22.96	25.50	-4.18	-6.71
86	6.62	36.37	33.46	-29.75	-26.84
87	2.11	6.25	6.25	-4.14	-4.14
88	20.31	14.29	14.12	6.03	6.19
89	3.51	6.07	4.59	-2.55	-1.07
90	13.76	12.96	13.82	0.80	-0.06
91	9.11	11.60	14.38	-2.49	-5.27
92	2.63	12.30	9.10	-9.67	-6.47
93	81.09	72.50	68.75	8.59	12.34
94	10.63	7.29	7.44	3.34	3.19
95	8.53	10.82	10.28	-2.28	-1.75
96	28.22	31.70	30.23	-3.48	-2.02
97	5.41	14.45	11.67	-9.04	-6.26
98	58.66	45.57	46.00	13.09	12.66
99	3.55	8.65	7.75	-5.11	-4.20
100	12.33	25.93	24.63	-13.59	-12.30
101	10.98	11.28	10.33	-0.30	0.65
102	0.67	2.59	3.20	-1.92	-2.53
103	6.31	8.27	8.99	-1.96	-2.69
104	24.60	33.97	32.65	-9.37	-8.05
105	18.47	17.59	16.08	0.89	2.39
106	8.94	16.88	15.58	-7.95	-6.65
107	7.06	19.55	15.64	-12.49	-8.58
108	21.13	22.27	23.33	-1.14	-2.20
109	3.42	10.23	7.84	-6.81	-4.41
110	19.07	17.87	17.29	1.20	1.79
111	22.58	15.20	12.60	7.38	9.99

112	6.43	10.93	8.24	-4.50	-1.81
113	16.00	17.50	17.79	-1.50	-1.79
114	13.98	26.93	21.14	-12.95	-7.16
115	2.43	7.31	5.29	-4.89	-2.86
116	58.97	55.15	55.29	3.83	3.68
117	18.06	23.47	22.67	-5.41	-4.61
118	44.32	36.21	37.34	8.11	6.98
119	4.69	9.77	10.82	-5.08	-6.13
120	20.54	19.87	17.05	0.67	3.49
121	0.33	2.36	0.84	-2.03	-0.51
122	14.44	12.50	11.33	1.94	3.11
123	12.52	12.06	13.15	0.46	-0.63
124	20.50	11.26	9.04	9.24	11.46
125	14.25	17.62	15.44	-3.36	-1.18
126	7.05	10.11	8.50	-3.06	-1.45
127	10.56	9.97	9.36	0.59	1.21
128	1.79	4.49	1.95	-2.70	-0.16
129	14.02	23.92	24.95	-9.90	-10.93
130	8.92	15.17	14.45	-6.26	-5.53
131	2.87	5.60	5.60	-2.73	-2.73
132	22.69	17.43	16.53	5.26	6.17
133	16.39	15.09	15.38	1.30	1.01
134	54.84	14.14	15.37	40.70	39.47
135	13.87	18.33	16.11	-4.46	-2.24
136	12.86	19.36	16.47	-6.51	-3.62
137	10.93	28.48	29.82	-17.55	-18.89
138	17.02	27.40	25.80	-10.38	-8.78
139	3.20	12.95	10.26	-9.74	-7.06
140	21.89	25.72	23.41	-3.83	-1.52
141	4.03	11.50	10.04	-7.48	-6.02
142	9.64	13.11	11.71	-3.47	-2.07
143	2.84	2.95	2.21	-0.11	0.63
144	15.07	12.33	10.44	2.74	4.63
145	1.01	1.52	0.76	-0.51	0.25
146	5.32	8.12	8.27	-2.80	-2.95
147	9.44	12.31	12.13	-2.88	-2.69
148	21.06	20.51	18.30	0.55	2.77
149	15.81	5.21	5.61	10.59	10.19
150	2.64	6.21	4.77	-3.57	-2.13
151	11.32	15.15	12.68	-3.84	-1.36
152	7.98	15.06	11.87	-7.08	-3.90
153	1.72	4.34	3.18	-2.61	-1.46
154	15.66	25.34	23.58	-9.69	-7.92
155	12.83	18.56	20.64	-5.74	-7.82
156	9.77	9.69	10.37	0.07	-0.61
157	14.98	11.98	10.82	2.99	4.15
158	57.44	70.76	71.86	-13.32	-14.42
159	20.51	15.55	11.99	4.96	8.53
160	2.28	11.11	9.64	-8.83	-7.36
161	9.77	20.43	21.65	-10.66	-11.88
162	16.00	19.08	22.11	-3.08	-6.11
163	77.74	63.35	56.97	14.38	20.77
164	23.17	27.32	30.39	-4.15	-7.22
165	39.46	35.18	39.98	4.28	-0.52
166	8.80	13.77	13.11	-4.97	-4.31
167	20.28	13.22	10.76	7.06	9.52
168	17.17	10.95	8.28	6.22	8.89
169	6.70	3.21	3.06	3.49	3.64
170	34.31	30.62	32.68	3.69	1.62
171	8.36	12.66	14.12	-4.30	-5.76

172	9.90	12.66	11.36	-2.77	-1.47
173	9.23	10.98	11.56	-1.75	-2.33
174	5.65	11.00	10.28	-5.35	-4.63
175	13.77	26.35	24.83	-12.58	-11.06
176	8.83	4.43	3.29	4.40	5.55
177	5.27	5.23	2.95	0.05	2.32
178	14.92	18.83	17.86	-3.91	-2.93
179	55.69	49.54	58.72	6.15	-3.03
180	2.28	10.08	9.11	-7.79	-6.82
181	28.92	28.06	25.06	0.86	3.86
182	26.02	30.71	30.71	-4.69	-4.69
183	5.19	3.00	3.00	2.19	2.19
184	1.80	2.47	1.89	-0.67	-0.09
185	1.76	2.53	2.70	-0.77	-0.94
186	12.06	13.58	12.86	-1.52	-0.80
187	7.86	8.65	9.13	-0.79	-1.27
188	7.37	13.31	12.75	-5.95	-5.38
189	8.70	8.91	10.40	-0.22	-1.70
190	44.22	39.47	39.16	4.75	5.06
191	28.94	39.60	37.08	-10.66	-8.14
192	21.64	35.96	32.12	-14.32	-10.48
193	4.43	11.60	7.52	-7.17	-3.09
194	1.52	6.76	6.10	-5.24	-4.58
195	25.16	27.38	27.38	-2.22	-2.22
196	19.11	20.47	16.56	-1.36	2.55
197	13.08	13.50	12.27	-0.42	0.81
198	3.60	13.66	10.69	-10.07	-7.10
199	24.25	23.95	22.62	0.31	1.64
200	54.71	44.64	39.76	10.07	14.95
201	11.82	8.12	7.60	3.70	4.22
202	65.21	40.18	35.85	25.03	29.36
203	34.85	34.82	31.70	0.04	3.16
204	24.94	25.24	25.24	-0.30	-0.30
205	42.04	28.49	27.63	13.55	14.41
206	27.26	20.64	18.36	6.63	8.91
207	0.74	3.89	3.39	-3.15	-2.64
208	11.36	13.01	11.27	-1.65	0.08
209	14.76	17.66	13.12	-2.90	1.63
210	21.29	27.26	24.94	-5.97	-3.65
211	19.37	11.35	9.43	8.02	9.94
212	10.34	7.48	5.65	2.85	4.69
213	33.51	39.16	39.45	-5.65	-5.94
214	1.90	6.87	5.81	-4.96	-3.91
215	35.40	27.52	30.51	7.88	4.88
216	3.89	6.74	6.09	-2.85	-2.20
217	14.81	15.66	13.94	-0.86	0.87
218	14.38	11.78	11.78	2.60	2.60
219	11.24	19.46	18.51	-8.22	-7.27
220	48.74	40.41	40.98	8.33	7.76
221	7.40	4.60	3.13	2.80	4.27
222	0.57	2.85	2.85	-2.28	-2.28
223	24.39	22.98	19.60	1.41	4.80
224	3.82	13.33	12.73	-9.51	-8.91
225	22.34	21.22	24.01	1.12	-1.67
226	17.72	25.10	25.38	-7.38	-7.67
227	27.03	23.99	22.47	3.04	4.56
228	10.63	19.56	16.73	-8.93	-6.10
229	14.17	24.76	21.92	-10.59	-7.75
230	17.01	20.21	19.21	-3.20	-2.20
231	13.51	20.03	19.86	-6.52	-6.35

232	36.33	30.92	27.11	5.41	9.22
233	1.82	1.12	0.56	0.70	1.26
234	2.05	15.37	16.62	-13.33	-14.57
235	14.00	11.59	10.73	2.41	3.27
236	9.47	17.93	15.54	-8.46	-6.07
237	30.82	35.66	37.96	-4.84	-7.14
238	23.71	26.11	27.07	-2.40	-3.36
239	7.15	6.00	6.57	1.15	0.58
240	22.98	24.27	24.43	-1.30	-1.45
241	32.08	40.03	39.08	-7.95	-7.00
242	37.35	38.73	40.81	-1.38	-3.46
243	32.31	34.12	35.15	-1.80	-2.83
244	34.23	34.36	36.50	-0.14	-2.28
245	38.77	37.81	37.19	0.96	1.58
246	9.18	8.14	7.14	1.04	2.04
247	38.35	22.33	21.33	16.02	17.02
248	28.10	21.00	20.29	7.10	7.80
249	10.34	17.56	17.13	-7.23	-6.79
250	45.32	43.00	42.19	2.32	3.13
251	72.29	74.31	82.60	-2.01	-10.31
252	12.66	16.34	12.80	-3.68	-0.13
253	54.70	32.50	29.84	22.20	24.86
254	26.33	28.04	30.62	-1.71	-4.29
255	21.97	20.96	21.43	1.01	0.54
256	20.98	29.32	29.16	-8.34	-8.18
257	22.94	22.19	23.65	0.75	-0.71
258	29.74	35.14	38.49	-5.41	-8.75
259	34.42	38.31	37.50	-3.88	-3.08
260	4.58	15.14	13.56	-10.56	-8.98
261	18.80	14.71	12.93	4.09	5.87
262	6.06	9.32	6.55	-3.26	-0.49
263	4.47	10.39	9.58	-5.92	-5.11
264	22.22	19.22	22.77	3.00	-0.55
265	17.17	24.57	23.28	-7.40	-6.11
266	3.32	8.59	9.81	-5.26	-6.49
267	29.33	23.76	22.09	5.57	7.24
268	15.76	12.08	12.42	3.68	3.35
269	23.20	8.92	6.58	14.28	16.63
270	17.78	13.44	15.32	4.34	2.47
271	50.04	51.56	51.72	-1.52	-1.68
272	13.01	15.43	12.47	-2.41	0.54
273	31.61	43.01	41.44	-11.40	-9.82
274	7.49	16.13	14.68	-8.65	-7.19
275	7.92	13.44	12.57	-5.52	-4.65
276	3.53	5.48	6.54	-1.95	-3.02
277	14.30	4.69	2.51	9.62	11.79
278	18.41	17.14	16.81	1.27	1.60
279	1.48	7.44	5.54	-5.96	-4.07
280	25.02	23.31	21.33	1.70	3.68
281	20.35	27.11	19.90	-6.76	0.46
282	6.39	12.91	10.08	-6.52	-3.69
283	69.16	58.78	66.02	10.38	3.14
284	7.66	6.65	6.96	1.01	0.70
285	16.03	26.02	20.76	-9.99	-4.73
286	7.14	3.50	3.18	3.65	3.96
287	13.43	2.58	2.29	10.86	11.14
288	19.10	24.51	23.70	-5.41	-4.60
289	41.70	25.56	22.20	16.14	19.51
290	18.80	27.87	29.77	-9.07	-10.96
291	2.21	1.19	1.19	1.02	1.02

292	3.86	6.69	5.73	-2.83	-1.87
293	30.19	36.76	38.24	-6.57	-8.05
294	49.05	42.54	41.08	6.51	7.98
295	24.10	26.15	24.65	-2.05	-0.55
296	13.26	18.30	15.69	-5.04	-2.43
297	12.97	18.24	15.00	-5.27	-2.03
298	13.85	24.19	24.04	-10.34	-10.18
299	9.12	20.68	21.14	-11.56	-12.02
300	25.29	30.46	29.07	-5.17	-3.78
301	28.78	21.26	21.12	7.52	7.67
302	1.86	6.81	5.65	-4.95	-3.79
303	15.77	17.22	14.81	-1.45	0.97
304	1.46	5.51	4.37	-4.05	-2.92
305	4.04	9.86	8.24	-5.81	-4.20
306	14.01	17.39	17.39	-3.38	-3.38
307	14.13	18.17	21.07	-4.04	-6.94
308	5.45	6.42	6.08	-0.97	-0.63
309	32.90	27.36	25.79	5.54	7.12
310	14.23	17.21	18.32	-2.98	-4.08
311	23.21	27.89	29.10	-4.68	-5.89
312	27.58	19.77	17.73	7.81	9.85
313	17.56	24.80	20.97	-7.24	-3.41
314	51.17	57.86	61.93	-6.70	-10.77
315	9.24	9.36	8.30	-0.11	0.94
316	12.19	14.80	11.64	-2.61	0.55
317	22.26	26.02	30.68	-3.76	-8.42
318	1.96	3.98	4.16	-2.01	-2.19
319	13.13	20.04	15.50	-6.91	-2.37
320	12.42	19.44	21.27	-7.01	-8.84
321	16.33	14.71	14.85	1.62	1.48
322	26.60	32.95	31.58	-6.35	-4.98
323	19.90	14.85	14.85	5.05	5.05
324	16.41	17.43	15.89	-1.02	0.52
325	16.15	20.96	18.68	-4.81	-2.53
326	8.50	10.85	7.29	-2.35	1.20
327	20.78	27.14	27.88	-6.36	-7.10
328	19.52	21.99	19.55	-2.47	-0.03
329	14.28	20.04	17.94	-5.77	-3.66
330	11.36	14.74	11.09	-3.37	0.28
331	21.64	19.74	18.42	1.90	3.22
332	21.99	33.63	26.04	-11.64	-4.06
333	14.38	19.75	14.40	-5.38	-0.02
334	9.14	15.93	14.77	-6.79	-5.63
335	40.49	39.43	36.57	1.06	3.92
336	14.56	30.36	28.41	-15.80	-13.85
337	4.76	8.12	6.94	-3.36	-2.18
338	13.04	20.06	19.46	-7.02	-6.42
339	4.44	6.59	3.63	-2.15	0.81
340	18.70	25.96	22.01	-7.26	-3.31
341	8.83	9.24	8.50	-0.41	0.33
342	19.86	21.86	21.86	-2.01	-2.01
343	33.82	36.66	37.58	-2.85	-3.76
344	33.55	33.21	34.83	0.34	-1.28
345	1.90	2.88	2.50	-0.98	-0.60
346	4.65	7.56	8.43	-2.90	-3.78
347	11.33	15.31	15.31	-3.99	-3.99
348	17.95	20.25	19.01	-2.30	-1.06
349	0.19	2.85	2.65	-2.67	-2.46
350	4.41	11.47	7.57	-7.06	-3.16
351	17.07	15.91	14.20	1.16	2.86

352	11.94	6.38	6.58	5.56	5.36
353	24.48	23.18	23.33	1.30	1.14
354	4.48	3.63	3.47	0.84	1.00
355	5.89	5.99	5.51	-0.10	0.39
356	12.64	16.05	16.05	-3.40	-3.40
357	7.87	16.14	15.90	-8.27	-8.03
358	16.50	7.60	8.89	8.90	7.61
359	3.40	8.97	7.06	-5.57	-3.66
360	14.83	14.88	12.28	-0.05	2.55
361	23.76	30.39	27.75	-6.63	-4.00
362	1.42	6.33	3.80	-4.91	-2.38
363	3.13	6.23	5.79	-3.09	-2.66
364	3.93	5.34	3.56	-1.41	0.37
365	0.98	3.64	3.19	-2.67	-2.21
366	17.33	27.99	29.51	-10.67	-12.19
367	24.65	30.76	31.11	-6.11	-6.45
368	5.73	6.80	6.96	-1.08	-1.23
369	14.24	19.01	18.11	-4.77	-3.87
370	16.01	12.74	10.16	3.27	5.85
371	30.27	21.53	20.09	8.74	10.18
372	7.96	13.26	12.38	-5.31	-4.42
373	21.87	22.40	23.13	-0.53	-1.27
374	3.21	6.01	5.22	-2.80	-2.01
375	36.26	27.02	21.10	9.24	15.16
376	11.27	16.31	13.57	-5.04	-2.29
377	14.86	14.39	14.71	0.48	0.15
378	57.93	54.31	56.65	3.63	1.28
379	39.46	39.23	48.78	0.23	-9.32
380	11.73	14.62	13.29	-2.89	-1.56
381	1.42	1.48	1.18	-0.05	0.24
382	12.38	17.64	13.37	-5.25	-0.98
383	4.86	13.40	6.89	-8.54	-2.02
384	28.87	24.12	25.60	4.75	3.27
385	14.17	21.10	18.93	-6.93	-4.76
386	6.84	12.80	10.83	-5.96	-3.99
387	12.43	21.74	17.65	-9.31	-5.22
388	5.11	11.37	12.84	-6.26	-7.74
389	12.64	7.14	5.83	5.51	6.82
390	3.15	4.44	4.93	-1.29	-1.79
391	1.93	1.86	1.86	0.08	0.08
392	8.43	4.11	4.74	4.32	3.69
393	5.66	8.24	9.68	-2.58	-4.02
394	1.63	6.01	5.66	-4.38	-4.04
395	2.96	19.57	20.62	-16.61	-17.66
396	22.62	43.56	41.69	-20.95	-19.07
397	24.95	17.98	14.15	6.98	10.81
398	8.24	7.95	6.79	0.29	1.45
399	16.93	14.80	15.09	2.13	1.84
400	11.52	13.64	12.84	-2.12	-1.32
401	2.89	5.63	3.69	-2.75	-0.80
402	17.30	21.08	22.12	-3.78	-4.82
403	13.37	19.76	16.68	-6.39	-3.31
404	25.71	16.96	18.26	8.76	7.45
405	12.00	20.52	17.77	-8.52	-5.77
406	19.04	27.91	25.94	-8.86	-6.90
407	15.64	22.52	21.87	-6.88	-6.23
408	28.65	25.06	23.50	3.60	5.15
409	20.53	39.90	37.77	-19.38	-17.24
410	23.28	23.55	18.79	-0.28	4.49
411	23.36	41.49	37.86	-18.13	-14.51

412	12.15	17.67	17.21	-5.53	-5.06
413	35.16	38.66	40.11	-3.50	-4.95
414	3.03	11.39	11.08	-8.36	-8.05
415	24.80	21.81	21.81	3.00	3.00
416	2.30	6.36	6.95	-4.06	-4.65
417	5.94	1.01	0.40	4.93	5.53
418	14.14	15.07	14.72	-0.93	-0.58
419	4.05	9.06	9.53	-5.01	-5.48
420	2.54	14.30	13.57	-11.76	-11.03
421	13.33	19.56	18.10	-6.22	-4.77
422	16.66	13.39	10.27	3.27	6.39
423	11.20	20.78	17.59	-9.59	-6.39
424	18.01	20.74	16.62	-2.73	1.39
425	9.32	23.69	22.67	-14.37	-13.35
426	7.00	8.76	7.27	-1.76	-0.27
427	9.74	14.91	17.04	-5.17	-7.30
428	4.63	5.69	6.44	-1.06	-1.80
429	12.13	9.94	7.88	2.20	4.26
430	2.53	11.00	6.94	-8.47	-4.41
431	8.63	13.69	10.03	-5.07	-1.40
432	21.67	22.56	19.16	-0.89	2.52
433	47.62	46.86	47.58	0.76	0.04
434	9.82	10.42	8.25	-0.60	1.57
435	5.94	17.06	13.68	-11.12	-7.74
436	15.87	19.57	20.81	-3.69	-4.93
437	18.86	28.17	25.30	-9.31	-6.44
438	10.86	8.69	8.25	2.17	2.61
439	6.73	4.70	3.38	2.03	3.35
440	32.92	25.72	24.13	7.20	8.78
441	17.32	12.32	11.97	4.99	5.34
442	8.04	11.87	8.35	-3.83	-0.31
443	24.00	38.42	33.07	-14.42	-9.07
444	1.72	6.44	5.31	-4.72	-3.59
445	4.44	8.42	8.59	-3.98	-4.15
446	4.92	15.71	14.42	-10.79	-9.50
447	12.37	11.48	10.10	0.89	2.27
448	21.22	26.75	25.25	-5.53	-4.03
449	1.42	7.06	6.32	-5.64	-4.90
450	22.62	33.70	34.26	-11.08	-11.64
451	5.50	11.74	9.23	-6.24	-3.72
452	17.14	16.00	15.84	1.14	1.30
453	1.53	1.65	2.10	-0.12	-0.57
454	42.34	48.26	52.53	-5.92	-10.19
455	5.57	6.83	5.64	-1.26	-0.08
456	10.09	12.16	9.41	-2.07	0.68
457	21.27	19.05	18.29	2.21	2.98
458	10.72	15.35	13.74	-4.63	-3.02
459	8.08	9.23	7.47	-1.15	0.61
460	14.91	22.01	16.40	-7.11	-1.49
461	6.82	15.90	17.62	-9.09	-10.80
462	21.30	27.71	30.46	-6.41	-9.17
463	12.60	6.65	6.49	5.95	6.11
464	6.31	9.50	10.67	-3.19	-4.36
465	5.60	7.92	6.47	-2.32	-0.86
466	20.03	11.73	11.14	8.29	8.89
467	14.85	23.72	24.07	-8.88	-9.22
468	17.45	17.91	18.49	-0.46	-1.05
469	4.24	9.70	9.70	-5.46	-5.46
470	14.96	18.83	16.44	-3.87	-1.47
471	48.71	51.48	49.95	-2.76	-1.24

472	33.19	23.73	23.88	9.46	9.31
473	30.16	21.91	20.69	8.25	9.47
474	23.10	28.08	28.41	-4.98	-5.31
475	12.65	22.67	24.80	-10.02	-12.15
476	0.00	5.17	3.60	-5.17	-3.60
477	37.76	26.20	25.75	11.57	12.02
478	6.85	5.37	4.47	1.48	2.37
479	28.20	32.49	32.04	-4.28	-3.83
480	14.65	27.90	28.35	-13.26	-13.70
481	10.24	7.53	7.23	2.71	3.00
482	1.94	0.36	0.18	1.58	1.76
483	2.71	3.52	2.68	-0.80	0.03
484	1.69	2.28	1.85	-0.59	-0.17
485	16.45	19.90	19.47	-3.45	-3.02
486	5.14	8.04	7.53	-2.89	-2.39
487	3.47	7.06	6.01	-3.59	-2.54
488	7.06	7.37	4.86	-0.32	2.19
489	9.24	8.70	7.13	0.54	2.11
490	44.28	28.50	27.27	15.78	17.01
491	5.41	10.00	7.00	-4.59	-1.59
492	22.14	31.02	35.03	-8.88	-12.89
493	20.49	17.98	18.15	2.51	2.34
494	6.39	3.14	1.49	3.25	4.90
495	14.20	5.86	5.47	8.34	8.73
496	10.94	14.18	12.20	-3.24	-1.26
497	4.57	3.56	2.70	1.01	1.87
498	15.34	9.03	11.33	6.31	4.01
499	34.55	33.08	36.83	1.47	-2.27
500	12.30	18.71	18.55	-6.41	-6.25
501	3.55	6.99	4.66	-3.44	-1.11
502	5.11	3.67	3.84	1.44	1.27
503	29.49	27.29	29.79	2.20	-0.30
504	27.23	26.49	25.93	0.74	1.30
505	6.84	11.02	12.31	-4.18	-5.47
506	13.44	18.63	16.20	-5.18	-2.75
507	25.76	22.98	20.56	2.78	5.20
508	5.13	7.25	6.72	-2.12	-1.59
509	4.94	9.38	5.98	-4.44	-1.04
510	35.28	47.62	48.43	-12.35	-13.16
511	10.89	24.40	23.64	-13.51	-12.75
512	38.14	43.88	44.06	-5.74	-5.91
513	43.41	47.99	50.43	-4.58	-7.02
514	8.62	8.98	8.37	-0.36	0.25
515	11.54	3.49	3.19	8.05	8.35
516	7.20	16.30	12.23	-9.10	-5.03
517	32.85	26.90	24.19	5.96	8.66
518	7.99	16.71	13.74	-8.72	-5.75
519	1.02	4.78	4.94	-3.76	-3.92
520	34.43	34.21	35.97	0.22	-1.55
521	7.91	13.03	11.91	-5.12	-4.00
522	83.33	79.21	80.21	4.12	3.12
523	23.00	21.16	19.29	1.84	3.71
524	8.10	17.95	14.91	-9.85	-6.81
525	46.48	39.94	38.96	6.54	7.52
526	11.49	8.10	7.48	3.40	4.01
527	27.88	18.20	16.02	9.68	11.86
528	3.99	10.12	11.04	-6.13	-7.05
529	19.30	20.10	24.03	-0.79	-4.72
530	8.24	10.51	7.48	-2.27	0.76
531	13.21	18.52	16.40	-5.32	-3.19

532	18.24	18.35	18.50	-0.11	-0.26
533	16.00	15.03	15.76	0.97	0.24
534	10.39	10.07	8.68	0.32	1.71
535	8.71	5.91	3.99	2.80	4.72
536	18.30	15.78	15.07	2.52	3.23
537	2.54	3.78	1.39	-1.24	1.14
538	18.45	24.71	26.89	-6.26	-8.44
539	7.76	10.28	10.71	-2.52	-2.95
540	7.62	12.15	12.45	-4.52	-4.83
541	9.40	10.41	9.62	-1.00	-0.22
542	21.16	16.14	15.12	5.02	6.05
543	18.87	17.06	15.64	1.81	3.23
544	9.42	10.30	9.72	-0.88	-0.30
545	27.96	24.29	20.92	3.67	7.04
546	33.39	40.40	38.11	-7.00	-4.72
547	10.19	11.35	9.66	-1.16	0.53
548	71.45	82.52	87.69	-11.07	-16.25
549	12.49	10.10	11.60	2.39	0.88
550	18.54	9.69	7.18	8.85	11.36
551	24.34	22.84	19.11	1.50	5.23
552	5.93	12.78	9.03	-6.85	-3.10
553	6.41	10.85	10.04	-4.44	-3.63
554	2.37	4.21	4.21	-1.84	-1.84
555	62.49	38.11	33.57	24.38	28.92
556	17.60	21.03	21.03	-3.42	-3.42
557	2.70	9.12	8.93	-6.42	-6.23
558	31.53	25.64	24.08	5.90	7.45
559	3.23	11.84	11.33	-8.62	-8.10
560	15.19	13.35	11.32	1.85	3.88
561	7.93	11.27	9.68	-3.34	-1.75
562	9.50	10.50	9.75	-1.00	-0.25
563	2.99	6.85	4.32	-3.86	-1.33
564	19.78	24.70	25.00	-4.92	-5.22
565	9.11	4.60	4.76	4.52	4.36
566	8.23	6.95	5.33	1.28	2.89
567	8.37	12.47	12.80	-4.10	-4.43
568	6.12	4.06	3.92	2.06	2.20
569	23.66	11.02	9.38	12.64	14.29
570	3.40	1.05	1.40	2.35	2.00
571	8.94	10.29	9.12	-1.35	-0.17
572	20.57	16.54	16.38	4.03	4.19
573	13.01	22.05	20.02	-9.04	-7.01
574	14.69	16.96	13.75	-2.26	0.94
575	0.83	13.47	8.40	-12.64	-7.57
576	28.71	33.23	32.88	-4.52	-4.17
577	1.79	2.94	2.42	-1.15	-0.63
578	15.25	15.86	14.61	-0.61	0.64
579	2.38	9.85	8.09	-7.48	-5.71
580	31.03	38.03	41.38	-7.01	-10.35
581	27.18	27.02	25.98	0.16	1.19
582	9.31	12.97	8.81	-3.66	0.50
583	16.54	14.68	12.74	1.86	3.80
584	8.09	14.35	11.77	-6.27	-3.69
585	6.38	11.18	9.41	-4.79	-3.03
586	53.93	51.65	56.42	2.28	-2.49
587	13.77	8.94	8.76	4.84	5.01
588	3.11	6.07	3.64	-2.96	-0.53
589	6.96	12.25	14.32	-5.30	-7.36
590	7.71	18.94	18.02	-11.23	-10.31
591	2.45	5.58	3.77	-3.13	-1.33

592	10.62	16.44	13.06	-5.81	-2.44
593	2.23	3.09	2.80	-0.86	-0.57
594	20.78	12.89	10.69	7.88	10.09
595	4.54	3.30	2.60	1.24	1.94
596	7.33	5.89	5.36	1.44	1.97
597	5.49	4.08	4.51	1.41	0.98
598	11.07	22.94	23.71	-11.87	-12.64
599	33.56	33.51	31.91	0.05	1.65
600	21.80	28.69	27.78	-6.90	-5.98
601	8.25	16.47	14.02	-8.22	-5.78
602	37.57	40.01	37.74	-2.44	-0.17
603	10.15	5.62	5.46	4.53	4.69
604	25.84	38.39	31.75	-12.55	-5.91
605	5.43	7.56	10.30	-2.14	-4.87
606	41.20	47.53	52.54	-6.33	-11.34
607	3.19	8.02	7.84	-4.83	-4.64
608	4.81	6.11	4.89	-1.30	-0.08
609	69.56	57.09	54.96	12.47	14.60
610	6.17	11.70	7.08	-5.54	-0.92
611	26.59	33.55	38.11	-6.96	-11.52
612	0.94	2.58	3.49	-1.65	-2.56
613	11.65	12.62	11.90	-0.97	-0.25
614	33.38	8.92	7.75	24.46	25.63
615	8.60	11.82	11.97	-3.22	-3.37
616	2.56	10.34	7.30	-7.79	-4.75
617	13.92	14.44	12.88	-0.52	1.04
618	3.86	12.90	9.78	-9.04	-5.93
619	6.87	1.31	1.02	5.56	5.85
620	48.06	35.67	32.54	12.38	15.52
621	33.46	33.33	33.18	0.12	0.27
622	9.32	5.73	4.47	3.60	4.85
623	6.19	25.79	22.68	-19.60	-16.48
624	10.12	22.28	19.77	-12.16	-9.65
625	1.06	4.35	4.52	-3.29	-3.45
626	9.46	6.51	7.35	2.95	2.11
627	69.00	60.36	56.15	8.63	12.85
628	28.58	32.49	30.55	-3.91	-1.97
629	27.11	29.65	30.09	-2.54	-2.98
630	5.77	9.49	7.19	-3.72	-1.42
631	11.83	12.52	10.14	-0.70	1.69
632	6.68	7.97	8.49	-1.29	-1.81
633	95.97	88.94	83.95	7.03	12.02
634	18.31	15.00	15.58	3.31	2.73
635	29.10	33.60	28.87	-4.49	0.23
636	9.70	9.31	6.67	0.39	3.03
637	12.33	13.82	12.15	-1.48	0.19
638	3.47	4.22	3.61	-0.75	-0.14
639	33.52	30.42	31.40	3.10	2.12
640	6.60	10.85	8.42	-4.26	-1.83
641	14.84	20.19	19.86	-5.35	-5.02
642	9.41	14.06	13.58	-4.66	-4.17
643	14.47	25.79	27.67	-11.32	-13.20
644	2.04	3.27	3.71	-1.22	-1.67
645	3.11	5.29	4.96	-2.18	-1.85
646	2.29	10.18	8.57	-7.89	-6.27
647	22.15	17.85	16.84	4.30	5.31
648	4.33	7.05	4.27	-2.73	0.06
649	15.98	24.29	27.04	-8.31	-11.06
650	12.51	13.67	10.57	-1.16	1.93
651	12.45	16.94	18.05	-4.48	-5.60

652	23.32	20.13	23.46	3.19	-0.14
653	21.52	23.88	24.32	-2.37	-2.80
654	4.66	10.12	6.69	-5.46	-2.03
655	52.61	57.71	56.54	-5.10	-3.93
656	30.40	13.66	12.60	16.74	17.80
657	16.37	17.95	17.37	-1.58	-1.00
658	1.92	8.83	7.38	-6.91	-5.47
659	4.54	4.92	3.91	-0.38	0.63
660	11.58	14.73	9.93	-3.15	1.65
661	3.43	7.60	4.56	-4.17	-1.13
662	28.21	18.68	18.68	9.53	9.53
663	3.02	6.47	7.06	-3.45	-4.04
664	17.28	23.37	23.93	-6.08	-6.65
665	7.63	15.86	16.04	-8.23	-8.42
666	5.81	7.98	4.39	-2.17	1.42
667	35.50	33.66	30.32	1.85	5.19
668	2.68	1.71	2.28	0.97	0.40
669	0.70	4.34	4.18	-3.64	-3.47
670	39.35	45.49	44.88	-6.13	-5.52
671	5.95	9.47	8.16	-3.52	-2.21
672	23.68	22.10	20.97	1.58	2.71
673	10.52	17.95	19.84	-7.43	-9.31
674	43.08	44.13	42.23	-1.05	0.84
675	8.35	12.15	8.96	-3.80	-0.61
676	34.81	14.76	14.06	20.05	20.74
677	5.32	7.94	6.76	-2.62	-1.44
678	16.87	27.83	29.12	-10.96	-12.25
679	3.51	11.54	11.91	-8.03	-8.40
680	3.69	8.67	7.51	-4.99	-3.83
681	15.02	7.47	6.87	7.55	8.14
682	35.81	42.97	46.44	-7.16	-10.63
683	9.35	8.58	6.70	0.77	2.64
684	0.92	1.88	1.41	-0.96	-0.49
685	13.25	16.03	17.61	-2.78	-4.36
686	52.08	39.37	37.50	12.71	14.58
687	22.66	21.69	21.38	0.97	1.27
688	15.48	19.96	22.31	-4.48	-6.83
689	4.84	5.42	4.68	-0.58	0.16
690	19.96	12.52	12.10	7.44	7.86
691	39.42	19.99	19.70	19.43	19.72
692	1.28	7.04	4.59	-5.76	-3.30
693	8.30	13.18	11.73	-4.88	-3.43
694	45.11	34.54	33.67	10.57	11.43
695	12.18	18.24	18.53	-6.07	-6.36
696	12.16	21.84	22.43	-9.68	-10.27
697	6.73	5.24	4.29	1.49	2.44
698	10.87	10.38	7.23	0.49	3.64
699	30.24	25.78	26.44	4.46	3.80
700	6.71	20.82	17.54	-14.11	-10.82
701	36.57	31.46	27.48	5.11	9.09
702	13.92	11.77	9.16	2.15	4.76
703	18.14	24.80	18.56	-6.66	-0.42
704	13.17	14.54	13.78	-1.37	-0.61
705	0.38	2.61	1.20	-2.23	-0.83
706	12.84	12.31	12.63	0.53	0.20
707	2.47	5.44	4.56	-2.97	-2.09
708	3.07	12.02	10.86	-8.95	-7.79
709	9.05	13.04	8.35	-3.99	0.70
710	4.09	5.92	4.91	-1.83	-0.82
711	5.29	7.30	8.23	-2.01	-2.94

712	19.57	18.22	15.21	1.36	4.36
713	4.04	15.59	15.74	-11.55	-11.70
714	2.22	3.11	2.64	-0.89	-0.42
715	24.21	26.04	25.71	-1.83	-1.50
716	8.80	8.85	7.40	-0.05	1.40
717	9.58	12.50	10.69	-2.92	-1.11
718	12.61	10.86	9.27	1.75	3.34
719	4.05	5.93	4.44	-1.88	-0.40
720	66.61	53.11	47.78	13.50	18.83
721	14.81	8.60	8.23	6.21	6.58
722	15.62	18.60	19.04	-2.98	-3.42
723	4.93	4.83	5.86	0.09	-0.93
724	17.81	11.25	7.92	6.56	9.89
725	8.96	14.77	11.41	-5.81	-2.45
726	4.18	8.73	8.24	-4.55	-4.06
727	6.59	10.86	10.71	-4.27	-4.13
728	2.34	6.94	5.06	-4.60	-2.72
729	13.62	14.02	11.27	-0.40	2.34
730	3.53	6.12	3.45	-2.59	0.08
731	2.45	5.25	3.56	-2.80	-1.11
732	15.34	15.75	13.73	-0.41	1.61
733	14.15	12.67	10.83	1.48	3.31
734	98.64	79.98	80.41	18.66	18.24
735	10.71	20.62	21.23	-9.91	-10.52
736	1.64	3.96	2.59	-2.31	-0.94
737	21.82	19.12	15.99	2.70	5.83
738	33.80	25.99	29.70	7.81	4.10
739	12.59	16.54	16.23	-3.96	-3.64
740	10.30	3.18	2.71	7.11	7.59
741	9.17	17.83	15.92	-8.67	-6.76
742	7.78	12.05	9.61	-4.27	-1.83
743	13.07	9.41	34.93	3.66	-21.86
744	58.66	64.01	64.98	-5.35	-6.32
745	23.48	24.71	22.10	-1.23	1.38
746	48.42	53.34	51.72	-4.93	-3.31
747	35.71	33.80	37.02	1.91	-1.31
748	1.26	2.92	3.08	-1.66	-1.82
749	6.03	4.54	4.38	1.49	1.64
750	13.05	11.98	9.66	1.06	3.38
751	22.74	27.63	28.39	-4.90	-5.66
752	24.28	13.56	8.98	10.72	15.30
753	1.88	10.21	8.61	-8.33	-6.72
754	64.32	41.49	40.97	22.82	23.34
755	10.63	9.86	9.70	0.77	0.93
756	7.14	2.90	1.45	4.24	5.69
757	11.65	14.36	10.54	-2.70	1.11
758	16.29	30.18	27.31	-13.89	-11.03
759	15.24	1.04	0.60	14.20	14.65
760	4.24	9.32	7.86	-5.08	-3.62
761	15.56	14.00	13.45	1.55	2.11
762	9.43	10.02	9.47	-0.60	-0.04
763	25.10	24.46	21.66	0.64	3.44
764	23.60	28.44	33.76	-4.84	-10.16
765	2.41	5.07	5.36	-2.66	-2.95
766	19.35	21.38	22.84	-2.03	-3.49
767	16.96	18.59	18.10	-1.63	-1.14
768	16.97	24.70	25.76	-7.73	-8.79
769	25.46	27.88	28.04	-2.42	-2.58
770	11.56	9.33	6.67	2.22	4.89
771	0.33	1.35	1.35	-1.02	-1.02

772	6.07	10.92	9.34	-4.85	-3.27
773	16.42	15.62	15.91	0.80	0.51
774	2.29	13.36	10.33	-11.07	-8.04
775	10.14	10.38	8.33	-0.24	1.80
776	1.31	8.55	8.99	-7.23	-7.68
777	4.99	6.07	3.94	-1.08	1.05
778	68.81	77.68	82.87	-8.87	-14.06
779	45.44	36.29	32.95	9.16	12.50
780	34.70	28.09	25.51	6.62	9.20
781	10.70	4.66	3.50	6.04	7.20
782	8.56	12.80	11.16	-4.24	-2.60
783	9.17	7.14	9.11	2.03	0.06
784	6.83	9.56	9.56	-2.74	-2.74
785	1.74	4.31	4.83	-2.57	-3.08
786	2.55	11.02	8.42	-8.47	-5.88
787	1.39	6.77	5.42	-5.38	-4.03
788	23.12	14.12	13.26	9.00	9.86
789	2.98	5.36	6.52	-2.38	-3.54
790	8.90	17.45	15.04	-8.56	-6.14
791	11.76	18.30	18.47	-6.55	-6.71
792	28.52	29.68	27.07	-1.16	1.45
793	18.83	24.70	25.00	-5.87	-6.17
794	2.85	6.86	5.52	-4.01	-2.67
795	2.14	5.90	4.97	-3.76	-2.83
796	29.64	35.00	33.71	-5.36	-4.07
797	43.40	48.97	45.89	-5.57	-2.49
798	4.22	7.04	7.19	-2.82	-2.97
799	39.95	29.56	34.12	10.40	5.84
800	41.48	37.88	34.23	3.60	7.25
801	7.67	10.27	7.93	-2.60	-0.26
802	6.18	3.88	4.04	2.30	2.14
803	22.44	22.46	18.94	-0.03	3.50
804	22.91	29.32	28.13	-6.40	-5.21
805	17.40	15.03	11.94	2.37	5.46
806	12.05	7.21	5.06	4.84	6.98
807	5.10	10.56	7.88	-5.45	-2.78
808	12.85	12.65	11.32	0.20	1.52
809	36.57	46.76	48.53	-10.20	-11.96
810	23.71	20.23	18.56	3.48	5.15
811	3.15	6.95	7.09	-3.80	-3.94
812	1.43	5.09	4.07	-3.66	-2.64
813	15.43	14.72	12.62	0.71	2.81
814	4.93	5.70	6.24	-0.77	-1.31
815	17.05	8.20	8.20	8.85	8.85
816	12.84	7.74	8.73	5.11	4.11
817	66.71	54.41	59.12	12.30	7.59
818	3.41	6.34	4.27	-2.92	-0.86
819	19.29	19.28	21.03	0.02	-1.74
820	28.32	27.27	27.27	1.05	1.05
821	4.17	9.57	8.41	-5.40	-4.24
822	8.50	11.96	10.83	-3.46	-2.33
823	13.01	19.62	18.26	-6.61	-5.24
824	14.95	11.44	11.00	3.51	3.94
825	19.95	20.96	20.79	-1.01	-0.84
826	4.51	5.62	3.64	-1.11	0.86
827	15.17	16.11	14.37	-0.94	0.80
828	4.77	3.26	4.04	1.51	0.73
829	2.02	4.53	2.91	-2.51	-0.89
830	12.12	15.86	13.29	-3.74	-1.17
831	13.12	3.78	3.18	9.34	9.94

832	5.35	4.25	4.10	1.09	1.25
833	2.10	1.78	1.62	0.32	0.48
834	3.65	10.97	10.37	-7.32	-6.72
835	5.67	12.38	12.82	-6.71	-7.15
836	14.15	15.23	14.06	-1.09	0.08
837	2.94	10.57	10.71	-7.62	-7.77
838	4.82	4.80	4.62	0.02	0.20
839	3.88	4.85	3.56	-0.97	0.32
840	5.53	12.37	10.48	-6.83	-4.95
841	9.55	10.13	8.32	-0.59	1.23
842	5.69	9.70	9.85	-4.01	-4.15
843	7.12	12.38	9.17	-5.26	-2.05
844	0.92	9.58	7.31	-8.65	-6.38
845	10.35	10.39	7.64	-0.03	2.72
846	31.09	40.88	45.49	-9.80	-14.41
847	7.69	6.80	7.45	0.88	0.24
848	40.06	38.96	36.92	1.10	3.15
849	3.20	8.03	5.30	-4.83	-2.10
850	14.61	23.21	25.29	-8.60	-10.67
851	6.24	11.77	8.60	-5.53	-2.36
852	5.92	5.80	5.95	0.12	-0.03
853	102.78	88.47	96.48	14.31	6.30
854	43.03	40.01	35.57	3.01	7.46
855	2.18	5.74	5.20	-3.56	-3.02
856	3.77	9.60	6.64	-5.83	-2.88
857	8.58	9.87	8.69	-1.29	-0.11
858	5.52	7.86	6.35	-2.35	-0.83
859	22.33	30.93	30.59	-8.60	-8.25
860	9.17	15.40	13.72	-6.23	-4.55
861	1.82	6.54	4.22	-4.72	-2.40
862	10.41	15.36	15.03	-4.95	-4.62
863	3.37	10.28	9.41	-6.91	-6.04
864	3.45	12.98	8.15	-9.53	-4.70
865	3.48	8.80	8.33	-5.32	-4.85
866	14.81	12.74	14.04	2.07	0.77
867	30.60	30.44	27.41	0.16	3.19
868	30.86	34.71	31.12	-3.85	-0.26
869	23.92	33.51	34.99	-9.59	-11.07
870	6.49	8.94	7.18	-2.45	-0.69
871	36.89	36.03	31.76	0.86	5.12
872	23.07	25.62	26.39	-2.55	-3.32
873	3.81	5.96	5.37	-2.15	-1.56
874	25.99	29.94	30.52	-3.95	-4.53
875	21.65	26.82	30.06	-5.17	-8.41
876	10.76	13.75	11.44	-3.00	-0.68
877	6.80	8.85	8.56	-2.05	-1.76
878	1.76	3.83	3.54	-2.07	-1.77
879	21.28	23.31	22.59	-2.03	-1.30
880	3.62	15.03	13.11	-11.41	-9.50
881	15.00	16.97	19.25	-1.97	-4.25
882	49.39	52.80	59.62	-3.42	-10.24
883	26.49	25.44	23.40	1.06	3.09
884	6.77	8.24	8.09	-1.47	-1.32
885	10.95	15.36	10.44	-4.41	0.51
886	19.74	19.11	16.40	0.63	3.33
887	12.43	16.04	15.06	-3.60	-2.63
888	5.39	8.98	9.12	-3.59	-3.73
889	3.33	13.97	11.21	-10.64	-7.88
890	11.70	10.37	11.28	1.33	0.42
891	24.78	23.88	22.82	0.89	1.96

892	46.44	46.91	48.97	-0.48	-2.53
893	14.61	15.96	16.76	-1.35	-2.14
894	2.20	3.24	1.94	-1.04	0.26
895	12.64	9.99	8.54	2.65	4.10
896	21.45	16.47	14.51	4.99	6.94
897	6.74	5.65	5.50	1.09	1.24
898	19.85	26.50	27.22	-6.65	-7.37
899	7.65	8.96	7.55	-1.31	0.09
900	4.36	7.11	5.51	-2.75	-1.15
901	5.43	5.83	4.48	-0.40	0.95
902	13.90	13.75	12.89	0.15	1.01
903	27.22	17.86	18.17	9.36	9.05
904	19.36	16.96	15.89	2.40	3.47
905	4.87	12.31	10.86	-7.44	-5.99
906	121.33	94.73	80.95	26.60	40.38
907	30.70	35.55	34.24	-4.84	-3.54
908	1.18	6.95	5.37	-5.77	-4.19
909	41.47	46.62	46.03	-5.15	-4.56
910	13.97	13.80	10.06	0.18	3.91
911	18.42	27.46	21.80	-9.04	-3.38
912	3.24	6.76	6.92	-3.51	-3.68
913	3.79	11.51	11.71	-7.72	-7.92
914	13.27	12.11	10.04	1.17	3.23
915	12.43	8.08	5.33	4.35	7.10
916	2.25	4.62	2.89	-2.37	-0.64
917	29.12	25.76	27.05	3.37	2.07
918	20.00	10.00	7.66	10.00	12.34
919	14.27	8.77	9.21	5.50	5.06
920	3.79	3.81	2.41	-0.02	1.38
921	24.19	23.05	21.63	1.15	2.56
922	16.64	17.67	13.15	-1.03	3.49
923	14.79	28.96	25.63	-14.16	-10.84
924	2.98	7.49	6.60	-4.51	-3.63
925	68.37	70.42	73.82	-2.05	-5.45
926	32.28	25.00	23.31	7.28	8.97
927	17.73	11.04	11.37	6.68	6.35
928	13.35	18.91	16.81	-5.55	-3.45
929	1.02	4.90	2.94	-3.89	-1.92
930	15.25	17.83	17.83	-2.58	-2.58
931	1.93	7.53	4.78	-5.60	-2.84
932	2.32	9.58	6.94	-7.26	-4.62
933	12.99	14.77	13.01	-1.78	-0.02
934	7.22	14.11	10.95	-6.89	-3.73
935	15.63	11.42	8.94	4.20	6.69
936	3.61	2.42	1.78	1.19	1.83
937	10.93	11.66	10.10	-0.73	0.82
938	11.75	15.93	16.94	-4.17	-5.19
939	70.76	59.54	61.33	11.22	9.43
940	3.06	8.62	8.81	-5.56	-5.76
941	24.11	17.79	16.32	6.31	7.78
942	11.11	21.10	24.35	-9.99	-13.24
943	14.81	26.49	21.28	-11.68	-6.47
Mean	**16.4**	**18.0**	**17.1**	**-1.62**	**-0.74**
SD	**15.1**	**13.5**	**14.0**	**6.39**	**6.67**

AHI: Apnea hypopnea index, SD: Standard deviation, Estimated AHI was subtracted from actual AHI to calculate the differences, Positive (+) and negative (-) differences indicate underestimation and overestimation respectively.

References

Abhang, P. A., Gawali, B. W., and Mehrotra, S. C. (2016). Technical aspects of brain rhythms and speech parameters. In *Introduction to EEG-and Speech-Based Emotion Recognition*, 51-79.

Akin, M. and Sezgin, N. (2010). Classıfication of sleep apnea by using wavelet transform and artificial neural networks. *Expert Systems with Applications, 37*(2), 1600-1607.

Al-Angari, H. M. and Sahakian, A. V. (2012). Automated recognition of obstructive sleep apnea syndrome using support vector machine classifier. *IEEE Transactions on Information Technology in Biomedicine, 16*(3), 463-468.

Al-Mardini, M., Aloul, F., Sagahyroon, A., and Al-Husseini, L. (2014). Classifying obstructive sleep apnea using smartphones. *Journal of Biomedical Informatics, 52*, 251-259.

Alsubie, H. S. and BaHammam, A. S. (2017). Obstructive sleep apnoea: children are not little adults. *Paediatric Respiratory Reviews, 21*, 72-79.

Alvarez-Estevez, D. and Moret-Bonillo, V. (2009). Fuzzy reasoning used to detect apneic events in the sleep apnea-hypopnea syndrome. *Expert Systems with Applications, 36*(4), 7778-7785.

Álvarez, D., Cerezo-Hernández, A., Crespo, A., Gutiérrez-Tobal, G. C., Vaquerizo-Villar, F., Barroso-García, V., *et al.* (2020). A machine learning-based test for adult sleep apnoea screening at home using oximetry and airflow. *Scientific Reports, 10*(1), 1-12.

Alvarez, D., Gutierrez, G., Marcos, J. V., del Campo, F., and Hornero, R. (2010). *Spectral analysis of single-channel airflow and oxygen saturation recordings in obstructive sleep apnea detection.* Paper presented at the 2010 Annual International Conference of the IEEE Engineering in Medicine and Biology Society.

Alvarez, D., Hornero, R., Abasolo, D., del Campo, F., and Zamarron, C. (2006). Nonlinear characteristics of blood oxygen saturation from nocturnal oximetry for obstructive sleep apnoea detection. *Physiological Measurement, 27*(4), 399.

Alvarez, D., Hornero, R., Garcia, M., del Campo, F., and Zamarron, C. (2007). Improving diagnostic ability of blood oxygen saturation from overnight pulse oximetry in obstructive sleep apnea detection by means of central tendency measure. *Artificial Intelligence in Medicine, 41*(1), 13-24.

Alvarez, D., Hornero, R., Garcia, M., del Campo, F., Zamarron, C., and Lopez, M. (2006). *Cross approximate entropy analysis of nocturnal oximetry signals in the diagnosis of the obstructive sleep apnea syndrome.* Paper presented at the 2006 Annual International Conference of the IEEE Engineering in Medicine and Biology Society.

Alvarez, D., Hornero, R., Marcos, J., del Campo, F., and Lopez, M. (2007). *Obstructive sleep apnea detection using clustering classification of nonlinear features from nocturnal oximetry.* Paper presented at the 2007 Annual International Conference of the IEEE Engineering in Medicine and Biology Society.

Alvarez, D., Hornero, R., Marcos, J. V., and del Campo, F. (2010). Multivariate analysis of blood oxygen saturation recordings in obstructive sleep apnea diagnosis. *IEEE Transactions on Biomedical Engineering, 57*(12), 2816-2824.

Alvarez, D., Hornero, R., Marcos, J. V., del Campo, F., and Lopez, M. (2009). *Spectral analysis of electroencephalogram and oximetric signals in obstructive sleep apnea diagnosis.* Paper presented at the 2009 Annual International Conference of the IEEE Engineering in Medicine and Biology Society.

Aminoff, M. J. (2012). Electroencephalography: general principles and clinical applications. In. *Aminoff's Electrodiagnosis in Clinical Neurology: Expert Consult-Online and Print*, 37.

Armitage, R. (1995). The distribution of EEG frequencies in REM and NREM sleep stages in healthy young adults. *Sleep, 18*(5), 334-341.

Atkinson, K. E. (2008). *An introduction to numerical analysis*. New York: John wiley & sons.

Avci, C. and Akbas, A. (2015). Sleep apnea classification based on respiration signals by using ensemble methods. *Bio-Medical Materials and Engineering*, *26*(1), 1703-1710.

Ayappa, I., Norman, R. G., Seelall, V., and Rapoport, D. M. (2008). Validation of a self-applied unattended monitor for sleep disordered breathing. *Journal of Clinical Sleep Medicine, 4*(1), 26-37.

Bandla, H. P. and Gozal, D. (2000). Dynamic changes in EEG spectra during obstructive apnea in children. *Pediatric Pulmonology, 29*(5), 359-365.

Belhumeur, P. N., Hespanha, J. P., and Kriegman, D. J. (1997). Eigenfaces vs. fisherfaces: Recognition using class specific linear projection. *IEEE Transactions on Pattern Analysis and Machine Intelligence*, *19*(7), 711-720.

Ben-Israel, N., Tarasiuk, A., and Zigel, Y. (2010). *Nocturnal sound analysis for the diagnosis of obstructive sleep apnea.* Paper presented at the 2010 Annual International Conference of the IEEE Engineering in Medicine and Biology Society.

Ben-Israel, N., Tarasiuk, A., and Zigel, Y. (2012). Obstructive apnea hypopnea index estimation by analysis of nocturnal snoring signals in adults. *Sleep, 35*(9), 1299-1305.

Berger, M., Oksenberg, A., Silverberg, D. S., Arons, E., Radwan, H., and Iaina, A. (1997). Avoiding the supine position during sleep lowers 24 h blood pressure in obstructive sleep apnea (OSA) patients. *Journal of Human Hypertension, 11*(10), 657-664.

Berry, R. B., Brooks, R., Gamaldo, C., Harding, S. M., Lloyd, R. M., Quan, *et al.* (2017). AASM scoring manual updates for 2017 (version 2.4). *Journal of Clinical Sleep Medicine, 13*(5), 665-666.

Berry, R. B., Budhiraja, R., Gottlieb, D. J., Gozal, D., Iber, C., Kapur, V. K., *et al.* (2012). Rules for scoring respiratory events in sleep: update of the 2007 AASM manual for the scoring of sleep and associated events. *Journal of Clinical Sleep Medicine, 8*(5), 597-619.

Bianchi, M. T., Lipoma, T., Darling, C., Alameddine, Y., and Westover, M. B. (2014). Automated sleep apnea quantification based on respiratory movement. *International Journal of Medical Sciences, 11*(8), 796-802.

Bishop, C. M. (2006). *Pattern recognition and machine learning*: springer.

Bowes, G. (1984). Arousal responses to respiratory stimuli during sleep. *Sleep and Breathing, 21*, 137-161.

Breiman, L. (1996). Bagging predictors. *Machine Learning, 24*(2), 123-140.

Broughton, R. and Hasan, J. (1995). Quantitative topographic electroencephalographic mapping during drowsiness and sleep onset. *Journal of Clinical Neurophysiology, 12*(4), 372-386.

Burgos, A., Goni, A., Illarramendi, A., and Bermudez, J. (2010). Real-time detection of apneas on a PDA. *IEEE Transactions on Information Technology in Biomedicine, 14*(4), 995-1002.

Carmes, K., Kempfner, L., Sorensen, H. B., and Jennum, P. (2014). *Novel method for detection of Sleep Apnoea using respiration signals.* Paper presented at the 2014 Annual International Conference of the IEEE Engineering in Medicine and Biology Society.

Cartwright, K. V. (2016). Simpson's Rule Integration with MS Excel and Irregularly-spaced Data. *Journal of Mathematical Science and Mathematics Education, 11*(2), 34-42.

Casasent, D. and Wang, Y. (2005). *Automatic target recognition using new support vector machine.* Paper presented at the 2005 IEEE International Joint Conference on Neural Networks.

Caseiro, P., Fonseca-Pinto, R., and Andrade, A. (2010). Screening of obstructive sleep apnea using Hilbert–Huang decomposition of oronasal airway pressure recordings. *Medical Engineering and Physics, 32*(6), 561-568.

Chai-Coetzer, C. L., Antic, N. A., Rowland, L. S., Catcheside, P. G., Esterman, A., Reed, *et al.* (2011). A simplified model of screening questionnaire and home monitoring for obstructive sleep apnoea in primary care. *Thorax, 66*(3), 213-219.

Chang, S. J. and Chae, K. Y. (2010). Obstructive sleep apnea syndrome in children: Epidemiology, pathophysiology, diagnosis and sequelae. *Korean Journal of Pediatrics, 53*(10), 863.

Charbonneau, M., Marin, J. M., Olha, A., Kimoff, R. J., Levy, R. D., and Cosio, M. G. (1994). Changes in obstructive sleep apnea characteristics through the night. *Chest, 106*(6), 1695-1701.

Chesson, A. L., Ferber, R. A., Fry, J. M., Grigg-Damberger, M., Hartse, K. M., Hurwitz, T. D., *et al.* (1997). Practice parameters for the indications for polysomnography and related procedures. *Sleep, 20*(6), 406-422.

Chung, F., Liao, P., Elsaid, H., Islam, S., Shapiro, C. M., and Sun, Y. (2012). Oxygen desaturation index from nocturnal oximetry: a sensitive and specific tool to detect sleep-disordered breathing in surgical patients. *Anesthesia and Analgesia, 114*(5), 993-1000.

Ciolek, M., Niedzwiecki, M., Sieklicki, S., Drozdowski, J., and Siebert, J. (2015). Automated detection of sleep apnea and hypopnea events based on robust airflow envelope tracking in the presence of breathing artifacts. *IEEE Journal of Biomedical and Health Informatics, 19*(2), 418-429.

Coenen, F. and Leng, P. (2007). The effect of threshold values on association rule based classification accuracy. *Data and Knowledge Engineering, 60*(2), 345-360.

Coito, A. L., Belo, D., Paiva, T., and Sanches, J. M. (2011). *Topographic EEG brain mapping before, during and after Obstructive Sleep Apnea Episodes.* Paper presented at the 2011 IEEE International Symposium on Biomedical Imaging: from Nano to Macro.

Corder, G. W. and Foreman, D. I. (2011). Nonparametric statistics for non-statisticians. In: John Wiley & Sons, Inc.

Cruz, A. A. (2007). *Global surveillance, prevention and control of chronic respiratory diseases: a comprehensive approach*: World Health Organization.

Cvetkovic, D., Ubeyli, E. D., Holland, G., and Cosic, I. (2010). Alterations in sleep EEG activity during the hypopnoea episodes. *Journal of Medical Systems, 34*(4), 485-491.

Cybenko, G. (1989). Approximation by superpositions of a sigmoidal function. *Mathematics of Control, Signals and Systems, 2*(4), 303-314.

de Almeida, F. R., Ayas, N. T., Otsuka, R., Ueda, H., Hamilton, P., Ryan, F. C., *et al.* (2006). Nasal pressure recordings to detect obstructive sleep apnea. *Sleep and Breathing, 10*(2), 62-69.

de Chazal, P., Heneghan, C., Sheridan, E., Reilly, R., Nolan, P., and O'Malley, M. (2003). Automated processing of the single-lead electrocardiogram for the detection of obstructive sleep apnoea. *IEEE Transactions on Biomedical Engineering, 50*(6), 686-696.

de Oliveira, A. C. T., Martinez, D., Vasconcelos, L. F. T., Gonçalves, S. C., do Carmo Lenz, M., Fuchs, S. C., *et al.* (2009). Diagnosis of obstructive sleep apnea syndrome and its outcomes with home portable monitoring. *Chest, 135*(2), 330-336.

del Campo, F., Hornero, R., Zamarron, C., Abasolo, D. E., and Alvarez, D. (2006). Oxygen saturation regularity analysis in the diagnosis of obstructive sleep apnea. *Artificial Intelligence in Medicine, 37*(2), 111-118.

Dement, W. and Kleitman, N. (1957). Cyclic variations in EEG during sleep and their relation to eye movements, body motility, and dreaming. *Electroencephalography and Clinical Neurophysiology, 9*(4), 673-690.

Dingli, K., Assimakopoulos, T., Fietze, I., Witt, C., Wraith, P. K., and Douglas, N. J. (2002). Electroencephalographic spectral analysis: detection of cortical activity changes in sleep apnoea patients. *European Respiratory Journal, 20*(5), 1246-1253.

Draper, N. R. and Smith, H. (2014). *Applied regression analysis* (Vol. 326): John Wiley & Sons.

Dudani, S. A. (1976). The distance-weighted k-nearest-neighbor rule. *IEEE Transactions on Systems, Man, and Cybernetics*, *6*(4), 325-327.

Dunn, O. J. (1961). Multiple comparisons among means. *Journal of the American Statistical Association, 56*(293), 52-64.

Dunn, O. J. (1964). Multiple comparisons using rank sums. *Technometrics, 6*(3), 241-252.

Efron, B., Hastie, T., Johnstone, I., and Tibshirani, R. (2004). Least angle regression. *The Annals of Statistics, 32*(2), 407-499.

Erman, M. K., Stewart, D., Einhorn, D., Gordon, N., and Casal, E. (2007). Validation of the ApneaLink™ for the screening of sleep apnea: a novel and simple single-channel recording device. *Journal of Clinical Sleep Medicine, 3*(4), 387-392.

Ferber, R., Millman, R., Coppola, M., Fleetham, J., Murray, C. F., Iber, C., *et al.* (1994). Portable recording in the assessment of obstructive sleep apnea. ASDA standards of practice. *Sleep, 17*(4), 378-392.

Fontenla-Romero, O., Guijarro-Berdinas, B., Alonso-Betanzos, A., and Moret-Bonillo, V. (2005). A new method for sleep apnea classification using wavelets and feedforward neural networks. *Artificial Intelligence in Medicine, 34*(1), 65-76.

Glass, G. V. (1966). Testing homogeneity of variances. *American Educational Research Journal, 3*(3), 187-190.

Gleeson, K., Zwillich, C. W., and White, D. P. (1990). The Influence of Increasing Ventilatory Effort on Arousal from Sleep. *American Review of Respiratory Disease, 142*, 295-300.

Grigg-Damberger, M., Gozal, D., Marcus, C. L., Quan, S. F., Rosen, C. L., Chervin, R. D., *et al.* (2007). The visual scoring of sleep and arousal in infants and children. *Journal of Clinical Sleep Medicine, 3*(2), 201-240.

Grover, S. S. and Pittman, S. D. (2008). Automated detection of sleep disordered breathing using a nasal pressure monitoring device. *Sleep and Breathing, 12*(4), 339-345.

Guijarro-Berdinas, B., Hernandez-Pereira, E., and Peteiro-Barral, D. (2012). A mixture of experts for classifying sleep apneas. *Expert Systems with Applications, 39*(8), 7084-7092.

Gutiérrez-Tobal, G. C., Álvarez, D., Crespo, A., Del Campo, F., and Hornero, R. (2018). Evaluation of machine-learning approaches to estimate sleep apnea severity from at-home oximetry recordings. *IEEE Journal of Biomedical and Health Informatics, 23*(2), 882-892.

Gutierrez-Tobal, G. C., Alvarez, D., del Campo, F., and Hornero, R. (2016). Utility of adaboost to detect sleep apnea-hypopnea syndrome from single-channel airflow. *IEEE Transactions on Biomedical Engineering, 63*(3), 636-646.

Gutierrez-Tobal, G. C., Alvarez, D., Marcos, J. V., del Campo, F., and Hornero, R. (2013). Pattern recognition in airflow recordings to assist in the sleep apnoea–hypopnoea syndrome diagnosis. *Medical and Biological Engineering and Computing, 51*(12), 1367-1380.

Gutierrez-Tobal, G. C., Hornero, R., Alvarez, D., Marcos, J. V., and del Campo, F. (2012). Linear and nonlinear analysis of airflow recordings to help in sleep apnoea–hypopnoea syndrome diagnosis. *Physiological Measurement, 33*(7), 1261.

Hamann, B. and Chen, J. (1994). Data point selection for piecewise linear curve approximation. *Computer Aided Geometric Design, 11*(3), 289-301.

Han, J., Shin, H. B., Jeong, D. U., and Park, K. S. (2008). Detection of apneic events from single channel nasal airflow using 2nd derivative method. *Computer Methods and Programs in Biomedicine, 91*(3), 199-207.

Harrell Jr, F. E., Lee, K. L., Califf, R. M., Pryor, D. B., and Rosati, R. A. (1984). Regression modelling strategies for improved prognostic prediction. *Statistics in Medicine, 3*(2), 143-152.

Hassan, A. R. and Haque, M. A. (2017). An expert system for automated identification of obstructive sleep apnea from single-lead ECG using random under sampling boosting. *Neurocomputing, 235*, 122-130.

Haykin, S. (1994). *Neural networks* (Vol. 2): Prentice hall New York.

Holz, J., Piosczyk, H., Feige, B., Spiegelhalder, K., Baglioni, C., Riemann, D., *et al.* (2012). EEG sigma and slow-wave activity during NREM sleep correlate with overnight declarative and procedural memory consolidation. *Journal of Sleep Research, 21*(6), 612-619.

Hornero, R., Alvarez, D., Abasolo, D., del Campo, F., and Zamarron, C. (2007). Utility of approximate entropy from overnight pulse oximetry data in the diagnosis of the obstructive sleep apnea syndrome. *IEEE Transactions on Biomedical Engineering, 54*(1), 107-113.

Howell, D. C. (2009). *Statistical methods for psychology*: Cengage Learning.

Huang, S. H., Teng, N. C., Wang, K. J., Chen, K. H., Lee, H. C., and Wang, P. C. (2015). Use of oximetry as a screening tool for obstructive sleep apnea: a case study in Taiwan. *Journal of Medical Systems, 39*(3), 29.

Huang, W., Guo, B., Shen, Y., and Tang, X. (2017). A novel method to precisely detect apnea and hypopnea events by airflow and oximetry signals. *Computers in Biology and Medicine, 88*, 32-40.

Jin, J. and Sanchez-Sinencio, E. (2015). A home sleep apnea screening device with time-domain signal processing and autonomous scoring capability. *IEEE Transactions on Biomedical Circuits and Systems, 9*(1), 96-104.

Jung, D., Hwang, S., Cho, J., Choi, B., Baek, H., Lee, Y., *et al.* (2018). Real-time automatic apneic event detection using nocturnal pulse oximetry. *IEEE Transactions on Biomedical Engineering, 65*(3), 706-712.

Kagawa, M., Tojima, H., and Matsui, T. (2016). Non-contact diagnostic system for sleep apnea–hypopnea syndrome based on amplitude and phase analysis of thoracic and abdominal Doppler radars. *Medical and Biological Engineering and Computing, 54*(5), 789-798.

Kaimakamis, E., Bratsas, C., Sichletidis, L., Karvounis, C., and Maglaveras, N. (2009). *Screening of patients with Obstructive Sleep Apnea Syndrome using C4.5 algorithm based on non linear analysis of respiratory signals during sleep.* Paper presented at the 2009 Annual International Conference of the IEEE Engineering in Medicine and Biology Society.

Kaimakamis, E., Tsara, V., Bratsas, C., Sichletidis, L., Karvounis, C., and Maglaveras, N. (2016). Evaluation of a decision support system for obstructive sleep apnea with nonlinear analysis of respiratory signals. *PloS One, 11*(3), e0150163.

Kass, J. E., Akers, S. M., Bartter, T. C., and Pratter, M. R. (1996). Rapid-eye-movement-specific sleep-disordered breathing: a possible cause of excessive daytime sleepiness. *American Journal of Respiratory and Critical Care Medicine, 154*(1), 167-169.

Kimoff, R. J., Cheong, T. H., Olha, A. E., Charbonneau, M., Levy, R. D., Cosio, M. G., *et al.* (1994). Mechanisms of apnea termination in obstructive sleep apnea. Role of chemoreceptor and mechanoreceptor stimuli. *American Journal of Respiratory and Critical Care Medicine, 149*(3), 707-714.

Kljajic, Z., Roje, Z., Becic, K., Capkun, V., Vilovic, K., Ivanisevic, P., *et al.* (2017). Formula for the prediction of apnea/hypopnea index in children with obstructive sleep apnea without polysomnography according to the clinical parameters: Is it reliable? *International Journal of Pediatric Otorhinolaryngology, 100*, 168-173.

Koley, B. L. and Dey, D. (2013). Real-time adaptive apnea and hypopnea event detection methodology for portable sleep apnea monitoring devices. *IEEE Transactions on Biomedical Engineering, 60*(12), 3354-3363.

Koley, B. L. and Dey, D. (2014). On-Line detection of apnea/hypopnea events using SpO_2 signal: a rule-based approach employing binary classifier models. *IEEE Journal of Biomedical and Health Informatics, 18*(1), 231-239.

Koo, T. K. and Li, M. Y. (2016). A guideline of selecting and reporting intraclass correlation coefficients for reliability research. *Journal of Chiropractic Medicine, 15*(2), 155-163.

Koves, P. (1999). *Obstructive Sleep Apnea Syndrome*. Budapest, Hungary: Springer-Verlag.

Kruskal, W. H. and Wallis, W. A. (1952). Use of ranks in one-criterion variance analysis. *Journal of the American Statistical Association, 47*(260), 583-621.

Kryger, M. H. (2000). Diagnosis and management of sleep apnea syndrome. *Clinical Cornerstone, 2*(5), 39-44.

Kryger, M. H., Roos, L., Delaive, K., Walld, R., and Horrocks, J. (1996). Utilization of health care services in patients with severe obstructive sleep apnea. *Sleep, 19*(9), 111-116.

Kushida, C. A., Littner, M. R., Morgenthaler, T., Alessi, C. A., Bailey, D., Coleman Jr, J., *et al.* (2005). Practice parameters for the indications for polysomnography and related procedures: an update for 2005. *Sleep, 28*(4), 499-523.

Lee, H., Park, J., Kim, H., and Lee, K. J. (2016). New rule-based algorithm for real-time detecting sleep apnea and hypopnea events using a nasal pressure signal. *Journal of Medical Systems, 40*(12), 282.

Lee, Y. K., Bister, M., Blanchfield, P., and Salleh, Y. M. (2004). *Automated detection of obstructive apnea and hypopnea events from oxygen saturation signal.* Paper presented at the 26th Annual International Conference of the IEEE Engineering in Medicine and Biology Society.

Liu, D., Pang, Z., and Lloyd, S. R. (2008). A neural network method for detection of obstructive sleep apnea and narcolepsy based on pupil size and EEG. *IEEE Transactions on Neural Networks, 19*(2), 308-318.

Maali, Y. and Al-Jumaily, A. (2013). Multi neural networks investigation based sleep apnea prediction. *Procedia Computer Science, 24*, 97-102.

Mandrekar, J. N. (2010). Receiver operating characteristic curve in diagnostic test assessment. *Journal of Thoracic Oncology, 5*(9), 1315-1316.

Marcos, J. V., Hornero, R., Alvarez, D., del Campo, F., and Aboy, M. (2010). Automated detection of obstructive sleep apnoea syndrome from oxygen saturation recordings using linear discriminant analysis. *Medical and Biological Engineering and Computing, 48*(9), 895-902.

Marcos, J. V., Hornero, R., Alvarez, D., del Campo, F., and Lopez, M. (2007). *Applying neural network classifiers in the diagnosis of the obstructive sleep apnea syndrome from*

nocturnal pulse oximetric recordings. Paper presented at the 2007 Annual International Conference of the IEEE Engineering in Medicine and Biology Society.

Marcos, J. V., Hornero, R., Alvarez, D., del Campo, F., Lopez, M., and Zamarron, C. (2008). Radial basis function classifiers to help in the diagnosis of the obstructive sleep apnoea syndrome from nocturnal oximetry. *Medical and Biological Engineering and Computing, 46*(4), 323-332.

Marcos, J. V., Hornero, R., Alvarez, D., del Campo, F., and Zamarron, C. (2009a). Assessment of four statistical pattern recognition techniques to assist in obstructive sleep apnoea diagnosis from nocturnal oximetry. *Medical Engineering and Physics, 31*(8), 971-978.

Marcos, J. V., Hornero, R., Alvarez, D., del Campo, F., and Zamarron, C. (2009b). *A classification algorithm based on spectral features from nocturnal oximetry and support vector machines to assist in the diagnosis of obstructive sleep apnea.* Paper presented at the 2009 Annual International Conference of the IEEE Engineering in Medicine and Biology Society.

Marcos, J. V., Hornero, R., Alvarez, D., del Campo, F., Zamarron, C., and Lopez, M. (2008a). *Single layer network classifiers to assist in the detection of obstructive sleep apnea syndrome from oximetry data.* Paper presented at the 2008 Annual International Conference of the IEEE Engineering in Medicine and Biology Society.

Marcos, J. V., Hornero, R., Alvarez, D., del Campo, F., Zamarron, C., and Lopez, M. (2008b). Utility of multilayer perceptron neural network classifiers in the diagnosis of the obstructive sleep apnoea syndrome from nocturnal oximetry. *Computer Methods and Programs in Biomedicine, 92*(1), 79-89.

Marcos, J. V., Hornero, R., Nabney, I. T., Alvarez, D., and del Campo, F. (2011). *Analysis of nocturnal oxygen saturation recordings using kernel entropy to assist in sleep apnea-hypopnea diagnosis.* Paper presented at the 2011 Annual International Conference of the IEEE Engineering in Medicine and Biology Society.

Marcuse, L. V., Fields, M. C., and Yoo, J. J. (2015). *Rowan's Primer of EEG* (2nd ed.). New York: Elsevier.

Masdeu, M. J., Ayappa, I., Hwang, D., Mooney, A. M., and Rapoport, D. M. (2010). Impact of clinical assessment on use of data from unattended limited monitoring as opposed to full-in lab PSG in sleep disordered breathing. *Journal of Clinical Sleep Medicine, 6*(1), 51-58.

McHugh, M. L. (2012). Interrater reliability: the kappa statistic. *Biochemia Medica, 22*(3), 276-282.

Mendez, M. O., Corthout, J., van Huffel, S., Matteucci, M., Penzel, T., Cerutti, S., *et al.* (2010). Automatic screening of obstructive sleep apnea from the ECG based on empirical mode decomposition and wavelet analysis. *Physiological Measurement, 31*(3), 273.

Morales, J. F., Varon, C., Deviaene, M., Borzee, P., Testelmans, D., Buyse, B., *et al.* (2017). *Sleep apnea hypopnea syndrome classification in spo 2 signals using wavelet decomposition and phase space reconstruction.* Paper presented at the 2017 IEEE International Conference on Wearable and Implantable Body Sensor Networks.

Morillo, D. S. and Gross, N. (2013). Probabilistic neural network approach for the detection of SAHS from overnight pulse oximetry. *Medical and Biological Engineering and Computing, 51*(3), 305-315.

Morillo, D. S., Rojas, J. L., Crespo, L. F., Leon, A., and Gross, N. (2009). Poincaré analysis of an overnight arterial oxygen saturation signal applied to the diagnosis of sleep apnea hypopnea syndrome. *Physiological Measurement, 30*(4), 405.

Morsy, A. A. and Al-Ashmouny, K. M. (2006). *Sleep apnea detection using an adaptive fuzzy logic based screening system.* Paper presented at the 2005 Annual International Conference of the IEEE Engineering in Medicine and Biology Society.

Muthuswamy, J. and Thakor, N. V. (1998). Spectral analysis methods for neurological signals. *Journal of Neuroscience Methods, 83*(1), 1-14.

Nakano, H., Tanigawa, T., Furukawa, T., and Nishima, S. (2007). Automatic detection of sleep-disordered breathing from a single-channel airflow record. *European Respiratory Journal, 29*(4), 728-736.

Nakano, H., Tanigawa, T., Ohnishi, Y., Uemori, H., Senzaki, K., Furukawa, T., *et al.* (2008). Validation of a single-channel airflow monitor for screening of sleep-disordered breathing. *European Respiratory Journal, 32*(4), 1060-1067.

Nattie, E. and Li, A. (2009). Central nervous chemoreceptors and respiratory drive. *Encyclopedia of Neuroscience*, 617-619.

Nazeran, H., Almas, A., Behbehani, K., Burk, J., and Lucas, E. (2001). *A fuzzy inference system for detection of obstructive sleep apnea.* Paper presented at the 2001 Annual International Conference of the IEEE Engineering in Medicine and Biology Society.

Nelder, J. A. and Baker, R. J. (1972). *Generalized linear models*. In: Wiley, New York.

Ng, A. S., Chung, J. W., Gohel, M. D., Yu, W. W., Fan, K. L., and Wong, T. K. (2008). Evaluation of the performance of using mean absolute amplitude analysis of thoracic and abdominal signals for immediate indication of sleep apnoea events. *Journal of Clinical Nursing, 17*(17), 2360-2366.

Nie, N. H., Bent, D. H., and Hull, C. H. (1975). *SPSS: Statistical package for the social sciences* (Vol. 227). New York: McGraw-Hill.

Niedermeyer, E. and da Silva, F. H. (2005). *Electroencephalography: basic principles, clinical applications, and related fields*: Lippincott Williams & Wilkins.

Norman, R. G., Ahmed, M. M., Walsleben, J. A., and Rapoport, D. M. (1997). Detection of respiratory events during NPSG: nasal cannula/pressure sensor versus thermistor. *Sleep, 20*(12), 1175-1184.

Oeverland, B., Skatvedt, O., Kvaerner, K. J., and Akre, H. (2002). Pulseoximetry: sufficient to diagnose severe sleep apnea. *Sleep Medicine, 3*(2), 133-138.

Oppenheim, A. V., Willsky, A. S., and Young, I. T. (1983). *Signals and Systems*. London: Prentice Hall.

Otero, A., Felix, P., and Alvarez, M. R. (2011). Algorithms for the analysis of polysomnographic recordings with customizable criteria. *Expert Systems with Applications, 38*(8), 10133-10146.

Otero, A., Felix, P., Alvarez, M. R., and Zamarron, C. (2008). *Fuzzy structural algorithms to identify and characterize apnea and hypopnea episodes.* Paper presented at the 2008 Annual International Conference of the IEEE Engineering in Medicine and Biology Society.

Otero, A., Felix, P., Barro, S., and Zamarron, C. (2012). A structural knowledge-based proposal for the identification and characterization of apnoea episodes. *Applied Soft Computing, 12*(1), 516-526.

Penzel, T., Moody, G. B., Mark, R. G., Goldberger, A. L., and Peter, J. H. (2000). *The apnea-ECG database.* Paper presented at the Computers in Cardiology.

Peppard, P. E., Young, T., Barnet, J. H., Palta, M., Hagen, E. W., and Hla, K. M. (2013). Increased prevalence of sleep-disordered breathing in adults. *American Journal of Epidemiology, 177*(9), 1006-1014.

Perez-Padilla, R., West, P., and Kryger, M. H. (1983). Sighs during sleep in adult humans. *Sleep, 6*(3), 234-243.

Pombo, N., Garcia, N., Felizardo, V., and Bousson, K. (2014). *Big data reduction using RBFNN: A predictive model for ECG waveform for eHealth platform integration.* Paper presented at the 2014 IEEE International Conference on e-Health Networking, Applications and Services.

Quan, S. F., Howard, B. V., Iber, C., Kiley, J. P., Nieto, F. J., O'Connor, G. T., *et al.* (1997). The sleep heart health study: design, rationale, and methods. *Sleep, 20*(12), 1077-1085.

Ragette, R., Wang, Y., Weinreich, G., and Teschler, H. (2010). Diagnostic performance of single airflow channel recording (ApneaLink) in home diagnosis of sleep apnea. *Sleep and Breathing, 14*(2), 109-114.

Rathnayake, S. I., Wood, I. A., Abeyratne, U. R., and Hukins, C. (2010). Nonlinear features for single-channel diagnosis of sleep-disordered breathing diseases. *IEEE Transactions on Biomedical Engineering, 57*(8), 1973-1981.

Rofail, L. M., Wong, K. K., Unger, G., Marks, G. B., and Grunstein, R. R. (2010). The utility of single-channel nasal airflow pressure transducer in the diagnosis of OSA at home. *Sleep, 33*(8), 1097-1105.

Rolon, R. E., Larrateguy, L. D., di Persia, L. E., Spies, R. D., and Rufiner, H. L. (2017). Discriminative methods based on sparse representations of pulse oximetry signals for sleep apnea–hypopnea detection. *Biomedical Signal Processing and Control, 33*, 358-367.

Rosenberg, R. S. and Van Hout, S. (2014). The american academy of sleep medicine inter-scorer reliability program: respiratory events. *Journal of Clinical Sleep Medicine, 10*(4), 447-454.

Salisbury, J. I. and Sun, Y. (2007). Rapid screening test for sleep apnea using a nonlinear and nonstationary signal processing technique. *Medical Engineering and Physics, 29*(3), 336-343.

Sanchez-Morillo, D., Lopez-Gordo, M. A., and Leon, A. (2014). Novel multiclass classification for home-based diagnosis of sleep apnea hypopnea syndrome. *Expert Systems with Applications, 41*(4), 1654-1662.

Scher, M. S. (2017). Pediatric neurophysiologic evaluation. In. In *Swaiman's Pediatric Neurology* (pp. 87-96): Elsevier.

Schramm, D., Scheidt, B., Hubler, A., Frenzel, J., Holthausen, K., and Breidbach, O. (2000). Spectral analysis of electroencephalogram during sleep-related apneas in pre-term and term born infants in the first weeks of life. *Clinical Neurophysiology, 111*(10), 1788-1791.

Schulz, H. (2008). Rethinking sleep analysis comment on the AASM manual for the scoring of sleep and associated events. *Journal of Clinical Sleep Medicine, 4*(02), 99-103.

Selvaraj, N. and Narasimhan, R. (2013). *Detection of sleep apnea on a per-second basis using respiratory signals.* Paper presented at the 2013 Annual International Conference of the IEEE Engineering in Medicine and Biology Society.

Series, F., Cormier, Y., and La Forge, J. (1990). Influence of Apnea Type and Sleep Stage on Nocturnal. *American Review of Respiratory Disease, 141*, 1522-1526.

Sezgin, N. and Tagluk, M. E. (2009). Energy based feature extraction for classification of sleep apnea syndrome. *Computers in Biology and Medicine, 39*(11), 1043-1050.

Shapiro, S. S. and Francia, R. S. (1972). An approximate analysis of variance test for normality. *Journal of the American Statistical Association, 67*(337), 215-216.

Sharma, H. and Sharma, K. (2016). An algorithm for sleep apnea detection from single-lead ECG using Hermite basis functions. *Computers in Biology and Medicine, 77*, 116-124.

Shochat, T., Hadas, N., Kerkhofs, M., Herchuelz, A., Penzel, T., Peter, J., *et al.* (2002). The SleepStripTM: an apnoea screener for the early detection of sleep apnoea syndrome. *European Respiratory Journal, 19*(1), 121-126.

Slater, G. and Steier, J. (2012). Excessive daytime sleepiness in sleep disorders. *Journal of Thoracic Disease, 4*(6), 608.

Song, C., Liu, K., Zhang, X., Chen, L., and Xian, X. (2016). An obstructive sleep apnea detection approach using a discriminative hidden Markov model from ECG signals. *IEEE Transactions on Biomedical Engineering, 63*(7), 1532-1542.

Specht, D. F. (1990). Probabilistic neural networks. *Neural Networks, 3*(1), 109-118.

Suykens, J. A. and Vandewalle, J. (1999). Least squares support vector machine classifiers. *Neural Processing Letters, 9*(3), 293-300.

Tagluk, M. E. and Sezgin, N. (2010). Classification of sleep apnea through sub-band energy of abdominal effort signal using wavelets+ neural networks. *Journal of Medical Systems, 34*(6), 1111-1119.

Tagluk, M. E. and Sezgin, N. (2011). A new approach for estimation of obstructive sleep apnea syndrome. *Expert Systems with Applications, 38*(5), 5346-5351.

Thommandram, A., Eklund, J. M., and McGregor, C. (2013). *Detection of apnoea from respiratory time series data using clinically recognizable features and kNN classification.* Paper presented at the 2013 Annual International Conference of the IEEE Engineering in Medicine and Biology Society.

Tian, J. Y. and Liu, J. Q. (2006). *Apnea detection based on time delay neural network.* Paper presented at the 2005 Annual International Conference of the IEEE Engineering in Medicine and Biology Society.

Travieso, C. M., Alonso, J. B., del Pozo, M., Ticay, J. R., and Castellanos-Dominguez, G. (2014). Building a Cepstrum-HMM kernel for Apnea identification. *Neurocomputing, 132*, 159-165.

Uddin, M., Chow, C., and Su, S. (2018). Classification methods to detect sleep apnea in adults based on respiratory and oximetry signals: a systematic review. *Physiological Measurement, 39*(3), 03TR01.

Uddin, M., Su, S., Chen, W., and Chow, C. (2019). Dynamic changes in electroencephalogram spectral power with varying apnea duration in older adults. *Journal of Sleep Research, 28*(6), e12850.

Urtnasan, E., Park, J. U., Joo, E. Y., and Lee, K. J. (2018). Automated detection of obstructive sleep apnea events from a single-lead electrocardiogram using a convolutional neural network. *Journal of Medical Systems, 42*(6), 104.

Varady, P., Bongar, S., and Benyo, Z. (2003). Detection of airway obstructions and sleep apnea by analyzing the phase relation of respiration movement signals. *IEEE Transactions on Instrumentation and Measurement, 52*(1), 2-6.

Varady, P., Micsik, T., Benedek, S., and Benyo, Z. (2002). A novel method for the detection of apnea and hypopnea events in respiration signals. *IEEE Transactions on Biomedical Engineering, 49*(9), 936-942.

Waibel, A., Hanazawa, T., Hinton, G., Shikano, K., and Lang, K. J. (1989). Phoneme recognition using time-delay neural networks. *IEEE Transactions on Acoustics, Speech, and Signal Processing*, *37*(3), 328-339.

Ward, K. L., McArdle, N., James, A., Bremner, A. P., Simpson, L., Cooper, M. N., *et al.* (2015). A comprehensive evaluation of a two-channel portable monitor to "rule in" obstructive sleep apnea. *Journal of Clinical Sleep Medicine, 11*(4), 433-444.

Welch, P. (1967). The use of fast Fourier transform for the estimation of power spectra: a method based on time averaging over short, modified periodograms. *IEEE Transactions on Audio and Electroacoustics, 15*(2), 70-73.

Wong, K. K., Jankelson, D., Reid, A., Unger, G., Dungan, G., Hedner, J. A., *et al.* (2008). Diagnostic test evaluation of a nasal flow monitor for obstructive sleep apnea detection in sleep apnea research. *Behavior Research Methods, 40*(1), 360-366.

Xavier, P., Behbehani, K., Watenpaugh, D., and Burk, J. R. (2007). *Detecting electroencephalography variations due to sleep disordered breathing events.* Paper presented at the 2007 Annual International Conference of the IEEE Engineering in Medicine and Biology Society.

Yang, J. S., Nicholas, C. L., Nixon, G. M., Davey, M. J., Anderson, V., Walker, A. M., *et al.* (2012). EEG spectral analysis of apnoeic events confirms visual scoring in childhood sleep disordered breathing. *Sleep and Breathing, 16*(2), 491-497.

Yang, J. S., Nicholas, C. L., Nixon, G. M., Davey, M. J., Anderson, V., Walker, A. M., *et al.* (2010). Determining sleep quality in children with sleep disordered breathing: EEG spectral analysis compared with conventional polysomnography. *Sleep, 33*(9), 1165-1172.

Younes, M. (2004). Role of arousals in the pathogenesis of obstructive sleep apnea. *American Journal of Respiratory and Critical Care Medicine, 169*(5), 623-633.

Young, T., Peppard, P. E., and Gottlieb, D. J. (2002). Epidemiology of obstructive sleep apnea: a population health perspective. *American Journal of Respiratory and Critical Care Medicine, 165*(9), 1217-1239.

Zadeh, L. A. (1965). Fuzzy sets. *Information and Control, 8*(3), 338-353.

Zamarron, C., Romero, P. V., Gude, F., Amaro, A., and Rodriguez, J. R. (2001). Screening of obstructive sleep apnoea: heart rate spectral analysis of nocturnal pulse oximetric recording. *Respiratory Medicine, 95*(9), 759-765.

Zarei, A. and Asl, B. (2019). Automatic detection of obstructive sleep apnea using wavelet transform and entropy-based features from single-lead ECG signal. *IEEE Journal of Biomedical and Health Informatics, 23*(3), 1011-1021.

Zhang, G. Q., Cui, L., Mueller, R., Tao, S., Kim, M., Rueschman, M., *et al.* (2018). The National Sleep Research Resource: towards a sleep data commons. *Journal of the American Medical Informatics Association, 25*(10), 1351-1358.

Zhang, J., Zhang, Q., Wang, Y., and Qiu, C. (2013). *A real-time auto-adjustable smart pillow system for sleep apnea detection and treatment.* Paper presented at the 2013 ACM/IEEE International Conference on Information Processing in Sensor Networks.